Electronic Thesis and Dissertation Repository

1-13-2020 2:00 PM

Effects of Drinking Water Treatment Processes on Removal of Algal Matter and Subsequent Water Quality

Ziming Zhao
The University of Western Ontario

Supervisor
Dr. Madhumita B Ray
The University of Western Ontario

Follow this and additional works at: https://ir.lib.uwo.ca/etd

Part of the Environmental Engineering Commons, and the Other Chemical Engineering Commons

Abstract

Seasonal algal blooms in drinking water sources have increased significantly over the recent past as a result of increased temperature and nutrient loading in surface water due to agricultural and surface runoff. More than 95% of algal cells can be removed by coagulation and flocculation processes. However, algal organic matter (AOM) is not removed well during coagulation, thus causes several operational challenges in drinking water treatment. This research was conducted to investigate the effectiveness of coagulation, granular activated carbon adsorption, and filtration processes on AOM removal and to evaluate disinfection by-products formation potential with/without UV irradiation.

Initially, coagulation performance for the treatment of algae-laden raw water was investigated systematically by central composite design using response surface methodology. The main mechanism of algae and AOM removal was charge neutralization at an optimum pH of around 6.0. Thereafter, the optimum coagulation conditions using alum for AOM of six different algal and cyanobacterial species were determined. The AOM removal by coagulation correlated well with the hydrophobicity of the AOM solution. The disinfection by-product formation potential of the AOM due to chlorination was determined after coagulation.

The efficiency and mechanism of AOM removal by granular activated carbon (GAC) adsorption were determined by batch adsorption experiments. The adsorption equilibrium data followed both Langmuir and Freundlich models. The adsorption process followed a pseudo-second-order kinetic model, and the calculated thermodynamic parameters indicated that GAC adsorption for AOM removal was spontaneous and endothermic in nature.

The fouling behavior of the microfiltration membranes after GAC adsorption pre-treatment was investigated and the filtration resistance and AOM removal efficiency were determined. The GAC adsorption increased the removal of AOM, decreased membrane fouling, and identified intermediate blocking as the major fouling mechanism of the membrane.

The effects of combined low-pressure ultraviolet (LPUV) irradiation and chlorination on the disinfection byproducts (DBPs) formation from AOM was investigated for common algae existed in surface water, AOM degradation was likely promoted by photodegradation of aromatics, and chlorine oxidation/substitution. Insights obtained of this work will help in properly designing and operating the AOM removal and reducing DBPs formation during water treatment of algae-laden source water.

Keywords: algae, algal organic matter, coagulation-flocculation, granular activated carbon, filtration, membrane fouling, chlorination, UV irradiation, disinfection by-products.

Summary for lay audience

Algal blooms frequently occur in surface water, such as rivers, lakes, reservoirs as a result of climate change and frequent eutrophication, causing deterioration of water quality in drinking water supplies. There are multiple barriers, including coagulation, clarification, filtration and disinfection processes applied in drinking water treatment plants to remove pathogens, viruses, and other contaminants and make the treated water safe enough for potable use. Although algal cells are removed well ($> 95\%$) during conventional processes of drinking water treatment, algal organic matter (AOM), as the metabolites of algae cells, is not removed well during coagulation. AOM causes several challenges in drinking water treatment such as increased coagulant demand, blocking the activated carbon adsorption sites, growth of biofilm causing membrane fouling, and increased formation of disinfection by-products (DBP) during chlorination.

This research was conducted to investigate the effects of treatment including coagulation, granular activated carbon (GAC) adsorption, filtration processes for AOM removal and evaluation of disinfection by-products formation potential with/without UV irradiation for six different species of algae and cyanobacteria. The results indicated that an average of 47.4% of AOM in terms of dissolved organic carbon (DOC) can be removed at the optimum coagulation-flocculation condition. The specific ultraviolet absorbance (SUVA) and hydrophobicity of AOM can be used as surrogate parameters to predict coagulation-flocculation efficiency. GAC could remove AOM, mitigating the irreversible fouling of a microfiltration membrane. Commonly applied UV irradiation dose of 40 mJ/cm^2 insignificantly affects DBP formation, more attention should be given to evaluate the feasibility of enhanced UV irradiation dosage on the degradation of AOM from some algal species. The experimental results obtained in this research are useful for determining the optimal coagulation, GAC adsorption and microfiltration conditions to be adopted and to minimize the DBP formation in treated drinking water.

Co-Authorship Statements

Chapter 3

Title of the paper: Optimization and modeling of coagulation-flocculation to remove algae and organic matter from surface water by response surface methodology

Authors: Ziming Zhao, Wenjun Sun, Madhumita B. Ray, Ajay K Ray, Tianyin Huang, Jiabin Chen

Status: Published

Journal: Frontiers of Environmental Science & Engineering

Individual contributions: The experimental plan was developed by Ziming Zhao under the supervision of Dr. Wenjun Sun and Dr. Madhumita B. Ray, while the execution of the plan, data analysis, and writing of the manuscript predominantly completed by Ziming Zhao under the supervision of Dr. Madhumita B. Ray. Dr. Ajay Ray assisted in the modeling part of the work. Dr. Tianyin Huang provided the experimental facilities and chemicals, Dr. Jiabin Chen was involved in the water sample collection and transportation in China.

Reference: Zhao, Z., Sun, W., Ray, M.B. et al. Front. Environ. Sci. Eng. (2019) 13: 75. https://doi.org/10.1007/s11783-019-1159-7,

---

Chapter 4

Title of the paper: Coagulation and disinfection by-products formation potential of extracellular and intracellular matter of algae and cyanobacteria

---

Authors: Ziming Zhao, Wenjun Sun, Ajay K Ray, Ted Mao, and Madhumita B. Ray

Status: Published

Journal: Chemosphere

Individual contributions: The experimental plan was developed by Ziming Zhao under the supervision of Madhumita B. Ray, while the execution of the plan, data analysis, and writing of the manuscript predominantly completed by Ziming Zhao under the supervision of Dr. Madhumita B. Ray; Dr. A. Ray helped with the analytical equipment and other lab facilities and lab-space. Dr. Wenjun Sun and Dr. Ted Mao gave the practical insights relevant for the treatment plants.

Chapter 5

Title of the paper: Adsorption of algal organic matter onto granular activated carbon

Authors: Ziming Zhao and Madhumita B. Ray

Status: Final draft to be submitted to Separation and Purification Technology

Individual contributions: The experimental plan was developed by Ziming Zhao under the supervision of Madhumita B. Ray, while the execution of the plan, data analysis, and writing of the manuscript predominantly completed by Ziming Zhao under the supervision of Dr. Madhumita B. Ray.

Chapter 6

Title of the paper: Granular activated carbon adsorption of algal organic matter in mitigating microfiltration membrane fouling

Authors: Ziming Zhao and Madhumita B. Ray

Status: In preparation for submission to Chemical Engineering Journal.

Individual contributions: The experimental plan was developed by Ziming Zhao under the supervision of Dr. Madhumita B. Ray, while the execution of the plan, data analysis, and writing of the manuscript completed by Ziming Zhao under the supervision of Dr. Madhumita B. Ray.

Chapter 7

Title of the paper: Impact of UV irradiation on disinfection by-product formation by post chlorination

Authors: Ziming Zhao, Wenjun Sun, Ted Mao, and Madhumita B. Ray

Status: In preparation for submission to J of Environmental Management.

Individual contributions: The experimental plan was developed by Ziming Zhao under the supervision of Dr. Ted Mao and Dr. Madhumita B. Ray, Dr. Wenjun Sun gave the practical insights relevant for the treatment plants. The execution of the plan, data analysis, and writing of the manuscript predominantly completed by Ziming Zhao under the supervision of Dr. Madhumita B. Ray.

Acknowledgements

"The highest excellence is like that of water"

"上善若水"

Laozi (Around 571-471 BC)

Table of Contents

List of Tables

List of Figures

List of Appendices

List of Abbreviations

AG	*Aulacoseira granulata f. curvatulum*
ANN	artificial neural networks
ANOVA	analysis of variance
AOM	algal organic matter
AP	aromatic protein-like
BCAA	bromochloroacetic acid
BCAN	bromochloroacetonitrile
BDCM	bromodichloromethane
BPNN	backpropagation neural network algorithm
CCD	central composite design
C-DBPs	carbonaceous DBPs
COD	chemical organic demand
CPCC	Canadian Phycological Culture Centre
CV	*Chlorella vulgaris*
DBAA	dibromoacetic acid
DBCM	dibromochloromethane
DBPFP	DBP formation potential
DBPR	Disinfectants and Disinfection By-products Rule
DBPs	disinfection by-products
DCAA	dichloroacetic acid
DCAN	dichloroacetonitrile
DHAA	dihaloacetic acid
DOC	dissolved organic carbon
DOM	dissolved organic matter
DWTPs	drinking water treatment plants
ECD	electron capture detector
EEM-PARAFAC	excitation–emission matrix coupled with parallel factor analysis
EOM	extracellular organic matter

FA	fulvic-like
FTIR	Fourier transform infrared spectrophotometer
GAC	granular activated carbon
GC	gas chromatography
HA	humic acid
HAA	haloacetic acids
HAAFP	haloacetic acids formation potential
HABs	harmful algal blooms
HAN	haloacetonitrile
HOBr	hypobromous acid
HOI	hypoiodous acid
HPI	hydrophilic
HPO	hydrophobic
HPSEC	high performance size exclusion chromatography
IF	irreversible fouling
IOM	intracellular organic matter
IUPAC	International Institute of Pure and Applied Chemistry
LPUV	low pressure ultraviolet
MA	*Microcystis aeruginosa*
MBAA	monobromoacetic acid
MCAA	monochloroacetic acid
MC-LR	microcystin-LR
MF	microfiltration
MIB	2-mentylisoborneol
MLR	multiple linear regression
MPUV	medium pressure ultraviolet
MSE	mean squared error
Msp	*Merismopedia sp.*
MTBE	methyl *tert* butyl ether
MW	molecular weight
N-DBP	nitrogenous DBP

NDIR	non-dispersive infrared adsorption
NDMA	N-nitrosodimethylamine
NF	nanofiltration
N-HPI	neutral hydrophilic fractions
NMR	nuclear magnetic resonance
NOM	natural organic matter
OCD	organic carbon detector
OCRIF	Ontario China Research Initiative Fund
OD	optical density
OLS	ordinary least squares
PAC	powdered activated carbon
PT	*Phaeodactylum tricornutum*
PVC	polyvinyl chloride
PVDF	polyvinylidene difluoride
R^2	correlation coefficient
RC	residual chlorine
RF	reversible fouling
RO	reverse osmosis
RSM	response surface methodology
SMP	soluble microbial product-like materials
SNWD	south to north water diversion
SQ	*Scenedesmus quadricauda*
SRNOM	Suwannee river NOM
SUVA	specific ultraviolet absorbance
TBM	tribromomethane
TC	total chlorine residual
TCAA	trichloroacetic acid
TCM	trichloromethane
TEP	transparent exopolymer particles
TF	total fouling
THAA	trihaloacetic acid

THM	trihalomethanes
THMFP	trihalomethanes formation potential
TMP	transmembrane pressure
TPI	transphilic
UF	ultrafiltration
UFC	uniform formation conditions
USEPA	United States Environment Protection Agency
UTOX	unknown total organic halide
UV_{254}	ultraviolet absorbance at 254 nm
UVD	ultraviolet detector
WHO	World Health Organization
WTPs	water treatment plants
XDLVO	the extended Derjaguin–Landau–Verwey–Overbeek
XPS	X-ray photoelectron spectroscopy

Chapter 1

1 Introduction

1.1 Background and motivations

At present, about 1.1 billion people worldwide lack access to improved water supply, and about 2.4 billion people are under the risk of exposures to waterborne diseases such as typhoid fever, cholera, diarrhea etc. because of the inadequate sanitation facilities [1]. Over 1.8 billion people will experience absolute water scarcity, and 2/3 of the world will be living under water-stressed conditions by 2025 [2]. The dire situation requires effective management of water resources, source water protection and development of cost-effective treatment technologies.

1.2 Algal bloom and related water issues

Surface water such as lakes, reservoirs, rivers, etc., are important drinking water sources worldwide that have experienced varying degrees of eutrophication in recent years [3-5]. Large-scale outbreaks of algal blooms due to eutrophication have caused severe deterioration of water quality in many places [6]. Algal blooms generally occur in the presence of high concentrations of nutrients, especially with warm, sunny, and calm hydraulic conditions. Harmful algal blooms (HABs) are proliferations of microscopic algae that potentially create health hazards to environment by producing toxins (i.e., microcystin) or bioactive compounds that accumulate in shellfish or fish, or through the accumulation of biomass of *microcystis aeruginosa* that subsequently affects the co-existing organisms and alters food chains in negative ways [7]. The outbreak of algal bloom leads to the death of aquatic organism and livestock as well as serious water quality deterioration.

The presence of algae in water affects various water treatment processes such as coagulation, sedimentation, and filtration in drinking water treatment plants. Moreover, toxins produced by some cyanobacteria and decomposed algal matter cause odor problem [8], leading to serious deterioration of water quality. In addition, the outbreak of algal

bloom, or death of algae releases algal organic matter (AOM) in water, which are potential precursors of the disinfection by-products (DBPs) formed due to chlorination and chloramination. Occasionally, chemical pre-oxidation and enhanced coagulation are applied to remove algae. High dosage of pre-oxidants may lead to cell damage causing the release of intracellular substances including odors and toxins. Algal matter in water causes several problems such as: 1) the increase of coagulant dose, 2) filter clogging and shortening of the filter operation cycle, and increasing the difficulty of backwash, 3) increase the chlorine demand and formation of disinfection by-products, 4) produce odorous substances, toxicity and degrade water taste, 5) increase the risk of waterborne organism reproduction in the distribution system [9].

Algal blooms in recent past had caused several serious water supply crises in China. A water quality survey of 26 major lakes and reservoirs of China in 2011 indicated that the percentage of investigated water source with class I – III, IV – V and worse than class V (water quality decreases with increasing class) were 42.3%, 50% and 7.7%, respectively [10]. There are many species of algae present in surface water in China. Based on the analysis of water quality of 11 reservoirs in Fujian Province, it was reported that the dominant algal species were Chlorophyta (40.58%), Cyanophyta (22.91%), Bacillariophyta (21.61%), and Chrysophyta (6.91%) [11]. Lake Taihu, the third largest freshwater lake in China, a large shallow eutrophic lake, is dominated by *Microcystis* spp. In 2007, a severe cyanobacterial bloom took place in the Lake Taihu, the only drinking water supply in the city of Wuxi, China, leaving approximately two million residents without drinking water for over a week [12]. In 2013 and 2014, Wu et al. [13] investigated 51 main rivers in China to determine the effect of nutrient on algae biomass during summer and winter in inflows of Taihu basin, China.

There has been growing concern over the cyanobacterial growth in North America and internationally, for the huge impact that excessive bloom and the carcinogenic algal toxins bring about. Massive algal blooms have been observed via satellite in the lower Great Lakes area since the mid-1990s [12]. In 2011, the western basin of Lake Erie had experienced the largest blooms since 2002 [14]. The bloom, extending over 5,000 km^2, comprised essentially with toxic *Microcystis* led to closure of beaches and drinking water advisories

in both Canada and the US [15]. The 2013 bloom was reported as one of the worst on record as it was the first time a water treatment plant in Ohio was taken off-line because of the concentration of cyanotoxins exceeding the treatment capacity and limit [16]. In 2014, there was a closure of drinking water supplies in the city of Toledo due to cyanobacterial bloom, resulted over 400,000 residents with no access to water for several days. As a consequence, in late 2015, a new Drinking Water Protection act had been brought up which requires the USEPA to develop and submit a plan for evaluating and managing risks related to algal toxins in drinking water provided by public water facilities [17].

1.3 South to north water diversion in China

The City of Beijing and many smaller cities across northern China suffer from persistent water scarcity and deteriorated source water quality. In order to resolve the urgent water shortage, The Chinese central government developed the "South to North Water Diversion (SNWD)" project. The middle route of the SNWD project originates at the Danjiangkou reservoir and aims to deliver 30 million m^3 of water to northern China every day. A portion of the diverted water will be stored in Miyun reservoir and used as a new water source for the City of Beijing. The total length of the main canal, which crosses the North China Plain, is approximately 1277 km, with an annual diversion capacity of 9.5×10^9 m^3 water; about 1.0×10^9 m^3 of diversion alone is allocated to Beijing as the source water for water treatment plants (WTPs) [18]. With the SNWD project completed by 2014, two new water treatment plants have been built by Beijing Waterworks Group with additional water capacity of 1,000 million liters per day. In addition, the existing water treatment plants must be upgraded in order to accommodate the change of water sources.

Realizing the different characteristics of new water sources and the lack of engineering experiences in constructing and operating such large water infrastructure, concerns have been raised in terms of the uncertainty of water quality, as well as impact of the ecological conditions in the storage reservoirs and effectiveness of current water treatment practices. The methods for monitoring and forecasting were intensely studied to ensure water diversion capability [19]. It is noticed that due to runoff and rain water infiltration, water quality is negatively affected in many parts of the channel. In the water body of the SNWD

project, 31 types of phytoplanktons were detected in the winter; 15 detected species were diatom (48.39%), seven were blue algae, six were green algae, and one each of cryptophyta, dinoflagellate, and chrysophyceae was present. Based on extensive monitoring data collected by the researchers and governmental agencies in China, various chemical and microbiological contaminants have been identified in some lakes and reservoirs. Among the most important are pathogenic protozoans (*Giardia* and *Cryptosporidium*), algal toxins, organic micropollutants and disinfection by-products resulting from chlorination. Multi-barrier treatment approaches including physicochemical pre-treatment, activated carbon adsorption, membrane filtration and disinfection (e.g., UV + chlorine) are required to ensure a safe supply of drinking water [20-22]. These technologies are established for removal of natural organic matter derived from detritus plant and animal materials, limited knowledge and engineering experiences exist for algal matter treatment, requiring control laboratory studies to develop optimum treatment options. Generated results can be used for systematic integration and process optimization resulting in great savings in capital, operation, and maintenance costs due to the scale of water treatment infrastructure.

1.4 Research objectives

Based on the aforementioned summary of the technical challenges and as a part of Ontario China Research Initiative Fund (OCRIF) the main objectives of this research are to:

(i) Evaluate and optimize the coagulation-flocculation process for algae and algal organic matter removal from algae-laden water; (ii) investigate the DBP formation potential during chlorination from different algae-laden water to determine the relationship between released AOM and DBP formation; (iii) assess the influence of granular activated carbon (GAC) adsorption for the AOM removal; (iv) investigate the feasibility of GAC adsorption to mitigate microfiltration (MF) membrane fouling due to various dissolved organic matter (DOM) derived from different algae; and (v) assess the influence of chlorine combined with UV dosage on DBP formation from algal matter. The different algae species chosen in this work are based on the water quality found in the SNWD project.

1.5 Thesis structure

This thesis includes 8 chapters and follows the "Integrated-Article Format" as outlined in the UWO thesis regulations. Chapter 1 presents a general introduction of the research problem and specific research objectives. Chapter 2 gives a broad literature review of algae and algal organic matter related issues in the water environment and drinking water treatment plants. Following the literature review, Chapter 3 to Chapter 7 present five projects towards the evaluation of coagulation-flocculation, adsorption, filtration and disinfection processes to remove six species of algae and the derived AOM. The projects details are as follows.

Chapter 3 describes the optimization and modeling of coagulation-flocculation to remove algae and organic matter from surface water by response surface methodology.

Chapter 4 includes work aimed at the investigation of the AOM removal performance by coagulation and disinfection by-product formation potential of AOM derived from four different algal and two cyanobacterial species.

Chapter 5 presents the isotherms, kinetics, and mechanism for the adsorption of dissolved organic matter onto GAC. The influences of GAC dosage, contact time, solution pH and temperature on the removal of DOM were investigated systematically

Chapter 6 evaluates the feasibility of granular activated carbon adsorption of dissolved organic matter in mitigating microfiltration membrane fouling.

Chapter 7 describes the impact of UV irradiation on disinfection by-product formation by post chlorination. The comparison of DBP formation was made between with and without UV irradiation of each DOM.

Finally, a general discussion with conclusions outlining the significance, limitations and possible future directions of this research is presented in Chapter 8.

References

[1]   M.W. Rosegrant, X. Cai, S.A. Cline, World water and food to 2025: dealing with scarcity, Intl Food Policy Res Inst2002.

[2]   S.T. Magwaza, L.S. Magwaza, A.O. Odindo, A. Mditshwa, Hydroponic technology as decentralised system for domestic wastewater treatment and vegetable production in urban agriculture: A review, Science of the Total Environment 698 (2020) 134154.

[3]   X. Jin, Q. Xu, C. Huang, Current status and future tendency of lake eutrophication in China, Science in China Series C: Life Sciences 48 (2005) 948-954.

[4]   Y. Xu, Q. Cai, L. Ye, S. Zhou, X. Han, Spring diatom blooming phases in a representative eutrophic bay of the Three-Gorges Reservoir, China, Journal of Freshwater Ecology 24 (2009) 191-198.

[5]   X. Liu, X. Lu, Y. Chen, The effects of temperature and nutrient ratios on Microcystis blooms in Lake Taihu, China: an 11-year investigation, Harmful Algae 10 (2011) 337-343.

[6]   D.M. Anderson, P.M. Glibert, J.M. Burkholder, Harmful algal blooms and eutrophication: nutrient sources, composition, and consequences, Estuaries 25 (2002) 704-726.

[7]   J. Ramsdell, D. Anderson, P. Glibert, HARRNESS: harmful algal research and response: a national environmental science strategy 2005-2015, Ecological Society of America, Washington, DC (2005).

[8]   D.R.U. Knappe, R.C. Belk, D.S. Birley, S.R. Gandy, N. Rastogi, A.H. Rike, Algae detection and removal strategies for drinking water treatment plants, (2004).

[9]   J. Yang, X. Yu, L. Liu, W. Zhang, P. Guo, Algae community and trophic state of subtropical reservoirs in southeast Fujian, China, Environmental Science and Pollution Research 19 (2012) 1432-1442.

[10]   China Environment Bulletin, Ministry of Environmental Protection of the People's Republic of China (2011).

[11]   J. Yang, X.Q. Yu, L.M. Liu, W.J. Zhang, P.Y. Guo, Algae community and trophic state of subtropical reservoirs in southeast Fujian, China, Environmental Science and Pollution Research 19 (2012) 1432-1442.

[12] R.H. Becker, M.I. Sultan, G.L. Boyer, M.R. Twiss, E. Konopko, Mapping cyanobacterial blooms in the Great Lakes using MODIS, Journal of Great Lakes Research 35 (2009) 447-453.

[13] P. Wu, B. Qin, G. Yu, J. Deng, J. Zhou, Effects of nutrient on algae biomass during summer and winter in inflow rivers of Taihu basin, China, Water Environment Research 88 (2016) 665-672.

[14] T.B. Bridgeman, J.D. Chaffin, J.E. Filbrun, A novel method for tracking western Lake Erie Microcystis blooms, 2002-2011, Journal of Great Lakes Research 39 (2013) 83-89.

[15] A.M. Michalak, E.J. Anderson, D. Beletsky, S. Boland, N.S. Bosch, T.B. Bridgeman, J.D. Chaffin, K. Cho, R. Confesor, I. Daloglu, J.V. Depinto, M.A. Evans, G.L. Fahnenstiel, L. He, J.C. Ho, L. Jenkins, T.H. Johengen, K.C. Kuo, E. Laporte, X. Liu, M.R. McWilliams, M.R. Moore, D.J. Posselt, R.P. Richards, D. Scavia, A.L. Steiner, E. Verhamme, D.M. Wright, M.a. Zagorski, Record-setting algal bloom in Lake Erie caused by agricultural and meteorological trends consistent with expected future conditions., Proceedings of the National Academy of Sciences of the United States of America 110 (2013) 6448-6452.

[16] F.R. Pick, Blooming algae: a Canadian perspective on the rise of toxic cyanobacteria, Canadian Journal of Fisheries and Aquatic Sciences 73 (2016) 1-10.

[17] U.S. EPA, "Algal Toxin Risk Assessment and Management Strategic Plan for Drinking Water", Office of Water, Cincinnati., 2015.

[18] C. Liu, H. Zheng, South-to-north water transfer schemes for China, International Journal of Water Resources Development 18 (2002) 453-471.

[19] Z. Wang, D. Shao, H. Yang, S. Yang, Prediction of water quality in south to north water transfer project of China based on GA-optimized general regression neural network, Water Science & Technology: Water Supply 15 (2015) 150.

[20] Y.R. Hu, T.Y. Zhang, L. Jiang, Y. Luo, S.J. Yao, D. Zhang, K.F. Lin, C.Z. Cui, Occurrence and reduction of antibiotic resistance genes in conventional and advanced drinking water treatment processes, Science of the Total Environment 669 (2019) 777-784.

[21] S.S. Marais, E.J. Ncube, T.A.M. Msagati, B.B. Mamba, T.T.I. Nkambule, Comparison of natural organic matter removal by ultrafiltration, granular activated carbon filtration and full scale conventional water treatment, Journal of environmental chemical engineering 6 (2018) 6282-6289.

[22]   S.Y. Zhang, S. Gitungo, L. Axe, J.E. Dyksen, R.F. Raczko, A pilot plant study using conventional and advanced water treatment processes: Evaluating removal efficiency of indicator compounds representative of pharmaceuticals and personal care products, Water Research 105 (2016) 85-96.

Chapter 2

2 Literature Review

2.1 Introduction

Algae are a group of eukaryotic oxygenic photosynthetic microorganisms with organelles such as chloroplast and nucleus, existing in various habitats including freshwater, marine water, moist rocks and wet soils. Sunlight, carbon dioxide, water and nutrients like nitrogen and phosphorus are required for their sustenance and growth[1]. Algae are classified based on cell wall chemistry, morphology, chlorophyll and accessory pigments. Commonly found algal groups in aqueous systems include green algae, dinoflagellates, diatoms, euglenoids, brown algae, golden-brown algae and red algae [2]. While as the primary producers, algae play the most significant positive role in the aquatic food web, their presence in potable water sources causes many challenges. Of particular interest in this research project are the issues related to the presence of dissolved organic matter originated from algae, which are reviewed in this section.

2.2 Algae and algal organic matter

2.2.1 Algal species in drinking water source

Water quality of lakes and reservoirs varies considerablely in the world; however, algal species present in an aquatic system vary in a small range. For example, diatoms thrive in cold water, whereas green and blue-green algae are dominant in warm, shallow and nutrition-rich water bodies [3].

Commonly found algae and cyanobacteria in drinking water sources (Table 2.1) include blue-green algae (Cyanophyceae), green algae (Chlorophyceae), euglenoids (Euglenophyceae), dinoflagellates (Dinophyceae), cryptomonads (Cryptophyceae), yellow-green algae (Xanthophyceae), golden algae (Chrysophyceae) and diatoms (Bacillariophy) [4].

Table 2.1 List of common algae observed in drinking water sources [3, 4]

Algae species	Characteristics	Growth Condition	Typical genera
Blue-green algae (Cyanobacteria)	Contains phycocyanin, allophycocyanin and chlorophyll *a*, gives blue, blue-green color. Produce cyanotoxins, perform oxygenic photosynthesis	Warm, eutrophic water, above 25 ∘C	*Anabaena, Aphanizomenon, Microcystis and Oscillatoria*
Green algae	Contains chlorophyll *a* and *b*, green color. Some genera are associated with unpleasant taste and odor and filter clogging problems	Summer	*Ankistrodesmus, Chlamydomonas, Chlorella, Scenedesmus*
Euglenoids	Contains chlorophyll *a* and *b*, green color, capable of photosynthesis	Summer	
Dinoflagellates	Capable of photosynthesis and feeding on bacteria, small planktonic algae. Brownish color, some genera are associated with unpleasant taste and odor problems, 90% of them live in ocean.	Summer and fall	*Ceratium, Peridinium*
Cryptomonads	Contains chlorophyll *a* and *c2*, and pigments masking the color of chlorophyll. May appear blue, blue-green, reddish, yellow-brown, olive-green. Light sensitive and prefer nutrient-enriched water.	Temperate climate throughout winter	*Cryptomonas, Chroomonas, Rhodomonas*

Yellow green Algae	Rarely present in large quantities. Contains chlorophyll *a* β-carotene, and many pigments, appears yellow-green, bright green	Low temperature	*Tribonema*
Golden algae	Commonly associated with unpleasant taste and odor.	Summer	*Synura, Dinobryon*
Diatom	Commonly associated with unpleasant taste, odor and filter clogging. Appear in brown color. Siliceous cell wall consists of polymerized silicic acid. Perform oxygenic photosynthesis at water temperature of 5∘C	Spring Oligotrophic waters, optimum temperature at 10-20 ∘C	*Asterionella, Cyclotella, Tabellaria, Fragilaria Melosira*

2.2.2 AOM concentration with cultivation time

Algal organic matter (AOM) is released into water duo to metabolic excretion and autolysis of algal cells [5]. AOM is categorized as extracellular organic matter (EOM) [6], excreted to surrounding environment by living algae cells [7] and intracellular organic matter (IOM), released due to natural rupture of cells in the declining growth phase. IOM can be deliberately released during pre-oxidation [8, 9] (in treatment plants), grinding [10, 11] or a freezing-thawing sequence [6, 12, 13].

Generally, the growth of algae and bacteria is a complex process with numerous catabolic and anabolic reactions resulting in cell division [14]. Therefore, the both extracellular and intracellular organic matter vary significantly with the algal species and can range from a few mg/L to around 100 mg/L [15]. AOM production increased with cultivation time for all the algae investigated [15-17].

A typical microbial growth curve is divided into four main phases, namely lag, exponential, stationary, and decline phase. Since most algal cells present good integrity in the early stage when the cells are young and medium is fresh, AOM in the medium is mainly due to EOM, with only little IOM released at that time [16]. The EOM release rate is much higher in the exponential phase than that in the stationary phase [17, 18]. Dissolved organic matter contents produced from AOM extraction, nevertheless, is much higher in the stationary stage than that in exponential stage [16, 17, 19-21]. The occurrence of cell autolysis and rupture under poor nutrient conditions lead to IOM releasing into culture media with a marked increase in AOM during the decline phase [15, 19]. The IOM content seems to be much higher than that of EOM in many cases, e.g., the dissolved organic carbon (DOC) of IOM from *M. aeruginosa* in the exponential phase is three to six times [22]] higher than the DOC from EOM. Therefore, it is vital to avoid the algal cells breaking and subsequent release of AOM [23], which affects the effectiveness of water treatment processes [20, 24, 25]. With increasing eutrophication of aquatic environments, organic matter (OM) originating from algal cells is a significant fraction (up to 50%) of natural organic matter (NOM) in surface waters [26, 27].

2.2.3 Characterization of algal organic matter

The AOM is comprised of various compounds such as polysaccharides, oligosaccharides, proteins, peptides, amino acids, traceable organic acid; exact composition varies with algae species [15]. There are many investigations presenting approximate chemical compositions of different algae. Becker et al. presented a general overview of major constituents of different algae species [28]. Composition of some commonly found species is provided in Table 2.2.

Table 2.2 Composition of different algal matter (% of dry matter).

Alga	Carbohydrates	Protein	Lipids	References
Anabaena cylindrical	25 – 30	43 - 56	4 - 7	[29]
Aphanizomenon flos-aquae	23	62	3	[28]
Arthrospira maxima	13 – 16	60 - 71	6 - 7	[28]
Aulacoseira granulata f. curvata	36.3	47.9	15.8	[30]
Chlamydomonas rheinhardii	17	48	21	[28]
Chlorella pyrenoidosa	24-28	54-60	11-12	[30, 31]
Chlorella vulgaris	12 – 17	51 - 58	14-24	[28, 32]
Euglena gracilis	14 – 18	39 - 61	14 - 20	[29]
Merismopedia sp.	35-57	29 - 45	NA	[33]
Microcystis aeruginosa	4.0 - 10.1	37 - 52	NA	[34]
Oscillatoria sp.	42 – 52	41 - 48	5 - 8	[29]
Phaedactylum. Tricornutum	11.2-26.1	36.4-53.2	18.0-32.6	[35, 36]
Porphyridium cruentum	40 – 57	28 - 39	9 - 14	[28]
Scenedesmus obliquus	10 – 27	50 - 65	7 - 14	[28, 30]
Scenedesmus quadricauda	3.7-24.8	4.4-9.5	6.9-10.6	[37]
Spirogyra sp.	33 – 64	6 - 20	11 - 21	[28]
Spirulina platensis	8 – 14	46 - 63	4 - 9	[28]
Syenchocaccus sp.	15	63	11	[28]

When comparing to NOM, AOM appears to contain more organic nitrogen and hydrophilic content, less aromatic carbon content and much lower specific ultraviolet absorbance (SUVA < 2 L/mg/m) [26]. It was reported that both EOM and IOM are hydrophilic with low SUVA. Compared to EOM, IOM is richer in proteins or peptides, more hydrophilic with lower SUVA value. Molecular weight fractionation showed that both EOM and IOM of cyanobacteria, green algae and diatom contain large portions of low-MW (below 1 k Da) compounds and some high-MW (over 100 k Da) polysaccharides [20]. IOM has a higher portion of total organic nitrogen, it also contains higher fraction of amino acids but lower fraction of aliphatic amines than EOM [6].

To further characterize the composition of algal organic matter, several methods have been reported in the literature, including UV-visible absorbance, fluorescence/HPLC [6], excitation emission matrix (EEM) [38], Fourier transform infrared spectrophotometry (FTIR) [39], H-NMR spectroscopy [40]. Currently, the most commonly used methods for the physiochemical characterization of AOM are: (1) DOC and dissolved organic nitrogen (DON) analysis, (2) spectrophotometry such as ultraviolet (UV) absorbance and fluorescence-excitation emission matrix (EEM), (3) hydrophobicity analysis by resin fractionation, (4) molecular weight distribution by high performance size exclusion chromatography (HPSEC). The summary of physicochemical properties of AOM is shown in Table 2.3.

Table 2.3 Physicochemical properties of AOM for various algal species at stationary growth phase.

Algal species	AOM	DOC (mg/L)	SUVA (L/mg m)	HPI (%)	EEM* (%)	MW	References
Green algae							
Scenedesmus subspicatus	EOM		1.18	54			[41]
	EOM	14.3					
	IOM	19.7					
Chlorella vulgarus	EOM	27 ± 9.7	0.54	60	SMP, AP, HA, and FA	< 1 kDa:30% >30 kDa: 62%	[16]
Chlorella sp.	EOM		1.34		HA, and FA		[10]
	IOM		0.78		Aromatic, aliphatic protein-like		
Chlorella sp.	IOM				AP:65, SMP:23, HA:3, FA:9	< 1 kDa: 19% >30 kDa: 44%	[42]
Chlamydomonas geitleri	EOM	21	0.6 ± 0.2	73			[20]
	IOM	33	0.3 ± 0.1	89			
Blue-green algae							

Microcystis aeruginosa	EOM		1.22		HA and SMP		[43]
	IOM		0.83		HA and SMP		
	EOM	18.0±2.3	0.48	57	SMP, AP	< 1 kDa:38% >30 kDa: 55%	[16]
	EOM	70	0.7 ± 0.3	69			[20]
	IOM	63	0.4 ± 0.2	87			
	EOM	18.4±0.4	1.01±0.03	51	HA, protein-like	< 1 kDa: 24% >30 kDa: 53%	[44]
	EOM	67.1					[15]
	IOM	32.1					
	EOM	11	0.11	61			[19]
	EOM	11	2.66				[45]
	IOM		1.09				
	IOM				AP:33, SMP:14.5, HA:22.5, FA:30	< 1 kDa: 24% >30 kDa: 35%	[42]
	EOM	27.6	0.88	41	SMP, AP	< 1 kDa:25% >30 kDa: 6%	[46]
	IOM	16.7	1.79	26.8	HA-like, FA-like substances a	< 1 kDa:25% >30 kDa: 61%	

Diatom							
Aulacoseira granulata f. curvata	EOM	3.6±1	0.58	64	SMP, AP	< 1 kDa:30% >30 kDa: 53%	[16]
Fragilaria crotonensis	EOM	48	0.7 ± 0.3	74			[20]
	IOM	53	0.4 ± 0.1	90			

Note: * DOC: dissolved organic matter; SUVA: specific ultraviolet absorbance; HPI: hydrophilic; EEM: Excitation-emission matrix fluorescence, AP: aromatic protein-like; SMP: soluble microbial product-like materials; HA: humic-like; FA: fulvic-like.

2.2.3.1 Total organic carbon (TOC) / dissolved organic carbon (DOC)

Water quality parameters such as TOC and DOC are commonly applied in water treatment processes. The TOC is the sum of the dissolved and particulate organic carbon, of which the inorganic carbon is removed via acidification. The organic carbon in water after filtered through a 0.45 μm membrane filter is defined as DOC [47]. The produced CO_2 is measured by non-dispersive infrared absorption (NDIR) after passing through a scrubber tube to remove interferences [48].

2.2.3.2 UV absorbance

UV-Vis spectroscopy plays an important role in analysing water chemistry [49]. The wavelengths between 220 to 280 nm are used as the most appropriate for NOM analysis, the absorbance at 254 nm is due to the aromatic groups of DOM [47]. SUVA is defined as the UV absorbance of a water sample at 254 nm normalized with the DOC concentration. It is calculated by dividing the UV absorbance (in cm^{-1}) at 254 nm by the DOC of the sample (in mg/L) and then expressed in unit of L/mg-m [50]. It has been widely used to evaluate the aromaticity or hydrophobic/hydrophilicity (HPO/HPI) properties of aqueous solution [47]. Absorbance of aromatic and humic substances at 254 nm is higher than aliphatic and non-humic substances[51]. Therefore, it represents the quantitative fraction of aromatic and humic content of aqueous system [52]. It can be seen in Table 2.3 that both EOM and IOM exhibit lower SUVA values (less than 2 mg/L-m) than that typically obtained for NOM [53], which may be due to more hydrophilic fraction compared to aromatic contents in AOM as compared to NOM [9, 26, 52].

2.2.3.3 Fluorescence spectroscopy

Fluorescence spectroscopy has been gaining attention in the water industry due to its highly sensitive and selective on-line water quality monitoring [54]. The specific excitation and emission wavelengths are the characteristics of molecular conformation, known as fluorophore. These fluorophores can be used to describe the structural compositions of the humic substances [47]. There are two major fluorescence peaks in a typical raw water including humic-like and protein-like fluorescence [55, 56] or three peaks described as humic-like, fulvic-like and tryptophan-like fluorophores [57, 58]. An online fluorescence

probe was applied to detect cyanobacterial and algal cell by 3D-fluorescent excitation–emission matrix (3D-EEMs) spectroscopy. The fluorescence of amino acid-like substance at λex/em = 290/345 nm dominated the AOM derived from *C. vulgaris*, λex/em = 355/475 nm dominated the spectra for *M. aeruginosa*, which has been associated with NOM previously. Significant correlations were also observed between the fluorescence signatures and DOC. This pigment fluorescence method presented an opportunity to obtain detail information on the AOM property and its treatability [59]. A summary of fluorescence property of selected AOM is given in Table 2.3.**.**

2.2.3.4 Resin fractionation

The most common approach for isolation of hydrophobic and hydrophilic organic matter from aqueous solution is using selective adsorption processes by polymeric resins. Non-ionic macroporous sorbents composed of acrylic esters (XAD-8 or DAX-8) or styrene divinylbenzene (XAD-4) are commonly used. DAX-8 and XAD-4 resin were used to adsorb the hydrophobic (HPO) and transphilic (TPI) portion fractions of NOM, respectively, the compounds that remained in the solution were collected as the hydrophilic (HPI) portion [60].

2.2.3.5 High performance size exclusion chromatography (HPSEC)

HPSEC is a powerful technique which has been widely used to characterize both quantitative and qualitative properties and MW variation of DOM in various water sources [61-63]. All types of organic carbon in water sample, including aliphatic and aromatic components can be measured by HPSEC coupled organic carbon (OCD) and/or UV detector (UVD) systems [61, 62, 64]. The measurement of molecular size and molecular weight profile derived from HPSEC combined with peak-fitting prediction can be used to model and predict the treatment unit performance for both NOM and AOM removal after coagulation and filtration [20, 62, 63, 65].

2.3 Drinking water treatment processes

In surface water, colloids and suspended particles, including organic content (humic and fulvic acids) and inorganic minerals, bacteria, virus, and algae, can contribute to turbidity,

color, odors and tastes in the surface waters. As shown in Figure 2.1, the size of particulates that can be removed by coagulation ranges from 0.001 μm to 10 μm. Humic acid, viruses, , bacteria and some species of algae and a portion of their metabolites have particle size within this range [66], and can be removed with colloids.
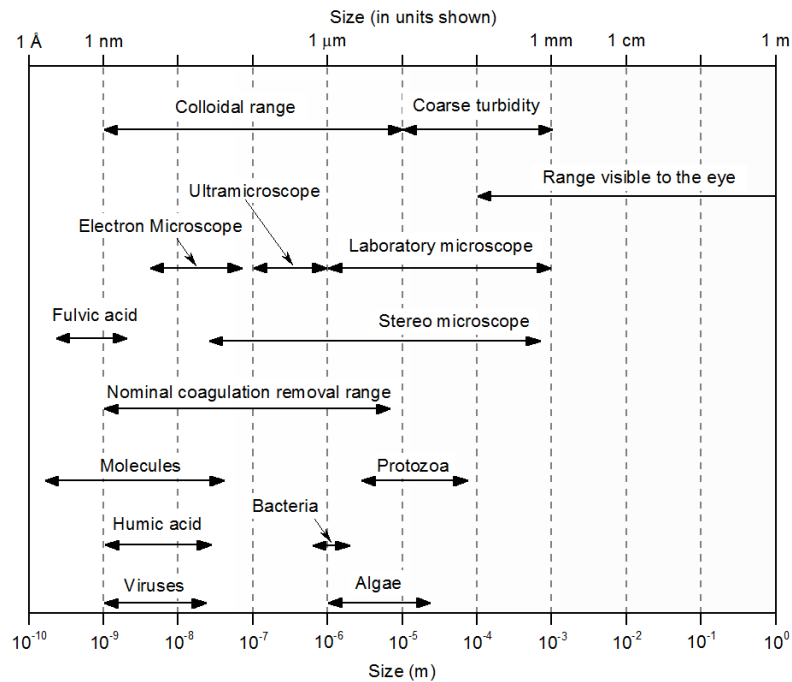
Figure 2.1 Particle size distribution in aqueous system. (Redrawn from [66, 67]).

Modern water treatment processes provide multiple barriers to produce potable water, including pre-oxidation, coagulation/flocculation, sedimentation and disinfection as shown in Figure 2.2.
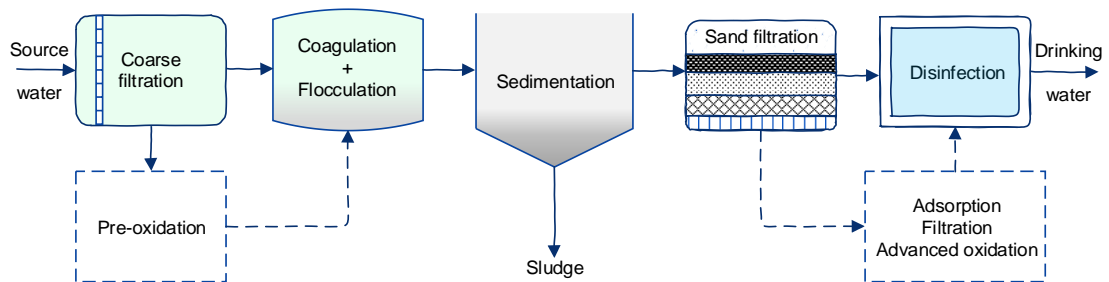
Figure 2.2 Overview of drinking water treatment. (Redrawn from [68])

Raw water is passed through a coarse filter, which removes large floating objects or suspended solids, such as plastic bags, leaves, etc., without removing dissolved organics, algae/cyanobacteria and their metabolites [68].

An optional pre-oxidation by chlorine, ozone or permanganate and ferrate aims to promote the efficiency of downstream treatment, such as coagulation; however, pre-oxidation processes damage the membrane of algae and cyanobacteria causing cell lysis and the release of algal toxins or IOM [69]. The effect of pre-oxidation by permanganate and ozone on coagulation by aluminum sulphate to remove *Microcystis aeruginosa* in aqueous solution was previously investigated by Xie et al., in which the results indicted that pre-oxidation improved cell removal during coagulation; however, more nitrogenous and lower-MW substance were produced because of the destroyed cell walls and membrane after pre-oxidation. The organic matter adsorbed on the cells' surface can be released after pre-oxidation with permanganate even without causing cell lysis [70]. Another study reported that permanganate pre-oxidation resulted with the release of EOM from cells of *Chlorella* sp.. [71]. However, pre-oxidation is becoming necessary in many drinking water facilities that are affected by invasive species such as zebra-mussel and zooplanktons, which affect the downstream equipment like membranes [68].

2.3.1 Coagulation & flocculation

Coagulation and flocculation shown in Figure 2.2 are the essential and most commonly used processes for both particulates and organic matter removal in treatment plants [72]. Full or partial removal of suspended particles and colloids, dissolved organic and/or inorganic matter, microorganisms such as bacteria, algae or viruses, can occur due to coagulation. Coagulants that are used in water treatment include inorganic salts (e.g., iron and aluminum), inorganic polymers (e.g., ploymeric aluminum chloride) and organic polymers with high MW and long chains. The addition of iron or aluminum salts as coagulants is to neutralize negatively charged colloids and suspended particles to prevent electrostatic repulsion between them and facilitating microflocs formation. Thereafter, the formed microflocs tend to agglomerate and form bigger particles, which are removed by sedimentation. In the flocculation process, various types of polyelectrolyte may also be added as coagulant aids or flocculants, which might be beneficial in turbidity removal in

conjunction with metal coagulants, but may have less significance in disinfection by-products (DBP) precursor removal because of the ineffectiveness in removal of dissolved organic matter (DOC) [73].

2.3.1.1 Factors affecting coagulation and flocculation

There are various parameters that affect the coagulation performance, including coagulant type, dose, water properties and coagulation condition, a summary of these influences are tabulated in Table 2.4.

Table 2.4 Factors affecting coagulation and flocculation [74, 75].

Coagulant applications	Raw water properties	Coagulation condition
Coagulants type (metallic salts and polymers) Coagulants dosage Coagulants aids	pH, alkalinity Turbidity, Ionic intensity Total dissolved carbon Organic matter composition Temperature	Rapid Mixing speed and time Slow Mixing speed and time Settling time

The two widely used coagulants are metal salts and polymers, and the most common metallic coagulants in drinking water treatment are aluminum sulfate and ferric chloride [76]. The selection of a specific coagulant depends on various factors including the required removal, cost, availability, storage, application and safety. The most important factor influencing the effectiveness of metal-based coagulants is pH [77]. Theoretically, at a optimum pH, the solubility of hydrolysed alum product is minimal and major faction of coagulant is converted to solid floc particles [78]. Negatively charged aluminum species are generated when pH is increased above the optimal value, and the positively-charged dissolved aluminum species are formed at a lower pH [79]. For the pH value of less than 3 or higher than 11, the destabilization potential is significantly decreased, the formed micro-flocs will not be able to aggregate into large flocs resulting in poor coagulation efficiency [80].

Generally, the dosage of coagulant applied depends on the content of suspended solids or content of water. However, the maximum treatment efficiency exists at an optimum dosage,

and decreases once coagulant is overdosed [81]. The reversely charged colloidal particles caused by the coagulant overdose results in colloids re-stabilization, consequently, decreasing the coagulation efficiency [82].

To meet the requirements of Disinfectants and Disinfection By-products Rule (DBPR), an enhanced coagulation was proposed by United States Environment Protection Agency (USEPA) [83] to minimize DBP formation by greater removal of NOM by changing coagulant type, dosage and pH to improve the total organic matter removal. The commonly applied alum dosage ranges from 5-150 mg/L for enhanced coagulation [84, 85]. Due to the health concern about aluminum, ferric chloride is used as an alternative coagulant, especially for water bodies with low turbidity, high dissolved matter and a moderate pH [86]. Polyelectrolytes can be used as an effective coagulation aids with relatively low dosage ranging from 1.5-10 mg/L for better coagulation.

2.3.1.2 Theory of coagulation

Coagulants are used to destabilize the charged colloids and suspended particles in aqueous solution. Based on the classical theory, four mechanisms of coagulation include the double layer compression, charge neutralization, adsorption and inter-particle bridging and enmeshment in precipitate, as shown in Figure 2.3 [86, 87].
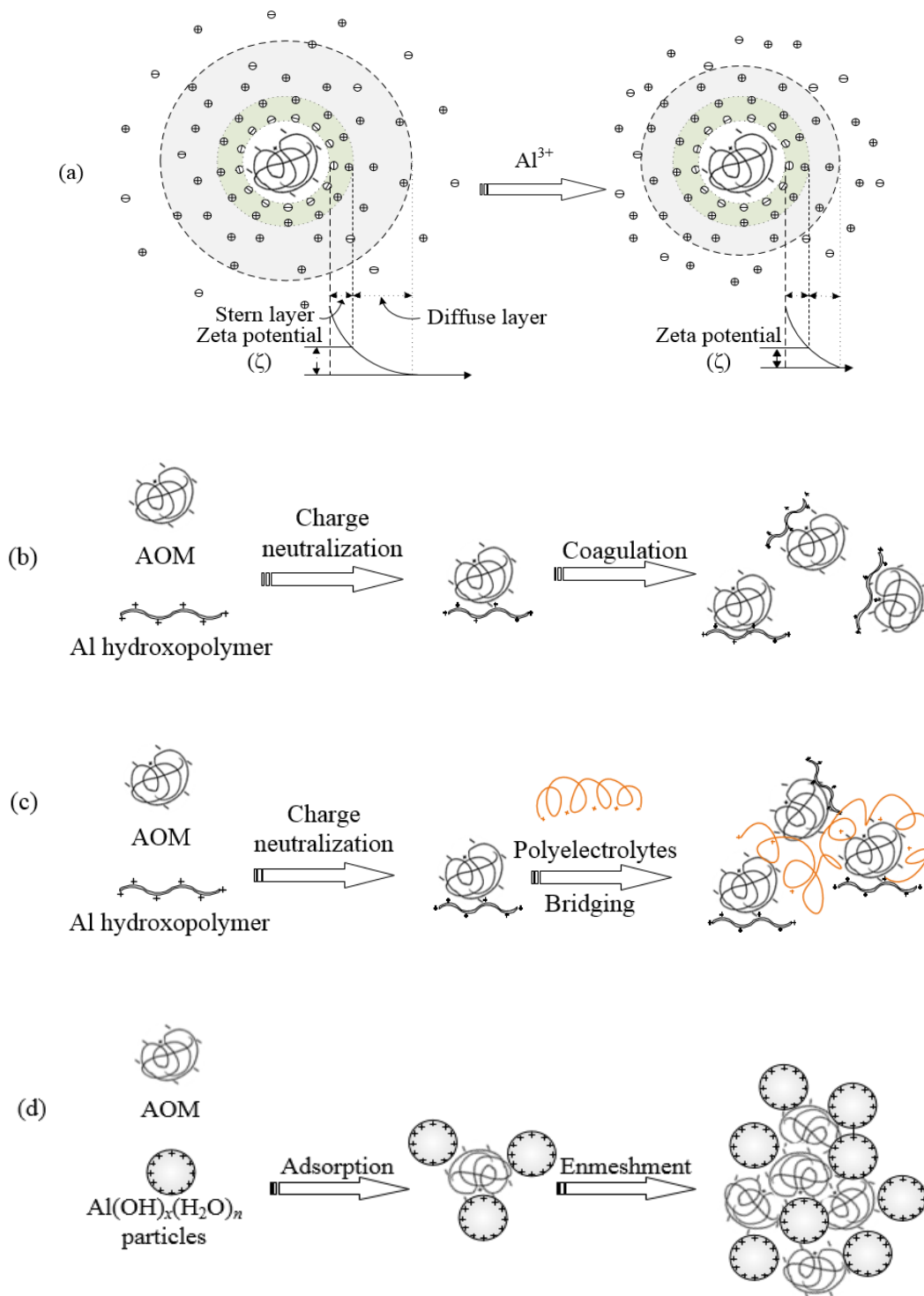
Figure 2.3 Mechanisms of coagulation-flocculation: (a) Double layer compression, (b) Charge neutralization, (c) Interparticle bridging, (d) Sweep coagulation. (Redrawn from [26, 88])

The negatively charged colloid particles attract ions of opposite charge to form a dense layer adjacent to the particle and is known as stern layer. The diffuse layer is formed as the result of dynamic equilibrium between excess positive ion attracted by the negatively charged core colloids and repulsion force from stern layer. These two layers in the interfacial region of colloid particles are known as the double layer[88]. Once a coagulant (positively charged) is added into a colloidal system, the double layer will be compressed because of electrostatic attraction between the ions and colloids. Even though double layer compression does not dominate the colloid destabilization process in water treatment, it is a critical destabilization mechanism in natural aquatic systems, such as the formation of delta in estuaries [86].

In the charge neutralization mechanism, the destabilization of colloidal particles occurs by neutralization through electrostatic interaction of the coagulant with counter-ions. Inter-particle bridging destabilization occurs when polyelectrolytes with highly active surface and linear or branched structure are used as the coagulation aid to facilitate the aggregation of micro-floc during flocculation process. The polymer adsorbs on colloidal particle and then extends the linear or branched chain to attach other particles, consequently, forming an inter-particle bridge. The formation of hydroxide precipitate occurs at higher coagulation dosages. The insoluble, amorphous precipitates entrap or enmesh colloids and the method is known as sweep coagulation or enmeshment[88].

2.3.1.3 AOM removal by coagulation

Aluminum salts, especially alum, are the most widespread used coagulants to remove turbidity, colour caused by NOM in all surface water and many groundwater [89]. With the negatively charged surface, algal cells are well removed (> 95%) during coagulation and flocculation processes in drinking water treatment [90-92]. The AOM, including both EOM and IOM originated from algal cell, is a significant fraction of NOM in algae-laden water body. AOM is not removed well by coagulation [5] and cause serious impacts on water treatment performance, including higher coagulant demand, fouling of the membrane, clogging of the adsorption sites of activated carbon, and formation of DBPs [5, 26, 43, 67, 93]. In contrast with algal cell removal, the investigation on AOM removal by coagulation is limited; literature available on AOM removal is summarized in Table 2.5.

The performance of aluminum and ferric coagulants for AOM-laden water was found to be comparable, although optimum pH range of coagulation by aluminum was higher than that of ferric coagulant [94]. The removal performance for both algal cell and AOM was mainly dependent on the pH and coagulant dosage, because of the presence of excessive negative charge on AOM [26]. The electrostatic interactions on coagulation are determined by the ratio of positive and negative charge in aqueous solution. A strong stoichiometric relationship between algal cell surface area and alum dosage was indicated and higher alum dosage was required as a result of coexistence of EOM and cells [95]. The removal of dissolved organic matter (DOM) in algae-laden surface water was investigated using poly-aluminum chloride as the coagulant. The aromatic-like substances with small portion of NOM was removed with algae due to coagulation based on the analysis of DOC, SUVA, and fluorescence excitation-emission (EEM) matrix spectroscopy, while the fulvic-like and tryptophon-like substances were not removed [96].

Guo et al. [57] reported a removal of 38.7% and 51.4% in terms of DOC and UV_{254}, respectively from the IOM of *Microcystic aeruginosa* obtained by enhanced coagulation at an alum dose of 5 mg/L as Al. The maximum removal of 42.3% and 61.5% was achieved at pH 6.5 for DOC and UV_{254}, respectively. A comparison with DOC, the higher UV_{254} removal indicated the superiority of alum to remove the aromatic substances present in IOM of *Microcystic aeruginosa*. Another research was carried out to investigate the coagulation performance to remove IOM derived from *Microcystis aeruginosa* spiked in raw water [97]. The results indicated that the removal efficiency was dependent on pH, type of coagulant and its dosage. The IOM removal efficiency was 46% for ferric sulphate and 41% for aluminum sulphate. The polysaccharides and proteins in IOM were mainly removed with a higher efficiency than other components.

EOM can form complexes with coagulants significantly increases the coagulants demand and reduces the coagulation efficiency [98-100], however, it was also reported that algal EOM can improve the treatment efficiency acting as a flocculation aid [101]. Another contradictory results was also reported that hydrophobic (HPO) fractions of IOM derived from *Microcystis aeruginosa* were more than that of EOM [34], while algal IOM was also reported to be mostly hydrophilic resultant with low removal performance during

coagulation [23]. Those contradictory results indicate that the effects of AOM on coagulation are algae species dependence [102] and also vary with algal growth stage and the distribution of HPI and HPO fraction of AOM [103].

Table 2.5 Studies on the removal of AOM by coagulation.

Water source and characteristics	Main reaction condition	Key results	References
Synthetic solutions including bovine serum albumin, peptides/proteins of *M. aeruginosa* and peat humic substance DOC: 8-13 mg/L	$Al_2(SO_4)_3$ dosage of 0.2-10 mg/L, Reaction time: around 15 min mixing shear rates: 50-200 s^{-1}.	▪ Up to 83% and 65% removals of DOC and HS was achieved under the optimum coagulant dose of 1.6 mg Al /L, and pH 5.5-6.2. ▪ The algal peptides/proteins positively impacted the overall removal efficiency of humic substance reducing the coagulant for Al-based coagulation process.	[104]
Algal turbid water with the turbidity of 20 NTU, pH: 8.7 Zeta potential: -19.7 mV	$FeCl_3$ dosage of 0.03-0.2 mmol/L, pH: 5-9 Stirring rate: 40-200 rpm, 40 min;	▪ Around 97% of turbidity removal efficiency was obtained under the optimal $FeCl_3$ dosage of 15 mg/L.	[105]
IOM solution of *M. aeruginosa* prepared with suspended Kaolin with DOC of 8.4 mg/L, UV_{254} of 0.09 cm-1, pH with	$Al_2(SO_4)_3$ dosage of 0.2-10 mg/L, 200 rpm for 2 min then by 40 rpm for 15 min followed by 30 min sedimentation	▪ The removal efficiency of IOM increased with higher alum doses, the maximum removal was 99.7%, 51.4%, and 38.7% for OD680, UV_{254}, DOC, respectively, by alum at 5 mg/L. The maximum removal of 61.5% for UV_{254}, 42.3% for DOC was achieved at pH 6.5.	[57]

7.0 and turbidity of 30 NTU.		▪ The higher UV_{254} removal than that of DOC implied the superiority of alum to remove the aromatic IOM species. ▪ The complexes formed by Al ions and proteins improved the removal efficiency. High MW fraction of IOM presented higher removal in terms of DOC and UV_{254}, and the sweep flocculation was the major mechanism	
EOM solution of *M. aeruginosa* harvested at the stationary growth phase, DOC = 3.2 mg/L	Polymeric aluminum with dosage of 0.4 mg Al / mg DOC, with / without MnO_2-aided	▪ high-MW fraction, and hydrophobic fraction of EOM was preferentially removed. ▪ Addition of permanganate improved EOM removal due to bridging of small flocs formed by metal bonding functional groups of EOM	[106]
AOM-surface water mixed solution (DOC ratio of 1:1) with DOC of 3 mg/L	Titanium sulfate with dosage 5-35 mg/L	▪ Maximum UV_{254} removal (60 %) was obtained for IOM of *M. aeruginosa*, which is higher than that of EOM (30%) at dosage of 15 mg/L ▪ The high-MW portion of IOM improved the coagulation by bridging flocculants	[72]

2.3.2 Granular activated carbon adsorption

Adsorption is a commonly used treatment process that can remove trace impurities, such as pesticide, cyanotoxins, etc. from water. Owing to the high porosity and large specific surface area (Table 2.6), activated carbon provides abundant adsorption sites for removing impurities [107]. Granular activated carbon (GAC) adsorption is one of the most widely employed technologies for the removal of DOM, turbidity, micropollutants, and DBP [108-110]. With proper design and maintenance, a GAC adsorption unit can be operated cost-effectively for several years to remove trace organic pollutants and NOM from industrial and municipal waters [111, 112]. Adsorption of DOM onto activated carbon is influenced by a number of physicochemical properties of both adsorbent and adsorbate, as well as solution properties such as initial DOM concentration, ionic strength, pH, molecular size distribution of DOM, and water temperature [113, 114]. A summary of influencing factors is presented below.

2.3.2.1 Effect of types of GAC

The characteristics of GAC such as particle size, surface area, pore volume and pore distribution depends on the material used and manufacturing process. A comparison of the properties of active carbon derived from different raw materials is presented in (Table 2.6). An investigation was performed to evaluate the adsorption performance to remove β-ionone by four types of commercial GAC, including cocoanut activated carbon (YK), nutshell activated carbon (GK) and two kinds of coal-based activated carbon (MZ-A and MZ-B)[111]. The equilibrium adsorption capacity of 19.43 mg/g by YK carbon, followed by GK carbon, MZ-A carbon and MZ-B carbon with the minimal capacity of 16.58 mg/g was obtained.

Table 2.6 Characteristics of activated carbon from various material source.

Raw materials	Density kg/L	Surface area m^2/g	Application	References
Coconut shells	1.4	700-2500	Vapor phase adsorption	[115-117]
Anthracite	1.5-1.8	500-2300	water purification, chemical recovery	[118, 119]
Macadamia nutshell		1718		[120]
Bitumen	1.25-1.50	400-1300	Wastewater treatment	[121]
Apricot stones		1190	Water purification	[122]
Almond shells		1005-1315	Water purification	[123]
Corn cob		400-1600	Wastewater treatment	[124, 125]
Wood	0.4-0.8	240-500	Aqueous phase adsorption	[117, 126]
Lignite	1.00-1.35	280-400	Wastewater treatment, gas vapor adsorption	[127]

The GAC is categorized based on pore size: micropores (< 2 nm), mesopores (2-50 nm) and macropores (>50 nm), according to the International Institute of Pure and Applied Chemistry (IUPAC) [128]. A study indicated that the presence of micropores is crucial for the removal of geosmin and 2-mentylisoborneol (MIB), which had size in the range of 0.55-6.3 nm [129]. Because of the predominant irregular-shaped micropores and some closed pore structures of commercial activated carbon, the adsorption of many antibiotics, such as tylosin and tetracycline and bulky molecules (i.e., alkylphenolic surfactants) involve size-exclusion effect [130]. A high adsorption potential is expected when the size of target molecules is in the range of pores of GAC [111].

2.3.2.2 Effect of AOM

The physiochemical properties of a DOM mixture can significantly alter the effectiveness of GAC adsorption. The characteristics of solute include aromaticity, hydrophobicity, polarizability, water solubility, size and charge [131-134]. Most investigations to date have

evaluated the removal of NOM [135-137] or specific micropollutants in the presence of NOM by activated carbon adsorption [110, 138, 139]. Only a few studies have emphasized on the adsorption of AOM as a major component of NOM in source water instead of pure AOM only [26, 140, 141]. A previous study of GAC adsorption for the removal of two algal odorants in water demonstrated that pH had a different impact on GAC adsorption. An Ideal Solution Adsorption model was developed to predict adsorption behavior. The low MW fraction in NOM could significantly inhibit algal odorants removal by GAC adsorption [142]. The comparison experiments were carried out to evaluate the competitive adsorption of two herbicides in the presence of peptides fraction derived from *Microcystis aeruginosa* onto two type of GAC. The study presented that low MW (700 -1700 Da) of AOM peptides played an essential role of adsorption competition between herbicides and peptides [143].The equilibrium and kinetic adsorption experiments were performed to investigate the effects of solution pH and ionic strengths on the removal efficiency of peptides derived from *Microcystis aeruginosa* by two types of GAC. The investigation demonstrated that the removal performance can be improved by the increase of ionic strength and the decrease of solution pH; the hydrogen bonds and electrostatic interaction between the peptides and GAC were the predominant adsorption mechanisms [144]. Another previous study investigated the GAC adsorption of three low-MW amino acids derived from cyanobacteria with the variation of initial concentration of amino acid, ionic strength and solution pH. The results indicated that removal efficiencies decreased with the increase of solution ion strength. Electrostatic interaction, hydrogen bonds and hydrophobic interaction dominated the GAC adsorption process for the removal of individual amino acid under specific solution pH and type of GAC applied [140]. The initial concentration of absorbate is regarded as an important driving force to facilitate the adsorption process by overcoming the mass transfer resistance between the solid and aqueous phases [145]. The adsorption of β-ionone onto GAC increased with the increase of initial concentration from 0.3 to 2.0 mg/L, which demonstrated that, with more contact chance between active adsorption sites of GAC and adsorbate of higher concentration, the adsorption sites occupied by β-ionone increased with the increase of initial concentration and accounted for the increase in adsorption [111].

2.3.2.3 Effect of solution properties

Generally, with a decrease in solution pH, the negatively charged functional groups on both GAC and adsorbate become protonated, decreasing the electrostatic repulsion force between GAC and adsorbate, consequently resulting in an increase of the adsorption efficiency [146]. A significant effect of pH on adsorption of peptides from IOM of *M. aeruginosa* onto GAC was observed in these studies [143, 144]. The formation of hydrogen bonds between protonated surface of GAC and protonated functional groups of peptides may result in high adsorption capacity at pH 5. The adsorption kinetics of clofibric acid onto activated carbon indicated that pH was a crucial parameter which strongly influenced the adsorption efficiency; highest adsorption efficiency was achieved at pH 2.0 and decreased with increase of pH [147]. A sigmoidal adsorption isotherm was fitted to the Dubinin-Astakhov equation and the solvation energy of the dissociated and undissociated forms of clofibric acid could explain the dependence of solution pH and isotherm adsorption shape. The adsorption of triclosan on activated carbon with variation of solution pH and ionic strength was conducted [148]. Solution pH had significant impact on the solute ionization degree and surface charge of sorbent, and resulted in high triclosan sorption in the acidic pH range. The increased adsorption capacity was also found with an increase in the ionic strength of the solution. Batch and column adsorption experiments with GAC were employed to remove dissolved organic matter (DOM) with variation of water temperature (5, 20, and 35°C) [149]. A positive effect of temperature on DOM adsorption was observed with batch and column experiments for various surface and synthesized water. The enhanced adsorption of DOM with increasing temperature is due to the entropic effect. The mean size of DOM molecules decreased with the increase of temperature [149] leading to an increased accessible GAC surface area, molecular self-association also was changed with temperature [150]. Inhibition of adsorption of water molecules onto carbon surface at high temperature also occurred due to increase in hydrophobic adsorption sites.

Previous studies on AOM adsorption on activated carbon had focused primarily on the removal of cyanotoxins, taste and odor compounds. However, GAC adsorption could also be an effective option for the removal of the low-MW AOM fraction, which is poorly

removed by coagulation. Therefore, systematic investigation of adsorption effectiveness of AOM from various types of algae is still high required.

2.3.3 Membrane filtration

Membrane filtration processes can efficiently remove cyanobacteria and their toxins [68]. Membranes are commonly applied in filtration processes and made of polymeric, ceramic, organo-mineral, or metals with a variety of pore sizes that physically strain particles, pathogens etc., from the influent water [151]. Porous membranes are categorized according to the nominal pore size and working pressure. Low-pressure membranes (microfiltration (0.1-10 μm) and ultrafiltration(0.01-0.1 μm)) have larger pore sizes and are applied for filtration, while high-pressure membranes (nanofiltration (around 1 nm) and reverse osmosis (0.1 nm)) have much smaller pore sizes and are employed to modify the chemical characteristics of water. The characteristics of common membrane filtration processes are summarized in Table 2.7.

Table 2.7 Characteristics of common membrane filtration processes [3, 151, 152].

Filtration Type	Pore size (µm)	Transmembrane pressure, TMP (MPa)	Mechanism	Target Contaminants
Microfiltration (MF)	0.1-1.0	0.03-0.3	Sieving	Particulate substance such as algae, Giardia, Crypto, bacteria, and clays
Ultrafiltration (UF)	0.005-0.1	0.05-0.5	Sieving	All substances removed by MF with humic acids and some viruses
Nanofiltration (NF)	0.001-0.005	0.5-1.5	Diffusion + exclusion	All substances removed by MF and UF plus dissolved metals and salts
Reverse osmosis (RO)	< 0.001	5-8	Diffusion + exclusion	All substances removed by MF, UF and NF plus smaller dissolved metals and salts

The nominal pore size determines what contaminants can be removed from the low-pressure membranes process. Microfiltration is commonly applied as a purification process to remove particulate material due to increasing water recycle demand and stringent discharge standards [153]. Ultrafiltration membranes can detain a fraction of the smaller particles that could pass microfiltration membranes. These membranes can replace the conventional treatment processes or can be used as an advanced treatment downstream of any combination of conventional treatment processes.

However, fouling of membranes due to the presence of organic matter in source water is a major challenge significantly affecting the efficiency of membrane filtration in water treatment. A previous study indicated that AOM can cause greater flux decline for both polymeric and ceramic membranes than that from humic acid and fulvic acid [154]. To mitigate membrane fouling, a number of factors influencing membrane filtration and fouling mitigation have been investigated, including membrane characteristics, solution properties and operating conditions were shown in Table 2.8.

Table 2.8 Factors affecting membrane fouling and fouling mitigation strategies [155].

Membrane characteristics	Solution properties	Operating conditions	Mitigation strategies
Membrane material, pore size and distribution, hydrophilicity, affinity, surface charge, zeta potential, surface roughness, membrane integrity.	Concentration, particle size, components and properties, pH, ion intensity	Configuration temperature, transmembrane pressure, cross-flow velocity	Feed pretreatment, mechanical scouring, chemical backwashing/cleaning, ultrasonic cleaning, membrane surface modification

2.3.3.1 Process parameters for membrane filtration and fouling mechanism

To elucidate fouling process, the classic membrane fouling models were developed based on blocking mechanism, including complete blocking, standard blocking, intermediate

blocking and cake filtration [156-160]. A schematic representation of blocking fouling is shown in Figure 2.4.

(a) Complete block   (b) Standard blocking

(c) Intermediate blocking   (d) Cake filtration
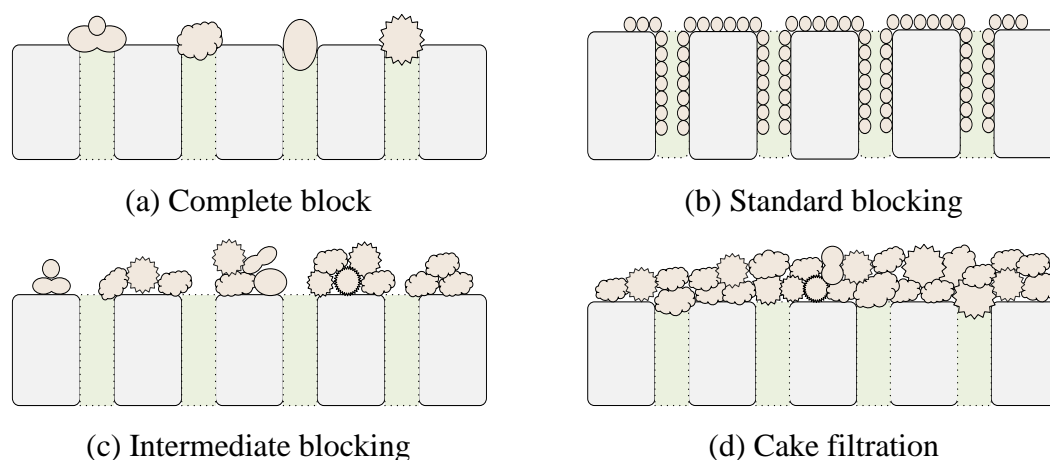
Figure 2.4 Schematic representation of the different fouling mechanisms of membrane filtration. (Redrawn from [159])

The instantaneous flux of filtration was obtained by numerically differentiating the cumulative volume filtered (*V*) per unit membrane area after exponential smoothing and analyzing it using block laws listed in Table 2.9.

Table 2.9 Classic membrane fouling models [156, 157].

Model	Equation	Description
Cake filtration	$\dfrac{1}{J} = \dfrac{1}{J_0} + k_c V$	Particles deposit on the membrane surface and cake layer forms, which helps in filtering.
Intermediate blocking	$J = J_0 \exp\left(-k_i V\right)$	Particles settle on each other and may block some membrane pores.
Standard blocking	$J = J_0 \left(1 - \dfrac{k_s}{2} V\right)^2$	Particles deposit on the internal pore walls decreasing the pore diameter.
Complete blocking	$J = J_0 - k_b V$	Particles block pores when reaching the membrane surfaces without superposition of particles.

where J_0 is the initial permeate flux, V is the accumulative volume and k_c, k_i, k_s, k_b are fitting parameters describing cake filtration, intermediate blocking, standard blocking, and complete blocking, respectively. To determine the dominant fouling mechanisms for each DOM on MF membrane, the experimental data are fitted to the model equations with R-squared (R^2) values demonstrating the goodness of modeling fit [106].

2.3.3.2 Impact of AOM on membrane filtration

Earlier, studies have identified AOM, instead of algal cells and debris, as the main membranes foulants for the treatment of algae-laden water [161-164]. In a comparison study of flux decline caused by algae cells (*S. quadricauda*) in deionized water, algal suspension and the derived AOM; although around 15% flux decline was observed from AOM less than the 70% decline caused by algae cells, the AOM which contained polysaccharides, proteins and lipids caused more irreversible fouling during UF filtration [165]. Membrane fouling involving AOM includes both irreversible fouling (i.e., adsorption of foulants inside membrane pore) and reversible fouling (e.g., membrane surface deposition), strongly influenced by the AOM characteristics such as charge, hydrophobicity and molecular weight distribution [161, 166]. Compared to algal cells, AOM caused a less total decline of flux in the initial stage, but a much more rapid flux decline during ultrafiltration of an AOM solution [161, 167]. It was indicated that irreversible plugging and pore narrowing was formed by low-MW AOM, and cake filtration occurred when a majority of biopolymers deposited on surface of membrane through size exclusion. Thereafter, the formed cake layer can serve as a dynamic barrier to adsorb/screen more low-MW substances and biopolymers for AOM [168, 169]. It was verified that the formed cake layer by AOM cannot be compacted because of a relatively low compressibility [167]. The cake formation caused by algal AOM has been considered to be more responsible than pore narrowing and plugging for UF fouling process [167, 170].

The hydrophilicity of AOM affects the fouling reversibility of ultrafiltration membrane for algae harvesting [161]. It was reported that the hydrophilic non-acid (HPI-NA) fraction of AOM derived from *C. zofingiensis* presented higher irreversible and total resistance than that from hydrophilic acid (HPI-A) and hydrophobic acid (HPO-A). The formation of

hydrogen bonding between hydrophilic polyvinyl chloride (PVC) membrane and carbohydrates in HPI-NA fraction can account for the compact cake layer formation. Similarly, much greater irreversible and total fouling were caused by IOM with more hydrophilic and large molecules than that by EOM extracted from *M. aeruginosa*. The adhesion energy of EOM-membrane and EOM-foulants were lower than the IOM-IOM cohesion energy and IOM-membrane adhesion energy. Cake formation was the major fouling mechanism for UF of IOM; however, both pore plugging and cake formation were responsible for EOM UF fouling [170].

The impact of the hydrophilic fraction on AOM fouling can be mitigated by selection of a hydrophobic membrane [23]. The polysaccharides in AOM are the major foulants for hydrophilic membrane, but account for only a fraction of irreversible fouling for hydrophobic polyethersulfone (PES) membrane. On the contrary, the hydrophobic fraction of AOM was considered as the primary contributor for irreversible fouling because of high protein content and strong interaction with hydrophobic PES membrane. The membrane pores were blocked by small MW factions, even though they dominated the total fouling by cake formation because of the strong affinity to water [171]. It was also confirmed that hydrophobic fraction of EOM derived from *M. aeruginosa* was mainly the tryptophan-like substance, which had a strong tendency to attach onto hydrophobic PES membrane based on the excitation–emission matrix coupled with parallel factor analysis (EEM-PARAFAC) [172]. A similar trend was also observed for MF fouling [161, 167]. Due to pore clogging and cake formation, the permeate flux can be reduced to 20% after 90 min on a commercial tubular ceramic MF membrane. The large MW (>20 kDa) of AOM released from *M. aeruginosa* was detained and formed cake layer as a dynamic barrier to remove smaller MW (< 500 Da) substances. The relatively high MW (~1000 Da) with 32% of total DOC presented the main irreversible fouling by being trapped in membrane pores, thus the cake/gel filtration dominated the AOM fouling in MF process. Meanwhile, hydrophobic substances in the outer layer can be removed easily by hydraulic backwashing due to the weak affinity between the foulants and hydrophilic membrane [166].

The electrostatic interaction between membrane surface and AOM can also affect membrane fouling and AOM removal [23]. An investigation concluded that AOM of

Chlorella sp. with lower negative charge demonstrated a more tendency to be attached to negatively charged MF membrane resulted a higher rejection of small to medium-MW organics and higher irreversible fouling resistance than that due to AOM of *M. aeruginosa* [173]. The interaction energy between membrane and AOM from different algal species was investigated earlier [174]. The results indicated that the adhesion energy between hydrophilic MF membrane and neutral hydrophilic (N-HPI) fraction of AOM was higher than other AOM fractions based on the extended Derjaguin-Landau-Verwey-Overbeek (XDLVO) theory.

As the dominant fraction of AOM matrix on a membrane surface, carbohydrates have a high diversity of structures and components, with complex biochemical properties [175, 176]. In addition, the properties of carbohydrates can alter dramatically with cultivation time, medium and environmental conditions [168, 177-179]. As a special faction of AOM, transparent exopolymer particles (TEP), which are released by algal cells via metabolic activity, cell lysis or breakage [180], have attracted increasing concern in the studies on membrane fouling [23]. TEP in carbohydrates can facilitate carbohydrates aggregation via intermolecular adhesion and subsequently alter the cake layer structure [168, 179]. In addition, the growth of biofilms on membrane surface can also be promoted by TEP [181-184] and then change the foulant matrix [168]. It is noted that special attention still is needed to pay on the characteristic of AOM and the structural properties of AOM fouling matrix. Although a much stronger correlation was suggested between fouling potential of organic matter and their characteristics than that with the organic concentration [185, 186], the AOM concentration in feed solution should be of concern due to its direct correlation with the flux decline of AOM fouling in MF/UF membrane processes [162, 169, 183, 187].

2.3.3.3 Mitigation strategies for membrane fouling

The impact of membrane fouling by AOM solution can be mitigated by several strategies, mainly including pretreatment of the feedwater, optimization of filtration conditions and modification of membrane cleaning procedures [23, 26]. Pretreatments of AOM solution prior to membrane filtration include coagulation-flocculation [106, 188-190], adsorption [168, 191-194], advanced oxidation [195] or their combination [196]. For instance, when coagulation was applied at optimal coagulation dose (5 mg Al^{3+}/L and 10 mg Fe^{3+}/L) as the

pretreatment to remove AOM released from *M. aeruginosa*, over 90% reversible and 65 % irreversible fouling reduction can be achieved, significantly ameliorating the fouling of a ceramic MF membrane. The effective removal of high MW biopolymer (> 20 kDa) by coagulation was primarily responsible for the reduction of AOM fouling during subsequent filtration [189]. A significant alleviation of flux decline caused by EOM of *M. aeruginosa* was achieved after polymeric aluminum (0.4 mg Al mg^{-1} DOC) coagulation removed up to 18% of organic substance, mainly high MW (>100 kDa) components of EOM. Due to oxidation and adsorption by manganese oxide, the potassium permanganate-aided Al coagulation presented greater EOM removal than Al coagulation alone, and resulted in better membrane permeability and fouling reversibility [106]. It was presented that compressibility of the AOM cake/gel layer and fouling potential can be significantly decreased using coagulant doses > 1 mg Fe/L. Precipitated iron hydroxide can effectively adsorb, aggregate biopolymer of AOM, mitigating UF membrane fouling [190] .

To avoid the potential damage to algal cells by chemical pretreatment, physical pretreatments such as activated carbon adsorption or adsorption combined with other processes were investigated to remove AOM prior to filtration [168, 191-193]. A previous investigation of fouling behavior by various AOMs found that membrane fouling was heavily affected by algal species and characteristics of AOM [197]. Two powdered activated carbon (PAC) dosing approaches including addition of PAC into the bulk feed solution and pre-depositing PAC onto the surface of membrane were applied to evaluate the reduction of membrane fouling by EOM of *M. aeruginosa* [198]. The pre-mixed PAC adsorption mitigated membrane fouling attributed to the formation of a porous fouling layer favoring the rejection of EOM and subsequent physical cleaning. Another investigation demonstrated that the addition of PAC significantly alleviated the transmembrane pressure and improved the AOM removal in terms of DOC ($10.9\pm1.7\%$), UV$_{254}$ ($27.1\pm1.7\%$) and microcystins ($40.8 \pm 4.2\%$). Only minor influence was observed on the rejection of hydrophilic high MW components such as carbohydrates and proteins in AOM [168, 199]. GAC adsorption has been regarded as one of cost-effective and environmentally-friendly technology for drinking water treatment processes for removal of lower MW and hydrophilic fraction of NOM, it has also been applied as a pre-treatment process for membrane filtration to mitigate membrane fouling and improve the permeate quality in

membrane-based treatment systems [199-201]. A hybrid membrane-activated carbon process was applied for the pre-treatment of produced water from oil/gas field, the results presented that GAC not only improved conductivity and COD removal efficiencies, but also reduced cake formation on the membrane surface [202]. It was presented that a GAC adsorption can remove DOC (especially the low-MW compounds) [199] and assimilable organic compounds (AOC) [203]. Another study [204] mentioned that coupling GAC to downstream MF process can reduce membrane fouling significantly with improved product water quality. It was also reported that PAC reduced the irreversible UF membrane fouling and decreased the chemical cleaning frequency, although it was ineffective for the mitigation of reversible membrane fouling and permeate flux [194].

An alternative strategy for fouling control is the careful selection and operation of membrane processes. Special attention should be paid to the morphology (i.e., pore size and distribution, surface roughness), surface charge and hydrophobicity/hydrophilicity [23, 205-208]. It was mentioned that AOM is more susceptible to form fouling on HPO membranes with more adsorptive and irreversible fouling and faster flux decline than HPI membranes [206, 209]. A minor difference in flux decline was also observed between HPI and HPO membranes; however, the irreversible fouling on HPO membrane was found to be slightly greater than that HPI counterpart, due to the stronger attractive interaction induced by adhesion [207]. The opposite results were also observed that the hydrophilic PVDF MF membrane presented lower AOM permeability due to the high attraction of hydrophilic membrane (up to 20 mW of zeta potential) for the AOM foulants.

The control of flux and crossflow velocity can also impact the membrane fouling formation when a cross-flow membrane system was applied [210, 211]. For instance, a remarkable reduction of algae deposition was obtained when higher air bubbling and flow rate were used during cross-flow microfiltration of *Chlorella sorokiniana* suspension [211]. It was demonstrated that the total filtration resistance can be reduced by increasing cross-flow velocity of MF; however, the pore blocking resistance was enhanced because of deep entrapment of AOM inside of membrane pores under high cross-flow velocity induced by higher TMP [212].

Membrane fouling by AOM can be controlled via selection of HPI membranes, feed solution pretreatment and optimization of hydraulic conditions. The exact balance of each fouling mechanism heavily depends on AOM property and concentration, and further research is required to improve elucidation of the fouling propensity by AOM. Interactions between AOM and NOM could induce a more aggressive fouling, this still requires further research.

2.3.4 Disinfection by-products formation from algal organic matter

2.3.4.1 Chlorination and DBP formation

Chlorination is a widely used disinfection process in drinking water plants for inactivation of pathogenic organisms (bacteria, protozoa, viruses etc.) due to higher inactivation efficiency and residual chlorine in water preventing microbial revival throughout the distribution system [213]. However, the reaction between chlorine and organic matter, anthropogenic contaminants and halides existing in the source water can produce undesirable DBPs, some of which are cytotoxic, carcinogenic or genotoxic compounds and have been associated with specific forms of cancer and birth defects [9, 214-217]. Over the last 40 years, more than 600 DBPs have been identified in drinking waters, including from initially the trihalomethanes (THMs), to now a great number of halogenated and non-halogenated organic and inorganic compounds [218, 219]. Trihalomethanes (THM) and haloacetic acids (HAA) are of two most prevalent groups of DBPs produced during disinfection, representing about 25% of the halogenated DBPs formed on weight basis [52, 220]. DBP formation is strongly impacted by the hydrophobic fraction of the dissolved organic matter [221]. The major classes of DBPs produced during chlorination, WHO guideline for maximum concentration and the potential health effects [222, 223], are summarized in Table 2.10.

Table 2.10 Important groups of DBPs produced during chlorination [218, 222-225].

Class of DBPs	Common compounds	WHO guideline (µg/L)	Health effects
Trihalomethanes (THM)	Chloroform	300	Cancer, liver, kidney and reproductive effects
	Bromodichloromethane	60	Cancer, liver, kidney and reproductive effects
	Dibromochloromethane	100	Nervous system, liver, kidney and reproductive effects
	Bromoform	100	Cancer, liver, kidney and reproductive effects
Haloacetic acids (HAA)	Dichloroacetic acid	50	Cancer and reproductive and developmental effects
	Trichloroacetic acid	200	Liver, kidney, spleen and developmental effects
	Monochloroacetic acid	20	
Haloacetonitrile (HAN)	Trichloroacetonitrile	Not establishing	Cancer, mutagenic and clastogenic effects
	Dichloroacetonitrile	20	
	Dibromoacetonitrile	70	
Other halonitrile	Cyanogen chloride	70	
Halogenated aldehydes and ketones	Formaldehyde	Not establishing	Mutagenic
Haloaldehyde	Chloral hydrate	10	
Halophenols	2-Chlorophenol	Not establishing	Cancer and tumor promoter

Halonitromethane	Chloropicrin	Not establishing
Inorganic Compounds	Bromate	10
	Chlorate	700
	Chlorite	700

It should be noted that the potential health effects summarized in Table 2.10 were based on the observations of mammalian cell transformation *in vitro* induced by the DBPs concentrated or extracted from drinking water. Without consideration of exposure via inhalation or dermal routes, no evidence has shown the carcinogenic effects in rodents *in vito* studies with exposure via the drinking water. People are exposed to water of a mixture of more than 600 identified DBPs and numberless unidentified compounds as well via ingestion, inhalation and dermal route, although most of DBPs present a relatively weak carcinogenic potency [218]. To better elucidate the toxicological effects of DBPs in drinking water, full epidemiological investigations are still needed with considerations of various exposure routes to concentrates or extracts from drinking water treated by different disinfection methods for various water sources [226].

2.3.4.2 Factors affecting DBP formation

The DBP formation is affected by several factors, including chlorine dose, contact time, water quality variable, such as type and abundance of organic matter present, DOC, UV_{254}, pH and temperature [227]. Thus, understanding the effects of these parameters is crucial before any conclusion can be drawn [73]. As the major halogenated DBPs, THMs and HAAs can accumulate in disinfected water since most of them are chemically stable. However, there are still many chemically unstable DBPs which are subject to further oxidation or hydrolysis, so that chlorine dose and contact time have great impacts on the type and amount of DBPs [222]. The World Health Organization (WHO) recommended a chlorine concentration at the delivery point of 0.5 mg/L should be applied [228]. Insufficient chlorine can result in the waterborne pathogen revival, thus exposing an increasing health risk from waterborne pathogens, but chlorine overdose can not only affect the taste of treated water, but also increase the health risk by escalated total DBP formation [213]. For instance, with the chlorine dose increase from 5 to 20 mg/L, the total THM formation increased from 70 to 85 µg/L during the chlorination of Nile River water [229]. Contact time with chlorine plays an important role on all DBP formation. It was reported that total THM formation increased by 150% after four days chlorination compared to that observed with 1 day. In addition, the different trends among THM species were also observed the formation of DBCM, BDCM, and TCM at four days was increased by 115%,

130% and 170% than that formed in one day, respectively, which indicated that longer contact time elevates THM formation potential [230].

Generally, the DBP formation rate increases with increasing temperature; however, it is a kinetically controlled process since higher temperature also accelerates the degradation of DBPs and promotes the depletion of chlorine residual [222]. It was observed that chlorine depletion accelerated as temperature increased from 3 to 34°C, meanwhile the DBP formation increased correspondingly with temperature escalating from 3 to 20°C, with a shift of DBP speciation as the results of further temperature increase from 20 to 34°C [231]. This implicated that DBP formation potential will be maximized under higher ambient temperature during summer [232].

The impact of pH on DBP formation is more complicated due to chemical alteration of reaction rate of the rate-control step of chlorination [233]. It was proposed that the majority of DBP formation decreased with increase in pH, while THMs compounds are of important exception because of significant influence of base-catalyzed hydrolysis mechanism (shown in Figure 2.5 [227]) promoting the THMs formation in alkaline pH [222, 234]. The previous investigation indicated that the yield of dihaloacetic acid (DHAA) and THM increased with the pH increasing from 5 to 10, but the opposite results were observed for trihaloacetic acid (THAA) and unknown total organic halide (UTOX), which may be attributed to the dehalogenation and hydrolysis at higher pH [227].
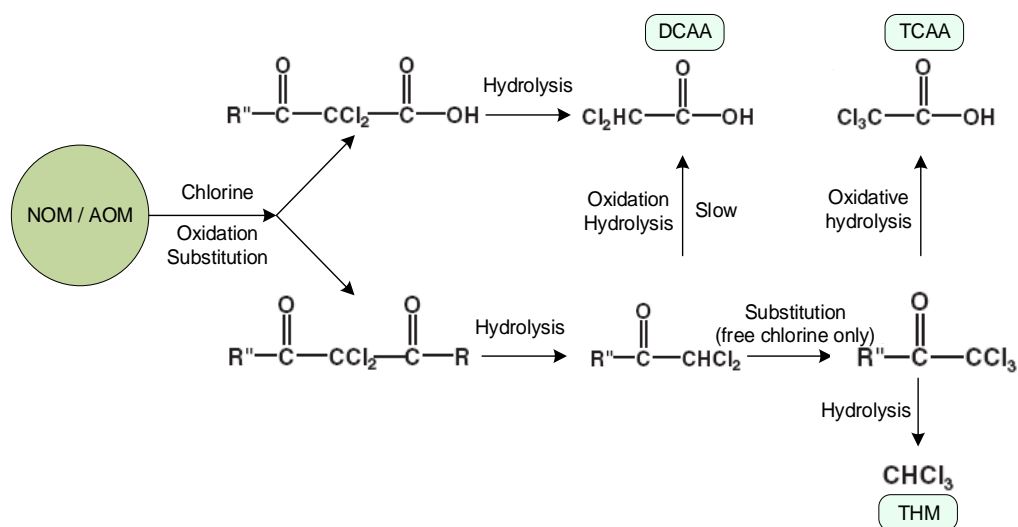
Figure 2.5 Formation and degradation pathway of THM and HAA from NOM.
(Redrawn from [227])

The effect of inorganic constituents, such as bromide and iodide, has been investigated in details in terms of speciation and amount of DBP formation. Because of high oxidation potential, chlorine can rapidly oxidize bromide and iodide to hypobromous acid (HOBr) and hypoiodous acid (HOI), which are known to be more effective in substitution reaction than chlorine upon exposure to NOM [235]. It has been observed that brominated THMs are dominant species over the major chlorinated THMs [73] in natural water, bromine incorporation level into THM formation was higher at around 50% than that chlorine at 5-10%. A similar trend was also observed in HAA formation [234]. It was reported that the total yields of THMs and HAA were increased by 18-74% and 2-35%, respectively, when 2-30 μM of bromide was added into raw water [236]. The brominated DBPs (Br-DBPs) and iodinated DBPs (I-DBPs) with greater cytotoxicity and genotoxicity[237, 238] upon chlorination have attracted increasing concerns.Thus, water treatment plants need to monitor the bromide levels and evaluate the suitability of their chlorination procedure.

The amount of organic matter presented in water, measured as DOC and UV_{254}, have been observed to correlate well with THM formation [52]. A strong correlation ($R^2 = 0.93$) between SUVA at a wavelength 280 nm and dichloracetic acid (DCAA) formation has been found upon chlorination of natural water sample [239]. This correlation might be attributed

to the aromatic structure as the primary active sites attacked by oxidant such as chlorine [240]. The functional groups of organic matter, such as phenolic functional groups has been observed to play an important role with good correlation with THM formation. It might be accounted for its electron-donating property with more tendency to incorporate chlorine than electron-withdrawing groups such as carboxylic[73].

2.3.4.3 DBP formation from AOM during chlorination

AOM are commonly dominated by hydrophilic polysaccharides and hydrophobic proteins in algae-contaminated water [241], which has been widely regarded as an important precursor of DBP in drinking water [10]. DBP formation by chlorination during disinfection of algae-laden water is of a great concern due to frequent occurrence of algal bloom in surface source water body. Previous investigations on the impact of AOM on disinfection have focused on the formation of carbonaceous DBP, especially, haloacetic acids (HAAs) and trihalomethanes (THMs) during chlorination of AOM (including EOM and IOM) originated from various algae species. The characteristics of AOM vary with the algal species, cultivation condition, such as nutrient content, pH, temperature and hydraulic mixing [242, 243]. Consequently, the DBP formation may vary considerably with the algal genus, algal growth, biochemical composition and the applied conditions of chlorination treatment (dose, pH and contact time) [244-247]. For better comparison, the DBP formation potential in terms of HAAs and THMs formation from AOM of several most abundant algal species under stationary growth phase are summarized in Table 2.11 [26, 243].

Table 2.11 Carbonaceous DBP formation potential from AOM of various algae under stationary growth phase.

Algal species	Chlorination condition	HAAFP (µg/mg-C)		THMFP (µg/mg-C)		Reference
		EOM	IOM	EOM	IOM	
Green algae						
Chlorella vulgaris	pH=7.2, RC[a] > 0.5 mg/L, 22ºC, 3 days			13		[248]
Chlorella sp.	pH=7,Cl$_2$:DOC= 5, 25ºC, 7 days	24	28	6	10	[11]
	pH=7, Cl$_2$:DOC= 5, 25ºC, 7 days	20	26	10	12	[10]
Scenedesmus quadricauda	pH=7, RC=0.5-1.2 mg/L, 20ºC,7 days	36[d]		20[c]		[41]
Cyanobacteria						
Microcystis aeruginosa	pH=7,Cl$_2$:DOC= 5, 25ºC, 3 days			8	15	[43]
	pH=7.2, RC > 0.5 mg/L, 22ºC, 3 days			12		[248]
	pH=7, RC>0.5mg/L, 21ºC, 7 days	11		17		[249]
	pH=7, RC=0.5-1.2 mg/L, 20ºC, 7 days	29		43		[41]
	pH=7, Cl$_2$:DOC= 5, 25ºC, 7 days	55[b]	68[b]	32[c]	21[c]	[250]
	pH=8.5, Cl$_2$:DOC= 3, 25ºC, 3 days	36	41	27	28	[13]
	pH=7, RC>0.5mg/L, 21ºC, 7 days	66[d]		28		[251]
	pH=7, Cl$_2$:DOC = 5(EOM),3 (IOM), 22ºC, 3 days	11[b]	14[b]	17[c]	28[c]	[6]

Species	Conditions				Reference
Aphanizomenon flos-aquae	pH=7, RC=0.5-1.2 mg/L, 20°C, 7 days	25	57		[41]
Anabaena flos-aquae	pH=7, RC=0.5-1.2 mg/L, 20°C, 7 days	19	27[c]		[41]
	pH=7, RC>0.5mg/L, 21°C, 7 days	48[d]	26		[251]
Diatom					
Asterionella formosa	pH=7, RC=0.5-1.2 mg/L, 20°C, 7 days	24[d]	19[c]		[41]
Aulacoseira granulata f. curvata	pH=7, RC=0.5-1.2 mg/L, 20°C, 7 days	13[d]	20[c]		[41]
Chaetoceros muelleri	pH=7, Cl$_2$:DOC= 5, 20°C, 7 days		29		[252]
Cyclotella meneghiniana	pH=7, chlorine dose = 12.8 mg/L, DOC = 1.2 mg/L, 25°C, 3 days		10[c]	12[c]	[253]

Note: a: RC refers the residual chlorine, b: HAA yield as DCAA, c: THM yield as TCM, d: HAA yield as DCAA and TCAA.

It can be seen from Table 2.11, the formation potential of THMs and HAA derived from EOM and IOM vary widely with algal species and experimental conditions. For the tested algal species, HAAFP is higher than THMFP for both EOM and IOM under similar experimental condition. For example, specific HAA reactivity (HAAFP) from EOM of green algae, cyanobacteria, diatoms, is 24 μg/mg-C, 55 μg/mg-C and 24 μg/mg-C, respectively, whereas specific THM reactivity (THMFP) from three algal species is 6 μg/mg-C, 32 μg/mg-C, 19 μg/mg-C, respectively, for a 7-days disinfection time. The opposite result of DBPFP of EOM was also observed that the HAAFP was less than THMFP under identical experimental conditions, which might be attributed to the specific growth condition affecting the properties of AOM. It was also observed that IOM forms higher HAAs and THMs than EOM, even though the available data for IOM is insufficient. The difference of DBPFP between EOM and IOM within various algae is unclear and more investigations are needed.

2.3.4.4 The impact of ultraviolet (UV) irradiation for DBP formation

Ultraviolet light (UV) treatment as a cost-effective and easily operation disinfection system has attracted increasing interests in water treatment industry. There are four spectrums range UV based on the wavelength, i.e., UV-A (315-400 nm), UV-B (280-315 nm), UV-C (200-280 nm), and Vacuum UV (100-200 nm) for inactivation. Because of the strong absorbance by nucleic acids. UV-C range is considered as the most germicidally active UV range [254]. Several types of UV lamps are commercially available, but the most commonly used include low pressure (LP) UV lamps, which emit monochromatically at 254 nm, and medium pressure (MP) lamps emitting higher intensity polychromatic germicidal UV light in the range 200 to 400 nm. Many factors, such as, UV wavelength, dosage and source water quality, may affect the UV irradiation performance.

There is no significant impact of UV radiation on water quality parameters, such as TOC, turbidity and pH for a dosage up to 4-5 times of usual UV disinfection dose of 40 mJ/cm^2 [255]. Thus, it does not produce regulated DBPs (THMs or HAAs) nor increase DBP formation upon subsequent chlorination [256, 257], and about 25% UV disinfection utilities in United States are applied as an alternative to chlorination to meet the stringent limits on

THMs and HAAs [258]. However, previous studies indicated that UV irradiation can fragment dissolved organic matter to lower MW products and enhance biodegradable substance formation [259-262], but no or low impact was observed on THMs and HAAs formation [263, 264]. However, the opposite results have also been presented [265]. A statistically significant change has been observed in the DBP formation from chlorination after UV irradiation for 4 different water sources. The results indicated that the increase of chloroform formation was the most significant ($\approx$ 112%) with the UV exposure of 60 mJ/cm^2 [266]. Previous studies majorly focused on the UV irradiation using relatively higher UV dosage (14-1,000 J/cm^2) on the NOM with DOC level from 5-17.4 mg/L, which is relatively higher than drinking water source in practice [265]. Only a few studies are reported that evaluated UV irradiation on DBP formation from AOM with subsequent chlorination. UV irradiation at dosage of 100 mJ/cm^2 and 1,000 mJ/cm^2, can effectively reduce the THMs and DHAA formation from EOM and IOM of *M. aeruginosa*. In addition, an increase in THMs and DHAA formation was also observed after 100 mJ/cm^2 dosage of UV irradiation in the presence of bromide (50 μg/L) [56]. The reduction in HAA formation from AOM of *Chlorella* sp. was observed after UV irradiation with dosage up to 396 mJ/cm^2, while nitrogenous DBPs (N-DBP) increased during subsequent chlorination [267]. Considering the limited research and inconsistent results, further investigation is needed to evaluate the impact of UV irradiation on DBP formation from algae-laden water source.

2.4 Knowledge gaps and research directions

The undesirable occurrence of AOM in source water heavily impacts the treatability and safety of drinking water. To minimize the risk of the breakout of waterborne diseases and mitigate the potential toxic DBP formation, multiple barriers, including coagulation, adsorption and filtration processes are applied prior to disinfection in drinking water treatment plants. The NOM, including fulvic and humic acids as major precursors of DBPs have attracted wide attention. However, the AOM comprised of both EOM and IOM as the DBPs precursors had not been investigated extensively within the entire drinking water treatment processes. The summary of existing research indicates the following:

- As the primary treatment process, AOM removal by coagulation-flocculation has been reported in previous research, but most of the work focused on removal efficiency for one or two algal species. Chemical characteristics such as AOM composition, molecular weight distribution during various growth phases were determined and coagulation performance was related to these properties. However, these properties depend heavily on species and growth phase, requiring dedicated studies specific to a target algae. Comprehensive studies relating coagulation performance of various algal matter to the fundamental properties such as the hydrophobicity, hydrophilicity and SUVA are required.

- Previous studies on AOM adsorption on activated carbon had focused primarily on cyanotoxins, taste and odor compounds. GAC adsorption could also be an effective option for the removal of the low-MW AOM fraction, which is poorly removed by coagulation. Systematic studies on adsorption effectiveness of AOM by GAC and its combination with microfiltration to mitigate the membrane fouling are required.

- The specific DBPFP of AOM varies with algae species and growth phase, thus it is difficult to predict the potentiality of DBP formation in water sample contaminated by the mixture of different algal species in raw water. Further investigations performed under identical conditions are needed to compare the performance of treatment technologies on DBP formation. In addition, the impact of UV irradiation on DBP formation from AOM still requires more research considering the limited studies and inconsistent results presented in literature.

Based on the gaps identified in the literature, the overall objective of this PhD research is to characterize the performance of commonly used processes in drinking water treatment plants namely coagulation-flocculation, GAC adsorption, membrane filtration and UV-chlorination using several commonly found algae from different groups. The comprehensive research will help to develop a treatment framework for the treatment plants.

References

[1]   R. Bailey, Organisms that use photosynthesis, in: ThoughtCo (Ed.), 2019.

[2]   I.L. Pepper, T.J. Gentry, Chapter 2 - Microorganisms Found in the Environment, in: I.L. Pepper, C.P. Gerba, T.J. Gentry (Eds.) Environmental Microbiology (Third Edition), Academic Press, San Diego, 2015, pp. 9-36.

[3]   M.J. Brandt, K.M. Johnson, A.J. Elphinston, D.D. Ratnayaka, Twort's Water Supply, Butterworth-Heinemann2016.

[4]   D.R. Knappe, Algae detection and removal strategies for drinking water treatment plants, American Water Works Association2004.

[5]   B. Ghernaout, D. Ghernaout, A. Saiba, Algae and cyanotoxins removal by coagulation/flocculation: A review, Desalination and Water Treatment 20 (2010) 133-143.

[6]   J.Y. Fang, X. Yang, J. Ma, C. Shang, Q.A. Zhao, Characterization of algal organic matter and formation of DBPs from chlor(am)ination, Water Research 44 (2010) 5897-5906.

[7]   A. Paralkar, J.K. Edzwald, Effect of ozone on EOM and coagulation., Journal - American Water Works Association 88 (1996) 143-154.

[8]   L.A. Coral, A. Zamyadi, B. Barbeau, F.J. Bassetti, F.R. Lapolli, M. Prévost, Oxidation of Microcystis aeruginosa and Anabaena flos-aquae by ozone: Impacts on cell integrity and chlorination by-product formation, Water Research 47 (2013) 2983-2994.

[9]   A. Tomlinson, M. Drikas, J.D. Brookes, The role of phytoplankton as pre-cursors for disinfection by-product formation upon chlorination, Water Research 102 (2016) 229-240.

[10]   L.C. Hua, J.L. Lin, P.C. Chen, C.P. Huang, Chemical structures of extra- and intra-cellular algogenic organic matters as precursors to the formation of carbonaceous disinfection byproducts, Chemical Engineering Journal 328 (2017) 1022-1030.

[11]   L.-C. Hua, J.-L. Lin, M.-Y. Syue, C. Huang, P.-C. Chen, Optical properties of algogenic organic matter within the growth period of Chlorella sp. and predicting their disinfection by-product formation, Science of the Total Environment 621 (2018) 1467-1474.

[12]   S. Zhou, Y. Shao, N. Gao, S. Zhu, L. Li, J. Deng, M. Zhu, Removal of Microcystis aeruginosa by potassium ferrate (VI): Impacts on cells integrity, intracellular organic matter release and disinfection by-products formation, Chemical Engineering Journal 251 (2014) 304-309.

[13]   S.Q. Zhou, S.M. Zhu, Y.S. Shao, N.Y. Gao, Characteristics of C-, N-DBPs formation from algal organic matter: Role of molecular weight fractions and impacts of pre-ozonation, Water Research 72 (2015) 381-390.

[14]   R.M. Maier, I.L. Pepper, Bacterial growth, Environmental Microbiology, Elsevier2015, pp. 37-56.

[15]   M. Pivokonsky, O. Kloucek, L. Pivokonska, Evaluation of the production, composition and aluminum and iron complexation of algogenic organic matter, Water Research 40 (2006) 3045-3052.

[16]   R.K. Henderson, A. Baker, S.A. Parsons, B. Jefferson, Characterisation of algogenic organic matter extracted from cyanobacteria, green algae and diatoms, Water Research 42 (2008) 3435-3445.

[17]   W.-J. Huang, C.-H. Lai, Y.-L. Cheng, Evaluation of extracellular products and mutagenicity in cyanobacteria cultures separated from a eutrophic reservoir, Science of the Total Environment 377 (2007) 214-223.

[18]   R. Chrost, M. Faust, Organic carbon release by phytoplankton: its composition and utilization by bacterioplankton, Journal of Plankton Research 5 (1983) 477-493.

[19]   M. Leloup, R. Nicolau, V. Pallier, C. Yéprémian, G. Feuillade-Cathalifaud, Organic matter produced by algae and cyanobacteria: Quantitative and qualitative characterization, Journal of Environmental Sciences 25 (2013) 1089-1097.

[20]   M. Pivokonsky, J. Safarikova, M. Baresova, L. Pivokonska, I. Kopecka, A comparison of the character of algal extracellular versus cellular organic matter produced by cyanobacterium, diatom and green alga, Water Research 51 (2014) 37-46.

[21]   L.O. Villacorte, Y. Ekowati, T.R. Neu, J.M. Kleijn, H. Winters, G. Amy, J.C. Schippers, M.D. Kennedy, Characterisation of algal organic matter produced by bloom-forming marine and freshwater algae, Water Research 73 (2015) 216-230.

[22]   H.S. Ou, N.Y. Gao, Y. Deng, J.L. Qiao, K.J. Zhang, T. Li, L. Dong, Mechanistic studies of Microcystic aeruginosa inactivation and degradation by UV-C irradiation and chlorination with poly-synchronous analyses, Desalination 272 (2011) 107-119.

[23]   Y. Zhang, Q. Fu, Algal fouling of microfiltration and ultrafiltration membranes and control strategies: A review, Separation and Purification Technology 203 (2018) 193-208.

[24]   L. Li, Z.M. Wang, L.C. Rietveld, N.Y. Gao, J.Y. Hu, D.Q. Yin, S.L. Yu, Comparison of the Effects of Extracellular and Intracellular Organic Matter Extracted From Microcystis aeruginosa on Ultrafiltration Membrane Fouling: Dynamics and Mechanisms, Environmental Science & Technology 48 (2014) 14549-14557.

[25]   Y. Zhang, C.Y. Tang, G. Li, The role of hydrodynamic conditions and pH on algal-rich water fouling of ultrafiltration, Water Research 46 (2012) 4783-4789.

[26]   M. Pivokonsky, J. Naceradska, I. Kopecka, M. Baresova, B. Jefferson, X. Li, R.K. Henderson, The impact of algogenic organic matter on water treatment plant operation and water quality: A review, Critical Reviews in Environmental Science and Technology 46 (2016) 291-335.

[27]   L.G. Linden, D.M. Lewis, M.D. Burch, J.D. Brookes, Interannual variability in rainfall and its impact on nutrient load and phytoplankton in Myponga Reservoir, South Australia, International Journal of River Basin Management 2 (2004) 169-179.

[28]   E.W. Becker, Micro-algae as a source of protein, Biotechnology Advances 25 (2007) 207-210.

[29]   D.M. Collyer, G. Fogg, Studies on fat accumulation by algae, Journal of Experimental Botany 6 (1955) 256-275.

[30]   J. Cao, D. Li, J. Wang, Studies on biochemical composition of 10 species of common freshwater phytoplankton, Acta Scientiarum Naturalium Universitatis Sunyatseni 36 (1997) 22-27.

[31]   C. Yang, Q. Hua, K. Shimizu, Energetics and carbon metabolism during growth of microalgal cells under photoautotrophic, mixotrophic and cyclic light-autotrophic/dark-heterotrophic conditions, Biochemical Engineering Journal 6 (2000) 87-102.

[32]   U.D. Enyidi, Chlorella vulgaris as Protein Source in the Diets of African Catfish Clarias gariepinus, Fishes 2 (2017) 17.

[33]   A. Konopka, M. Schnur, Biochemical composition and photosynthetic carbon metabolism of nutrient limited cultures of merismopedia tenuissima (cyanophyceae) Journal of Phycology 17 (1981) 118-122.

[34]   M. Li, P.N. Nkrumah, M. Xiao, Biochemical composition of Microcystis aeruginosa related to specific growth rate: insight into the effects of abiotic factors, Inland Waters 4 (2014) 357-362.

[35]   I.S. Chronakis, M. Madsen, 14 - Algal proteins, in: G.O. Phillips, P.A. Williams (Eds.) Handbook of Food Proteins, Woodhead Publishing2011, pp. 353-394.

[36]   C.M. Gatenby, D.M. Orcutt, D.A. Kreeger, B.C. Parker, V.A. Jones, R.J. Neves, Biochemical composition of three algal species proposed as food for captive freshwater mussels, Journal of applied phycology 15 (2003) 1-11.

[37]   E.A.I. Abdelkhalek, B. Mohamed, A. MOHAMMED, A. Lotfi, Growth performance and biochemical composition of nineteen microalgae collected from different Moroccan reservoirs, Mediterranean Marine Science 17 (2015) 323-332.

[38]   L. Li, N. Gao, Y. Deng, J. Yao, K. Zhang, Characterization of intracellular & extracellular algae organic matters (AOM) of Microcystic aeruginosa and formation of AOM-associated disinfection byproducts and odor & taste compounds, Water Research 46 (2012) 1233-1240.

[39]   S.Q. Zhou, Y.S. Shao, N.Y. Gao, Y. Deng, L. Li, J. Deng, C.Q. Tan, Characterization of algal organic matters of Microcystis aeruginosa: Biodegradability, DBP formation and membrane fouling potential, Water Research 52 (2014) 199-207.

[40]   Z. Rehmana, S. Jeonga, S. Tabatabaia, A. Emwasb, T. Leiknesa, Advanced characterization of dissolved organic matter released by bloom-forming marine algae, Desalination and Water Treatment 69 (2017) 1-11.

[41]   E.H. Goslan, C. Seigle, D. Purcell, R. Henderson, S.A. Parsons, B. Jefferson, S.J. Judd, Carbonaceous and nitrogenous disinfection by-product formation from algal organic matter, Chemosphere 170 (2017) 1-9.

[42]   L.-C. Hua, S.-J. Chao, C. Huang, Fluorescent and molecular weight dependence of THM and HAA formation from intracellular algogenic organic matter (IOM), Water Research 148 (2019) 231-238.

[43]   M.Q. Zhu, N.Y. Gao, W.H. Chu, S.Q. Zhou, Z.D. Zhang, Y.Q. Xu, Q. Dai, Impact of pre-ozonation on disinfection by-product formation and speciation from chlor(am)ination of algal organic matter of Microcystis aeruginosa, Ecotoxicology and Environmental Safety 120 (2015) 256-262.

[44]   F. Qu, H. Liang, J. He, J. Ma, Z. Wang, H. Yu, G. Li, Characterization of dissolved extracellular organic matter (dEOM) and bound extracellular organic matter (bEOM) of Microcystis aeruginosa and their impacts on UF membrane fouling, Water Research 46 (2012) 2881-2890.

[45]   J.X. Chen, N.Y. Gao, L. Li, M.Q. Zhu, J. Yang, X. Lu, Y.S. Zhang, Disinfection by-product formation during chlor(am)ination of algal organic matters (AOM) extracted from Microcystis aeruginosa: effect of growth phases, AOM and bromide concentration, Environmental Science and Pollution Research 24 (2017) 8469-8478.

[46]   G. Li, Y. Ren, L. Gu, Q. He, R. Deng, L.Z. Tang, Migration and transformation of nitrogen in algae organic matter (AOM) during the growth of Microcystis aeruginous, Desalination and Water Treatment 111 (2018) 79-87.

[47]   A. Matilainen, E.T. Gjessing, T. Lahtinen, L. Hed, A. Bhatnagar, M. Sillanpää, An overview of the methods used in the characterisation of natural organic matter (NOM) in relation to drinking water treatment, Chemosphere 83 (2011) 1431-1442.

[48]   P. Whitehead, Total Organic Carbon (TOC) and its Measurement, Pure Lab Water For Science, 2018.

[49]   H.-H. Perkampus, UV-VIS Spectroscopy and its Applications, Springer Science & Business Media2013.

[50]   B.B.a.J.W. Potter, Determination of Total Organic Carbon and Specific UV Absorbance at 254 nm in Source Water and Drinking Water, Mothed 415.3, U.S. Environmental Protection Agency, U.S. Environmental Protection Agency, Washington, DC, 2009.

[51]   A.M. Hansen, T.E. Kraus, B.A. Pellerin, J.A. Fleck, B.D. Downing, B.A. Bergamaschi, Optical properties of dissolved organic matter (DOM): Effects of biological and photolytic degradation, Limnology and Oceanography 61 (2016) 1015-1032.

[52]   G. Hua, D.A. Reckhow, I. Abusallout, Correlation between SUVA and DBP formation during chlorination and chloramination of NOM fractions from different sources, Chemosphere 130 (2015) 82-89.

[53]   M.C. S. Gora, Study on characteristics and removal of natural organic matter in drinking water systems in Newfoundland and Labrador, Department of Environment and Conservation, Department of Environment and Conservation,Water Management Division, 2011, pp. 205.

[54]   R. Henderson, Y. Shutova, A. Baker, A. Zamyadi, P. Le-Clech, A. Branch, G. Newcombe, S. Khan, R. Stuetz, Fluorescence: State-of-the-art monitoring for water treatment systems, Water: Journal of the Australian Water Association 42 (2015) 108.

[55]   S. Baghoth, M. Dignum, A. Grefte, J. Kroesbergen, G. Amy, Characterization of NOM in a drinking water treatment process train with no disinfectant residual, Water Science and Technology: Water Supply 9 (2009) 379-386.

[56]   S. Chen, J. Deng, L. Li, N.Y. Gao, Evaluation of disinfection by-product formation during chlor(am)ination from algal organic matter after UV irradiation, Environmental Science and Pollution Research 25 (2018) 5994-6002.

[57]   T.T. Guo, Y.L. Yang, R.P. Liu, X. Li, Enhanced removal of intracellular organic matters (IOM) from Microcystic aeruginosa by aluminum coagulation, Separation and Purification Technology 189 (2017) 279-287.

[58]   J. Fang, Formation and control of disinfection by-products in chlorination of B-G algae and algal organic matter (AOM), School of Municipal. & Environ. Eng., Harbin Institute of Technology, Harbin, 2010.

[59]   S. I. Khan, A. Zamyadi, N.R.H. Rao, X. Li, R.M. Stuetz, R.K. Henderson, Fluorescence spectroscopic characterisation of algal organic matter: towards

improved in situ fluorometer development, Environmental Science: Water Research & Technology 5 (2019) 417-432.

[60]   L. Xing, M.F. Murshed, T. Lo, R. Fabris, C.W. Chow, J. van Leeuwen, M. Drikas, D. Wang, Characterization of organic matter in alum treated drinking water using high performance liquid chromatography and resin fractionation, Chemical Engineering Journal 192 (2012) 186-191.

[61]   C.W. Chow, R. Fabris, J.v. Leeuwen, D. Wang, M. Drikas, Assessing natural organic matter treatability using high performance size exclusion chromatography, Environmental Science & Technology 42 (2008) 6683-6689.

[62]   E.N. Hidayah, Y.-C. Chou, H.-H. Yeh, Comparison between HPSEC-OCD and F-EEMs for assessing DBPs formation in water, Journal of Environmental Science and Health, Part A 52 (2017) 391-402.

[63]   C.-H. Lai, Y.-C. Chou, H.-H. Yeh, Assessing the interaction effects of coagulation pretreatment and membrane material on UF fouling control using HPSEC combined with peak-fitting, Journal of Membrane Science 474 (2015) 207-214.

[64]   N. Her, G. Amy, D. Foss, J. Cho, Y. Yoon, P. Kosenka, Optimization of method for detecting and characterizing NOM by HPLC− size exclusion chromatography with UV and on-line DOC detection, Environmental Science & Technology 36 (2002) 1069-1076.

[65]   W.W. Huang, X. Qin, B.Z. Dong, W.Z. Zhou, W.G. Lv, Fate and UF fouling behavior of algal extracellular and intracellular organic matter under the influence of copper ions, Science of the Total Environment 649 (2019) 1643-1652.

[66]   D. Hendricks, Fundamentals of water treatment unit processes: physical, chemical, and biological, Crc Press2016.

[67]   P.C. Xie, Y.Q. Chen, J. Ma, X. Zhang, J. Zou, Z.P. Wang, A mini review of preoxidation to improve coagulation, Chemosphere 155 (2016) 550-563.

[68]   S. Merel, D. Walker, R. Chicana, S. Snyder, E. Baures, O. Thomas, State of knowledge and concerns on cyanobacterial blooms and cyanotoxins, Environment International 59 (2013) 303-327.

[69]   A.A.M. Gad, S. El-Tawel, Effect of pre-oxidation by chlorine/permanganate on surface water characteristics and algal toxins, Desalination and Water Treatment 57 (2016) 17922-17934.

[70]   P.C. Xie, J. Ma, J.Y. Fang, Y.H. Guan, S.Y. Yue, X.C. Li, L.W. Chen, Comparison of Permanganate Preoxidation and Preozonation on Algae Containing Water: Cell Integrity, Characteristics, and Chlorinated Disinfection Byproduct Formation, Environmental Science & Technology 47 (2013) 14051-14061.

[71]   J.-J. Chen, H.-H. Yeh, I.-C. Tseng, Effect of ozone and permanganate on algae coagulation removal–Pilot and bench scale tests, Chemosphere 74 (2009) 840-846.

[72]   J. Xu, Y.X. Zhao, B.Y. Gao, S.L. Han, Q. Zhao, X.L. Liu, The influence of algal organic matter produced by Microcystis aeruginosa on coagulation-ultrafiltration treatment of natural organic matter, Chemosphere 196 (2018) 418-428.

[73]   S. Sinha, Coagulatibility of NOM and its effects on formation of chlorination DBPs, University of Colorado at Boulder (1999).

[74]   V. Kumar, N. Othman, S. Asharuddin, Applications of Natural Coagulants to Treat Wastewater− A Review, MATEC Web of Conferences, EDP Sciences, 2017, pp. 06016.

[75]   K.E. Lee, N. Morad, T.T. Teng, B.T. Poh, Development, characterization and the application of hybrid materials in coagulation/flocculation of wastewater: A review, Chemical Engineering Journal 203 (2012) 370-386.

[76]   A. Bahadori, M. Clark, B. Boyd, Essentials of water systems design in the oil, gas, and chemical processing industries, Springer Science & Business Media2013.

[77]   J.-J. Qin, M.H. Oo, K.A. Kekre, F. Knops, P. Miller, Impact of coagulation pH on enhanced removal of natural organic matter in treatment of reservoir water, Separation and Purification Technology 49 (2006) 295-298.

[78]   M. Sillanpää, M.C. Ncibi, A. Matilainen, M. Vepsäläinen, Removal of natural organic matter in drinking water treatment by coagulation: A comprehensive review, Chemosphere 190 (2018) 54-71.

[79]   D.J. Pernitsky, J.K. Edzwald, Selection of alum and polyaluminum coagulants: principles and applications, Journal of Water Supply: Research and Technology-Aqua 55 (2006) 121-141.

[80]   J.T. Wang, W.Y. Xu, J.J. Xu, D. Wei, H. Feng, Z.H. Xu, Effect of aluminum speciation and pH on in-line coagulation/diatomite microfiltration process: Correlations between aggregate characteristics and membrane fouling, Journal of Molecular Liquids 224 (2016) 492-501.

[81]   J. Zou, H. Zhu, F. Wang, H. Sui, J. Fan, Preparation of a new inorganic–organic composite flocculant used in solid–liquid separation for waste drilling fluid, Chemical Engineering Journal 171 (2011) 350-356.

[82]   W.P. Cheng, F.H. Chi, C.C. Li, R.F. Yu, A study on the removal of organic substances from low-turbidity and low-alkalinity water with metal-polysilicate coagulants, Colloids and Surfaces A: Physicochemical and Engineering Aspects 312 (2008) 238-244.

[83] U.E.P. Agency, Comprehensive Disinfectants and Disinfection Byproducts Rules (Stage 1 and Stage 2): Quick Reference Guide, (2006).

[84] U. EPA, Enhanced coagulation and enhanced precipitative softening guidance manual, Disinfectants and disinfection byproducts rule (DBPR) (1999).

[85] S.R. Poleneni, E. Inniss, H. Shi, J. Yang, B. Hua, J. Clamp, Enhanced Flocculation Using Drinking Water Treatment Plant Sedimentation Residual Solids, Water 11 (2019) 1821.

[86] J.H. Lehr, J. Keeley, Domestic, municipal, and industrial water supply and waste disposal, Wiley Interscience2005.

[87] N. Tzoupanos, A. Zouboulis, Coagulation-flocculation processes in water/wastewater treatment: the application of new generation of chemical reagents, 6th IASME/WSEAS International Conference Greece, 2008.

[88] T. Suopajärvi, Functionalized nanocelluloses in wastewater treatment applications, Acta Universitatis Ouluensis C 526 (2015).

[89] D. Ghernaout, B. Ghernaout, Sweep flocculation as a second form of charge neutralisation—a review, Desalination and Water Treatment 44 (2012) 15-28.

[90] C.X. Ma, H.Y. Pei, W.R. Hu, H.Z. Xu, Y. Jin, The lysis and regrowth of toxic cyanobacteria during storage of achitosan-aluminium chloride composite coagulated sludge: implications for drinking water sludge treatment, RSC Advances 6 (2016) 112756-112764.

[91] H.F. Miao, W.Y. Tao, The mechanisms of ozonation on cyanobacteria and its toxins removal, Separation and Purification Technology 66 (2009) 187-193.

[92] A. Gonzalez-Torres, J. Putnam, B. Jefferson, R.M. Stuetz, R.K. Henderson, Examination of the physical properties of Microcystis aeruginosa flocs produced on coagulation with metal salts, Water Research 60 (2014) 197-209.

[93] N. Zaouri, L. Gutierrez, L. Dramas, D. Garces, J.-P. Croue, Interfacial interactions between Skeletonema costatum extracellular organic matter and metal oxides: Implications for ceramic membrane filtration, Water Research 116 (2017) 194-202.

[94] J. Safarikova, M. Baresova, M. Pivokonsky, I. Kopecka, Influence of peptides and proteins produced by cyanobacterium Microcystis aeruginosa on the coagulation of turbid waters, Separation and Purification Technology 118 (2013) 49-57.

[95] R.K. Henderson, S.A. Parsons, B. Jefferson, The impact of differing cell and algogenic organic matter (AOM) characteristics on the coagulation and flotation of algae, Water Research 44 (2010) 3617-3624.

[96]   X.M. Tang, H.L. Zheng, C. Zhao, J. Zhai, B.Z. Liu, W. Chen, Z.A. Zhang, F. Li, Removal of dissolved organic matter from algae-polluted surface water by coagulation, Desalination and Water Treatment 57 (2016) 25337-25344.

[97]   M. Pivokonsky, L. Pivokonska, J. Baumeltova, P. Bubakova, The effect of cellular organic matter produced by cyanobacteria microcystis aeruginosa on water purification, Journal of Hydrology and Hydromechanics 57 (2009) 121-129.

[98]   T. Takaara, D. Sano, H. Konno, T. Omura, Cellular proteins of Microcystis aeruginosa inhibiting coagulation with polyaluminum chloride, Water Research 41 (2007) 1653-1658.

[99]   A.J. Garzon-Sanabria, S.S. Ramirez-Caballero, F.E. Moss, Z.L. Nikolov, Effect of algogenic organic matter (AOM) and sodium chloride on Nannochloropsis salina flocculation efficiency, Bioresource Technology 143 (2013) 231-237.

[100]   D. Ghernaout, The hydrophilic/hydrophobic ratio vs. dissolved organics removal by coagulation – A review, Journal of King Saud University - Science 26 (2014) 169-180.

[101]   C. Wan, M.A. Alam, X.-Q. Zhao, X.-Y. Zhang, S.-L. Guo, S.-H. Ho, J.-S. Chang, F.-W. Bai, Current progress and future prospect of microalgal biomass harvest using various flocculation technologies, Bioresource Technology 184 (2015) 251-257.

[102]   X.M. Tang, H.L. Zheng, B.Y. Gao, C.L. Zhao, B.Z. Liu, W. Chen, J.S. Guo, Interactions of specific extracellular organic matter and polyaluminum chloride and their roles in the algae-polluted water treatment, Journal of Hazardous Materials 332 (2017) 1-9.

[103]   M. Leloup, V. Pallier, R. Nicolau, G. Feuillade-Cathalifaud, Assessing Transformations of Algal Organic Matter in the Long-Term: Impacts of Humification-Like Processes, International Journal of Molecular Sciences 16 (2015) 18096-18110.

[104]   M. Pivokonsky, J. Naceradska, T. Brabenec, K. Novotna, M. Baresova, V. Janda, The impact of interactions between algal organic matter and humic substances on coagulation, Water Research 84 (2015) 278-285.

[105]   L. Chekli, C. Eripret, S.H. Park, S.A.A. Tabatabai, O. Vronska, B. Tamburic, J.H. Kim, H.K. Shon, Coagulation performance and floc characteristics of polytitanium tetrachloride (PTC) compared with titanium tetrachloride (TiCl4) and ferric chloride (FeCl3) in algal turbid water, Separation and Purification Technology 175 (2017) 99-106.

[106]   Z.S. Yan, B. Liu, F.S. Qu, A. Ding, H. Liang, Y. Zhao, G.B. Li, Control of ultrafiltration membrane fouling caused by algal extracellular organic matter (EOM)

using enhanced Al coagulation with permanganate, Separation and Purification Technology 172 (2017) 51-58.

[107] X. He, Y.-L. Liu, A. Conklin, J. Westrick, L.K. Weavers, D.D. Dionysiou, J.J. Lenhart, P.J. Mouser, D. Szlag, H.W. Walker, Toxic cyanobacteria and drinking water: Impacts, detection, and treatment, Harmful Algae 54 (2016) 174-193.

[108] J.C. Jeon, C.H. Jo, I. Choi, S.B. Kwon, E. Jang, T.M. Hwang, Analysis on the Natural Organic Matter and Disinfection By-Products in Full-scale Advanced Water Treatment Plant and Conventional Water Treatment Plant, Desalination and Water Treatment 51 (2013) 6288-6298.

[109] K.P. Lobanga, J. Haarhoff, S.J. van Staden, Treatability of South African surface waters by activated carbon, Water SA 39 (2013) 379-384.

[110] S. Jamil, P. Loganathan, A. Listowski, J. Kandasamy, C. Khourshed, S. Vigneswaran, Simultaneous removal of natural organic matter and micro-organic pollutants from reverse osmosis concentrate using granular activated carbon, Water Research 155 (2019) 106-114.

[111] J. Deng, Y.S. Shao, N.Y. Gao, S.Q. Zhou, X.H. Hu, Adsorption Characteristics of ss-Ionone in Water on Granular Activated Carbon, Clean-Soil Air Water 40 (2012) 1341-1348.

[112] C.A. Chiu, K. Hristovski, S. Huling, P. Westerhoff, In-situ regeneration of saturated granular activated carbon by an iron oxide nanocatalyst, Water Research 47 (2013) 1596-1603.

[113] B. Schreiber, D. Wald, V. Schmalz, E. Worch, Removal of dissolved organic compounds by granular activated carbon, in: L. Simeonov, E. Chirila (Eds.) Chemicals as Intentional and Accidental Global Environmental Threats, Springer, Dordrecht, 2006, pp. 397-+.

[114] M. Li, Effects of Natural Organic Matter on Contaminant Removal by Superfine Powdered Activated Carbon Coupled with Microfiltration Membranes, (2014).

[115] Z. Hu, M. Srinivasan, Preparation of high-surface-area activated carbons from coconut shell, Microporous and Mesoporous Materials 27 (1999) 11-18.

[116] K. Yang, J. Peng, C. Srinivasakannan, L. Zhang, H. Xia, X. Duan, Preparation of high surface area activated carbon from coconut shells using microwave heating, Bioresource Technology 101 (2010) 6163-6169.

[117] M. Yusufu, C. Ariahu, B. Igbabul, Production and characterization of activated carbon from selected local raw materials, African Journal of Pure and Applied Chemistry 6 (2012) 123-131.

[118] P. Nowicki, R. Pietrzak, H. Wachowska, Siberian anthracite as a precursor material for microporous activated carbons, Fuel 87 (2008) 2037-2040.

[119] J.W. Zondlo, M.R. Velez, Development of surface area and pore structure for activation of anthracite coal, Fuel Processing Technology 88 (2007) 369-374.

[120] A. Ahmadpour, D. Do, The preparation of activated carbon from macadamia nutshell by chemical activation, Carbon 35 (1997) 1723-1732.

[121] D. Cuhadaroglu, O.A. Uygun, Production and characterization of activated carbon from a bituminous coal by chemical activation, African Journal of Biotechnology 7 (2008).

[122] D. Savova, E. Apak, E. Ekinci, F. Yardim, N. Petrov, T. Budinova, M. Razvigorova, V. Minkova, Biomass conversion to carbon adsorbents and gas, Biomass and Bioenergy 21 (2001) 133-142.

[123] A. Marcilla, S. Garcıa-Garcıa, M. Asensio, J. Conesa, Influence of thermal treatment regime on the density and reactivity of activated carbons from almond shells, Carbon 38 (2000) 429-440.

[124] W. Tsai, C. Chang, S. Lee, Preparation and characterization of activated carbons from corn cob, Carbon 35 (1997) 1198-1200.

[125] W.T. Tsai, C.Y. Chang, S.Y. Wang, C.F. Chang, S.F. Chien, H.F. Sun, Preparation of activated carbons from corn cob catalyzed by potassium salts and subsequent gasification with CO2, Bioresource Technology 78 (2001) 203-208.

[126] B. Sivakumar, C. Kannan, S. Karthikeyan, Preparation and characterization of activated carbon prepared from balsamodendron caudatum wood waste through various activation processes, RASĀYAN Journal of Chemistry 5 (2012) 321-327.

[127] Y. Qi, A.F. Hoadley, A.L. Chaffee, G. Garnier, Characterisation of lignite as an industrial adsorbent, Fuel 90 (2011) 1567-1574.

[128] A.D. McNaught, A. Wilkinson, Compendium of chemical terminology. IUPAC recommendations, (1997).

[129] K.O. Nowack, F.S. Cannon, D.W. Mazyck, Enhancing activated carbon adsorption of 2-methylisoborneol: methane and steam treatments, Environmental Science & Technology 38 (2004) 276-284.

[130] L. Ji, F. Liu, Z. Xu, S. Zheng, D. Zhu, Adsorption of pharmaceutical antibiotics on template-synthesized ordered micro-and mesoporous carbons, Environmental Science & Technology 44 (2010) 3116-3122.

[131] L. Li, P.A. Quinlivan, D.R. Knappe, Effects of activated carbon surface chemistry and pore structure on the adsorption of organic contaminants from aqueous solution, Carbon 40 (2002) 2085-2100.

[132] D. De Ridder, M. McConville, A. Verliefde, L. Van der Aa, S. Heijman, J. Verberk, L. Rietveld, J. Van Dijk, Development of a predictive model to determine micropollutant removal using granular activated carbon, Drinking Water Engineering and Science 2 (2009) 57-62.

[133] D.J. De Ridder, L. Villacorte, A.R. Verliefde, J.Q. Verberk, S. Heijman, G.L. Amy, J.C. Van Dijk, Modeling equilibrium adsorption of organic micropollutants onto activated carbon, Water Research 44 (2010) 3077-3086.

[134] V. Yangali-Quintanilla, A. Sadmani, M. McConville, M. Kennedy, G. Amy, A QSAR model for predicting rejection of emerging contaminants (pharmaceuticals, endocrine disruptors) by nanofiltration membranes, Water Research 44 (2010) 373-384.

[135] K. Watson, M.J. Farre, F.D.L. Leusch, N. Knight, Using fluorescence-parallel factor analysis for assessing disinfection by-product formation and natural organic matter removal efficiency in secondary treated synthetic drinking waters, Science of the Total Environment 640 (2018) 31-40.

[136] N. Moona, K.R. Murphy, M. Bondelind, O. Bergstedt, T.J.R. Pettersson, Partial renewal of granular activated carbon biofilters for improved drinking water treatment, Environmental Science-Water Research & Technology 4 (2018) 529-538.

[137] A.H. Sulaymon, A.F.M. Ali, S.K. Al-Naseri, Natural organic matter removal from Tigris River water in Baghdad, Iraq, Desalination 245 (2009) 155-168.

[138] S. Alvarez-Torrellas, J.L. Sotelo, A. Rodriguez, G. Ovejero, J. Garcia, Influence of the natural organic matter in the removal of caffeine from water by fixed-bed column adsorption, International Journal of Environmental Science and Technology 14 (2017) 833-840.

[139] S.Y. Zhang, S. Gitungo, L. Axe, J.E. Dyksen, R.F. Raczko, A pilot plant study using conventional and advanced water treatment processes: Evaluating removal efficiency of indicator compounds representative of pharmaceuticals and personal care products, Water Research 105 (2016) 85-96.

[140] L. Cermakova, I. Kopecka, M. Pivokonsky, L. Pivokonska, V. Janda, Removal of cyanobacterial amino acids in water treatment by activated carbon adsorption, Separation and Purification Technology 173 (2017) 330-338.

[141] L. Li, H.C. Guo, C. Shao, S.L. Yu, D.Q. Yin, N.Y. Gao, N. Lu, Effect of algal organic matter (AOM) extracted from Microcystis aeruginosa on photo-degradation of Diuron, Chemical Engineering Journal 281 (2015) 265-271.

[142] K.J. Zhang, N.Y. Gao, Y. Deng, M.H. Shui, Y.L. Tang, Granular activated carbon (GAC) adsorption of two algal odorants, dimethyl trisulfide and beta-cyclocitral, Desalination 266 (2011) 231-237.

[143] P. Hnatukova, I. Kopecka, M. Pivokonsky, Adsorption of cellular peptides of Microcystis aeruginosa and two herbicides onto activated carbon: Effect of surface charge and interactions, Water Research 45 (2011) 3359-3368.

[144] I. Kopecka, M. Pivokonsky, L. Pivokonska, P. Hnatukova, J. Safarikova, Adsorption of peptides produced by cyanobacterium Microcystis aeruginosa onto granular activated carbon, Carbon 69 (2014) 595-608.

[145] Z. Aksu, E. Kabasakal, Batch adsorption of 2, 4-dichlorophenoxy-acetic acid (2, 4-D) from aqueous solution by granular activated carbon, Separation and Purification Technology 35 (2004) 223-240.

[146] B.A. Zachman, Understanding and predicting natural organic matter adsorption by granular activated carbon columns, University of Colorado at Boulder, Ann Arbor, 2005, pp. 332.

[147] A. Mestre, M. Pinto, J. Pires, J. Nogueira, A. Carvalho, Effect of solution pH on the removal of clofibric acid by cork-based activated carbons, Carbon 48 (2010) 972-980.

[148] S.K. Behera, S.-Y. Oh, H.-S. Park, Sorption of triclosan onto activated carbon, kaolinite and montmorillonite: effects of pH, ionic strength, and humic acid, Journal of Hazardous Materials 179 (2010) 684-691.

[149] B. Schreiber, T. Brinkmann, V. Schmalz, E. Worch, Adsorption of dissolved organic matter onto activated carbon - the influence of temperature, absorption wavelength, and molecular size, Water Research 39 (2005) 3449-3456.

[150] P. Conte, A. Piccolo, Conformational arrangement of dissolved humic substances. Influence of solution composition on association of humic molecules, Environmental Science & Technology 33 (1999) 1682-1690.

[151] A. Gonzalez-Perez, K.M. Persson, F. Lipnizki, Functional Channel Membranes for Drinking Water Production, Water 10 (2018) 11.

[152] H. Zhou, D.W. Smith, Advanced technologies in water and wastewater treatment, Canadian Journal of Civil Engineering 28 (2001) 49-66.

[153] S.G. Lehman, L. Liu, Application of ceramic membranes with pre-ozonation for treatment of secondary wastewater effluent, Water Research 43 (2009) 2020-2028.

[154] X.L. Zhang, L.H. Fan, F.A. Roddick, Impact of the Interaction between Aquatic Humic Substances and Algal Organic Matter on the Fouling of a Ceramic Microfiltration Membrane, Membranes 8 (2018) 10.

[155] Y. Liao, A. Bokhary, E. Maleki, B. Liao, A review of membrane fouling and its control in algal-related membrane processes, Bioresource Technology 264 (2018) 343-358.

[156] E.J. de la Casa, A. Guadix, R. Ibanez, F. Camacho, E.M. Guadix, A combined fouling model to describe the influence of the electrostatic environment on the cross-flow microfiltration of BSA, Journal of Membrane Science 318 (2008) 247-254.

[157] C. Duclos-Orsello, W. Li, C.-C. Ho, A three mechanism model to describe fouling of microfiltration membranes, Journal of Membrane Science 280 (2006) 856-866.

[158] R. Golbandi, M.A. Abdi, A.A. Babaluo, A.B. Khoshfetrat, T. Mohammadlou, Fouling study of TiO2-boehmite MF membrane in defatting of whey solution: Feed concentration and pH effects, Journal of Membrane Science 448 (2013) 135-142.

[159] E. Iritani, N. Katagiri, Developments of blocking filtration model in membrane filtration, KONA Powder and Particle Journal 33 (2016) 179-202.

[160] J.X. Liu, J. Tian, Z.H. Wang, D.S. Zhao, F. Jia, B.Z. Dong, Mechanism analysis of powdered activated carbon controlling microfiltration membrane fouling in surface water treatment, Colloids and Surfaces a-Physicochemical and Engineering Aspects 517 (2017) 45-51.

[161] W. Zhang, W. Zhang, X.Z. Zhang, P. Amendola, Q. Hu, Y.S. Chen, Characterization of dissolved organic matters responsible for ultrafiltration membrane fouling in algal harvesting, Algal Research-Biomass Biofuels and Bioproducts 2 (2013) 223-229.

[162] Y.-T. Chiou, M.-L. Hsieh, H.-H. Yeh, Effect of algal extracellular polymer substances on UF membrane fouling, Desalination 250 (2010) 648-652.

[163] D.A. Ladner, D.R. Vardon, M.M. Clark, Effects of shear on microfiltration and ultrafiltration fouling by marine bloom-forming algae, Journal of Membrane Science 356 (2010) 33-43.

[164] V. Discart, M.R. Bilad, D. Vandamme, I. Foubert, K. Muylaert, I. Vankelecom, Role of transparent exopolymeric particles in membrane fouling: Chlorella vulgaris broth filtration, Bioresource Technology 129 (2013) 18-25.

[165] X. Zhang, Q. Hu, M. Sommerfeld, E. Puruhito, Y. Chen, Harvesting algal biomass for biofuels using ultrafiltration membranes, Bioresource Technology 101 (2010) 5297-5304.

[166] X. Zhang, L. Fan, F.A. Roddick, Understanding the fouling of a ceramic microfiltration membrane caused by algal organic matter released from Microcystis aeruginosa, Journal of Membrane Science 447 (2013) 362-368.

[167] F. Qu, H. Liang, J. Tian, H. Yu, Z. Chen, G. Li, Ultrafiltration (UF) membrane fouling caused by cyanobateria: Fouling effects of cells and extracellular organics matter (EOM), Desalination 293 (2012) 30-37.

[168] Y. Zhang, J.Y. Tian, J. Nan, S.S. Gao, H. Liang, M.L. Wang, G.B. Li, Effect of PAC addition on immersed ultrafiltration for the treatment of algal-rich water, Journal of Hazardous Materials 186 (2011) 1415-1424.

[169] L.O. Villacorte, Y. Ekowati, H. Winters, G. Amy, J.C. Schippers, M.D. Kennedy, MF/UF rejection and fouling potential of algal organic matter from bloom-forming marine and freshwater algae, Desalination 367 (2015) 1-10.

[170] L. Li, Z. Wang, L.C. Rietveld, N. Gao, J. Hu, D. Yin, S. Yu, Comparison of the effects of extracellular and intracellular organic matter extracted from Microcystis aeruginosa on ultrafiltration membrane fouling: dynamics and mechanisms, Environmental Science & Technology 48 (2014) 14549-14557.

[171] F. Qu, H. Liang, Z. Wang, H. Wang, H. Yu, G. Li, Ultrafiltration membrane fouling by extracellular organic matters (EOM) of Microcystis aeruginosa in stationary phase: Influences of interfacial characteristics of foulants and fouling mechanisms, Water Research 46 (2012) 1490-1500.

[172] H.R. Yu, F.S. Qu, H. Liang, Z.S. Han, J. Ma, S.L. Shao, H.Q. Chang, G.B. Li, Understanding ultrafiltration membrane fouling by extracellular organic matter of Microcystis aeruginosa using fluorescence excitation-emission matrix coupled with parallel factor analysis, Desalination 337 (2014) 67-75.

[173] X. Zhang, M.E. Devanadera, F.A. Roddick, L. Fan, M.L.P. Dalida, Impact of algal organic matter released from Microcystis aeruginosa and Chlorella sp. on the fouling of a ceramic microfiltration membrane, Water Research 103 (2016) 391-400.

[174] W.W. Huang, H.Q. Chu, B.Z. Dong, Understanding the fouling of algogenic organic matter in microfiltration using membrane-foulant interaction energy analysis: Effects of organic hydrophobicity, Colloids and Surfaces B-Biointerfaces 122 (2014) 447-456.

[175] G.G. Leppard, The characterization of algal and microbial mucilages and their aggregates in aquatic ecosystems, Science of the Total Environment 165 (1995) 103-131.

[176] H.-C. Flemming, T.R. Neu, D.J. Wozniak, The EPS matrix: the "house of biofilm cells", Journal of bacteriology 189 (2007) 7945-7947.

[177] K. Mopper, K.S. Ramana, D.T. Drapeau, The role of surface-active carbohydrates in the flocculation of a diatom bloom in a mesocosm, Deep Sea Research Part II: Topical Studies in Oceanography 42 (1995) 47-73.

[178] G.A. Jackson, A model of the formation of marine algal flocs by physical coagulation processes, Deep Sea Research Part A. Oceanographic Research Papers 37 (1990) 1197-1211.

[179] L.H. Armbrecht, V. Smetacek, P. Assmy, C. Klaas, Cell death and aggregate formation in the giant diatom Coscinodiscus wailesii (Gran & Angst, 1931), Journal of experimental marine biology and ecology 452 (2014) 31-39.

[180] U. Passow, R. Shipe, A. Murray, D. Pak, M. Brzezinski, A. Alldredge, The origin of transparent exopolymer particles (TEP) and their role in the sedimentation of particulate matter, Continental Shelf Research 21 (2001) 327-346.

[181] T. Berman, M. Holenberg, Don't fall foul of biofilm through high TEP levels, Filtration & Separation 42 (2005) 30-32.

[182] L. Villacorte, Y. Ekowati, H. Calix-Ponce, V. Kisielius, J. Kleijn, J.S. Vrouwenvelder, J. Schippers, M. Kennedy, Biofouling in capillary and spiral wound membranes facilitated by marine algal bloom, Desalination 424 (2017) 74-84.

[183] T. Berman, R. Mizrahi, C.G. Dosoretz, Transparent exopolymer particles (TEP): A critical factor in aquatic biofilm initiation and fouling on filtration membranes, Desalination 276 (2011) 184-190.

[184] R. Ramanan, B.-H. Kim, D.-H. Cho, H.-M. Oh, H.-S. Kim, Algae–bacteria interactions: evolution, ecology and emerging applications, Biotechnology Advances 34 (2016) 14-29.

[185] N. Her, G. Amy, H.R. Park, M. Song, Characterizing algogenic organic matter (AOM) and evaluating associated NF membrane fouling, Water Research 38 (2004) 1427-1438.

[186] S. Babel, S. Takizawa, H. Ozaki, Factors affecting seasonal variation of membrane filtration resistance caused by Chlorella algae, Water Research 36 (2002) 1193-1202.

[187] F.S. Qu, H. Liang, J.G. He, J. Ma, Z.Z. Wang, H.R. Yu, G.B. Li, Characterization of dissolved extracellular organic matter (dEOM) and bound extracellular organic matter (bEOM) of Microcystis aeruginosa and their impacts on UF membrane fouling, Water Research 46 (2012) 2881-2890.

[188] S. Babel, S. Takizawa, Chemical pretreatment for reduction of membrane fouling caused by algae, Desalination 274 (2011) 171-176.

[189] X.L. Zhang, L.H. Fan, F.A. Roddick, Feedwater coagulation to mitigate the fouling of a ceramic MF membrane caused by soluble algal organic matter, Separation and Purification Technology 133 (2014) 221-226.

[190] S.A. Alizadeh Tabatabai, J.C. Schippers, M.D. Kennedy, Effect of coagulation on fouling potential and removal of algal organic matter in ultrafiltration pretreatment to seawater reverse osmosis, Water Research 59 (2014) 283-294.

[191] Y. Zhang, X.Y. Wang, H.J. Jia, B.G. Fu, R.W. Xu, Q. Fu, Algal fouling and extracellular organic matter removal in powdered activated carbon-submerged hollow fiber ultrafiltration membrane systems, Science of the Total Environment 671 (2019) 351-361.

[192] Y. Liu, X. Li, Y. Yang, S. Liang, Fouling control of PAC/UF process for treating algal-rich water, Desalination 355 (2015) 75-82.

[193] K. Li, F. Qu, H. Liang, S. Shao, Z.-s. Han, H. Chang, X. Du, G. Li, Performance of mesoporous adsorbent resin and powdered activated carbon in mitigating ultrafiltration membrane fouling caused by algal extracellular organic matter, Desalination 336 (2014) 129-137.

[194] M. Campinas, M.J. Rosa, Assessing PAC contribution to the NOM fouling control in PAC/UF systems, Water Research 44 (2010) 1636-1644.

[195] X.L. Zhang, L.H. Fan, F.A. Roddick, Effect of feedwater pre-treatment using UV/H2O2 for mitigating the fouling of a ceramic MF membrane caused by soluble algal organic matter, Journal of Membrane Science 493 (2015) 683-689.

[196] W.W. Huang, H.Q. Chu, B.Z. Dong, M.L. Hu, Y. Yu, A membrane combined process to cope with algae blooms in water, Desalination 355 (2015) 99-109.

[197] W.W. Huang, H.Q. Chu, B.Z. Dong, J.X. Liu, Evaluation of different algogenic organic matters on the fouling of microfiltration membranes, Desalination 344 (2014) 329-338.

[198] Y. Zhang, H. Jia, X. Wang, C. Ma, R. Xu, Q. Fu, S. Li, Comparing the effects of pre-deposited and pre-mixed powdered activated carbons on algal fouling during ultrafiltration, Algal Research 44 (2019) 101687.

[199] S. Metsamuuronen, M. Sillanpaa, A. Bhatnagar, M. Manttari, Natural Organic Matter Removal from Drinking Water by Membrane Technology, Separation and Purification Reviews 43 (2014) 1-61.

[200] B.K. Mayer, C. Johnson, Y. Yang, N. Wellenstein, E. Maher, P.J. McNamara, From micro to macro-contaminants: The impact of low-energy titanium dioxide photocatalysis followed by filtration on the mitigation of drinking water organics, Chemosphere 217 (2019) 111-121.

[201] Y. Rasouli, M. Abbasi, S.A. Hashemifard, Investigation of in-line coagulation-MF hybrid process for oily wastewater treatment by using novel ceramic membranes, Journal of Cleaner Production 161 (2017) 545-559.

[202] B. Kose‑Mutlu, M.E. Ersahin, H. Ozgun, R. Kaya, C. Kinaci, I. Koyuncu, Influence of powdered and granular activated carbon system as a pre‑treatment alternative for membrane filtration of produced water, Journal of Chemical Technology & Biotechnology 92 (2017) 283-291.

[203] G. Naidu, S. Jeong, S. Vigneswaran, S.A. Rice, Microbial activity in biofilter used as a pretreatment for seawater desalination, Desalination 309 (2013) 254-260.

[204] J.W. Hatt, E. Germain, S.J. Judd, Granular activated carbon for removal of organic matter and turbidity from secondary wastewater, Water Science and Technology 67 (2013) 846-853.

[205] M. Rickman, J. Pellegrino, R. Davis, Fouling phenomena during membrane filtration of microalgae, Journal of Membrane Science 423 (2012) 33-42.

[206] F. Qu, H. Liang, J. Zhou, J. Nan, S. Shao, J. Zhang, G. Li, Ultrafiltration membrane fouling caused by extracellular organic matter (EOM) from Microcystis aeruginosa: effects of membrane pore size and surface hydrophobicity, Journal of Membrane Science 449 (2014) 58-66.

[207] S.Q. Zhou, Y.S. Shao, N.Y. Gao, L. Li, J. Deng, C.Q. Tan, M.Q. Zhu, Influence of hydrophobic/hydrophilic fractions of extracellular organic matters of Microcystis aeruginosa on ultrafiltration membrane fouling, Science of the Total Environment 470 (2014) 201-207.

[208] V. Discart, M. Bilad, R. Moorkens, H. Arafat, I.F. Vankelecom, Decreasing membrane fouling during Chlorella vulgaris broth filtration via membrane development and coagulant assisted filtration, Algal Research 9 (2015) 55-64.

[209] X. Sun, C. Wang, Y. Tong, W. Wang, J. Wei, Microalgae filtration by UF membranes: influence of three membrane materials, Desalination and Water Treatment 52 (2014) 5229-5236.

[210] P. Pongpairoj, R. Field, Z. Cui, F. Wicaksana, A.G. Fane, Transmission of and fouling by long chain molecules during crossflow microfiltration of algal suspensions: influence of shear, Desalination and Water Treatment 35 (2011) 138-149.

[211] F. Wicaksana, A.G. Fane, P. Pongpairoj, R. Field, Microfiltration of algae (Chlorella sorokiniana): Critical flux, fouling and transmission, Journal of Membrane Science 387 (2012) 83-92.

[212] A. Ahmad, N.M. Yasin, C. Derek, J. Lim, Crossflow microfiltration of microalgae biomass for biofuel production, Desalination 302 (2012) 65-70.

[213] R. Sadiq, M.J. Rodriguez, Disinfection by-products (DBPs) in drinking water and predictive models for their occurrence: a review, Science of the Total Environment 321 (2004) 21-46.

[214] M.T. Yang, X.R. Zhang, Halopyrroles: A New Group of Highly Toxic Disinfection Byproducts Formed in Chlorinated Saline Wastewater, Environmental Science & Technology 48 (2014) 11846-11852.

[215] W. Chu, S.W. Krasner, N. Gao, M.R. Templeton, D. Yin, Contribution of the antibiotic chloramphenicol and its analogues as precursors of dichloroacetamide and other disinfection byproducts in drinking water, Environmental Science & Technology 50 (2015) 388-396.

[216] S. Ding, W. Chu, S.W. Krasner, Y. Yu, C. Fang, B. Xu, N. Gao, The stability of chlorinated, brominated, and iodinated haloacetamides in drinking water, Water Research 142 (2018) 490-500.

[217] S. Ding, Y. Deng, T. Bond, C. Fang, Z. Cao, W. Chu, Disinfection byproduct formation during drinking water treatment and distribution: A review of unintended effects of engineering agents and materials, Water Research (2019).

[218] S.D. Richardson, M.J. Plewa, E.D. Wagner, R. Schoeny, D.M. DeMarini, Occurrence, genotoxicity, and carcinogenicity of regulated and emerging disinfection by-products in drinking water: A review and roadmap for research, Mutation Research/Reviews in Mutation Research 636 (2007) 178-242.

[219] C.H. Jeong, E.D. Wagner, V.R. Siebert, S. Anduri, S.D. Richardson, E.J. Daiber, A.B. McKague, M. Kogevinas, C.M. Villanueva, E.H. Goslan, Occurrence and toxicity of disinfection byproducts in European drinking waters in relation with the HIWATE epidemiology study, Environmental Science & Technology 46 (2012) 12120-12128.

[220] S.W. Krasner, H.S. Weinberg, S.D. Richardson, S.J. Pastor, R. Chinn, M.J. Sclimenti, G.D. Onstad, A.D. Thruston, Occurrence of a new generation of disinfection byproducts, Environmental Science & Technology 40 (2006) 7175-7185.

[221] A. Al-Omari, A. Muhammetoglu, E. Karadirek, A. Jiries, M. Batarseh, B. Topkaya, S. Soyupak, A Review on Formation and Decay Kinetics of Trihalomethanes in Water of Different Qualities, CLEAN - Soil, Air, Water 42 (2014) 1687-1700.

[222] E. Mcbean, Z. Zhu, W. Zeng, Systems analysis models for disinfection by-product formation in chlorinated drinking water in Ontario, Civil Engineering and Environmental Systems 25 (2008) 127-138.

[223] K. Gopal, S.S. Tripathy, J.L. Bersillon, S.P. Dubey, Chlorination byproducts, their toxicodynamics and removal from drinking water, Journal of Hazardous Materials 140 (2007) 1-6.

[224] S.E. Hrudey, Chlorination Disinfection By-Products (DBPs) in Drinking Water and Public Health in Canada: A Primer for Public Health Practitioners: Reviewing

Evidence from Over 30 Years of Research: A Knowledge Translation Review, National Collaborating Centre for Environmental Health2008.

[225] F. Edition, Guidelines for drinking-water quality, WHO chronicle 38 (2011) 104-108.

[226] I.W.G.o.t.E.o.C.R.t. Humans, W.H. Organization, I.A.f.R.o. Cancer, Some drinking-water disinfectants and contaminants, including arsenic, IARC2004.

[227] G. Hua, D.A. Reckhow, DBP formation during chlorination and chloramination: effect of reaction time, pH, dosage, and temperature, Journal‑American Water Works Association 100 (2008) 82-95.

[228] W.H. Organization, Guidelines for drinking-water quality fourth edition, 2012.

[229] M.A. El-Dib, R.K. Ali, THMs formation during chlorination of raw Nile river water, Water Research 29 (1995) 375-378.

[230] H. Sakai, S. Tokuhara, M. Murakami, K. Kosaka, K. Oguma, S. Takizawa, Comparison of chlorination and chloramination in carbonaceous and nitrogenous disinfection byproduct formation potentials with prolonged contact time, Water Research 88 (2016) 661-670.

[231] P. Roccaro, H.S. Chang, F.G.A. Vagliasindi, G.V. Korshin, Differential absorbance study of effects of temperature on chlorine consumption and formation of disinfection by-products in chlorinated water, Water Research 42 (2008) 1879-1888.

[232] A.D. Nikolaou, T.D. Lekkas, The Role of Natural Organic Matter during Formation of Chlorination By‑products: A Review, Acta hydrochimica et hydrobiologica 29 (2001) 63-77.

[233] T. Bond, E. Goslan, S. Parsons, B. Jefferson, Treatment of disinfection by‑product precursors, Environmental Technology 32 (2011) 1-25.

[234] T. Bond, E.H. Goslan, S.A. Parsons, B. Jefferson, A critical review of trihalomethane and haloacetic acid formation from natural organic matter surrogates, Environmental Technology Reviews 1 (2012) 93-113.

[235] J.M. Symons, S.W. Krasner, L.A. Simms, M. Sclimenti, Measurement of THM and precursor concentrations revisited: the effect of bromide ion, Journal‑American Water Works Association 85 (1993) 51-62.

[236] G.H. Hua, D.A. Reckhow, J. Kim, Effect of bromide and iodide ions on the formation and speciation of disinfection byproducts during chlorination, Environmental Science & Technology 40 (2006) 3050-3056.

[237] J.Y. Jiang, X.G. Zhang, X.H. Zhu, Y. Li, Removal of Intermediate Aromatic Halogenated DBPs by Activated Carbon Adsorption: A New Approach to

Controlling Halogenated DBPs in Chlorinated Drinking Water, Environmental Science & Technology 51 (2017) 3435-3444.

[238] W.A. Cheema, T. Manasfi, K.M.S. Kaarsholm, H.R. Andersen, J.L. Boudenne, Effect of medium-pressure UV-lamp treatment on disinfection by-products in chlorinated seawater swimming pool waters, Science of the Total Environment 599 (2017) 910-917.

[239] S.E. Duirk, R.L. Valentine, Modeling dichloroacetic acid formation from the reaction of monochloramine with natural organic matter, Water Research 40 (2006) 2667-2674.

[240] N. Ates, M. Kitis, U. Yetis, Formation of chlorination by-products. in waters with low SUVA-correlations with SUVA and differential UV spectroscopy, Water Research 41 (2007) 4139-4148.

[241] X. Zhang, L. Fan, F.A. Roddick, Influence of the characteristics of soluble algal organic matter released from Microcystis aeruginosa on the fouling of a ceramic microfiltration membrane, Journal of Membrane Science 425 (2013) 23-29.

[242] W. Huang, H. Chu, B. Dong, Characteristics of algogenic organic matter generated under different nutrient conditions and subsequent impact on microfiltration membrane fouling, Desalination 293 (2012) 104-111.

[243] L.C. Hua, C.H. Lai, G.S. Wang, T.F. Lin, C.P. Huang, Algogenic organic matter derived DBPs: Precursor characterization, formation, and future perspectives - A review, Critical Reviews in Environmental Science and Technology 49 (2019) 1803-1834.

[244] Y.S. Lui, H.C. Hong, G.J.S. Zheng, Y. Liang, Fractionated algal organic materials as precursors of disinfection by-products and mutagens upon chlorination, Journal of Hazardous Materials 209 (2012) 278-284.

[245] H. Lv, J. Yang, L. Liu, X. Yu, Z. Yu, P. Chiang, Temperature and nutrients are significant drivers of seasonal shift in phytoplankton community from a drinking water reservoir, subtropical China, Environmental Science and Pollution Research 21 (2014) 5917-5928.

[246] Y. Liang, Y.S. Lui, H. Hong, Fatty acids and algal lipids as precursors of chlorination by-products, Journal of Environmental Sciences 24 (2012) 1942-1946.

[247] Y.S. Lui, J.W. Qiu, Y.L. Zhang, M.H. Wong, Y. Liang, Algal-derived organic matter as precursors of disinfection by-products and mutagens upon chlorination, Water Research 45 (2011) 1454-1462.

[248] X. Yang, W.H. Guo, Q.Q. Shen, Formation of disinfection byproducts from chlor(am)ination of algal organic matter, Journal of Hazardous Materials 197 (2011) 378-388.

[249] J.Y. Fang, J. Ma, X. Yang, C. Shang, Formation of carbonaceous and nitrogenous disinfection by-products from the chlorination of Microcystis aeruginosa, Water Research 44 (2010) 1934-1940.

[250] L. Li, N.Y. Gao, Y. Deng, J.J. Yao, K.J. Zhang, Characterization of intracellular & extracellular algae organic matters (AOM) of Microcystic aeruginosa and formation of AOM-associated disinfection byproducts and odor & taste compounds, Water Research 46 (2012) 1233-1240.

[251] J. Huang, N. Graham, M.R. Templeton, Y. Zhang, C. Collins, M. Nieuwenhuijsen, A comparison of the role of two blue–green algae in THM and HAA formation, Water Research 43 (2009) 3009-3018.

[252] M.L. Nguyen, P. Westerhoff, L. Baker, Q. Hu, M. Esparza-Soto, M. Sommerfeld, Characteristics and reactivity of algae-produced dissolved organic carbon, Journal of Environmental Engineering-Asce 131 (2005) 1574-1582.

[253] X.B. Liao, J.J. Liu, M.L. Yang, H.F. Ma, B.L. Yuan, C.H. Huang, Evaluation of disinfection by-product formation potential (DBPFP) during chlorination of two algae species - Blue-green Microcystis aeruginosa and diatom Cyclotella meneghiniana, Science of the Total Environment 532 (2015) 540-547.

[254] J.K. Edzwald, Water Quality and Treatment A Handbook on Drinking Water, McGrawHill2010.

[255] J.R. Bolton, C.A. Cotton, The ultraviolet disinfection handbook, American Water Works Association2011.

[256] J.P. Malley, J.P. Shaw, J.R. Ropp, Evaluation of by-products produced by treatment of groundwaters with ultraviolet irradiation, AWWAR1996.

[257] J.P. Shaw, J.P. Malley Jr, S.A. Willoughby, Effects of UV irradiation on organic matter, Journal‐American Water Works Association 92 (2000) 157-167.

[258] A.D. Shah, A.D. Dotson, K.G. Linden, W.A. Mitch, Impact of UV disinfection combined with chlorination/chloramination on the formation of halonitromethanes and haloacetonitriles in drinking water, Environmental Science & Technology 45 (2011) 3657-3664.

[259] F.H. Frimmel, Impact of light on the properties of aquatic natural organic matter, Environment International 24 (1998) 559-571.

[260] J. Thomson, F.A. Roddick, M. Drikas, Vacuum ultraviolet irradiation for natural organic matter removal, Journal of Water Supply: Research and Technology-Aqua 53 (2004) 193-206.

[261] W. Buchanan, F. Roddick, N. Porter, M. Drikas, Fractionation of UV and VUV pretreated natural organic matter from drinking water, Environmental Science & Technology 39 (2005) 4647-4654.

[262] E.H. Goslan, F. Gurses, J. Banks, S.A. Parsons, An investigation into reservoir NOM reduction by UV photolysis and advanced oxidation processes, Chemosphere 65 (2006) 1113-1119.

[263] W. Liu, S. Andrews, J. Bolton, K. Linden, C. Sharpless, M. Stefan, Comparison of disinfection byproduct (DBP) formation from different UV technologies at bench scale, Water Science and Technology: Water Supply 2 (2002) 515-521.

[264] David Shepherd, Rowena Gee, Tom Hall, Paul Rumsby, G. Dillon, Effect of UV on the Chemical Composition of water including DBP formation_final report, 2015.

[265] Y. Choi, Y.J. Choi, The effects of UV disinfection on drinking water quality in distribution systems, Water Research 44 (2010) 115-122.

[266] W. Liu, L.M. Cheung, X. Yang, C. Shang, THM, HAA and CNCl formation from UV irradiation and chlor(am)ination of selected organic waters, Water Research 40 (2006) 2033-2043.

[267] F. Dong, Q. Lin, J. Deng, T. Zhang, C. Li, X. Zai, Impact of UV irradiation on Chlorella sp. damage and disinfection byproducts formation during subsequent chlorination of algal organic matter, Science of the Total Environment 671 (2019) 519-527.

Chapter 3

3 Optimization and Modeling for Coagulation-Flocculation to Remove Algae and Organic Matter from Surface Water by Response Surface Methodology[1]

3.1 Introduction

A persistent worldwide concern in drinking water treatment is the proliferation of algae and the resultant metabolites in source water. Rivers, lakes and reservoirs as important freshwater reserves in China are facing increasing threat of eutrophication [1]. According to the "China's Ecological Environment Statements Bulletin of 2017", about 30% of China's lakes and reservoirs suffer from mild to moderate level of eutrophication [2]. Lake Taihu is one of the largest freshwater lakes in eastern China affected by algal blooms periodically due to non-point nutrient run-off sources, while Lake Dianchi, a heavily polluted lake in Yunnan province shows both algal and fungi pollution. Algae bloom not only affects the ecology and aesthetic value of the aquatic system [3], it also derives multiple problems and pose many challenges to drinking water treatment, such as increasing coagulant demand, clogging filters [4, 5], taste and odor issues [6] and disinfection byproduct formation [7-9]. Blooms involving toxin-producing algal species even can pose serious threats to human health [10, 11]. The increasingly water eutrophication caused by cyanobacteria outbreak, resulted in several serious threats to local residential, commercial, industrial and agricultural production.

Many countries and the World Health Organization (WHO) have established a guideline (1-1.5 µg/L) for microcystin-LR (MC-LR), which is one of the most toxic cyanotoxin

---

[1] A version of this chapter has been published in a manuscript entitled "Z. Zhao, W. Sun, M.B. Ray, A.K. Ray, T. Huang, J. Chen, Optimization and modeling of coagulation-flocculation to remove algae and organic matter from surface water by response surface methodology, Frontiers of Environmental Science & Engineering 13 (2019) 75."

produced by *Microcystis aeruginosa* [12]. In 2007, the large-scale cyanobacteria outbreak in Lake Taihu from May to June caused a serious safety threat to drinking water and led to the disruption of water supplies to millions of people in Wuxi and its surrounding areas [13]. Lake Yangcheng is the third largest freshwater lake on the Taihu Plain. It is also the main drinking water source for Suzhou and Kunshan urban areas. As the second drinking water source for the city of Wuxi, Lake Yangcheng has been affected by severe eutrophication [14], which has resulted in the cyanobacteria blooms. Therefore, it is of vital importance to enhance the removal of algae and dissolved organic matter in the water treatment process.

Among the conventional water treatment processes, coagulation-flocculation is one of the economical methods to deal with "algal blooms" caused by the outbreak of microalgae [15]. As the primary barrier for algal removal in conventional drinking water treatment, several studies have focused on investigations of coagulation with/without pre-treatment for algae cells and the metabolites removal from raw water. It has been found that the removal of algal cells is easier than the removal of dissolved algal organic matter (AOM) [16]. More than 98% of algal cells could be removed by aluminum chloride dosage of 13 mg/L when the initial cell density was less than 1.0×10^6 cell/L [7]. However, for the combined coagulation and peroxidation processes, a poor removal of *Microcystis aeruginosa* cells and larger amount of trihalomethane (THM) formation occurred due to the release of AOM after peroxidation [17].

Considering the maximal algae removal with avoiding the lysis of algal cells to release AOM, it is necessary to enhance the coagulation conditions for maximum removal of algal cells and AOM without causing cell lysis. The success of this process implementation depends on how precisely pH and coagulant dosage are chosen with respect to the specific initial water quality.

Response surface methodology (RSM), as a combination of mathematical and statistical methods, has been widely applied for solving multivariable problems to optimize the process parameters with less number of experimental runs and analyzing the interaction between the parameters. The objectives of RSM are: (1) to develop approximating functions for predicting responses, and (2) to optimize the responses based on the factors

of interests [18]. The advantages of the RSM include a low number of tests, high precision of regression equations, and continuous analysis of various levels of test factors. It has been widely applied in engineering fields, such as biology, medicine and environment [19-24]. The most commonly used RSM method is the central composite design (CCD), which includes center points, factorial points, and axial points. From the CCD design, a quadratic approximation can be employed to develop a second-order response surface model for predicting the optimal point for a certain set of variables as follows:

$$\widehat{Y} = \beta_0 + \sum_{i=1}^{3} \beta_i x_i + \sum_{i=1}^{3} \beta_{ii} x_i^2 + \sum_{i<j}^{3} \beta_{ij} x_i x_j + \epsilon \qquad \text{(Eq. 3.1)}$$

Where $\widehat{Y}$ is the predicted response; β_0, β_i, β_{ii} and β_{ij} are the coefficients for the intercept, linear, square, and interaction term of regression, respectively, which can be derived from ordinary least squares (OLS) or multiple linear regression (MLR), x_i and x_j represent the coded values of independent variables, ϵ indicates the statistical error.

Artificial Neural Networks (ANN) are computing systems with learning algorithms and architectures inspired by the working and structure of the human brain. Although there is a considerable amount of investigations on various scenarios using both RSM and ANN techniques in the literatures [25, 26], only a few studies on the coagulation-flocculation process were presented with the methods of both RSM and ANN techniques. Gadekar developed an artificial neural network to predict color removal using aluminum-based coagulant to remove color from a disperse dye solution; the performance of the model had correlation coefficient (R^2) values greater than 0.90 [27]. To minimize settled water turbidity, It was reported that ANN can be applied to predict both the optimum carbon dioxide and coagulation dosages with R^2 values of 0.68 and 0.90, respectively [28].

Hence, the key motivation behind this study was to develop an approach to evaluate and predict coagulation process efficiency for the removal of turbidity, cells, DOC and UV_{254} absorbance of algae and organic matter using both RSM and ANN techniques. A two-level, three-factors CCD design was applied to investigate the correlation between experimental variables and responses as the removals of microalgae, turbidity and dissolved organic carbon (DOC) in a real surface water body to provide solutions for the treatment of algae and algal matter-rich raw water.

3.2 Materials and methods

3.2.1 Study site and sample collection

Lake Yangchen (31°25′N, 120°48′E), located between Lake Tai and the Yangtze River, has a surface area of about 20 km^2 and a mean depth of 1.9 m with an annual average temperature of 16-18 ℃. As the third-largest freshwater lake on the Taihu Plain, Lake Yangcheng is the major drinking water source in Suzhou and Kunshan urban areas, and the second drinking water source of Wuxi City. The water samples from the Lake Yangcheng were collected twice per month in a 25 L plastic container from July 15 to August 31, 2017. All samples were preserved in the fridge (≈ 5 ℃) before use within two weeks. The characteristics of raw water during the test period are shown in Table 3.1.

3.2.2 Coagulation-flocculation

Coagulant aluminum sulfate hydrate (Al$_2$(SO$_4$)$_3$·18H$_2$O), sodium hydroxide and hydrochloric acid for pH adjustment, were all of analytical grade and commercially available from Shanghai Lujie Chemical Reagent Co., Ltd., China. Coagulation tests were conducted using model ZR4-6 joint coagulation experiment mixer (Shenzhen Zhongshui Co., Ltd, China). Hemocytometer (Dark Line (0650010), Paul Marienfeld GmbH & Co., Germany) and microscope (CX-23, Olympus Co., Japan) were used for counting the algal cells before and after coagulation. The turbidity was measured using a Turbidity meter, (Hach 2100Q, Hach Company, USA). The DOC and UV$_{254}$ absorbance of water samples were measured using a Shimadzu TOC-L analyzer (CPH TOC, Shimadzu Scientific Instruments Ltd., Japan) and UV-Vis spectrophotometer (Model V-1200, Shanghai Meipuda Instrument Ltd., China), respectively.

Coagulation-flocculation experiments of 2 L algae-laden water were performed at room temperature, various pH, alum doses (mg Al/L) and initial cell densities. The pH of the test solution was adjusted by adding pre-determined amount of 0.1 M hydrochloric acid or 0.1 M sodium hydroxide solution prior to the coagulation. The algal suspension was mixed at the agitation speed (150 rpm) for 2 min followed by a low mix/flocculation of 25 rpm for 20 min, and finally a 30 min settling. The supernatant was taken from 2 cm below the water

surface for analysis of remaining cell density and turbidity. The DOC and UV_{254} absorbance were measured after filtering the supernatant through 0.45 µm membrane filter (Tianjin JINTENG Co., Ltd., China). The effects of alum dose, pH and initial cell density on coagulation performance experiments were conducted in duplicated and reported with average values, which were calculated from the supplementary data in Appendix A.

Table 3.1 Water quality characteristics of Lake Yangcheng.

Parameters	Range	Mean
pH	7.08 - 8.45	7.48
Temperature (℃)	25 – 28	27
Cell density (10^6 cell/ml)	4.2 - 5.8	4.6
Turbidity (NTU)	198 – 252	223
DOC (mg/L)	10.2 – 13.5	12.41
UV_{254} absorbance (m^{-1})	0.083 – 0.094	0.089

Quantitative characterization of algae species in water was carried out using alga counter (Algae C model from Wansheng Ltd., China) and an automatic identification software.

3.2.3 Response surface methodology with central composite design

Preliminary experiments indicated that three major variables affected coagulation-flocculation performance: coagulant dosage, pH and initial algal cell density, and experiments with single factor investigations narrowed the range of variables prior to experimental design. Based on those results, a complete set of the three-factor central CCD design shown in Table 3.2 was applied to investigate the effects of individual variables and their interactions on the removal of algal cell, turbidity, DOC and UV_{254} absorbance to determine the response pattern and optimum combination of variables. Fourteen experimental runs were augmented with six replications at the center values (zero level) to evaluate the experimental error. The significance of each variable's effect on responses can only be compared with a coded pattern because of their different units and limits of variation. For statistical calculations, the variable X_i was coded as x_i according to the following Equation 3.2:

$$x_i = (X_i - X_0) / \delta X \qquad \text{(Eq. 3.2)}$$

where X_i is the uncoded value of the ith independent variable, X_0 is the value of ith variable at the center point of the experimental range and δX is the step change [29].

Table 3.2 Analytical factors and levels for RSM experimental design.

Variables		Coded and actual levels				
		$-\alpha/-1.682$	-1	0	1	$+\alpha/1.682$
X_1	Alum dose（mg Al/L）	4.57	5.67	7.29	8.91	10.02
X_2	pH	4.66	5.00	5.50	6.00	6.34
X_3	Initial Cell Density（10^6 cell/ml）	2.32	3.00	4.00	5.00	5.68

Analysis of variance (ANOVA) was applied for data analyses to determine the interactions between the variables and the responses. The fit quality of polynomial regression models were demonstrated by the coefficient of determination R^2, and F-test and p-value (probability) evaluation were applied to check statistical significances with 95% confidence level.

3.2.4 Artificial neural network model

A feed-forward backpropagation neural network algorithm (BPNN) with three layers was developed by a neural network tool box of MATLAB software version 9.2.0 (R 2017a). Mathematically, the structure of a 3-layer ANN with n, m, and p the number of input, hidden and output nodes, respectively, is shown in Figure 3.1:
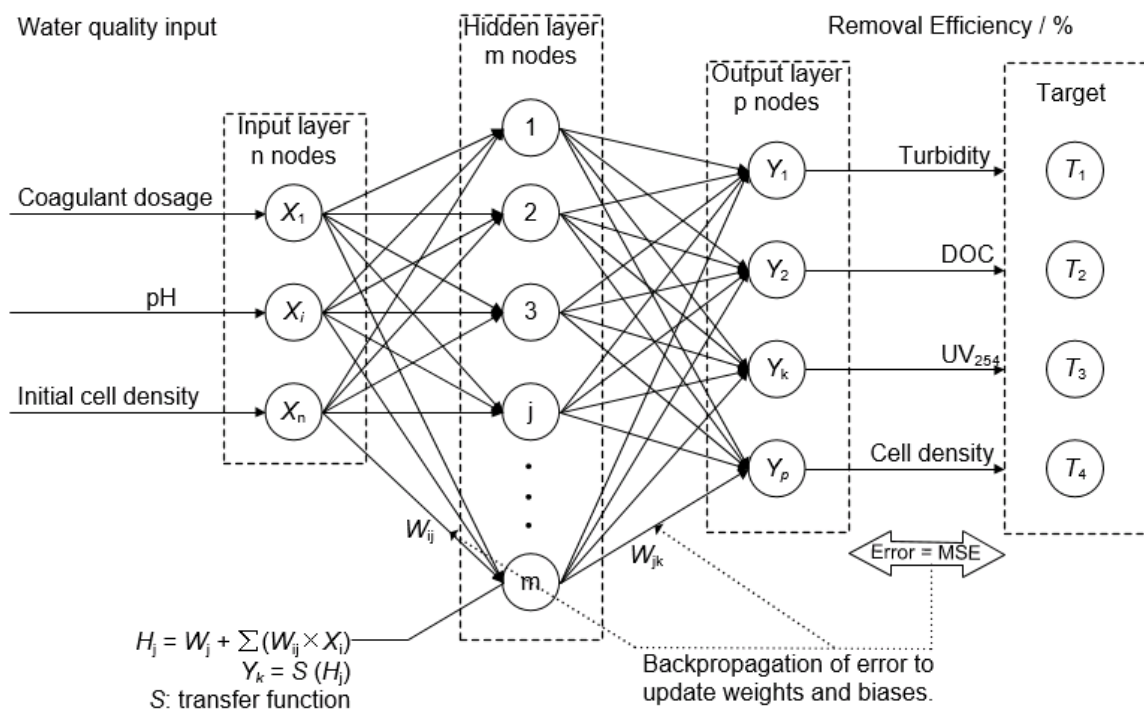
Figure 3.1 Architecture of the three layers backpropagation artificial neural network (BPNN).

where Y_k are the output values (responses) and X_i are the input values (variables) of the network; W_{ij} are the connection weights between the input layer and the hidden layer; W_{jk} are the connection weights between the hidden layer and the output layer; S is the transfer function. At each node, the weighted input signals are summed with a bias value (W_j). The combined input (H_i) then passes through the transfer function (S) to produce the output node (Y_k) as demonstrated in Figure 3.1 [30]. The Levenberg - Marquardt back propagation algorithm was used for ANN model training. The proposed neural networks had two transfer functions, of which the first transfer function was tansig and the second one was linear transfer function (purelin) [27].

A total of 44 data points, including the data from CCD experiments, single variable (alum dose, pH and initial cell density) and validation investigations, were used in ANN modelling. These data points were split randomly into training (70%), validation (15%), and test (15%) subsets. All variables values were normalized in the limits from -1 to +1 using the following Equation 3.3:

$$\text{Normalized data} = \left[\frac{2X_{AC}-(X_{min}+X_{max})}{X_{max}-X_{min}}\right] \text{[31, 32]} \qquad \text{(Eq. 3.3)}$$

To match the tangent sigmoid function applied in ANN modeling, where X_{AC}, X_{min} and X_{max} were the actual, minimum, and maximum data, respectively. A minimum mean squared error (MSE) shown as the following Equation 3.4, where Y_i and $\widehat{Y_i}$ were the ith experimental and predicted values were computed. The ANN model and the variation of experimental parameters were evaluated based on the minimum value of the MSE of the training and prediction set.

$$\text{MSE} = \frac{1}{n}\sum_{i=1}^{n}(Y_i - \widehat{Y_i})^2 \qquad \text{(Eq. 3.4)}$$

The training parameters were used with three input nodes, 8 to 10 hidden neurons and one output node with respect to one response each time, learning rule: Levenberg–Marquardt, number of epochs: 1000, error goal: 0.0001 in this study.

3.3 Results and discussion

3.3.1 Algae species distribution

As shown in Figure 3.2, more than 98% of the microalgae in the investigated water body were cyanobacteria (mainly *Microcystis*), only 0.1% and 0.34% of algae belonged to *Oscillatoria* in the two samples, while the concentration of *Nitzschia palea*, a diatom, was 1.55% and 1.67%, respectively, in the two samples. The amount of *Protosiphon*, a *Chlorophyta* detected in sample 2 shown in Figure 3.2(b), was only 0.03%. Considering the average cell density of 4.6×10^6 cell/ml, water sample was seriously contaminated by cyanobacterial bloom, which may be due to the surrounding municipal and industrial wastewater discharge containing high total phosphorus and total nitrogen into water under mild hydrological and weather condition [33]. Therefore, as shown in Figure 3.2, *Microcystis* dominated the phytoplankton community. The average specific UV absorbance (SUVA) of 0.7 L/(m·mg C) indicated that the dissolved organic matter in algae-laden water was predominately hydrophilic, with low SUVA value (0.3-1.7 L/(m·mg C)) [34].
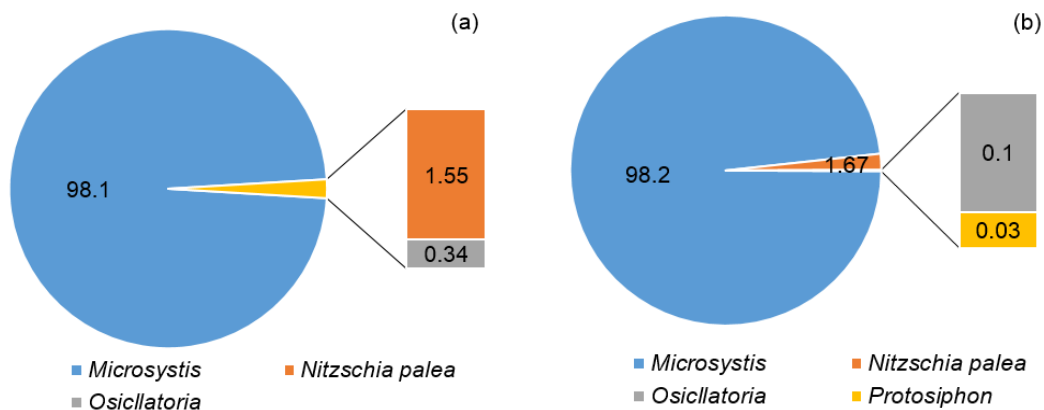
Figure 3.2 Algal species distribution in raw water.

3.3.2 Effect of alum dose on the coagulation performance

Aluminum sulfate (alum) is one of the most commonly applied coagulants in water treatment plants, due to its cost-effectivity and widespread availability [35]. The dosage of coagulant is the most vital parameter for algae and dissolved organic matter removal. The effects of alum dose on the coagulation performance for the removal of algal cells, turbidity, DOC and UV_{254} absorbance with initial cell density of $(4.9 \pm 0.3) \times 10^6$ cell/ml at the coagulant dosage range of $3.2 – 8.1$ mg Al/L (40-100 mg/L alum calculated using the mass of $Al_2 (SO_4)_3$ 18 H_2O) are presented in Figure 3.3.
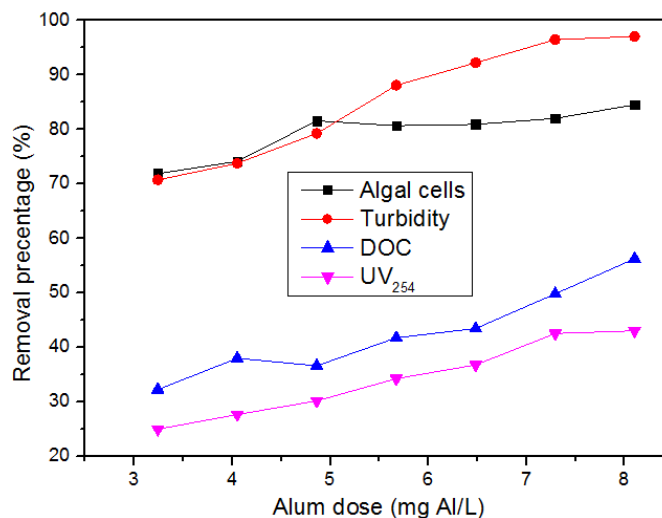
Figure 3.3 Effect of alum dosage on coagulation performance for the water samples with cell density of 4.55×10^6 cell/ml without pH adjustment.

The coagulation performance increased with the increasing of the coagulant dose for the removals of turbidity, DOC and UV_{254} absorbance, consistent with previous results of increased DOM removal with the increasing alum dose to a certain point [36]. However, higher alum dosage will contribute to relatively high aluminum residuals causing a possible health hazard, although this can be remediated, even be avoided, by pH control in the finished water [37]. It can be noted that the cell removal efficiency reached a plateau at dosage $\geq$ 4.86 mg Al/L with the maximum algal cell removal of 81.6 $\pm$ 5.8%. With the increase of alum dose, the removals efficiency of turbidity, DOC and UV_{254} absorbance increased up to 97.0 $\pm$ 1.4%, 56.3 $\pm$ 3.1% and 43.0 $\pm$ 0.1%, respectively, which can be explained by the higher charge neutralization ability with the increase of alum dose [38]. However, at a higher dose, charge reversal may occur and result in a reduction of the removal efficiency. Considering the potential health risk of high alum dosage, 7.3 mg Al/L was chosen as the appropriate alum dose for further experiments.

3.3.3 Effect of pH on the coagulation performance

The effect of pH on the coagulation performance was tested at variable pH between 4.5 and 7.0 with the same initial algal cell density and coagulant dosage of 7.3 mg Al/L (Figure 3.4). It can be noted that higher removals of all four responses occurred at lower pH of 4.5-6.0. The maximum algal cell removal of 94.2 $\pm$ 1.6% occurred at pH 6.0; however, for turbidity, DOC and UV_{254} absorbance removals, the maximum coagulation performance of 97.4 $\pm$ 0.2%, 53.2 $\pm$ 1.8%, and 47.7 $\pm$ 1.2% occurred at pH 5.5, 5.0 and 5.5, respectively. At pH lower than 5.5, positive hydrolyzates, such as $Al(OH)^{2+}$, $Al_2(OH)_2^{4+}$ were formed by alum, which neutralize the exterior negative charges of cell and colloids to promote the floc growth by physical or chemical adsorption of destabilized cell and DOM colloids [39]. At pH $\geq$ 6.0, $Al(OH)_4^-$ formed, which was not beneficial for negative charge neutralization of the cells [40].
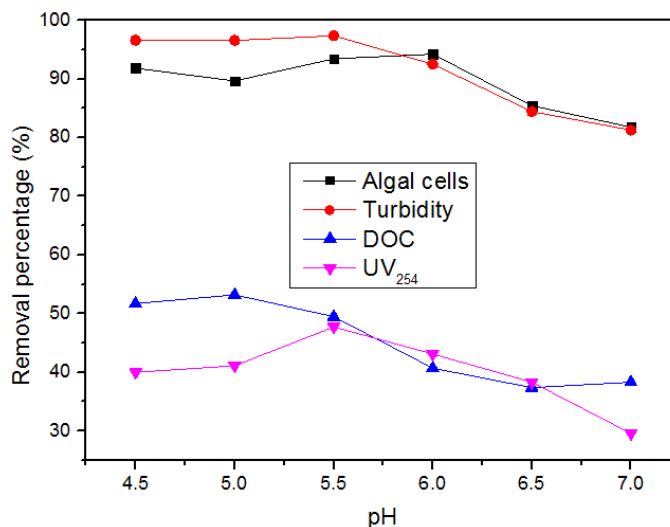
Figure 3.4 Effect of pH on coagulation performance for the water samples with cell density of 4.5×10^6 cell/ml under the coagulation dosage 7.30 mg Al/L.

It also indicated that the cationic $[H]^+$ to neutralize the surface charge of algal cell required was less than DOM in water, so that algal cell reached the maximum removal efficiency at a relatively higher pH of 6 compared to DOM (represented by DOC). The pH value of 5.5 was chosen as the most feasible pH for the removals of algal cells, turbidity, DOC, and UV_{254} absorbance.

3.3.4 Effect of initial cell density on the coagulation performance

It was noticed that the removal performance at various initial cell densities and the constant coagulant dosage resulted in different removal efficiencies. Thus, the relationship between initial cell density and required coagulant dosages on removal efficiency was further investigated at different cell density with fixed coagulation dosage and initial pH. It indicated that the four responses of coagulation performance increased initially then decreased with the increase of cell density as shown in Figure 3.5.
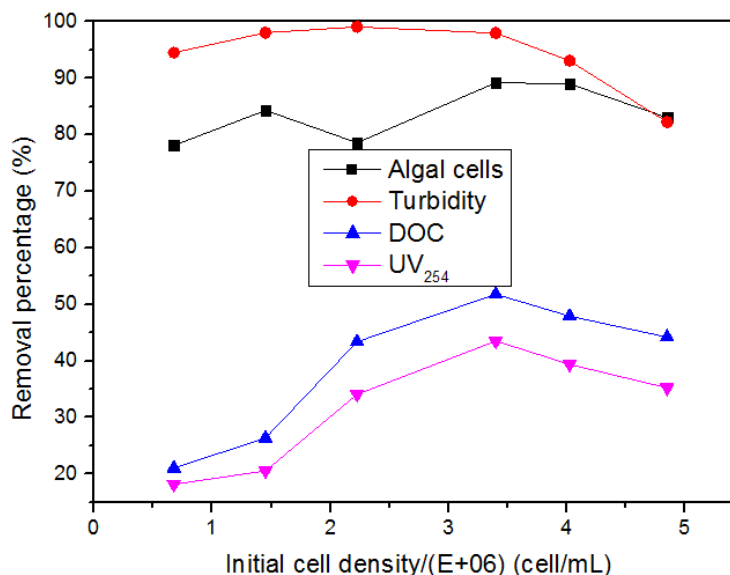
Figure 3.5 Effect of initial cell density on coagulation performance under the coagulation dosage 7.30 mg Al/L and pH of 5.5.

For the water sample with low cell density (less than 2×10^6 cell/L) and concentration of DOM, the dosage of 7.3 mg Al/L coagulant may be considered as overdose, as the re-stabilization of cell and organic matter occurred resulting in lower removal efficiency of algal cells, turbidity, DOC and UV_{254} absorbance. Once the cell density increased further with the increase of the concentration of DOM in water, the dosage of 7.3 mg Al/L coagulant demonstrated the maximum removal efficiency of the cell density of 3.3×10^6 cell/ml. The removal percentage decreased with the increase of cell density due to relatively insufficient coagulant dosage.

3.3.5 Response surface model and analysis of variance (ANOVA)

Due to the aforementioned factors, a set of central composite design (CCD) experiments for optimization of parameters, such as alum dose, coagulation pH, and initial cell density were performed to locate the maximum removal efficiency of algal cells, turbidity, DOC and UV_{254} absorbance by Design Expert 7.0 (trial version) from the experimental data shown in Table 3.3.

Table 3.3 CCD experimental design and experimental results.

Run	Experimental variables			Removal percentage (%)			
	Alum dosage/X_1 (mg Al/L)	pH/ X_2	Initial cell density/ X_3 (E+06 cell/mL)	Algal cells	Turbidity	DOC	UV$_{254}$
1	5.7	5.0	3.0	93.9	81.3	48.6	28.3
2	8.9	5.0	3.0	92.8	92.1	46.4	20.6
3	5.7	6.0	3.0	89.5	78.7	41.6	19.2
4	8.9	6.0	3.0	91.5	91.3	40.9	28.9
5	5.7	5.0	5.0	86.1	85.1	38.9	27.2
6	8.9	5.0	5.0	96.9	91.5	44.0	15.0
7	5.7	6.0	5.0	83.2	87.1	40.2	24.4
8	8.9	6.0	5.0	94.7	92.8	47.1	20.1
9	4.6	5.5	4.0	91.7	76.7	37.7	25.9
10	10.0	5.5	4.0	92.2	89.4	47.6	24.0
11	7.3	4.7	4.0	93.7	97.4	45.9	28.1
12	7.3	6.3	4.0	90.1	87.7	45.3	25.4
13	7.3	5.5	2.3	93.1	97.3	48.2	26.0
14	7.3	5.5	5.7	92.7	93.7	43.4	24.0
15	7.3	5.5	4.0	96.9	95.9	50.8	30.4
16	7.3	5.5	4.0	97.5	95.9	51.6	30.0
17	7.3	5.5	4.0	97.4	96.2	51.2	30.1
18	7.3	5.5	4.0	97.8	96.0	51.4	30.4
19	7.3	5.5	4.0	97.0	96.0	51.0	30.6
20	7.3	5.5	4.0	97.1	95.9	51.0	30.0

Based on the experimental and ANOVA results, the quadratic regression equations were developed on the basis of CCD experimental sets and input variables, where X_1, X_2, X_3, are the alum dosage (mg/L), coagulation pH and initial cell density (10^6 cell/ml), respectively, only significant items were presented in the regression equation presented in the Equation 3.5-3.8.

$$\textbf{Cell removal}/\% = -168.3 + 6.1\,X_1 + 89.1\,X_2 + 1.3\,X_3 + 1.6\,X_1X_3 - 0.8\,X_1^2$$

$$- 8.3\,X_2^2 - 1.7\,X_3^2, \qquad \text{(Eq. 3.5)}$$

$$\textbf{Turbidity removal}\ /\% = -217.0 + 30.7\,X_1 + 72.0\,X_2 - 1.9\,X_1^2 - 6.8\,X_2^2, \qquad \text{(Eq. 3.6)}$$

$$\textbf{DOC removal}\ /\% = -176.0 + 14.2\,X_1 + 76.3\,X_2 - 16.3\,X_3 + 1.2\,X_1X_3 + 4.2\,X_2X_3 - 1.2$$

$$X_1^2 - 8.6\,X_2^2 - 2.1\,X_3^2, \qquad \text{(Eq. 3.7)}$$

$$\textbf{UV}_{254}\ \textbf{absorbance removal}\ /\% = -137.9 - 3.4\,X_1 + 47.3\,X_2 + 28.2\,X_3 + 3.9\,X_1X_2 - 1.4$$

$$X_1X_3 - 0.9\,X_1^2 - 6.9\,X_2^2 - 2.4\,X_3^2, \qquad \text{(Eq. 3.8)}$$

To validate the response surface model from a statistical standpoint, the significance of the regression model and the lack-of-fit need to be addressed [26]. Generally, F-value or p value (also called the Prob>F value) are commonly used to evaluate the significance of the models. The larger F-value and correspondingly smaller p value, indicate the significance of the established regression model. A p value less than 0.05 represents that the design model is statistically significant. The p value for each regression model was less than 0.05 with the lowest values of 0.0006, which indicated that each of the regression model obtained above was significant. The precision of the model can be demonstrated by the coefficient determination (R^2) to quantify the strength of the correlation between the observed and predicted values and calculated as the following Equation 3.9 [41]:

$$R = \frac{\sum_{i=1}^{n}(Y_i - \bar{Y}_i)(\hat{Y}_i - \bar{\hat{Y}}_i)}{\sqrt{\sum_{i=1}^{n}(Y_i - \bar{Y}_i)^2}\sqrt{\sum_{i=1}^{n}(\hat{Y}_i - \bar{\hat{Y}}_i)^2}} \qquad \text{(Eq. 3.9)}$$

where i is the data number, Y_i is observed value, $\hat{Y}_i$ is predicted value, $\bar{Y}_i$ and $\bar{\hat{Y}}_i$ are the means of Y_i and $\hat{Y}_i$, respectively.

The R^2 values for turbidity, DOC, UV$_{254}$ absorbance, and cell removal efficiencies were determined as 0.901, 0.950, 0.893 and 0.890, respectively. The values of the coefficient of determination ($R^2 \geq 0.89$) indicated that more than 89% of the variability in the responses could be explained by the models. The obtained adequate precision (AP) of the models compares the range of the predicted values at the design points to the average prediction error, which indicates the signal-to-noise ratio and a ratio, greater than 4 is desirable [42]. In the present study, the obtained values with the minimum of 10.99 as shown in Table 3.4 indicated an adequate signal and suggested that the models can describe the relationship of variables and responses successfully.

Table 3.4 ANOVA Results for Regression Models.

ANOVA	Response			
	Turbidity	**DOC**	**UV$_{254}$**	**Algal cells**
R^2	0.909	0.952	0.893	0.890
p	0.0006	<0.0001	0.0002	<0.0001
Std. Dev.	2.7	1.4	1.9	1.7
Mean	90.9	46.1	25.9	93.3
C.V.%	3.0	2.8	7.3	1.8
PRESS	564.5	104.2	216.7	157.1
AP	11.1	15.8	11.0	11.6

The coefficient of variation (C.V.%) represents the ratio of the standard deviation to the average response value in the model. The smaller the value is, the smaller the dispersion in data. In this study, the maximum C.V.% value of 7.3% was less than 15% removal efficiency of UV$_{254}$ absorbance, which indicated that the reliability of the data was very high, and the experiment had high reproducibility. These findings revealed that the accuracy and ability of the polynomial models obtained for observed responses were appropriate and satisfactory.

Response surfaces for removal efficiency of the coagulation process for algae-laden lake water were created by Design-Expert 8.0 and shown in Figure 3.6. Based on ANOVA results, there was no interaction effect of the variables for turbidity removal. It indicated that alum dose and pH had the dominant effects on turbidity removal, initial cell density had insignificant effects even though turbidity increased with the increase of initial cell density in the experimental range. Figure 3.6(a) and (b) showed the response surface and contour plots for cell density and turbidity removal efficiency as a function of alum dose and pH at an initial cell density of 4.0×10^6 cell/ml. The highest removal efficiency (97.8%, 97.4% for algal cells and turbidity, respectively) occurred at the alum dosage of 7.3 mg Al/L and pH of 5.5. The lowest removal occurred at the higher pH of 6.0 and a low coagulant dose of 5.7 mg Al/L. It was found that the algal cells and turbidity removal efficiency presented the same pattern, which decreased with increasing pH up to 6.0 at the low coagulant dose of 5.7 mg Al/L.
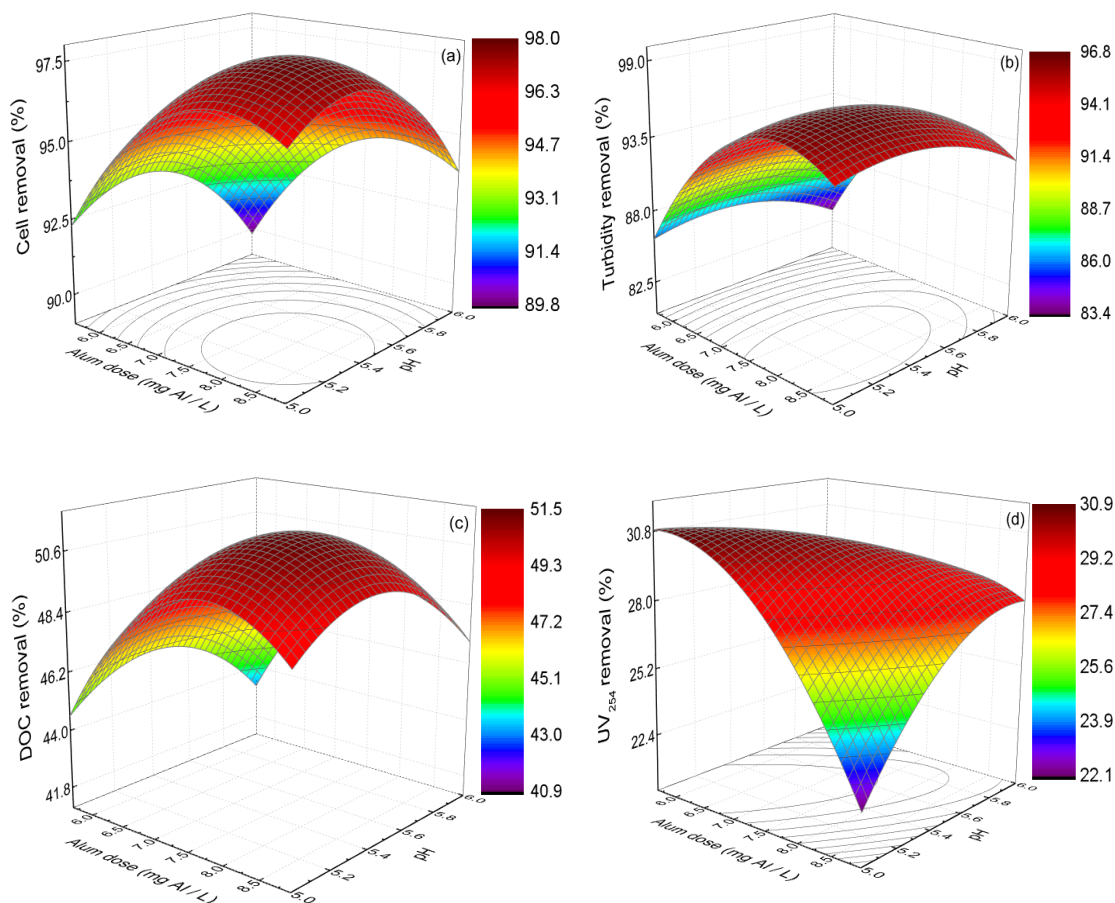
Figure 3.6 Surface plots of removal efficiency with the interaction of coagulant dosage and pH with initial cell density of 4.0×10^6 cell/ml, (a)Algal cells; (b)Turbidity; (c)DOC; (d)UV$_{254}$.

The interaction surface of DOC removal percentage (Figure 3.6(c)) showed a mound shape; axial steepness and surface curvature increase, which indicated that the interaction effect of coagulant dose and pH had a significant response to DOC removal efficiency. The response surface of UV$_{254}$ absorbance removal efficiency was shown in Figure 3.6(d); the UV$_{254}$ absorbance removal efficiency decreased significantly with the increase of initial cell density even at a high coagulation dose of 8.9 mg Al/L and pH of 5.5, which indicated that the alum applied could not remove aromatic compounds of water efficiently, and higher cell density competed with aromatics of water for coagulant dosage.

Using the optimization module by Design-Expert software, the optimum parameters of coagulation process were obtained for the removal of algal cells, turbidity, DOC and UV$_{254}$

absorbance. With these multiple responses, the overlaid contour plot (Figure 3.7) was used to visually demonstrate the optimal conditions range which the required responses can be simultaneously reached.
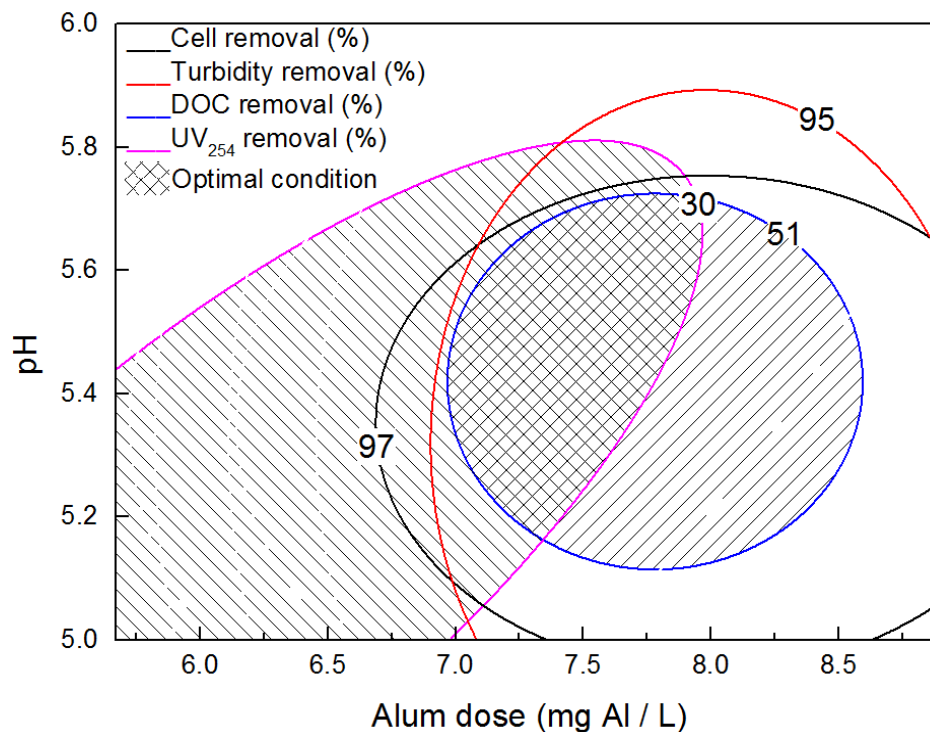
Figure 3.7 Overlaid contour plot for algal cells, turbidity, DOC and UV$_{254}$ removal percentage by alum coagulation. Data fitted by three-factor central composite design.

The optimum parameters of coagulation process were determined as follows: the dosage of coagulation 7.6 mg Al/L, pH of 5.4 and the initial algae concentration 3.8×10^6 cell/ml. The predicated removal percentage for algal cells, turbidity, DOC and UV$_{254}$ absorbance was $97.3 \pm 1.7\%$, $95.5 \pm 2.7\%$, $51.2 \pm 1.3\%$ and $30.3 \pm 2.7\%$, respectively.

The validation tests was conducted under the optimized conditions with the coagulant dosage of 7.5 mg Al/L, pH of 5.5 and the initial algae concentration of 4×10^6 cell/ml. The actual removal performances for algal cells, turbidity, DOC, and UV$_{254}$ absorbance were 97.3%, 95.4%, 48.7%, and 28.3%, respectively. Although the equivalent alum dosage of 1.97×10^{-9} mg Al/cell is less than that of 4.3×10^{-9} mg Al/cell presented by Gonzalez [43] who used a higher pH of 7.0 in their study, the optimized condition in the current study for

algae-laden water treatment obtained a relatively higher alum dose than usual 2.5-4.0 mg Al/L for drinking water treatment [22]. This indicated that polymer coagulant or coagulation aid may be needed to reduce the alum dosage or a combination with other treatment, for instance, air flotation may be used.

3.3.6 Artificial neural network

The ANN model has been applied extensively to predict nonlinear systems due to cost and time effectivity and high precision [44]. Table 3.5 demonstrates ANN topology, correlation coefficient (R^2) at training, validation, testing, and overall test and standard deviation.

Table 3.5 Performance of ANN network models.

Dependent responses	Topology	Correlation coefficient (R^2)*				Std. Dev.
		Training	Validation	Testing	All	
Algal cells	3 : 8 : 1	0.907	0.919	0.865	0.886	1.3
Turbidity	3 : 10 : 1	0.974	0.958	0.965	0.971	1.6
DOC	3 : 10 : 1	0.979	0.901	0.994	0.973	1.2
UV$_{254}$	3 : 10 : 1	0.947	0.943	0.813	0.898	1.4
Total	3 : 10 : 4	0.990	0.971	0.974	0.981	1.8

Note: The associated p value of each R^2 is less than 0.001.

The topology selected was based on the performance of networks, which gave minimum MSE and R^2 close to one. The training R^2 in all cases of models propose the highest value because the majority of the dataset (70%) were used for training repeatedly several times for adjusting the weights of the network. ANN-predicted values of removal efficiencies for algal cells, turbidity, DOC and UV$_{254}$ absorbance versus experimental data were presented in Figure 3.8. The linear regression analysis between ANN-predicted and observed values showed the minimum linear regression coefficient (R^2) of 0.886 for cell removal. The overall R^2 of the models is larger than 0.8 represents that the developed models are robust [45].
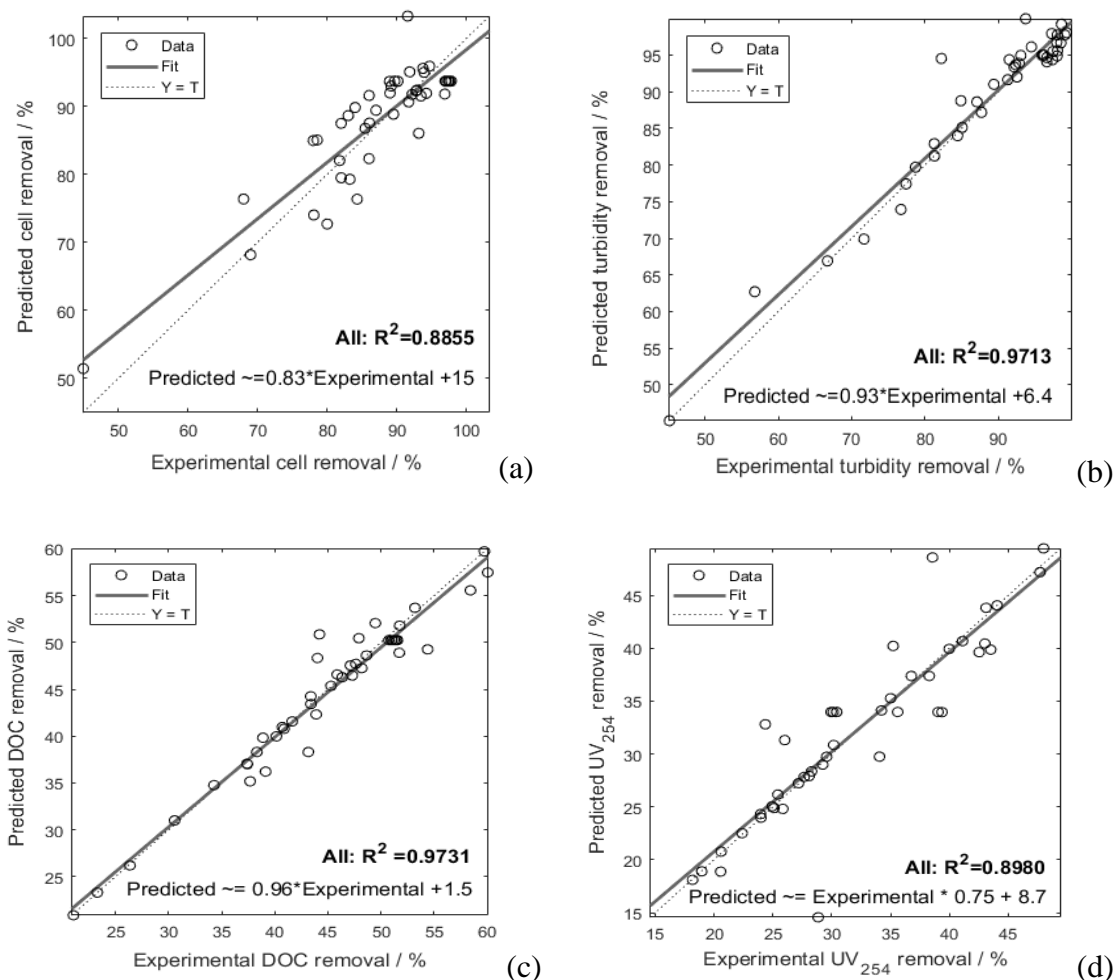
Figure 3.8 The plots of predicted vs. actual values of removal efficiency by BPNN, (a) algal cells; (b) turbidity; (c) DOC; (d) UV$_{254}$.

Linear regression analysis was carried out between the variables (coagulation dose, pH and initial cell density) and removal performance (algal cells, turbidity, DOC and UV$_{254}$ absorbance) values predicted by ANN and RSM models with their corresponding observed values. The largest standard deviation of these four responses from RSM and ANN were 2.7 (Table 3.4) and 1.6 (Table 3.5), respectively, which indicated that RSM model prediction presented a greater deviation than ANN predication. Both models presented stable responses, but the ANN models were better in data fitting and estimation capabilities. In comparison with RSM, ANN presented relatively higher average regression coefficient of 0.93 than 0.91 from RSM. The modeling results indicated that ANN was slightly more accurate for estimating the values of dependent variables as compared to the RSM models.

However, the RSM can be applied to analyze the factor effects (main and interactional) and propose regression equations for responses. Also, RSM can identify the significant main and interaction factors or insignificant terms in the model and thereby can reduce the complexity of the problem with assumption of quadratic non-linear correlation. However, ANN can easily overcome the limitations of RSM, inherently capture almost any form of non-linearity without the requirement of a standard experimental design to build the model [25].

3.3.7 Mechanism of algae and DOM removal by alum

It is well-known that four mechanisms of charge neutralization, adsorption, bridging, and sweep flocculation might be involved in coagulation process of natural colloids [46]. Alum undergoes hydrolysis to form variable mononuclear and polynuclear species depending on pH as shown by Equation 3.10.

$$Al(H_2O)_6^{3+} \leftrightarrow Al(OH)(H_2O)_5^{2+} \rightarrow Al_{13}O_4(OH)_{24}^{7+} \rightarrow Al(OH)_3 (S) \leftrightarrow Al(OH)_4^- \text{(Eq. 3.10)}$$

Based on the applied dosage of 4.6-10.0 mg Al/L, the concentration of alum (as $Al_2(SO_4)_3.14.3 H_2O$) was about 50.7-111.2 mg/L in the experiments. From the results presented in Table 3.3, it can be seen that the maximum cell removal of 97.8% occurred at pH 5.5. According to the coagulation domain diagram for alum dosage at various pH presented by [47], the region which corresponds to the dosage of 50.7-111.2 mg/L at pH 5.5 is in the sweep coagulation zone. In the pH range of 6.0-8.0, algal surfaces are negatively charged [48]. On the other hand, for alum coagulant, the dominant species of aluminum possibly are $Al_{13}O_4(OH)_{24}^{7+}$ and $Al(OH)_3 (S)$ at this pH range. The optimal coagulation for algae-laden natural water occurred around pH 5-6, which both algal cell and DOM are negatively charged, so that electrostatic interaction occurred between cationic aluminum species and cell/DOM. Therefore, both charge neutralization and sweep flocculation were possible mechanisms for the removal of algae and organic matter in present investigation. It was also indicated that charge neutralization and sweep flocculation to be the dominant mechanisms for DOM removal[46]. The reduced electrostatic repulsion between DOM colloidal particles/cells may facilitate initial aggregation of colloidal and fine suspended particulate to form microflocs [49], in addition,

the attached polyanions of DOM onto negative cell surface may also favor the agglomeration formation [50].

3.4 Conclusions

In the present study, the coagulation performance was investigated and optimized for the removal of algal cells and DOM from the eutrophic water sample of Lake Yangcheng. Based on the response surface analysis designed by CCD, the regression models for the coagulation performance were developed. A dosage of 7.57 mg Al/L and pH 5.42 was determined as optimal condition of coagulation for initial algal concentration of 3.83×10^6 cell/ml and an average initial DOC of 12.41 mg/L. Charge neutralization and sweep coagulation were the dominate mechanisms for the treatment of algae-laden natural water. The variance analysis of regression models and verification tests showed that the regression models were effective in fitting the experimental data. The ANN model was relatively more accurate in estimating the values of the coagulation performance. The models developed in this study may provide useful treatment options for the drinking water treatment plants drawing surface water affected by algal blooms.

References

[1]   L. Wang, X. Yan, J. Ma, X. Xu, Process analysis study on algae removal from eutrophic water in Taihu lake, Journal of Changzhou University (Natural Science Edition) 29 (2017) 41-45.

[2]   G. Li, China's Ecological Environment Statements Bulletin of 2017, Ministry of Ecology and Environment of People's Republic of China, China, 2018.

[3]   J. Lee, P.K. Rai, Y.J. Jeon, K.H. Kim, E.E. Kwon, The role of algae and cyanobacteria in the production and release of odorants in water, Environmental Pollution 227 (2017) 252-262.

[4]   M. Campinas, M.J.o. Rosa, Evaluation of cyanobacterial cells removal and lysis by ultrafiltration, Separation and Purification Technology 70 (2010) 345-353.

[5]   Y. Zhang, J.Y. Tian, J. Nan, S.S. Gao, H. Liang, M.L. Wang, G.B. Li, Effect of PAC addition on immersed ultrafiltration for the treatment of algal-rich water, Journal of Hazardous Materials 186 (2011) 1415-1424.

[6]   J.A. Westrick, D.C. Szlag, B.J. Southwell, J. Sinclair, A review of cyanobacteria and cyanotoxins removal/inactivation in drinking water treatment, Analytical and Bioanalytical Chemistry 397 (2010) 1705-1714.

[7]   Q. Shen, J. Zhu, L. Cheng, J. Zhang, Z. Zhang, X. Xu, Enhanced algae removal by drinking water treatment of chlorination coupled with coagulation, Desalination 271 (2011) 236-240.

[8]   R. Gough, P.J. Holliman, G.M. Cooke, C. Freeman, Characterisation of algogenic organic matter during an algal bloom and its implications for trihalomethane formation, Sustainability of Water Quality and Ecology 6 (2015) 11-19.

[9]   S.K. Engelage, W.T. Stringfellow, T. Letain, Disinfection Byproduct Formation Potentials of Wetlands, Agricultural Drains, and Rivers and the Effect of Biodegradation on Trihalomethane Precursors, Journal of Environmental Quality 38 (2009) 1901-1908.

[10]   A. Zamyadi, L.A. Coral, B. Barbeau, S. Dorner, F.R. Lapolli, M. Prévost, Fate of toxic cyanobacterial genera from natural bloom events during ozonation, Water Research 73 (2015) 204-215.

[11]   Y. Oyama, T. Fukushima, B. Matsushita, H. Matsuzaki, K. Kamiya, H. Kobinata, Monitoring levels of cyanobacterial blooms using the visual cyanobacteria index (VCI) and floating algae index (FAI), International Journal of Applied Earth Observation and Geoinformation 38 (2015) 335-348.

[12]   S. Merel, D. Walker, R. Chicana, S. Snyder, E. Baurès, O. Thomas, State of knowledge and concerns on cyanobacterial blooms and cyanotoxins, Environment International 59 (2013) 303-327.

[13]   Y. Sun, W. Wu, X.F. Xiao, H.F. Wu, W.Q. Sun, M.J. Ren, C.Y. ZHu, Y.Y. Xu, Research progress on removal of algae in water by flocculation, Chemical Research and Application 29 (2017) 153-159.

[14]   Y. Wang, W. Hu, Z. Peng, Y. Zeng, K. Rinke, Predicting Lake Eutrophication Responses to Multiple Scenarios of Lake Restoration: A Three-Dimensional Modeling Approach, Water 10 (2018) 994.

[15]   X.Y. Zheng, H.L. Zheng, S.Y. Zhao, W. Chen, Z.Q. Yan, L.H. Dong, Review on the removal of algae in source water by coagulation technology, Chemical Research and Application (2015) 1619-1624.

[16]   C.X. Ma, W.R. Hu, H.Y. Pei, H.Z. Xu, R.T. Pei, Enhancing integrated removal of Microcystis aeruginosa and adsorption of microcystins using chitosan-aluminum chloride combined coagulants: Effect of chemical dosing orders and coagulation mechanisms, Colloids and Surfaces a-Physicochemical and Engineering Aspects 490 (2016) 258-267.

[17]   J.-L. Lin, L.-C. Hua, S.K. Hung, C. Huang, Algal removal from cyanobacteria-rich waters by preoxidation-assisted coagulation–flotation: Effect of algogenic organic matter release on algal removal and trihalomethane formation, Journal of Environmental Sciences 63 (2018) 147-155.

[18]   N. Javadi, F.Z. Ashtiani, A. Fouladitajar, A.M. Zenooz, Experimental studies and statistical analysis of membrane fouling behavior and performance in microfiltration of microalgae by a gas sparging assisted process, Bioresource Technology 162 (2014) 350-357.

[19]   S.-C. Kim, Application of response surface method as an experimental design to optimize coagulation–flocculation process for pre-treating paper wastewater, Journal of Industrial and Engineering Chemistry 38 (2016) 93-102.

[20]   G. Halder, S. Dhawane, P.K. Barai, A. Das, Optimizing chromium (VI) adsorption onto superheated steam activated granular carbon through response surface methodology and artificial neural network, Environmental Progress & Sustainable Energy 34 (2015) 638-647.

[21]   J.-P. Wang, Y.-Z. Chen, X.-W. Ge, H.-Q. Yu, Optimization of coagulation–flocculation process for a paper-recycling wastewater treatment using response surface methodology, Colloids and Surfaces A 302 (2007) 204-210.

[22]   T.K. Trinh, L.S. Kang, Response surface methodological approach to optimize the coagulation–flocculation process in drinking water treatment, Chemical Engineering Research and Design 89 (2011) 1126-1135.

[23]   L. Li, S. Zhang, Q. He, X.B. Hu, Application of response surface method in experimeatal design and optimization, Research and Exploration in Laboratory 34 (2015).

[24]   H.R. Yang, Y.C. Fu, Q.X. Wang, Optimization of micro-polluted water treatment by response surface methodology, Journal of Anhui Agricultural Sciences 45 (2017) 48-50.

[25]   D. Bingöl, M. Hercan, S. Elevli, E. Kilic, Comparison of the results of response surface methodology and artificial neural network for the biosorption of lead using black cumin, Bioresource Technology 112 (2012) 111-115.

[26]   M. Khayet, C. Cojocaru, M. Essalhi, Artificial neural network modeling and response surface methodology of desalination by reverse osmosis, Journal of Membrane Science 368 (2011) 202-214.

[27]   M.R. Gadekar, M.M. Ahammed, Coagulation/flocculation process for dye removal using water treatment residuals: modelling through artificial neural networks, Desalination and Water Treatment 57 (2016) 26392-26400.

[28]   R.H. McArthur, R.C. Andrews, Development of artificial neural networks based confidence intervals and response surfaces for the optimization of coagulation performance, Water Science and Technology-Water Supply 15 (2015) 1079-1087.

[29]   Y. Wang, K. Chen, L. Mo, J. Li, J. Xu, Optimization of coagulation–flocculation process for papermaking-reconstituted tobacco slice wastewater treatment using response surface methodology, Journal of Industrial and Engineering Chemistry 20 (2014) 391-396.

[30]   M. Al-Abri, K. Al Anezi, A. Dakheel, N. Hilal, Humic substance coagulation: Artificial neural network simulation, Desalination 253 (2010) 153-157.

[31]   J.-N. Zhao, L.-X. Sun, Z.-C. Tan, Low-temperature heat capacities and thermodynamic properties of N-benzyloxycarbonyl-L-3-phenylalanine (C17H17NO4), Journal of Chemical & Engineering Data 55 (2010) 4267-4272.

[32]   C.G. Piuleac, S. Curteanu, M.A. Rodrigo, C. Saez, F.J. Fernandez, Optimization methodology based on neural networks and genetic algorithms applied to electro-coagulation processes, Central European Journal of Chemistry 11 (2013) 1213-1224.

[33]   J.R. Ma, J.M. Deng, B.Q. Qin, S.X. Long, Progress and prospects on cyanobacteria bloom-forming mechanism in lakes, Acta Ecologica Sinica 33 (2013) 3020-3030.

[34]   E.H. Goslan, C. Seigle, D. Purcell, R. Henderson, S.A. Parsons, B. Jefferson, S.J. Judd, Carbonaceous and nitrogenous disinfection by-product formation from algal organic matter, Chemosphere 170 (2017) 1-9.

[35]   P. Gebbie, An operator's guide to water treatment coagulants, In Proceedings of the 31st Annual Qld Water Industry Workshop—Operations SkillsRockhampton, Australia 2006, pp. 14-20.

[36]   G.D. Lanciné, K. Bamory, L. Raymond, S. Jean-Luc, B. Christelle, B. Jean, Coagulation-Flocculation treatment of a tropical surface water with alum for dissolved organic matter (DOM) removal: Influence of alum dose and pH adjustment, J Int Environmental Application & Science 3 (2008) 57-247.

[37]   A. Matilainen, M. Vepsalainen, M. Sillanpaa, Natural organic matter removal by coagulation during drinking water treatment: a review, Advances in Colloid and Interface Science 159 (2010) 189-197.

[38]   T.S. Aktas, F. Takeda, C. Maruo, M. Fujibayashi, O. Nishimura, Comparison of four kinds of coagulants for the removal of picophytoplankton, Desalination and Water Treatment 51 (2013) 3547-3557.

[39]   Z.L. Yang, B.Y. Gao, Q.Y. Yue, Y. Wang, Effect of pH on the coagulation performance of Al-based coagulants and residual aluminum speciation during the treatment of humic acid-kaolin synthetic water, Journal of Hazardous Materials 178 (2010) 596-603.

[40]   P. Zhang, Z. Wu, G. Zhang, G. Zeng, H. Zhang, J. Li, X. Song, J. Dong, Coagulation characteristics of polyaluminum chlorides PAC-Al30 on humic acid removal from water, Separation and Purification Technology 63 (2008) 642-647.

[41]   X. Xiao, J. He, H. Huang, T.R. Miller, G. Christakos, E.S. Reichwaldt, A. Ghadouani, S. Lin, X. Xu, J. Shi, A novel single-parameter approach for forecasting algal blooms, Water Research 108 (2017) 222-231.

[42]   T. Olmez-Hanci, I. Arslan-Alaton, G. Basar, Multivariate analysis of anionic, cationic and nonionic textile surfactant degradation with the H(2)O(2)/UV-C process by using the capabilities of response surface methodology, Journal of Hazardous Materials 185 (2011) 193-203.

[43]   A. Gonzalez-Torres, J. Putnam, B. Jefferson, R.M. Stuetz, R.K. Henderson, Examination of the physical properties of Microcystis aeruginosa flocs produced on coagulation with metal salts, Water Research 60 (2014) 197-209.

[44]   M. Moghaddari, F. Yousefi, M. Ghaedi, K. Dashtian, A simple approach for the sonochemical loading of Au, Ag and Pd nanoparticle on functionalized MWCNT and subsequent dispersion studies for removal of organic dyes: Artificial neural network and response surface methodology studies, Ultrasonics Sonochemistry 42 (2018) 422-433.

[45]   P. Kundu, A. Debsarkar, S. Mukherjee, Artificial neural network modeling for biological removal of organic carbon and nitrogen from slaughterhouse wastewater

in a sequencing batch reactor, Advances in Artificial Neural Systems 2013 (2013) 13.

[46]   T.T. Guo, Y.L. Yang, R.P. Liu, X. Li, Enhanced removal of intracellular organic matters (IOM) from Microcystic aeruginosa by aluminum coagulation, Separation and Purification Technology 189 (2017) 279-287.

[47]   A. Amirtharajah, K.M. Mills, Rapid‑mix design for mechanisms of alum coagulation, Journal‑American Water Works Association 74 (1982) 210-216.

[48]   A.L. Gonçalves, C. Ferreira, J.A. Loureiro, J.C. Pires, M. Simões, Surface physicochemical properties of selected single and mixed cultures of microalgae and cyanobacteria and their relationship with sedimentation kinetics, Bioresources and Bioprocessing 2 (2015) 21-31.

[49]   H.K. Agbovi, L.D. Wilson, Flocculation Optimization of Orthophosphate with FeCl3 and Alginate Using the Box-Behnken Response Surface Methodology, Industrial & Engineering Chemistry Research 56 (2017) 3145-3155.

[50]   M. Baresova, M. Pivokonsky, K. Novotna, J. Naceradska, T. Branyik, An application of cellular organic matter to coagulation of cyanobacterial cells (Merismopedia tenuissima), Water Research 122 (2017) 70-77.

Chapter 4

4 Coagulation and Disinfection By-Products Formation Potential of Extracellular and Intracellular Matter of Algae and Cyanobacteria[2]

4.1 Introduction

Due to climate change and abundance of nutrients, frequent eutrophication and outbreak of algal blooms and phytoplankton growth in surface water are of global concern [1-4]. While particulate algal cells are removed well (> 95%) during coagulation and flocculation processes in drinking water treatment [5-7], dissolved algal organic matter (AOM), which includes both extracellular organic matter (EOM) and intracellular organic matter (IOM), are not removed well during coagulation [8]. AOM causes a series of problems in drinking water treatment such as increased coagulant demand, growth of biofilm causing fouling of the membrane, blocking the activated carbon adsorption sites, and increased formation of precursors for disinfection by-product (DBP) during chlorination [8-12]. The majority of available literature focuses on the DBP formation from allochthonous natural organic matter (NOM) from detritus materials and vegetation, limited studies dealt with DBP formation from autochthonous NOM due to phytoplankton growth. Algal (or algogenic) organic matter (AOM) is composed of polysaccharide, proteins and humic-like substance, which has been classified as the autochthonous natural compounds in water [13]. The AOM is believed to comprise a substantial proportion of natural organic matter [12], and a dominant contributor to DBP precursors in surface water [14], and playing an important role in aquatic ecosystem [15], which emphasizes the importance of the investigation of AOM on water treatment processes.

While EOM is present at all stages of growth of the phytoplankton, chemical coagulants such as alum and pre-oxidation using chlorine (to facilitate better removal by coagulation)

---

[2] A version of this chapter has been published in Chemosphere with the title of "Z. M., Zhao, et al. "Coagulation and disinfection by-products formation potential of extracellular and intracellular matter of algae and cyanobacteria." Chemosphere 245 (2020): 125669."

may cause damage to algal cell integrity leading to the release of IOM, which cause taste, odor and toxicity in water [16]. Higher amount of trihalomethane (THM) formation occurred due to the release of IOM during pre-oxidation before coagulation [17]. IOM can also be released to treated water if coagulated species remain in the bottom of a sedimentation basin. However, the role of IOM vs EOM on the coagulation and disinfection by-production formation potential (DBPFP) is not well established due to lack of comprehensive control studies.

Contradictory results are reported in literature on the nature of EOM and IOM and their performance in water treatment processes. It was reported that algal IOM was mostly hydrophilic (HPI) [13] indicating low removal potential during coagulation, while IOM of *Microcystis aeruginosa* was reported to be more hydrophobic (HPO) than EOM [18]. Conversely, algal EOM can act as a flocculation aid improving the coagulation efficiency [19]. EOM also can form chelate complexes with metal coagulants, significantly increasing the required dosage and reducing the treatment efficiency [20-22]. Therefore, the effect of AOM on coagulation in water treatment is still contradictory and specific to algal species [23] as the distribution of HPO and HPI fractions of AOM varies depending on the type of algae and stage of growth [24].

To the best of my knowledge, there has been no systematic comparison of DBP formation followed by coagulation under identical treatment conditions for different species of algae and cyanobacteria. An earlier research investigated DBP formation from only EOM of three cyanobacteria, one diatom and one green algae [25]. However, they did not study the effect of coagulation on the removal of EOM. Comprehensive control studies are needed to determine the roles of specific AOM originating from commonly found, abundant algal species in surface water, their removal using coagulant dosages relevant to drinking water treatment, and subsequent DBPFP evaluation. The objectives of this study were to: (i) optimize the coagulation conditions to remove AOM originated from four species of algae *Chlorella vulgaris* (CV)*, Scenedesmus quadricauda* (SQ)*, Phaeodactylum tricornutum* (PT)*, and Aulacoseira granulata f. curvata.* (AG)*, and two cyanobacteria *Microcystis aeruginosa* (MA)*, Merismopedia* sp. (Msp), (ii) determine the IOM and EOM fractions of AOM for a known concentration of algal/cyanobacterial cells, (iii) determine HPO, HPI

and TPI fractions of the AOM, and their effect on the coagulation performance, and (iv) determine DBPFP after coagulation of the AOM of individual species. An attempt was undertaken to determine whether the common water quality parameter, SUVA, can be used as an indicator for both coagulation performance and DBPFP of algal matter.

Cyanobacteria (*Microcystis aeruginosa*, *Merismopedia* sp.) and green algae (*Chlorella vulgaris*, *Scenedesmus quadricauda*) are the most abundant freshwater photosynthetic species in surface water during a bloom [26-28]. Diatoms such as *Phaeodactylum tricornutum* and *Aulacoseira granulata f. curvata* contributing to high concentration (> 10 mg/L) of DOC, are the useful indicators of surface water eutrophication[29], causing significant problems in water treatment plants [30]. While nitrogenous DBPs are potentially more genotoxic than carbonaceous DBP, they are formed at a much lower concentration (Table 4.1). For example, *Microcystis aeruginosa* formed only 0.95 µg/mg-C haloacetonitriles (HANs) and 0.017 µg/mg-C NDMA compared to 18 µg/mg-C and 13.65 µg/mg-C of HAA and THM, respectively [31], and therefore was not determined in this work. For brevity, hereafter, the test species will be designated by the abbreviated names only.

Table 4.1 DBP formation potential from algal organic matter.

Algal species		Carbonaceous DBPs (C-DBP) (µg/mg C)		Nitrogenous DBPs (N-DBP) (µg/mg C)		Formation conditions	References
		HAAs	THMs	HANs	NDMA		
M. aeruginosa.	EOM	18	13.65	0.95	0.017	under 25°C for 3 days for AOM extracted	[31]
	IOM	14.25	21.3	3.73	0.017	at late exponential phase	
M. aeruginosa.	IOM [a]	117	64	1.2	0.01-0.052	under 23°C for 7 days with free chlorine	[32]
						residual of 7.6-11.1 mg/L	
S. subspicatus	EOM	37.5	20	1.1	NA	under 20°C for 7 days with 5 mg Cl_2/mg	[25]
M. aeruginosa	EOM	30	45	1.35	NA	C and chlorine residual 05-1.2 mg/L, then	
A. granulata	EOM	13.5	20	0.9	NA	quenched by ammonium chloride	

Note: a: The method of freeze−thaw sequences (−77 °C freezer, 35 °C water bath) and sonication (1 hour in an ice bath) to release the IOM. The cell debris was separated from the dissolved IOM through filtration (0.7 µm).

4.2 Materials and methods

4.2.1 Cultivation of algae and cyanobacteria

The four algal species and two cyanobacteria were purchased from the Canadian Phycological Culture Centre (CPCC) at Waterloo University (Waterloo, ON, Canada). They were cultivated in 2 L conical flasks in specific medium (shown in Table 4.2) for each species at 23 ± 2 ^{o}C using humidified air flow of 2 L/minute. All solutions were prepared from reagent-grade chemicals and Milli-Q water. Intermittent illumination (3000 lx) at a light/dark cycle (16/8 hours shift) was provided to simulate natural light condition [33]. The growth of each species was monitored by cell counting using hemocytometer under microscopy. Algae and cyanobacterial cultures were harvested at the stationary growth phase (25-30 days, depending on the species) [34] when the final cell concentrations were approximately $0.24\text{-}6.5 \times 10^7$ cells/ml.

4.2.2 AOM extraction

EOM of algae was separated from the harvested cell suspension using a centrifuge (Thermo Scientific Sorvall, Legend T Plus) at 3700 rpm and 30 minutes centrifugation time. Subsequently, a 0.45 µm filter (hydrophilic acrylic copolymer, Pall Corporation) was used to separate the supernatant containing EOM. The deposited algae on the filter was washed three times using Milli-Q water. Four different methods were attempted for lysis of the algal cells to obtain IOM as: (i) using a bead-beater at a frequency of 3500 rpm for 2 minutes mixing with silica beads [35]; (ii) applying ultrasonication at a frequency of 50 Hz for 10 minutes [36]; (iii) autoclaving at 120 ^{o}C [37] for 15-30 minutes [38]; (iv) 3 cycles of freeze (-18 ^{o}C) and thaw (40 ^{o}C) [39]. The resultant solution was then filtered using 0.45 µm membrane disc filters to obtain the IOM. The EOM and IOM stock solutions were stored at 4 ^{o}C for no more than 48 hours before characterization or preparing the feed water with a DOC concentration of approximately 10 mg/L for coagulation. This concentration was chosen to make the water quality comparable to NOM concentration in drinking water plants, which is around 2-10 mg/L [40].

4.2.3 Characterization of AOM

DOC of EOM and IOM was measured using a Shimadzu TOC–V$_{CPN}$ analyzer. Glucose solution was used as the standard to obtain the calibration curve with the detection limit of 0.1 mg/L. Temperature and pH were measured using a pH meter (Orion Model STAR A111). A UV/Vis spectrophotometer (Shimadzu Model 3600) was used to scan a range of absorbance values from 200 to 300 nm with a 1 cm quartz cell to obtain the UV absorbance at 254 nm (UV$_{254}$). The specific UV absorbance (SUVA = UV absorbance at 254 nm/DOC mg/L) (L·mg^{-1}·cm), the widely used parameter for characterizing aromaticity of organics, was determined for all AOM samples.

4.2.4 Determination of HPI and HPO fractions

The resin fractionation method had been used to separate organic matter of the source water into HPO, TPI, and HPI fractions by adsorption using DAX-8 (Supelite, USA) and XAD-4 (Amberlite, USA) resins in a column successively [41-43]. The process is based on surface adsorption equilibrium between the resin and the organic matter in water. The column capacity factor k' shown in the Equation 4.1 [44] is the ratio of the amount of organic matter retained by resin (C'_{ads}) to the concentration of initial organic matter influent ($C_{influent}$),

$$C'_{ads} = k' \times C_{influent} \qquad \text{(Eq. 4.1)}$$

The volume of influent passed through the column can be calculated using Equation 4.2 [44], where the void volume $V_0 = V_b \times P$, V_b is the bed volume of resin and P is the resin porosity (0.65). Several resin fractionation procedures and quantification methods were developed to partition organic matter in water samples [25, 42, 45]. A value of 50 for k' was generally accepted to be the column capacity for humic substances separation in previous investigations [46-51]. It was demonstrated that increasing the column capacity factor k' would cause lower retention of the hydrophobic fraction on the column due to higher flow rate causing decreased yield of hydrophobic fraction [44, 52, 53]. Therefore, a lower column capacity of 30 was applied in this study in order to adsorb most of the HPO fraction in AOM solutions by DAX-8 resin as:

$$V = 2V_0(1 + k') \qquad\qquad\qquad \text{(Eq. 4.2)}$$

where V is the volume of AOM solution passed through the column, V_0 is void volume and k' represents the column capacity.

About 310 mL EOM or IOM solution with initial DOC of 10.43 ± 0.80 mg/L, and pH 2 (adjusted by 10 M HCl) was passed through two 20 cm length glass columns connected in series and filled with 8 mL of DAX-8 and XAD-4 resin, respectively, using a constant flowrate of 3 mL/minute. While HPI fraction passes through both DAX-8 and XAD-4 columns, the HPO fraction is absorbed onto DAX-8 resin and transphilic fraction is absorbed onto the XAD-4 resin. Thereafter, the same volume (310 mL) of 0.1 M NaOH as the initial water sample, was applied to elute the HPO and TPI fractions from DAX-8 and XAD-4 column, respectively, using the same flowrate (3 mL/minute). DOC of each fraction was measured using the TOC analyzer described earlier. Before fractionation, the resins were rinsed with methanol, 0.1 M NaOH, 0.1 M HCl and Milli-Q water until the DOC of the effluent was same as that of Milli-Q water. Recovery of each fractionation determined from the DOC values was within 95-108 %.

4.2.5 Coagulation of AOM

Coagulation experiments were conducted using a Phipps & Bird programmable apparatus (Model PB900) with six stainless steel paddles at room temperature ($\sim$24 $^{\circ}$C) in 500 mL beakers. A commonly used coagulant ($Al_2(SO_4)_3 \cdot 18H_2O$) was added with a dosage varying from 30 to 60 mg/L (2.4-4.8 mg/L of Al^{3+}) at a pH between 5.0-8.0 (adjusted by adding either 1N HCl or 1N NaOH); a relatively higher dosage than usual 30 mg/L in drinking water treatment plant was tried as enhanced coagulation. Coagulation experiments included rapid mixing at 150 rpm for 2 minutes, followed by a slow stirring at a speed of 25 rpm for 20 minutes for floc growth. Thereafter, a settling time of 30 minutes was applied to precipitate the formed flocs, and the supernatant was analyzed to determine the residual DOC and UV_{254} values after coagulation. All experiments were performed in triplicated and reported with average values and standard deviation (n = 3).

4.2.6 Chlorination and DBPs analysis

Chlorination of the coagulated water was conducted according to the uniform formation conditions (UFC) at pH 8.0 ± 0.2 with a borate buffer solution [54]. Subsequently, a combined hypochlorite-buffer dosing solution was added to the water samples with the free chlorine dosage of 1.8 times of initial DOC of the water sample [55] and stored in headspace-free amber glass bottles in the dark at ambient temperature (20 ± 1 ^{o}C) for 24 hours and kept the residual free chlorine within 1.0 ± 0.4 mg/L. After 24 hours of incubation, the stoichiometric amount of ammonium chloride was added to quench the free residual chlorine in water to obtain the THMFP and HAAFP. The formation potentials of four major THM$_4$, trichloromethane (TCM), bromodichloromethane (BDCM), dibromochloromethane (DBCM) and tribromomethane (TBM), were extracted with methyl *tert* butyl ether (MTBE) by liquid-liquid extraction following the method of USEPA 551.1[56]. Six HAA$_6$, monochloroacetic acid (MCAA), monobromoacetic acid (MBAA), dichloroacetic acid (DCAA), dibromoacetic acid (DBAA), bromochloroacetic acid (BCAA), and trichloroacetic acid (TCAA) were extracted from water samples following the modified USEPA method 552.3 [57]. The DBPs were determined using a GC-ECD (Shimadzu GC-2014) with a BPX5 capillary column (30 m× 0.25 mm ID, 0.25 μm film thickness). DBP (μg/mg C) yields were normalized by dividing the concentration of DBP (in μg/L) by the DOC (in mg/L).

4.3 Results and discussion

4.3.1 Cell growth and EOM, IOM separation

All the algae and cyanobacteria (axenic cultures) were harvested at their stationary growth stage after 25-30 days of cultivation using conditions mentioned earlier. The maximum specific growth rates (μ_{max}, d^{-1}) of CV, SQ, MA, Msp, PT and AG were 0.514 day^{-1}, 0.362 day^{-1}, 0.553 day^{-1}, 0.602 day^{-1}, 0.869 day^{-1} and 0.585 day^{-1}, respectively, which are comparable with earlier studies at similar conditions [18, 58-60]. In the stationary phase, the algal population reached the maximum cell concentration of about 21.75×10^6 cell/mL for PT, 9.26×10^6 cell/mL for SQ, 9.30×10^6 cell/mL for Msp, 65.38×10^6 cell/mL for CV, 36.69×10^6 cell/mL for MA, and 2.35×10^6 cell/mL for AG. Of the two diatoms, PT and

AG, PT grew much faster than AG, followed by the two cyanobacteria. It should be noted that other than the prescribed growth medium for a particular species shown in Table 4.2, growth conditions such as temperature, oxygen flow and light exposure were kept consistent for all algae and were not optimized for any individual species.

In order to obtain the intracellular organic matter, several cell disintegration methods mentioned earlier were applied to a ubiquitous green algae, CV, and the results are shown in Figure 4.1. Of the various methods applied for extraction of IOM, autoclaving produced the maximum DOC and SUVA, followed by 3 cycles of freeze and thaw. However, autoclaving was not used in further experiments as some alteration (hydrolysis) and degradation of organics structure may occur during autoclaving [61].
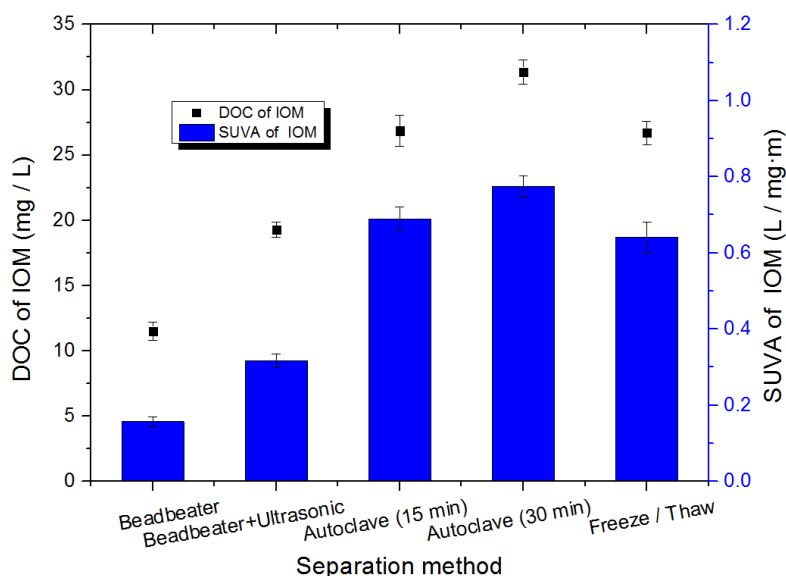
**Figure 4.1 DOC and SUVA of IOM from *C. vulgaris* with initial cell density of 6.5 ×
10^7 cell / ml obtained by different extraction methods.**

For these experiments, the DOC and SUVA values of EOM from CV were kept consistent at 34.09 ± 2.04 mg/L, and 0.26 ± 0.03, since all the algal suspensions were taken from the same stock solution. The EOM was separated using centrifugation and filtration as mentioned earlier. After each treatment, the released IOM is measured in terms of DOC and SUVA as shown in Figure 4.1 The maximum IOM production was achieved by autoclaving for 30 min with the DOC value of 31.37 mg/L, whereas commonly applied bead-beater with 2 min shaking could produce only 11.51 mg/L of DOC. Ultrasonic

treatment can facilitate the cell lysis due to the explosion of cavitation bubbles; however, the produced DOC of 19.27 mg L was lower than that of three cycles of freeze / thaw, and autoclave treatment for 15 min, which produced a similar IOM production with DOC value of 26.7 mg/L and 26.9 mg/L, respectively. Therefore, autoclaving produced the maximum DOC from the IOM, however, it was not used in further experiments as some alteration (hydrolysis) and degradation of organics structure may occur during autoclaving [1].

It should be noted that the chemical composition and microstructure can be affected by the rate of freezing and thawing. The structures of aromatics like gingerol and monocyclic like zingibevene were affected by the freezing and thawing time [37]. For consistency, freezing and thawing time kept constant at 12 hours at -18 C and 4 hours at 25 C, respectively [39]. Production of both EOM and IOM increased with cultivation time until the stationary phase was reached for all six species. DOC of EOM and IOM extracted from each species with cultivation days are shown in Figure 4.2.
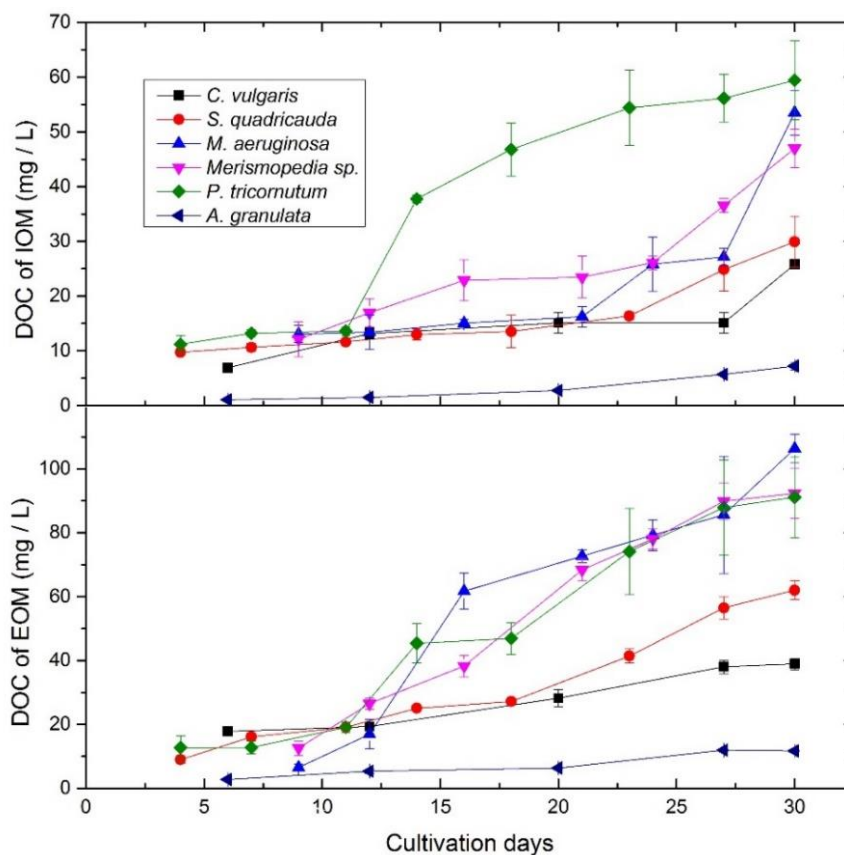
Figure 4.2 Organic matter produced from the algal species and cyanobacteria with cultivation time.

The constituents of cellular matter such as protein, carbohydrate and lipid vary significantly based on the species and their growth phase. Therefore, harvesting of the algae and cyanobacteria was conducted once they all reached stationary stage for consistency and the final values are summarized in Table 4.2.

Table 4.2 DOC of cellular material from the six species at the stationary stage.

Algae	Cell Density (cells/mL)	DOC (mg/L)		SUVA (L/m·mg)		Growth medium DOC (mg/L)	
		EOM*	IOM	EOM	IOM		
CV	6.5×10^7	28.61 ± 2.71	25.83 ±1.90	0.25	0.65	High salt	10.26
SQ	9.3×10^6	46.24 ± 0.08	24.84 ± 2.90	0.26	0.57	High salt	10.26
MA	3.7×10^7	68.45 ± 2.02	53.50 ± 1.86	0.55	0.67	3N-BBM	4.24
Msp	9.3×10^6	78.10± 3.15	46.97 ± 1.29	0.55	0.56	BG-11	4.25
PT	2.2×10^7	79.12 ± 4.99	56.13 ± 4.82	0.74	0.56	F / 2	8.76
AG	2.4×10^6	9.28 ± 0.23	7.21 ± 0.03	0.30	0.86	CHU 10	2.38

*the DOC value of the growth media was subtracted from the EOM DOC values, $^{\int}$ after 30 days cultivation at 23 ± 2ºC, 16/8 hours light/dark cycle and 2 L/minute aeration.

The diatom PT had the highest EOM excretion followed by the two species of cyanobacteria MA and Msp, and DOC of EOM from each species was higher than that of IOM at the stationary phase, which compares with the results from [62]. SUVA varied between 0.263 and 0.861 L/mg-m, as shown in Table 4.2 , showing relatively lower aromaticity compared to NOM in which can range from 1.8 to 4.4 L/m-mg [63]. SUVA values for the IOM were slightly higher than that of the EOM, except for PT which showed slightly higher SUVA for EOM than IOM. The IOM of diatom, AG showed the highest SUVA value. The SUVA followed the similar trend as the DOC, and compared well with the literature [64]. A low SUVA also suggests that IOM from CV is of more hydrophilic in nature [65] and mainly comprised of protein-like substances, instead of humic-like matters [39].

4.3.2 Removal of EOM and IOM by coagulation

A relatively wide range of alum dose (30-60 mg/L) was tested for the removal of DOC and UV_{254} of EOM and IOM (initial DOC of 8.5 ± 1.5 mg/L) of each species. Although the dosage of alum depends on initial DOC concentration, a typical dosage of 30 mg/L is quite common in a water treatment plant. The higher dosage was used to test whether enhanced

coagulation could be achieved using 40-60 mg/L (Figure 4.3). The results indicated that DOC removal efficiency generally increased with increasing alum dosage, but it reached a plateau around 40 mg/L for most cases with the exception of IOM of CV, EOM of SQ and EOM of Msp. Hence, there was no benefit in increasing alum dosage beyond this concentration for most of the cases. DOC removal efficiency of EOM followed the order of PT ($82.69 \pm 3.43\%$) > AG ($69.90 \pm 4.48\%$) > MA ($65.29 \pm 0.76\%$) > Msp ($59.99 \pm 4.42\%$) > CV ($24.95 \pm 0.83\%$) > SQ ($21.55 \pm 0.77\%$).
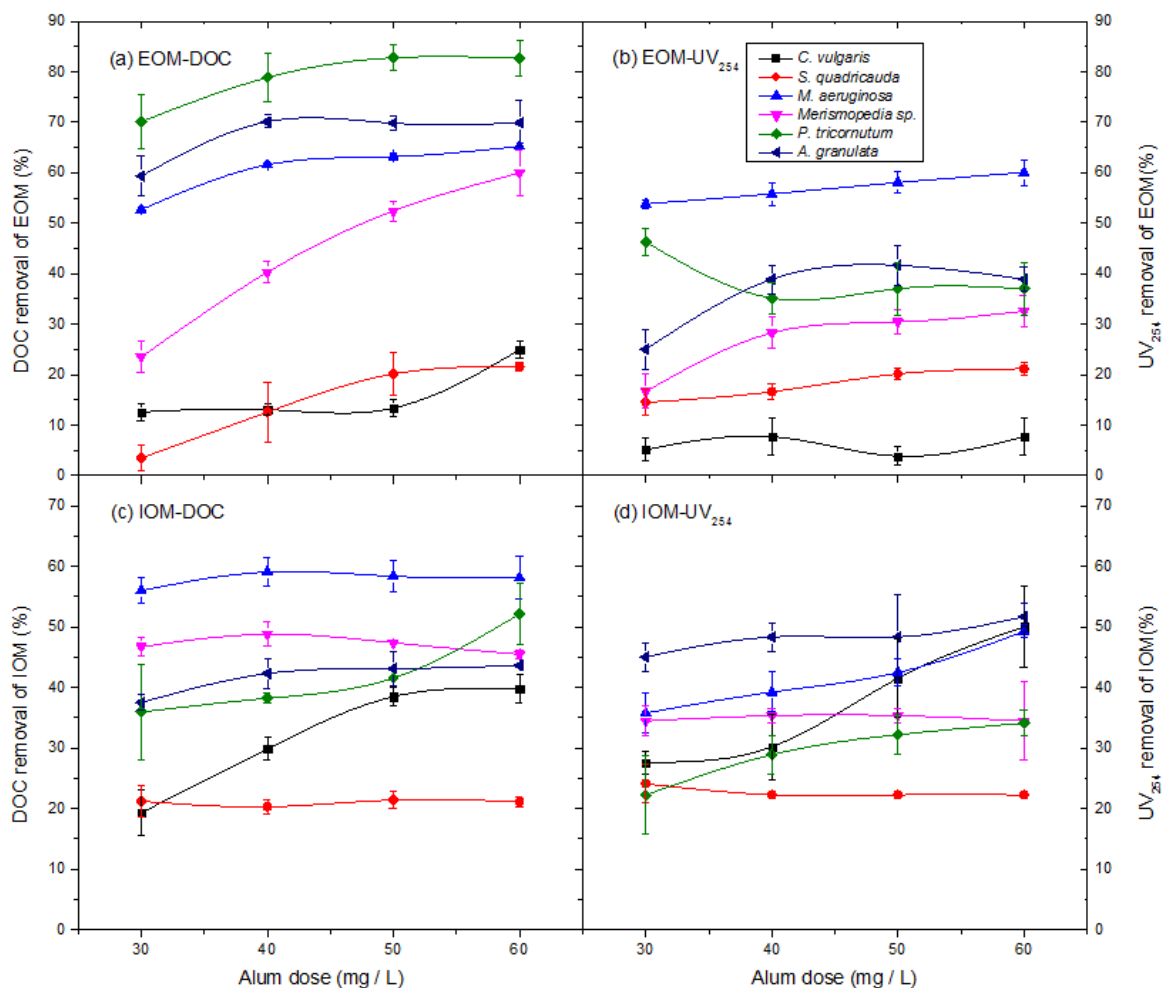
Figure 4.3 The effect of alum dosage on the removal of DOC and UV$_{254}$ of EOM (a, b) and IOM (c, d).

Comparing the results with EOM, removal of IOM was slightly lower than EOM and varied between $19.31 \pm 3.84\%$ and 59.09 ± 2.41 with highest removal occurred for MA and the lowest removal occurred for SQ. The removal efficiency of IOM at optimum condition of alum dosage of 40 mg /L and pH 5 followed the order of MA ($58.93 \pm 0.29\%$) > Msp ($49.28 \pm 0.32\%$) > AG ($47.50 \pm 1.24\%$) ≈ PT ($47.27 \pm 0.32\%$) > CV ($37.67 \pm 2.11\%$) > SQ ($20.54 \pm 2.01\%$). Thus, removal of AOM of CV and SQ by coagulation was not very effective.

The UV$_{254}$ removal followed a very similar trend as that of DOC removal. In most cases, DOC removal was correlated to the SUVA value of the species with some exceptions. In

general, aromatic compounds were better removed during coagulation. It was reported that for SUVA <3, DOC is hydrophilic, low in molecular weight and in charge density, and only slightly affected by coagulation [66]. This could explain the deviation in coagulation performance for both EOM and IOM with respect to SUVA as the SUVA of all cellular materials of AOM varied only from 0.24 to 0.861 L/m-mg. The results of coagulation of DOC and UV_{254} at dose of 30 mg/L and pH are presented in Table 4.3.

Table 4.3 The AOM removal by coagulation with an alum dosage of 30 mg/L and at pH 5 and 23°C.

Algae	EOM		IOM	
	DOC	UV_{254}	DOC	UV_{254}
CV	36.07 ± 1.30	43.75 ± 2.42	35.12 ± 0.32	43.41 ± 1.17
SQ	16.96 ± 0.84	19.35 ± 1.52	20.75 ± 0.31	19.83 ± 1.49
MA	76.40 ± 0.91	56.71 ± 1.49	61.81 ± 0.26	47.83 ± 2.05
Msp	59.62 ± 1.15	29.55 ± 3.21	41.42 ± 0.29	26.36 ± 1.29
PT	61.56 ± 7.29	32.60 ± 1.89	52.82 ± 7.17	82.00 ± 2.83
AG	70.51 ± 2.13	40.00 ± 4.95	36.07 ± 1.30	43.75 ± 2.42

The effect of pH on coagulation in the range of 5-8 was tested, and the results presented in Figure 4.4 indicated that the DOC removal for AOM decreased with increasing pH, which is consistent with an earlier study [67]. Maximum DOC removal for EOM occurred at pH 5-6; at pH 5 and at a coagulant dose of 30 mg/L, monomeric Al $(OH)^{2+}$ and polynuclear $Al_8((OH)_{20}^{4+})$ are the dominant species involved in charge neutralization of negative (especially carboxyl-) groups of AOM [68]. Once pH increases over 6.0, the formation of Al $(OH)_4^-$ species becomes dominant causing decreased DOC removal efficiency [69]. At pH 6 and a higher coagulant dose, restabilization may occur decreasing the removal of both DOC and UV_{254}. Since most of the dose-response curves remained flat at higher Al-dosage, charge reversal did not occur during AOM coagulation.

The effect of pH is more significant for the DOC removal than UV_{254} as can be seen in Figure 4.4. Aromaticity of algal matter is primarily due to proteins and amino acids, and pKa_1 of many aromatic acids is in the range of 1.82-2.83 with isoelectric points around

5.07-7.59 [70]. Therefore, in the test pH range, compounds contributing to aromaticity probably remained neutral and their removal was not affected significantly by pH. Interaction of EOM with soluble aluminum ions may cause EOM-metal complexes that will remain in solution until either the binding capacity of the EOM is satisfied, or the solubility of the metal-AOM complex is exceeded [71]. However, the complex formation potentially decreases the coagulation efficiency. The increase in DOC removal was incremental for an increase in pH from 5.0 to 6.0, with a maximum of 20% increase in EOM removal for Msp. For other algae, the increase in DOC removal was less than 8% when pH was decreased from 6.0 to 5.0. Conversely, low pH will require pH adjustment before final distribution of water. Considering the possibility of corrosion at lower pH and higher chemical consumption, although pH 5.0 and 40 mg/L may be considered as the enhanced coagulation condition for removal of both EOM and IOM, pH 6.0 was chosen for further experiments. During NOM coagulation, better performance was observed for hydrophobic fraction of the DOC [22]. Therefore, an effort was made in this work to fractionate the cellular materials of all six species and determine the effect of hydrophobicity on coagulation.
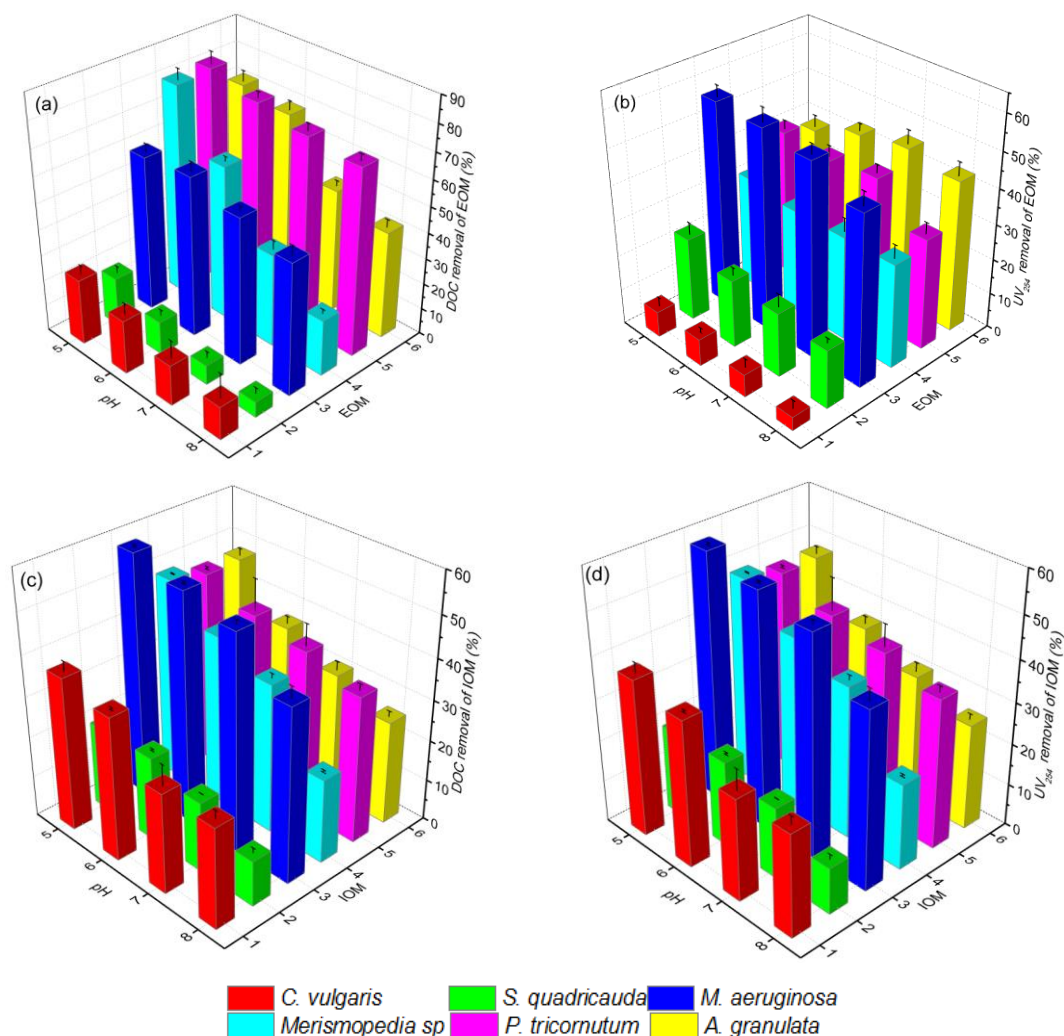
Figure 4.4 Effect of pH on DOC and UV$_{254}$ removal of EOM (a, b), of IOM (c, d) with initial DOC 8.5 ± 1.5 mg/L from individual algae and cyanobacteria.

4.3.3 Hydrophobicity of AOM and correlation with coagulation

The HPO, HPI and TPI contents of EOM and IOM are shown in Figure 4.5. The HPI fraction was the dominant fraction for all species and varied between 50 and 70%, consistent with earlier published results [26, 39, 72, 73]. Green algae has more HPI fraction than cyanobacteria, which is in accordance with Zhang et al. [73], where only 11% AOM of CV was HPO compared to 30% of MA [74]. In this work, the relatively higher HPO fraction in AOM of MA and MSP, 35.17±3.01% and 46.16 ±1.41%, respectively, compared to 30% HPO in MA-EOM [26, 75] is probably due to lower column capacity value of 30

used as explained earlier. The distribution of various fractions did not vary significantly between EOM and IOM, although PT (both EOM and IOM) and Msp (IOM) showed higher HPO fractions, causing the highest removal of AOM of PT by coagulation. The TPI of EOM/IOM from each species varies between 8.71 ± 0.95 % and 14.98 ± 0.66 %. TPI is of intermediate polarity isolated from the XAD-4 resin, and although the exact chemical identity of TPI is not known, they are more hydrophilic with a high proportion of carboxylic acid functionality [76] and may not be removed well due to coagulation. Except for PT, all the other species investigated in this work had higher HPO fraction in IOM than that in EOM, which is in agreement with the results from [77], where IOM from MA contained more HPO fraction with higher MW than EOM.
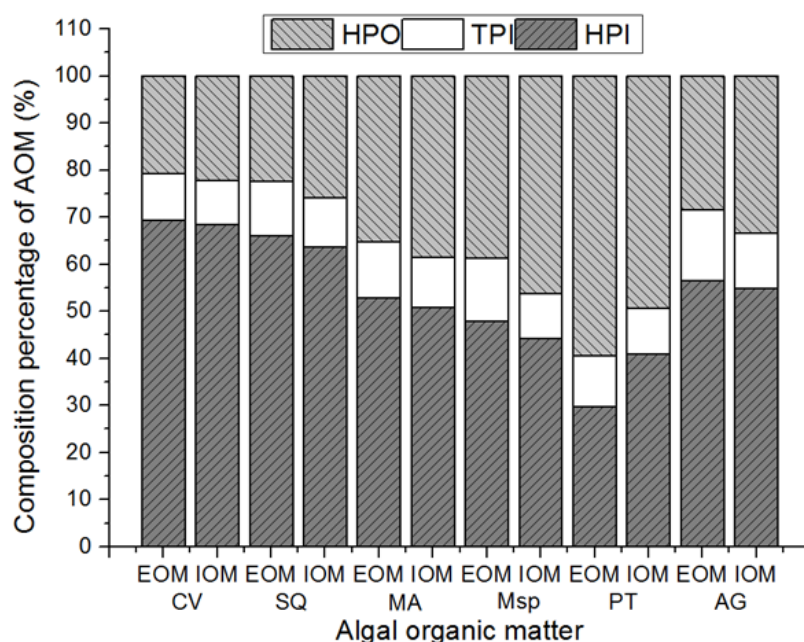
Figure 4.5 Resin fractionation results of EOM and IOM for the six species. (DOC recovery varied from 95-108%).

The cellular composition of each algal species collected from literatures was presented in Table 4.4. The HPI fraction including carbohydrates and proteins are dominant constituents of each species. All AOM investigated was predominately hydrophilic with low SUVA except PT. It has the highest amount of protein and lipid percentage than other algae, which may account for its relatively higher HPO ratio [78].

Table 4.4 Chemical composition of algal cell based on dry-weight*.

Algal species	Proteins (%)	Carbohydrates (%)	Lipids (%)	References
CV	54.65 ± 0.07	12.09 ± 3.17	12 ± 0.2	[5, 6]
SQ	7.15	50.4	35.7	[7]
MA	30-45	5-10	18.48-30.32	[8, 9]
Msp	29-45	35-57	10 ± 0.7	[6, 10]
PT	53.2	11.2	35.6	[11]
AG	47.9	36.3	15.8	[11]

* Organic solvent extraction was applied to isolate lipid after cell mechanical disruption

It was reported that the ratio of HPO and HPI organic matter can be used as an indicative parameter to quantify the treatability of NOM, especially DOC [22, 79]. During the coagulation-flocculation process, AOM can also act as a ligand to bind hydrous aluminum *in-situ* forming gelatinous precipitate, which can act as adsorption sites for further AOM [80]. Since the TPI fraction with carboxylic acid are more hydrophilic than hydrophobic, the DOC removal of AOM for all six species was plotted with the ratio of HPO to (HPI +TPI) (Figure 4.6).
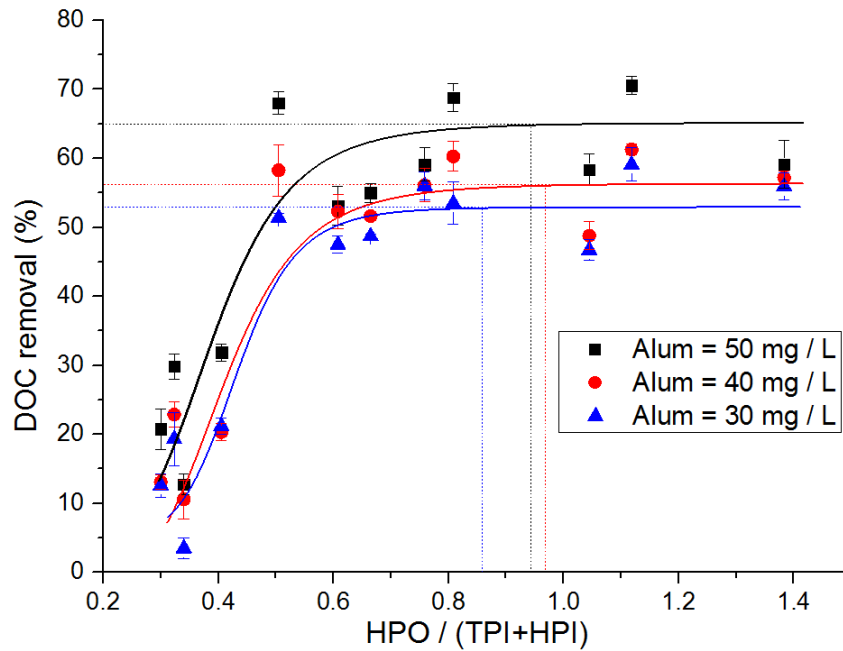
Figure 4.6 Correlation of HPO/(HPI+TPI) with DOC removal at different alum dosages.

The DOC removal increased with the increase of HPO/(HPI+TPI) ratio until the value reached 0.8 showing a non-linear behavior (fitted using Origin Pro 9.0 LangmuirEXT1 with the parameters shown in Table 4.5) [81]. Equation 4.3 shown below fitted the experimental data well with correlation co-efficient $R^2 \geq 85\%$ for alum dosage of 30 and 40 mg/:

$$y = \frac{a \cdot bx^{(1-c)}}{1 + bx^{(1-c)}}$$
(Eq. 4.3)

where, y represented the DOC removal percentage, which is equivalent to fractional coverage, θ, in the most used Langmuir adsorption isotherm $\theta = \frac{Kc}{1+Kc}$ [82]. The x is the ratio of HPO/(HPI+TPI), which indicates the hydrophobicity of AOM solution, and b is equal to the equilibrium constant K ($K = k_a/k_d$), where k_a and k_d are the rate constants for adsorption and desorption, respectively. The value of b in Equation (3) illustrates how the coagulant flocs or particulates surface sites become saturated as the hydrophobicity of the

solution rises. The magnitude of *b* quantifies the affinity of the AOM for surface adsorption. The *a* and *c* are fitting parameters without much physical significance.

The removal of AOM varies from 53.36% to 64.89% with the increase of alum dosage from 30 to 50 mg/L (Figure 4.6), more scatter in data can be seen at alum dosage of 50 mg/L. Such high alum dosage is also not advised due to adverse effect of Al^{3+} in treated water. The higher value of constant "*b*" (Table 4.5) at 30 mg/L indicates higher dependence of coagulation performance on dosage at lower HPO/(HPI+TPI) ratios.

It is interesting to see that higher than 65% AOM removal was not possible even at HPO/(HPI+TPI) $\geq$1.0 and at a higher alum dosage, and overdosing was not achieved, indicating charge reversal or restabilization of polymeric species were not factors, and no precipitation also can be observed.

Table 4.5 DOC removal parameters of AOM using alum at pH 6.

Alum dosage	Parameters			Regression	*p* value
mg/L	*a*	*b*	*c*	coefficient	
30	55.51	1322.67	-7.28	0.904	< 0.0001
40	57.38	248.89	-4.95	0.857	< 0.0001
50	65.25	259.27	-4.89	0.799	< 0.0001

4.3.4 DBP formation potential of various fractions of AOM

After chlorination using the UFC method, the specific DBPs produced by EOM and IOM from six species are shown in Figure 4.7. In agreement with the coagulation results presented earlier, *specific* THM and HAA formation potential remained constant for different doses of alum for all species. This is expected as the DBPFP was normalized with the corresponding DOC values; constant values indicate good reproducibility of coagulation and DBPFP experiments. A small increase/decrease in formation potential is mostly due to analytical error. Despite higher removal of DOC for PT, it showed the highest amount of DBP formation potential with 146.0 ± 16.64 µg/mg C of HAAs and 124.01 ± 11.07 µg/mg C of THM from the EOM, and 91.80 ± 1.02 µg/mg C HAAs and 75.91 ± 2.50 µg/mg C THM from the IOM, respectively, shown in Table 4.6. PT produced large amount

of AOM, especially relatively higher percentage of lipids causing higher amount of polyunsaturated fatty acids released by autolysis of the cells. Except PT and MA, IOM from four other species (CV, SQ, Msp and AG) presented higher specific HAAFP and THMFP than the corresponding EOM probably due to the higher aromatic and aliphatic proteinaceous substances in IOM with higher activity for chlorine substitution. Amino acids as the important constituents of algal organic matter have been reported for HAA formation [83], whereas carboxylic moieties in EOM likely to be unfavorable for substitution reaction with chlorine [84].
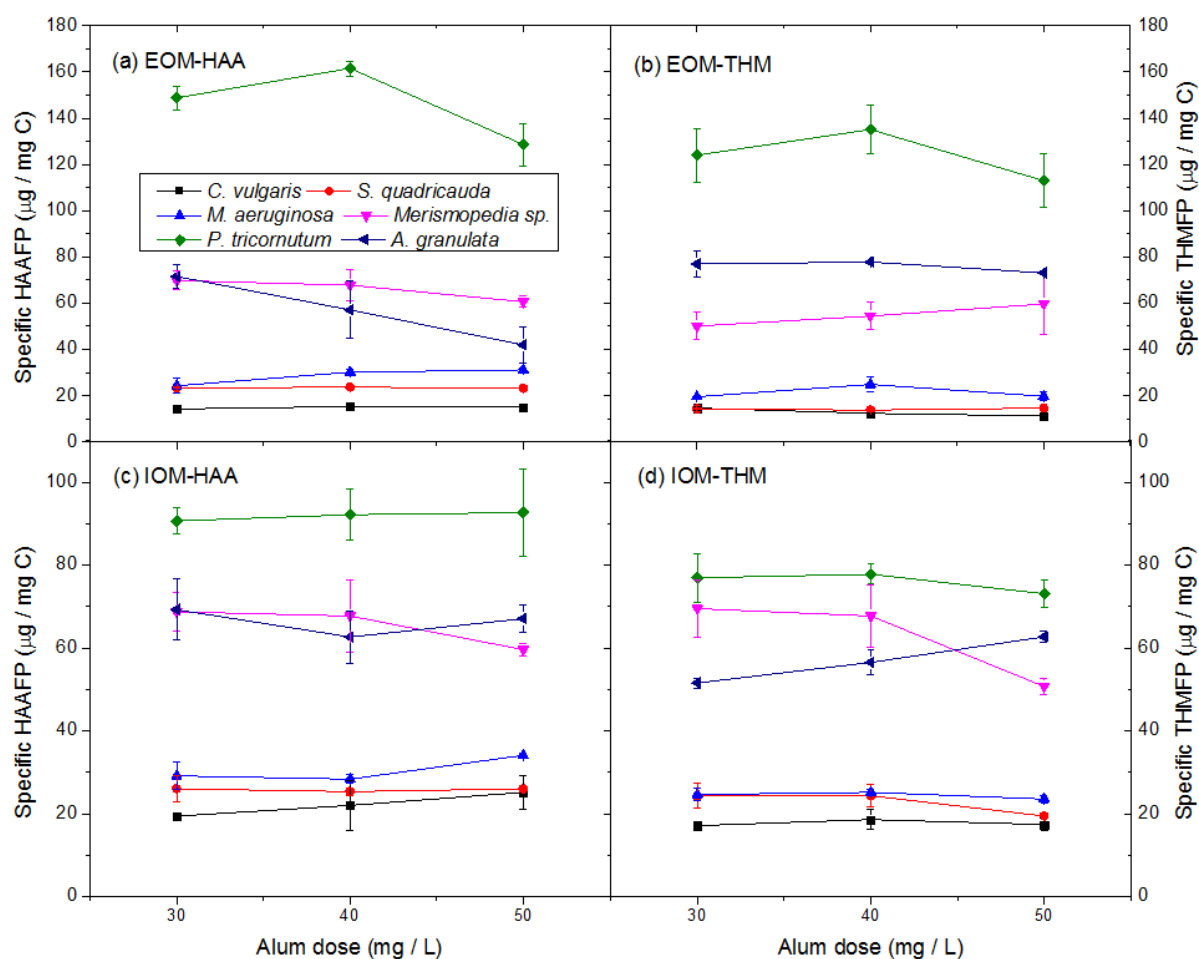
Figure 4.7 The specific DBP formation potential from different algal and cyanobacterial species after coagulation.

The DBPFP values produced in this work are in the range of limited values found in literature for different algae. A relatively higher proportion of HPO fraction in IOM than

EOM from MA was also reported by [62]. Higher THM formation for the MA-IOM with 20 μg/mg C as compared to 10 μg/mg C for the MA-EOM was reported [85]. Another study reported specific yields of chloroform, chloroacetic acid to be 32.44, 54.58 μg/mg C, respectively for MA-EOM, and 21.46, 68.29 μg/mg C for MA-IOM [62]. The two cyanobacteria (MA and Msp), with higher nitrogen fixation capability and releasing up to 45% of organic nitrogen [86], caused substantial amount of THM and HAA formation. Both MA and Msp contain significant amount of proteins in their AOM (Table 4.4); organic nitrogen also contributes to a large amount of active sites to derive THM and HAA [87, 88]. Amino acids can produce an unstable intermediate dichloroacetonitrile to react with chlorine and form THMs an HAAs [89].

Table 4.6 Average specific DBPFP for various species after coagulation.

Algae	Specific HAAFP (μg/mg C)		Specific THMFP (μg/mg C)	
	EOM	IOM	EOM	IOM
CV	14.83 ± 0.56	22.20 ± 2.86	12.66 ± 1.74	17.68 ± 0.77
SQ	23.36 ± 0.29	25.77 ± 0.41	14.17 ± 0.42	22.67 ± 2.83
MA	28.46 ± 3.74	30.52 ± 3.13	21.34 ± 2.98	24.44 ± 0.83
Msp	62.98 ± 4.82	65.30 ± 4.99	54.66 ± 4.78	62.61 ± 10.37
PT	146.26 ± 16.64	91.80 ± 1.02	124.01 ± 11.07	75.91 ± 2.50
AG	56.80 ± 14.83	66.30 ± 3.36	72.91 ± 2.50	56.92 ± 5.58

The correlation between SUVA and specific DBP formation potential (HAAPF and THMPF) from AOM is presented in Figure 4.8 with the correlation coefficients of 0.718 and 0.662 for specific HAAFP and specific THMFP, respectively.
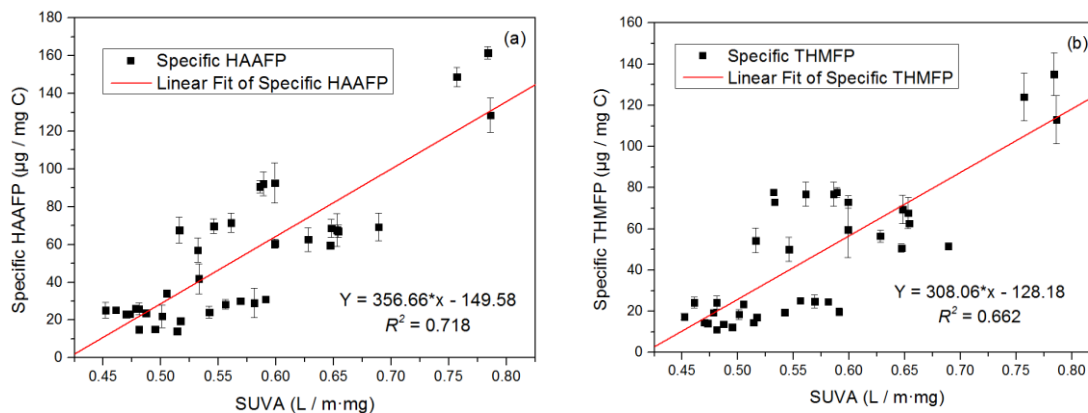
Figure 4.8 Correlation between SUVA of AOM and formation of HAAPF (a), THMFP (b).

Higher correlation coefficients 0.83 and 0.81 for HAAFP and THMFP, respectively with SUVA were presented in previous study [90], for NOM in algal-rich water with a DOC solution of much higher SUVA of 2-5 L/m·mg. Generally, DBPFP prediction capability of SUVA is weak in water with low SUVA values [91]. An attempt was made to evaluate the DBP formation potential of each fraction (HPI, TPI and HPO) from AOM, following the UFC method and the results are shown in Figure 4.9. It can be seen that the HPO fractions are the dominant DBP precursors; only exception of EOM of SQ, which had one of the lowest SUVA values. The results are consistent with an earlier study which more reactive HPO materials in water resulted higher DBPFP [92]. These results suggest that HPO/HPI ratio is a good indicator for THMFP for DOM irrespective of the nature and source of DOM.
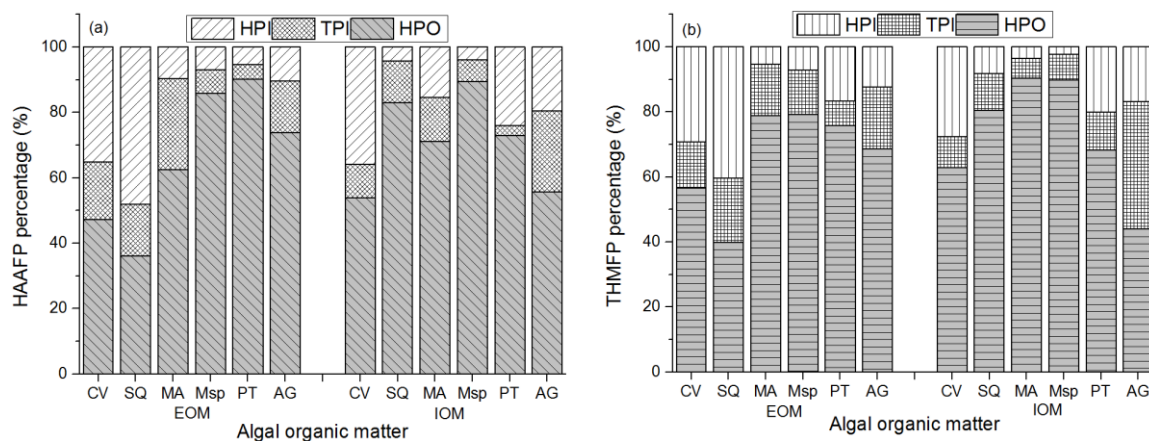
Figure 4.9 HAAFP and THMFP percentage of hydrophilic (HPI), transphilic (TPI) and hydrophobic (HPO) fractions of different species.

4.4 Conclusions

Coagulation performance and DBPFP for both extra- and intra-cellular materials of four algae and two cyanobacteria were determined. The work conclusively has shown that at optimum coagulation condition of pH 6 and alum dosage of 40 mg/L, an average of 47.43% and 40.43% AOM removal in terms of DOC and UV_{254} can be achieved, and removal correlated well with the HPO/(HPI +TPI) ratio and SUVA. The DBPFP was determined using uniform formation condition and the specific DBP value varied from 14.83 ± 0.56 μg/mg-C to 146.26 ± 16.64 μg/mg-C. The diatom, PT, produced the highest amount of DBP followed by the cyanobacterium Msp. The HPO fractions of cellular material contributed a majority of DBPFP, which are moderately correlated to SUVA ($R^2 \approx 0.662$-0.718), due to low SUVA values of the cellular materials. Although HPO fraction of the cellular material was removed better during coagulation, higher specific DBPFP also occurred for this fraction for most species. Similar to NOM, SUVA and hydrophobicity of AOM can be used as a surrogate parameter to predict the coagulation performance and DBPFP from algal matter. Although IOM produces higher amount of DBP, their concentration in natural water is low except for massive algal bloom collapse or during pre-oxidation before coagulation.

References

[1]   Z.S. Yan, B. Liu, F.S. Qu, A. Ding, H. Liang, Y. Zhao, G.B. Li, Control of ultrafiltration membrane fouling caused by algal extracellular organic matter (EOM) using enhanced Al coagulation with permanganate, Separation and Purification Technology 172 (2017) 51-58.

[2]   F.R. Pick, Blooming algae: a Canadian perspective on the rise of toxic cyanobacteria, Canadian Journal of Fisheries and Aquatic Sciences 73 (2016) 1-10.

[3]   S.C. Chang, C.H. Li, J.J. Lin, Y.H. Li, M.R. Lee, Effective removal of Microcystis aeruginosa and microcystin-LR using nanosilicate platelets, Chemosphere 99 (2014) 49-55.

[4]   A. Faruqi, M. Henderson, R.K. Henderson, R. Stuetz, B. Gladman, B. McDowall, A. Zamyadi, Removal of algal taste and odour compounds by granular and biological activated carbon in full-scale water treatment plants, Water Science and Technology-Water Supply 18 (2018) 1531-1544.

[5]   C.X. Ma, H.Y. Pei, W.R. Hu, H.Z. Xu, Y. Jin, The lysis and regrowth of toxic cyanobacteria during storage of achitosan-aluminium chloride composite coagulated sludge: implications for drinking water sludge treatment, RSC Advances 6 (2016) 112756-112764.

[6]   H.F. Miao, W.Y. Tao, The mechanisms of ozonation on cyanobacteria and its toxins removal, Separation and Purification Technology 66 (2009) 187-193.

[7]   A. Gonzalez-Torres, J. Putnam, B. Jefferson, R.M. Stuetz, R.K. Henderson, Examination of the physical properties of Microcystis aeruginosa flocs produced on coagulation with metal salts, Water Research 60 (2014) 197-209.

[8]   B. Ghernaout, D. Ghernaout, A. Saiba, Algae and cyanotoxins removal by coagulation/flocculation: A review, Desalination and Water Treatment 20 (2010) 133-143.

[9]   N. Zaouri, L. Gutierrez, L. Dramas, D. Garces, J.-P. Croue, Interfacial interactions between Skeletonema costatum extracellular organic matter and metal oxides: Implications for ceramic membrane filtration, Water Research 116 (2017) 194-202.

[10]   P.C. Xie, Y.Q. Chen, J. Ma, X. Zhang, J. Zou, Z.P. Wang, A mini review of preoxidation to improve coagulation, Chemosphere 155 (2016) 550-563.

[11]   M.Q. Zhu, N.Y. Gao, W.H. Chu, S.Q. Zhou, Z.D. Zhang, Y.Q. Xu, Q. Dai, Impact of pre-ozonation on disinfection by-product formation and speciation from chlor(am)ination of algal organic matter of Microcystis aeruginosa, Ecotoxicology and Environmental Safety 120 (2015) 256-262.

[12]   M. Pivokonsky, J. Naceradska, I. Kopecka, M. Baresova, B. Jefferson, X. Li, R.K. Henderson, The impact of algogenic organic matter on water treatment plant operation and water quality: A review, Critical Reviews in Environmental Science and Technology 46 (2016) 291-335.

[13]   Y. Zhang, Q. Fu, Algal fouling of microfiltration and ultrafiltration membranes and control strategies: A review, Separation and Purification Technology 203 (2018) 193-208.

[14]   A. Tomlinson, M. Drikas, J.D. Brookes, The role of phytoplankton as pre-cursors for disinfection by-product formation upon chlorination, Water Research 102 (2016) 229-240.

[15]   T. Li, B. Dong, Z. Liu, W. Chu, Characteristic of algogenic organic matter and its effect on UF membrane fouling, Water Science and Technology 64 (2011) 1685-1691.

[16]   C.W.K. Chow, M. Drikas, J. House, M.D. Burch, R.M.A. Velzeboer, The impact of conventional water treatment processes on cells of the cyanobacterium Microcystis aeruginosa, Water Research 33 (1999) 3253-3262.

[17]   J.-L. Lin, L.-C. Hua, S.K. Hung, C. Huang, Algal removal from cyanobacteria-rich waters by preoxidation-assisted coagulation–flotation: Effect of algogenic organic matter release on algal removal and trihalomethane formation, Journal of Environmental Sciences 63 (2018) 147-155.

[18]   M. Li, P.N. Nkrumah, M. Xiao, Biochemical composition of Microcystis aeruginosa related to specific growth rate: insight into the effects of abiotic factors, Inland Waters 4 (2014) 357-362.

[19]   C. Wan, M.A. Alam, X.-Q. Zhao, X.-Y. Zhang, S.-L. Guo, S.-H. Ho, J.-S. Chang, F.-W. Bai, Current progress and future prospect of microalgal biomass harvest using various flocculation technologies, Bioresource Technology 184 (2015) 251-257.

[20]   T. Takaara, D. Sano, H. Konno, T. Omura, Cellular proteins of Microcystis aeruginosa inhibiting coagulation with polyaluminum chloride, Water Research 41 (2007) 1653-1658.

[21]   A.J. Garzon-Sanabria, S.S. Ramirez-Caballero, F.E. Moss, Z.L. Nikolov, Effect of algogenic organic matter (AOM) and sodium chloride on Nannochloropsis salina flocculation efficiency, Bioresource Technology 143 (2013) 231-237.

[22]   D. Ghernaout, The hydrophilic/hydrophobic ratio vs. dissolved organics removal by coagulation – A review, Journal of King Saud University - Science 26 (2014) 169-180.

[23]   X.M. Tang, H.L. Zheng, B.Y. Gao, C.L. Zhao, B.Z. Liu, W. Chen, J.S. Guo, Interactions of specific extracellular organic matter and polyaluminum chloride and their roles in the algae-polluted water treatment, Journal of Hazardous Materials 332 (2017) 1-9.

[24]   M. Leloup, V. Pallier, R. Nicolau, G. Feuillade-Cathalifaud, Assessing Transformations of Algal Organic Matter in the Long-Term: Impacts of Humification-Like Processes, International Journal of Molecular Sciences 16 (2015) 18096-18110.

[25]   E.H. Goslan, C. Seigle, D. Purcell, R. Henderson, S.A. Parsons, B. Jefferson, S.J. Judd, Carbonaceous and nitrogenous disinfection by-product formation from algal organic matter, Chemosphere 170 (2017) 1-9.

[26]   R.K. Henderson, A. Baker, S.A. Parsons, B. Jefferson, Characterisation of algogenic organic matter extracted from cyanobacteria, green algae and diatoms, Water Research 42 (2008) 3435-3445.

[27]   H. Ou, N.Y. Gao, Y. Deng, J.L. Qiao, H. Wang, Immediate and long-term impacts of UV-C irradiation on photosynthetic capacity, survival and microcystin-LR release risk of Microcystis aeruginosa, Water Research 46 (2012) 1241-1250.

[28]   J. Naceradska, M. Pivokonsky, L. Pivokonska, M. Baresova, R.K. Henderson, A. Zamyadi, V. Janda, The impact of pre-oxidation with potassium permanganate on cyanobacterial organic matter removal by coagulation, Water Research 114 (2017) 42-49.

[29]   J.P. Smol, E.F. Stoermer, The diatoms: applications for the environmental and earth sciences, Cambridge University Press2010.

[30]   J.D. Plummer, J.K. Edzwald, Effect of ozone on algae as precursors for trihalomethane and haloacetic acid production, Environmental Science & Technology 35 (2001) 3661-3668.

[31]   S.Q. Zhou, S.M. Zhu, Y.S. Shao, N.Y. Gao, Characteristics of C-, N-DBPs formation from algal organic matter: Role of molecular weight fractions and impacts of pre-ozonation, Water Research 72 (2015) 381-390.

[32]   E.C. Wert, F.L. Rosario-Ortiz, Intracellular Organic Matter from Cyanobacteria as a Precursor for Carbonaceous and Nitrogenous Disinfection Byproducts, Environmental Science & Technology 47 (2013) 6332-6340.

[33]   L.O. Villacorte, Y. Ekowati, T.R. Neu, J.M. Kleijn, H. Winters, G. Amy, J.C. Schippers, M.D. Kennedy, Characterisation of algal organic matter produced by bloom-forming marine and freshwater algae, Water Research 73 (2015) 216-230.

[34]   H. Wang, D. Liu, L. Lu, Z. Zhao, Y. Xu, F. Cui, Degradation of algal organic matter using microbial fuel cells and its association with trihalomethane precursor removal, Bioresource Technology 116 (2012) 80-85.

[35]   J. Geciova, D. Bury, P. Jelen, Methods for disruption of microbial cells for potential use in the dairy industry—a review, International Dairy Journal 12 (2002) 541-553.

[36]   X. Wang, H. Miao, Y. Zhai, Study on the methods of alga cells fragmentation, Journal of Tianjin University of Science & Technology 22 (2007) 21.

[37]   P. Singha, K. Muthukumarappan, Quality changes and freezing time prediction during freezing and thawing of ginger, Food science & nutrition 4 (2016) 521-533.

[38]   P. Prabakaran, A.D. Ravindran, A comparative study on effective cell disruption methods for lipid extraction from microalgae, Letters in applied microbiology 53 (2011) 150-154.

[39]   L. Li, N.Y. Gao, Y. Deng, J.J. Yao, K.J. Zhang, Characterization of intracellular & extracellular algae organic matters (AOM) of Microcystic aeruginosa and formation of AOM-associated disinfection byproducts and odor & taste compounds, Water Research 46 (2012) 1233-1240.

[40]   S.A. Baghoth, Characterizing natural organic matter in drinking water treatment processes and trains, IHE Delft Institute for Water Education, Delft University of Technology, 2012.

[41]   F.S. Qu, H. Liang, J.G. He, J. Ma, Z.Z. Wang, H.R. Yu, G.B. Li, Characterization of dissolved extracellular organic matter (dEOM) and bound extracellular organic matter (bEOM) of Microcystis aeruginosa and their impacts on UF membrane fouling, Water Research 46 (2012) 2881-2890.

[42]   Y. Chen, B. Dong, N. Gao, J. Fan, Effect of coagulation pretreatment on fouling of an ultrafiltration membrane, Desalination 204 (2007) 181-188.

[43]   Z. Su, T. Liu, W. Yu, X. Li, N.J.D. Graham, Coagulation of surface water: Observations on the significance of biopolymers, Water Research 126 (2017) 144-152.

[44]   J. Labanowski, G. Feuillade, Dissolved organic matter: Precautions for the study of hydrophilic substances using XAD resins, Water Research 45 (2011) 315-327.

[45]   M.-L. Nguyen, P. Westerhoff, L. Baker, Q. Hu, M. Esparza-Soto, M. Sommerfeld, Characteristics and reactivity of algae-produced dissolved organic carbon, Journal of Environmental Engineering 131 (2005) 1574-1582.

[46]   D. Ma, B. Peng, Y. Zhang, B. Gao, Y. Wang, Q. Yue, Q. Li, Influences of dissolved organic matter characteristics on trihalomethanes formation during chlorine

disinfection of membrane bioreactor effluents, Bioresource Technology 165 (2014) 81-87.

[47] C. Piper, Development of a rapid fractionation tool for natural organic matter, Cranfield University, Cranfield University, 2010.

[48] M. Pivokonsky, J. Safarikova, M. Baresova, L. Pivokonska, I. Kopecka, A comparison of the character of algal extracellular versus cellular organic matter produced by cyanobacterium, diatom and green alga, Water Research 51 (2014) 37-46.

[49] L. Lin, B. Xu, Y.-L. Lin, C.-Y. Hu, T. Ye, T.-Y. Zhang, F.-X. Tian, A comparison of carbonaceous, nitrogenous and iodinated disinfection by-products formation potential in different dissolved organic fractions and their reduction in drinking water treatment processes, Separation and Purification Technology 133 (2014) 82-90.

[50] T.F. Marhaba, Y. Pu, K. Bengraine, Modified dissolved organic matter fractionation technique for natural water, Journal of Hazardous Materials 101 (2003) 43-53.

[51] A.T. Chow, Comparison of DAX-8 and XAD-8 resins for isolating disinfection byproduct precursors, Journal of Water Supply: Research and Technology-Aqua 55 (2006) 45-55.

[52] A. Shapiro, E. Karavanova, Fractionation of dissolved organic matter on the XAD resin, Moscow University soil science bulletin 69 (2014) 139-145.

[53] O. Orr, The characterization, isolation, and fractionation of natural organic matter from three surface waters, Environmental Engineering and Science, Clemson University, USA, 2009.

[54] R.S. Summers, S.M. Hooper, H.M. Shukairy, G. Solarik, D. Owen, Assessing DBP yield: uniform formation conditions, American Water Works Association. Journal 88 (1996) 80.

[55] X. Hu, Formation Potential of Disinfection By-products after Coagulation of Algal Matters, University of Western Ontario (2016).

[56] D.J. Munch, D.P. Hautman, Method 551.1: Determination of chlorination disinfection byproducts, chlorinated solvents, and halogenated pesticides/herbicides in drinking water by liquid-liquid extraction and gas chromatography with electron-capture detection, Methods for the Determination of organic compounds in drinking water (1995).

[57] M. Domino, B. Pepich, D. Munch, P. Fair, Y. Xie, Method 552.3 Determination of haloacetic acids and dalapon in drinking water by liquid-liquid microextraction,

derivatization, and gas chromatography with electron capture detection, Methods for the Determination of organic compounds in drinking water (2003).

[58]   S. Singh, P. Singh, Effect of temperature and light on the growth of algae species: a review, Renewable and Sustainable Energy Reviews 50 (2015) 431-444.

[59]   M. Podevin, I.A. Fotidis, D. De Francisci, P. Moller, I. Angelidaki, Detailing the start-up and microalgal growth performance of a full-scale photobioreactor operated with bioindustrial wastewater, Algal Research-Biomass Biofuels and Bioproducts 25 (2017) 101-108.

[60]   M. Li, W. Zhu, L. Gao, L. Lu, Changes in extracellular polysaccharide content and morphology of Microcystis aeruginosa at different specific growth rates, Journal of applied phycology 25 (2013) 1023-1030.

[61]   L. Barsanti, P. Gualtieri, Algae: anatomy, biochemistry, and biotechnology, Second Edition ed., CRC press2014.

[62]   G. Li, Y. Ren, L. Gu, Q. He, R. Deng, L.Z. Tang, Migration and transformation of nitrogen in algae organic matter (AOM) during the growth of Microcystis aeruginous, Desalination and Water Treatment 111 (2018) 79-87.

[63]   B. Edris, B. Hamed, M. FerdosKord, Determination of hydrophobic and hydrophilic fractions of natural organic matter in raw water of Zahedan water treatment plant, Health Scope 2012 (2012) 25-28.

[64]   A.M. Hansen, T.E. Kraus, B.A. Pellerin, J.A. Fleck, B.D. Downing, B.A. Bergamaschi, Optical properties of dissolved organic matter (DOM): Effects of biological and photolytic degradation, Limnology and Oceanography 61 (2016) 1015-1032.

[65]   X. Yang, W.H. Guo, Q.Q. Shen, Formation of disinfection byproducts from chlor(am)ination of algal organic matter, Journal of Hazardous Materials 197 (2011) 378-388.

[66]   J.K. Edzwald, Coagulation in drinking-water treatment - particles, organics and coagulants, Water Science and Technology 27 (1993) 21-35.

[67]   D. Shu-xuan, X. Hui, X. Feng, W. Dong-sheng, Y. Chang-qing, J. Ru-yuan, L. Yan-jing, Effects of Al species on coagulation efficiency, residual Al and floc properties in surface water treatment, Colloids and Surfaces A: Physicochemical and Engineering Aspects 459 (2014) 14-21.

[68]   C. Hu, H. Liu, J. Qu, D. Wang, J. Ru, Coagulation behavior of aluminum salts in eutrophic water: significance of Al13 species and pH control, Environmental Science & Technology 40 (2006) 325-331.

[69]   K.E. Lee, N. Morad, T.T. Teng, B.T. Poh, Development, characterization and the application of hybrid materials in coagulation/flocculation of wastewater: A review, Chemical Engineering Journal 203 (2012) 370-386.

[70]   I. Hunt, R. Spinney, Amino Acids, Peptides and Proteins Organic Chemistry On-Line Learning Center, McGraw-Hill Calgary, 2006.

[71]   J. Gregor, C. Nokes, E. Fenton, Optimising natural organic matter removal from low turbidity waters by controlled pH adjustment of aluminium coagulation, Water Research 31 (1997) 2949-2958.

[72]   N. Her, G. Amy, H.R. Park, M. Song, Characterizing algogenic organic matter (AOM) and evaluating associated NF membrane fouling, Water Research 38 (2004) 1427-1438.

[73]   X. Zhang, M.E. Devanadera, F.A. Roddick, L. Fan, M.L.P. Dalida, Impact of algal organic matter released from Microcystis aeruginosa and Chlorella sp. on the fouling of a ceramic microfiltration membrane, Water Research 103 (2016) 391-400.

[74]   R.K. Henderson, S.A. Parsons, B. Jefferson, The impact of differing cell and algogenic organic matter (AOM) characteristics on the coagulation and flotation of algae, Water Research 44 (2010) 3617-3624.

[75]   X. Zhang, L. Fan, F.A. Roddick, Understanding the fouling of a ceramic microfiltration membrane caused by algal organic matter released from Microcystis aeruginosa, Journal of Membrane Science 447 (2013) 362-368.

[76]   G.R. Aiken, D.M. McKnight, K. Thorn, E. Thurman, Isolation of hydrophilic organic acids from water using nonionic macroporous resins, Organic Geochemistry 18 (1992) 567-573.

[77]   J.Y. Fang, J. Ma, X. Yang, C. Shang, Formation of carbonaceous and nitrogenous disinfection by-products from the chlorination of Microcystis aeruginosa, Water Research 44 (2010) 1934-1940.

[78]   S. Prestegard, S. Erga, P. Steinrücken, S. Mjøs, G. Knutsen, J. Rohloff, Specific metabolites in a Phaeodactylum tricornutum strain isolated from western Norwegian fjord water, Marine Drugs 14 (2015) 9.

[79]   L. Xing, M.F. Murshed, T. Lo, R. Fabris, C.W. Chow, J. van Leeuwen, M. Drikas, D. Wang, Characterization of organic matter in alum treated drinking water using high performance liquid chromatography and resin fractionation, Chemical Engineering Journal 192 (2012) 186-191.

[80]   K. Chithra, N. Balasubramanian, Modeling electrocoagulation through adsorption kinetics, J. Model. Simul. Syst 1 (2010) 124-130.

[81]   Y. Jin, C. Liu, X. Sun, K. Lee, Y. Jung, K. Row, Adsorption Isotherms of Tryptophan Enantiomer on D-Tryptophan Molecular Imprinted Polymer, Asian Journal of Chemistry 24 (2012).

[82]   N. Ayawei, A.N. Ebelegi, D. Wankasi, Modelling and interpretation of adsorption isotherms, Journal of Chemistry 2017 (2017) 11.

[83]   T. Bond, E.H. Goslan, S.A. Parsons, B. Jefferson, Treatment of disinfection by-product precursors, Environmental Technology 32 (2011) 1-25.

[84]   L.C. Hua, J.L. Lin, P.C. Chen, C.P. Huang, Chemical structures of extra- and intra-cellular algogenic organic matters as precursors to the formation of carbonaceous disinfection byproducts, Chemical Engineering Journal 328 (2017) 1022-1030.

[85]   R.K. Ali, A.M.A. El-Aty, M.I. Badawy, A. Abdel-Karim, T.A. Gad-Allah, M.E. Ali, Impacts of Algal Cells and Humic acid on the Formation of Disinfection By-Products during chlorination of drinking water, J. Appl. Environ. Biol. Sci 5 (2015) 298-303.

[86]   P. Westerhoff, H. Mash, Dissolved organic nitrogen in drinking water supplies: a review, Journal of Water Supply Research and Technology-Aqua 51 (2002) 415-448.

[87]   I.G. Hwang, H.Y. Kim, K.S. Woo, J. Lee, H.S. Jeong, Biological activities of Maillard reaction products (MRPs) in a sugar–amino acid model system, Food Chemistry 126 (2011) 221-227.

[88]   J. Huang, N. Graham, M.R. Templeton, Y. Zhang, C. Collins, M. Nieuwenhuijsen, A comparison of the role of two blue–green algae in THM and HAA formation, Water Research 43 (2009) 3009-3018.

[89]   D.A. Reckhow, A.L. MacNeill, T.L. Platt, J.N. McClellan, Formation and degradation of dichloroacetonitrile in drinking waters, Journal of Water Supply: Research and Technology-Aqua 50 (2001) 1-13.

[90]   K.-Y. Park, Y.-J. Yu, S.-J. Yun, J.-H. Kweon, Natural organic matter removal from algal-rich water and disinfection by-products formation potential reduction by powdered activated carbon adsorption, Journal of Environmental Management 235 (2019) 310-318.

[91]   N. Ates, M. Kitis, U. Yetis, Formation of chlorination by-products in waters with low SUVA—correlations with SUVA and differential UV spectroscopy, Water Research 41 (2007) 4139-4148.

[92]   D.M. Golea, A. Upton, P. Jarvis, G. Moore, S. Sutherland, S.A. Parsons, S.J. Judd, THM and HAA formation from NOM in raw and treated surface waters, Water Research 112 (2017) 226-235.

Chapter 5

5 Adsorption of algal organic matter onto granular activated carbon

5.1 Introduction

Algae bloom in surface water is an increasing worldwide concern due to significant secretion of intracellular and extracellular material increasing the color and odor of the water. The released algal organic matter (AOM) is primarily composed of polysaccharides, proteins and lipids, and is the major component of the dissolved organic matter (DOM) in surface water sources [1]. DOM of water increases coagulation demand, causes clogging of the filter and membrane, and increases disinfection by-product (DBP) formation [2]. The conventional drinking water treatment processes, such as coagulation and flocculation, can effectively remove the particulate algae cells in drinking water plants. However, these processes are ineffective in removing the dissolved organic matter (DOM) derived from algae, only partial removal occurs at extended coagulation conditions [3, 4]. Our earlier research showed that a maximum of 50-60% removal of AOM from six different algae occurred by enhanced coagulation at a higher alum dose of 50 mg/L at pH 5.0-6.0 [5].

Activated carbon adsorption is regarded as one of most effective technologies employed widely to remove DOM, turbidity, and DBP precursors [6-8]. Using mostly once-through operation, powdered activated carbon (PAC) is commonly applied in water treatment plants for micropollutant removal [9] and odor and/or taste control [10]. Although, PAC is removed in a downstream filter in the treatment plant requiring no further treatment, there is potential for some leakage of carbon into treated water. Conversely, granular activated carbon (GAC) with proper bed design and routine maintenance can be used more effectively at low cost for several years to remove trace organics and natural organic matter from surface water [11, 12].

The removal of DOM by activated carbon adsorption is affected by a number of parameters including initial DOM concentration, ionic strength, pH, molecular size distribution of DOM, and temperature [13]. To date, most studies on the adsorption of AOM on activated carbon concentrated on the removal of natural organic matter (NOM) [14-16] or a specific micropollutant in presence of NOM [8, 17, 18], while algal matter is an integral part of NOM in a eutrophic water. Only a few studies have dealt with the adsorption of AOM [19, 20]; in most cases, water collected from surface water sources was treated using activated carbon, where the DOM is composed of both algal matter and humic acid. The equilibrium and kinetics of adsorption of two algal odorants, dimethyl trisulfide and *β*-cyclocitral on GAC were investigated in presence of NOM; NOM inhibited the adsorption rate for the two odorants [21]. No study was found on the adsorption of algal matter on activated carbon separated from the growth of algae in control conditions. For large-scale applications, leading to the objectives of the present work. In this work, adsorption of extracellular organic matter (EOM) from *C. vulgaris* (green algae), *Merismopedia* sp. (cyanobacterium), and *P. tricornutum* (diatom) was characterized and the adsorption behavior was compared with that of humic acid. Only EOM was tested in this work as intracellular organic matter (IOM) is only present in water when lysis of algal cells occurs under some stress conditions such as pre-oxidation due to chlorination and ozonation or in case of excess algal bloom [22, 23].

5.2 Materials and methods

5.2.1 Algal cultivation and algal organic matter preparation

Three algae strains were originally purchased from Canadian Phycological Culture Centre (*P. tricornutum* (PT), strain no. CPCC 162 cultivated in F/2 medium in artificial seawater, *Merismopedia* sp. (Msp)strain no. CPCC 711 cultured in BG-11 medium in deionized water) and University of Texas at Austin and Chlamydomonas Resource Center (*C. vulgaris* (CV), strain no. UTEX 2714 cultured in High Salt medium in deionized water). For the rest of the discussion in this paper, the algae species are referred by their abbreviated names shown in the parentheses. The algae strains were inoculated in sterilized media with illumination (3000 lx) of a 16/8 hours light / dark cycle at 25°C for 30 days when the algal species reach

stationary growth phase. EOM of algae was separated from the harvested cell suspension using a centrifuge (Thermo Scientific, Legend T Plus) at 3700 rpm for 30 min. Subsequently, the obtained supernatant was filtered by a 0.45 µm hydrophilic acrylic copolymer filters (Pall Corp.) to obtain EOM. Measured as DOM, algal extracellular materials are complex organics comprised of polysaccharides, proteins, lipids, etc. However, instead of individual constituents of algal matter, it is more practical to determine the adsorption capacity of activated carbon for the removal of AOM as DOM. Concentration of DOM in the samples before and after adsorption was quantified as dissolved organic carbon (DOC) using a Shimadzu TOC–V$_{CPN}$ analyzer which was calibrated by a standard glucose solution to obtain the calibration curve with the detection limit of 0.1 mg/L. Commercial humic acid (HA) with an average molecular weight of 39.098 kDa was purchased from Alfa Aesar (Thermo Fisher Scientific, CA). A stock solution of HA was stored in amber glass bottle and protected from the sunlight. HA working solution with approximately 7.5 mg/L of DOC was prepared from the stock solution and then filtered through 0.45 µm membrane filter mentioned above before being used in the experiments. The pH and temperature were measured using a pH meter (Orion Model STAR A111). The UV/Vis spectrophotometer (Shimadzu Model 3600) was used to scan a range of absorbance values from 200 to 300 nm with a 1 cm quartz cell to obtain the ultraviolet absorbance at 254 nm (UV$_{254}$) for the AOM.

The commercial granular activated carbon (GAC) was an extruded activated charcoal (CAS Number: 7440-44-0, Norit ROW 0.8 SUPRA) purchased from Sigma-Aldrich (Canada Co). The GAC surface properties were analyzed in an earlier work [23] at our lab: surface area ≈1400 m^2/g; microporous area ≈ 766 m^2/g; mesoporous area ≈ 634 m^2/g; pore size ≈ 2 nm; total pore volume ≈ 0.7 cm^3/g. The GAC was washed by Milli-Q water to remove the fines and then dried in an oven at 105 °C overnight, and subsequently stored in a desiccator prior to the experiments.

5.2.2. Batch adsorption experiments

The adsorption experiments were carried out in 500 mL Erlenmeyer flasks containing 400 mL of DOM (either AOM or humic acid) solution using a Max Q 400 Bench-top Orbital

Shaker (Thermo Scientific, Canada) operated at four temperatures (296, 303, 308 and 313K) using 200 rpm of agitation. Since surface- and ground-water contain DOC in the range of 2-10 mg/L [24], initial DOC concentration of both AOM and humic acid was kept in this range. The required amount of GAC was added into the DOM solution with an initial DOC of 7.4 ± 0.5 mg/L. The pH of solution was adjusted using 1M HCl or 1M NaOH to reach the initial pH values between 5-8 prior to adsorption. About 10 mL of samples were collected from each flask at certain time intervals and filtered through 0.45 μm membrane filter, followed by the DOC and UV$_{254}$ measurement. Triplicate experiments were performed at each adsorption condition.

through 0.45 μm membrane filter followed by the DOC and UV$_{254}$ measurement.

5.3 Results and discussion

The adsorption of AOM onto the GAC is affected by various factors such as contact time, the adsorbent dosage/adsorbate concentration, pH of the solution and temperature [25].

5.3.1. Influence of contact time

To determine the equilibrium time for maximum uptake, the adsorption experiments were performed with GAC dosage of 1.2 g/L for DOM solution with initial DOC of 7.50 ± 0.48 mg/L at 296 K for different contact time up to 12 h. It is indicated in Figure 5.1 that the removal of DOM by adsorption reached a plateau after 10 h, so that a contact time of 12 h was taken to be the equilibrium time, which is comparable to the adsorption of other organics on activated carbon such as humic acid [26]. It was also demonstrated in Figure 5.1 that the adsorption was relatively rapid within first 4 h and gradually slowed until it reached equilibrium after 10 h. This is typical of any adsorption process when initial rapid adsorption occurs due to the availability of a large amount of vacant surface sites. However, comparing adsorption of many organics on GAC [8, 20, 21, 27, 28], where most adsorption occurs within first few minutes, the adsorption of AOM is somewhat low. The rate of adsorption declined approximately after 10 h, as the remaining vacant sites on adsorbent are difficult to occupy probably because of the repulsive forces between DOM [27, 28]. It can be seen from Figure 5.1a, that the highest removal efficiency of 62.58 ± 0.23 %

occurred for CV-EOM followed by PT-EOM, HA and Msp-EOM, with 41.69 ± 0.62 %, 26.92 ± 0.23 % and 23.95 ± 0.07 %, respectively.
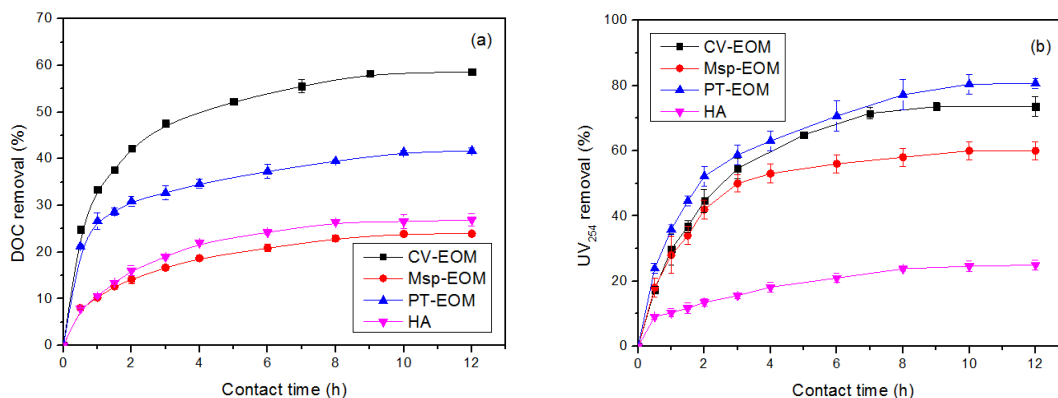
Figure 5.1 Effect of contact time on GAC adsorption for AOM removal as DOC (a) and UV_{254} (b) (initial DOC = 7.50 ± 0.48 mg/L, agitation speed = 200 rpm, GAC dosage = 1.2 g/L, pH =7 and Temperature = 296 K).

It was noted that UV_{254} removal for three EOM (Figure 5.1b) was higher than that of DOC removal, and HA showed a comparable removal percentage for both DOC and UV_{254}, which indicated that the aromatic and compounds containing unsaturated bonds or humic substances in DOM solution are the major substances to be adsorbed onto GAC. The hydrophobicity of the EOM of the tested in an earlier work in our group [5]. Although, the EOM of CV had the lowest amount of hydrophobic compounds compared to Msp and PT, highest adsorption occurred for the EOM of CV. The AOM of CV also had higher amounts of protein compared to PT and Msp [5]. This may be also due to the higher percentage of low molecular weight (< 1 kDa) fraction in in CV-EOM [29, 30]. In general, adsorption of EOM on GAC increased with the increased hydrophobicity; however, HA (MW > 39 kDa) and Msp-EOM comprised with higher portion of high molecular weight (1 < MW < 10 kDa) fraction [31] which resulted in the relatively low adsorption onto GAC [32].

5.3.2. Influence of GAC dosage

The influence of GAC dosage on the removal of DOM was determined in the range of 0.2 to 1.4 g/L, as shown in Figure 5.2. As expected, the percentage of DOM removal in terms

of DOC and UV_{254} increased with the increase of GAC dosage, as the number of available adsorption sites increased by increasing the adsorbent dose. However, at a larger dosage, agglomeration of GAC occurs reducing the adsorption sites. The removal of UV_{254} is typically higher than that of DOC, as aromatic compounds are better adsorbed on GAC.
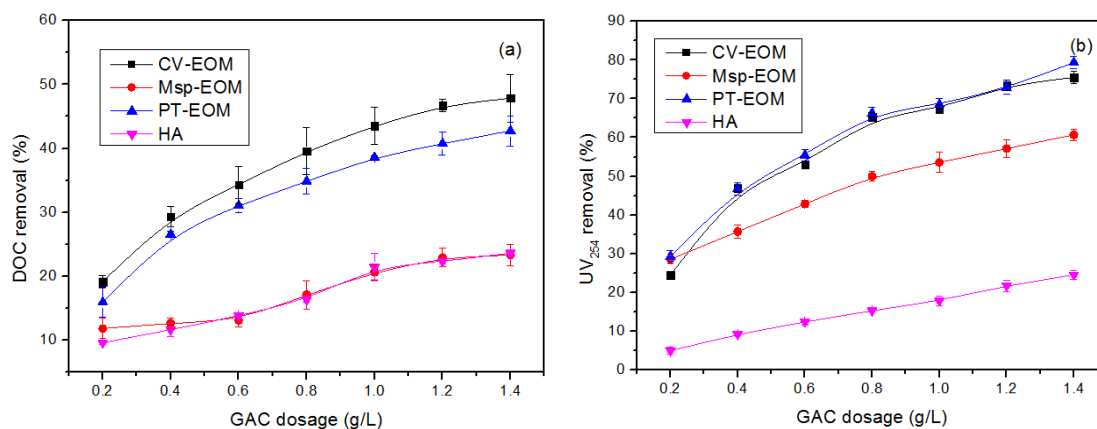
Figure 5.2 Effect of GAC dosage on AOM removal in term of DOC (a) and UV_{254} (b) (initial AOM concentration (DOC) = 7.4 ± 0.5 mg/L, agitation speed = 200 rpm, contact time = 12 hours, pH =7 and temperature = 296 K).

5.3.3. Influence of initial pH

The pH affects not only the surface charge of the adsorbent and the dissociation of functional groups on the active sites of the GAC, but also the degree of ionization of the DOM present in the solution [25, 33]. In this study, DOM adsorption by GAC was carried out in the pH range of 5.0-8.0. Figure 5.3 shows the effects of pH on the removal of DOM as DOC and UV_{254}. The extent of adsorption decreased significantly with pH increasing from 5.0-8.0, with the maximum adsorption efficiency for each species was attained at pH 5 with the DOC removal of 73.23 ± 2.96%, 53.02 ± 0.49%, 47.69 ± 3.71%, 22.65 ± 1.09%, for CV-EOM, PT-EOM, Msp-EOM and humic acid, respectively. UV_{254} removal also followed the same trend with highest removal occurring at the lowest pH of 5.0.
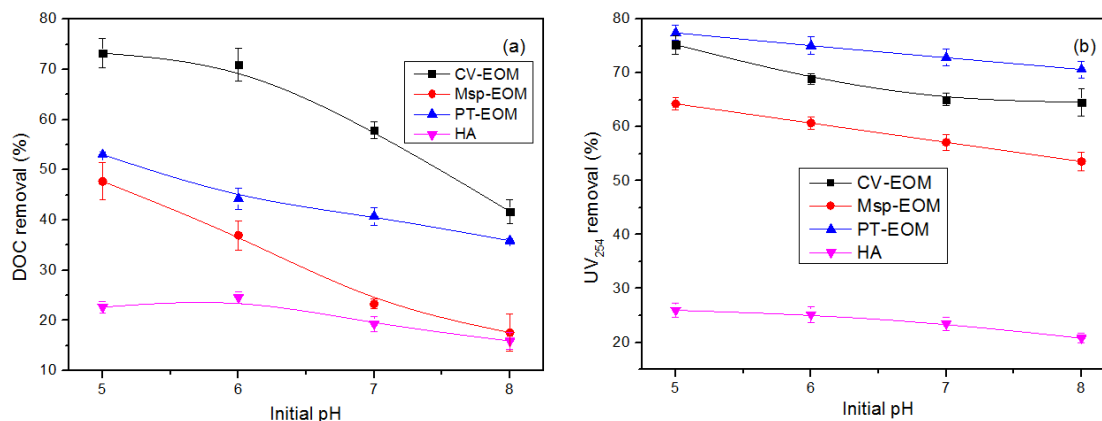
Figure 5.3 Effect of initial pH on GAC adsorption for AOM removal in term of DOC (a) and UV$_{254}$ (b) (initial DOC = 7.4 ± 0.5 mg/L, agitation speed = 200 rpm, contact time = 12 hours, GAC dosage = 1.2 g/L and temperature = 296 K).

Generally, DOM derived from algal cells or HA comprises of various polymeric components such as polysaccharide, lipid, proteins [34] and humic substances [35] with major functional groups such as carboxylic and phenolic, which are deprotonated at higher pH. The point of zero charge for the commercial GAC was determined to be 9.5 [36] Therefore, the GAC surface remained mostly positively charged at pH 5.0, and the higher adsorption at low pH is probably due to the electrostatic attraction between the positively charged GAC surface and partially deprotonated carboxylic and phenolic groups of AOM and HA, and also due to hydrophobic interactions between the carbon surface and the neutral compounds [37].

5.3.4. Effect of solution temperature

The influence of temperature from 296 K to 313 K on adsorption equilibrium is presented in Figure 5.4. It was observed that the removal of DOM from different algae increased with increase in temperature, which was in accordance with earlier results of increased adsorption of natural organic matter (NOM) [13, 38]. As shown in Figure 5.4a, CV-EOM presented the highest increase (18.46 %) with increasing temperature from 296 K to 313 K, followed by 9.54 %, 8.96 % and 5.54 % for Msp-EOM, PT-EOM and HA, respectively.

The UV$_{254}$ removal (Figure 5.4b) of each DOM was higher than the corresponding DOC; the highest increase (10.85%) in removal was observed from PT-EOM, followed by Msp-EOM, HA and CV-EOM with increased removal percentage of 9.29%, 8.15% and 0.87%, respectively.
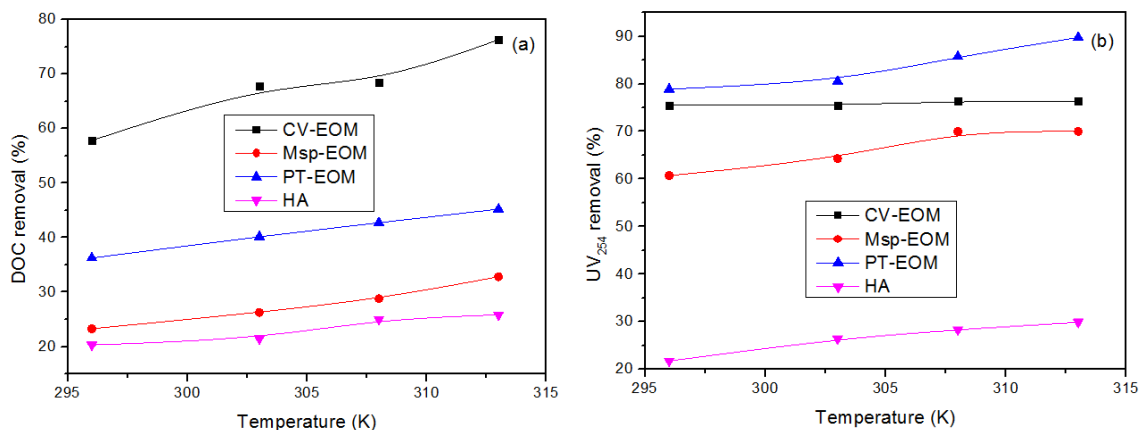
Figure 5.4 Effect of temperature on GAC adsorption for DOM removal in term of DOC (a) and UV$_{254}$ (b) (initial DOM concentration (DOC) = 7.42 ± 0.31 mg/L, agitation speed = 200 rpm, contact time = 12 hours, GAC dosage = 1.2 g/L and pH = 7.0).

This endothermic nature of the adsorption process indicates chemisorption of DOM on GAC surface. Similar increase in adsorption due to increase in temperature was seen by several researchers for the adsorption of NOM on GAC.[39] It was indicated that NOM forms larger aggregates at lower temperatures, but disintegrates into smaller molecules at higher temperatures, which can diffuse with relative ease into micropores of activated carbon, increasing adsorption at higher temperature.

5.3.5. Adsorption equilibrium

Both Langmuir and Freundlich models were applied to evaluate the most suitable adsorption isotherm for the DOM adsorption onto GAC. The Langmuir model was derived from the assumptions that adsorption occurs on a homogenous surface of an adsorbent and

forms a monolayer on the surface of the adsorbent, with uniform adsorption energies [40]. The linear form of the models can be expressed as the following Equations 5.1 and 5.2.

$$\frac{1}{q_e} = \frac{1}{q_m K_L} \frac{1}{C_e} + \frac{1}{q_m} \qquad \text{(Eq. 5.1)}$$

where C_e is the DOM concentration in solution (mg/L) at equilibrium, q_e denotes the amount adsorbed at equilibrium (mg/g), q_m is the maximum adsorption capacity of GAC (mg/g), K_L is the adsorption constant at equilibrium.

$$R_L = \frac{1}{1 + K_L C_0} \qquad \text{(Eq. 5.2)}$$

The R_L is the separation factor, which demonstrates the feature of the isotherms to be either irreversible ($R_L = 0$), favorable ($0 < R_L < 1$), linear ($R_L = 1$) or unfavorable ($R_L > 1$) [41].

The Freundlich model describes a multilayer adsorption with non-uniform affinity over a heterogeneous surface with non-uniform heat of adsorption [42]. The linear form of the Freundlich model can be expressed as the following Equation 5.3.

$$\log q_e = \log K_F + \frac{1}{n} \log C_e \qquad \text{(Eq. 5.3)}$$

where K_F is a constant associated with the adsorption capacity and $1/n$ is an empirical parameter relating the surface affinity, which varies with the heterogeneity of surface site energy distribution [20]. The calculated model parameters are summarized in Table 5.1 and the fitted models are shown in Figure 5.1.

To elucidate the adsorption capacity of GAC for each type of AOM, the equilibrium adsorption data for each AOM were analyzed using Langmuir, Freundlich Equation 5.1-5.3. The calculated parameters are summarized in Table 5.1.and shown in Figure 5.5.

Table 5.1 Analysis of Langmuir and Freundlich adsorption isotherm parameters by linear regression method.

Isotherm parameters	CV-EOM		Msp-EOM		PT-EOM		HA	
Langmuir adsorption	DOC	UV_{254}	DOC	UV_{254}	DOC	UV_{254}	DOC	UV_{254}
q_m (mg/g)	31.45	1.02	4.24	0.17	22.88	0.27	7.90	0.16
K_L	0.09	3.10	0.16	7.04	0.03	10.33	0.04	5.05
R_L	0.63	0.77	0.45	0.84	0.80	0.68	0.77	0.24
R^2	0.98	0.94	0.93	0.98	0.98	0.98	0.93	0.94
Freundlich adsorption								
K_F (L/g)	6.89	1.38	0.83	0.723	0.83	1.42	0.38	0.14
n	1.19	1.27	1.973	1.11	1.18	1.15	1.26	3.66
R^2	0.98	0.95	0.943	0.98	0.98	0.98	0.93	0.95

The R^2 values of the Langmuir (average $R^2 = 0.957$) and Freundlich (average $R^2 = 0.962$) isotherms for all DOM (for both DOC and UV_{254}) were all above 0.95 and indicated that the adsorption data were fitted well by both models. The maximum adsorption capacities of GAC for DOC removal calculated by the Langmuir model were 31.45 mg/g, 4.235 mg/g, 22.88 mg/g, and 7.899 mg/g for the DOC of CV-EOM, Msp-EOM, PT-EOM and HA, respectively. A comparable adsorption capacity (5 - 9 mg DOC/g GAC) for HA adsorption was also reported in previous study indicated that GAC presented a poor adsorption for high MW of HA. [32]. The adsorption capacity of Msp-EOM was the lowest, and comparing with the earlier work on the adsorption of naphthenic acids on the same GAC, the capacity for DOM is much lower compared to the naphthenic acids [36, 43]. The value of R_L from the Langmuir model varies from 0.241 to 0.880; in addition, the obtained values of n (within the range of 1.108 and 3.660) from the Freundlich model inferred that DOM removal by GAC was a favorable adsorption process [41], the values of n were more close to 1, which demonstrated that the surface heterogeneity of GAC is a less significant factor for adsorption [11].
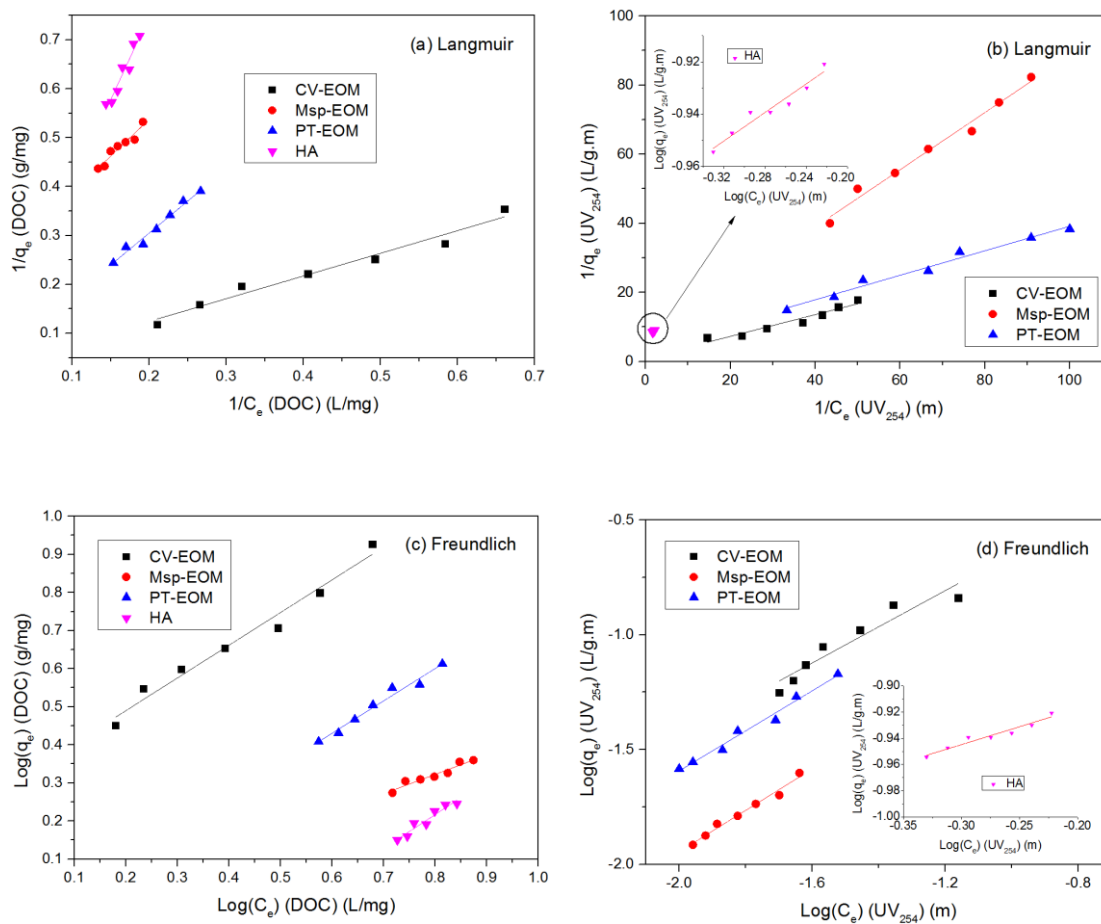
Figure 5.5 Adsorption isotherms of DOM onto GAC by Langmuir modeling for DOC (a) and UV$_{254}$ (b) removal, Freundlich modeling for DOC (c) and UV$_{254}$ (d) using C$_0$ = 7.373 ± 0.286 mg/L, T= 296 K, pH = 7, t =12h.

5.3.6. Adsorption kinetics

Adsorption kinetics quantitatively describes the rate of adsorption. The kinetics of DOM removal by GAC were analyzed using pseudo-first-order and pseudo-second-order models to fit the experimental data, the intraparticle diffusion model was also further applied to analyze the kinetic data [40].

The pseudo first-order model can be expressed by following linear Equation 5.4 and 5.5:

$$\log(q_e - q_t) = \log q_e - \frac{k_1}{2.303} t \qquad \text{(Eq. 5.4)}$$

$$q_t = \frac{(C_0 - C_t) V}{m} \qquad \text{(Eq. 5.5)}$$

Where k_1 (h^{-1}) is the pseudo-first-order adsorption kinetic constant; q_t is the amount of DOM adsorbed at time t (h); and q_e refers to the amount adsorbed at equilibrium, both in mg/g. C_0 is the initial DOM concentration in solution (mg/L), and C_t is the DOM concentration in solution at time t (h). The k_1 and q_e values are obtained by plotting log $(q_e - q_t)$ as a function of t.

The pseudo-second-order model derived from the adsorption capacity at equilibrium can be described by the following Equation 5.6:

$$\frac{t}{q_t} = \frac{1}{k_2 q_e^2} + \frac{t}{q_e} \qquad \text{(Eq. 5.6)}$$

where k_2 (g/mg min) is the rate constant at equilibrium for pseudo second-order adsorption. q_t and q_e ($mg.g^{-1}$) are the amounts of DOM adsorbed at time t and at equilibrium, respectively.

The calculated kinetic parameters including the first-order rate constant k_1, the second-order rate constant k_2, experimental equilibrium adsorption amount $q_{e, exp}$ and theoretical equilibrium adsorption amount $q_{e, cal}$ for each DOM, and regression coefficients (R^2), are presented in Table 5.2 and Figure 5.6.

The precision of model fitting was evaluated by the value of regression coefficients (R^2) and comparing the value of $q_{e, exp}$ and $q_{e,cal}$. The theoretical equilibrium adsorption capacities calculated from the pseudo-second-order model for each DOM compared well with the experimental data, with higher R^2 value demonstrating the validity and superiority of the second order model than pseudo-first-order model. Based on the findings, it can be

concluded that the pseudo-second-order model better describes DOM removal by GAC adsorption.
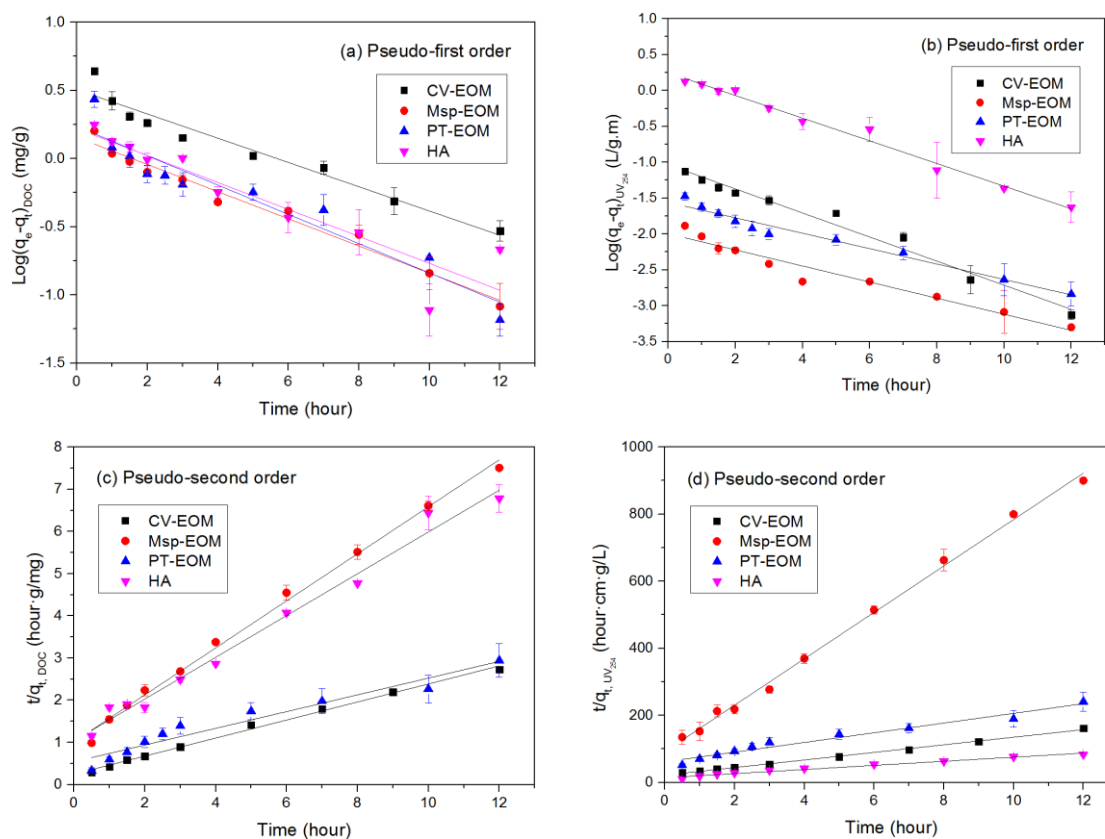
Figure 5.6 Kinetic modeling for AOM adsorption; Pseudo-first-order kinetic model DOC (a) and UV$_{254}$ (b); pseudo-second-order kinetic model DOC (c) and UV$_{254}$ (d), under adsorption condition of C$_0$ = 7.573 ± 0.359 mg/L, T= 296 K, pH = 7.

Table 5.2 Parameters of the pseudo-first and pseudo-second order kinetic models.

Kinetic parameters	CV-EOM		Msp-EOM		PT-EOM		HA	
Pseudo-first-order	DOC	UV_{254}	DOC	UV_{254}	DOC	UV_{254}	DOC	UV_{254}
k_1 (h^{-1})	0.21	0.39	0.23	0.26	0.25	0.25	0.23	0.36
$q_{e,cal}$ (mg/g)	3.21	0.09	1.43	0.01	1.72	0.03	1.66	0.57
Δq(%)	-26.8	24.4	-10.2	-22.6	-37.4	-18.9	-19.1	29.9
R^2	0.95	0.98	0.98	0.95	0.91	0.96	0.86	0.98
Pseudo-second-order								
k_2 (g/(mg·h)	0.18	5.91	0.43	52.1	0.17	3.41	0.24	2.65
$q_{e,cal}$ (mg/g)	4.67	0.09	1.52	0.01	3.357	0.07	2.02	0.16
Δq(%)	6.69	19.42	-4.82	11.13	21.77	4.57	-1.66	13.56
R^2	0.99	0.99	0.99	0.99	0.94	0.97	0.99	0.99
Intraparticle diffusion								
k_{d1} (mg/(g·h$^{0.5}$)	1.33	0.03	0.55	0.01	0.62	0.01	0.77	0.04
C_1	0.95	0.001	0.12	0.001	1.03	0.003	0.18	0.02
R^2	0.97	0.98	0.99	0.96	0.89	0.94	0.94	0.99
k_{d2} (mg/(g·h$^{0.5}$)	0.25	0.002	0.22	0.002	0.07	0.005	0.23	0.01
C_2	3.48	0.07	0.79	0.01	0.20	0.02	0.94	0.10
R^2	0.98	0.68	0.92	0.97	0.75	0.94	0.57	0.99
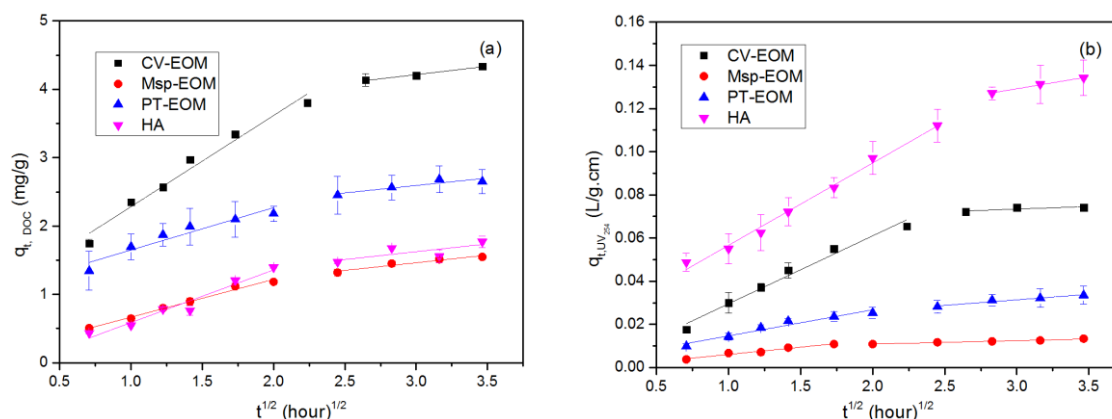
Figure 5.7 Intraparticle diffusion plot for GAC adsorption of DOM removal in term of DOC (a) and UV$_{254}$ (b) at C$_0$ = 7.573 ± 0.359 mg/L, T= 296 K, pH = 7.

The adsorption data were further analyzed to evaluate the role of diffusion (as a rate-controlling step) in the adsorption process by intraparticle diffusion model as shown in Equation 5.7.

$$q_t = k_d\sqrt{t} + C \qquad \text{(Eq. 5.7)}$$

where k_d is the intraparticle diffusion rate constant (mg·g^{-1} h$^{-1/2}$) and C is the intercept of linear plot of qt *vs.* $\sqrt{t}$, which is proportional to the thickness of boundary layer.

According to the intraparticle diffusion model, adsorbate uptake is proportional to the square root of contact time during the process of adsorption. The regression plot of *qt vs.* $\sqrt{t}$ should be linear if intraparticle diffusion process is involved and if the regression line passes through the origin, film diffusion is insignificant as $C = 0$ [44]. However, it is not always the case and both film diffusion and intraparticle diffusion may affect adsorption kinetics simultaneously [45]. For DOM adsorption on GAC, intraparticle diffusion was involved but was not the rate limiting step, since the regression lines did not pass through the origin as shown in Figure 5.7. The adsorption process of each DOM onto GAC includes two phases. For the first period, a linear phase with a steep slope was seen, which was followed by another linear phase with a shallow slope after 8 hours. Similar results were also reported by Qian et al [46] on haloform removal by GAC adsorption, indicating that

both film diffusion and intraparticle diffusion contributed to the adsorption process. The first phase is proposed to be the surface adsorption process in which DOM is quickly diffused to GAC surface through the boundary layer causing fast increase of qt $vs.$ $\sqrt{t}$. The intraparticle diffusion is the controlling process in the second phase in which the DOM diffuses into the intraparticle of the GAC and adsorbs onto the interior sites with a moderate increase of qt $vs.$ $\sqrt{t}$ till the adsorption equilibrium was reached [41, 47].

5.3.7. Thermodynamic properties

The standard Gibbs free-energy change (ΔG^{o}), enthalpy change (ΔH^{o}) and entropy change (ΔS^{o}) of the adsorption processes can be determined by the following Equation 5.8, 5.9 [21].

$$\Delta G^{o} = -RT \ln K_D \quad\quad\quad \text{(Eq. 5.8)}$$

$$\ln K_D = \frac{\Delta S^{0}}{R} - \frac{\Delta H^{0}}{RT} \quad\quad\quad \text{(Eq.5.9)}$$

Where T is the absolute temperature (K), R is the universal gas constant (8.314×J/(mol K)), and $K_D = q_e/C_e$ is the distribution coefficient (ml / g) of the solute between GAC and the solution in equilibrium [48]. The ΔH^{0} and ΔS^{0} can be calculated from the slope and intercept of the Van't Hoff plot of $\ln K_D$ as a function of $1/T$ as shown in Figure 5.8.
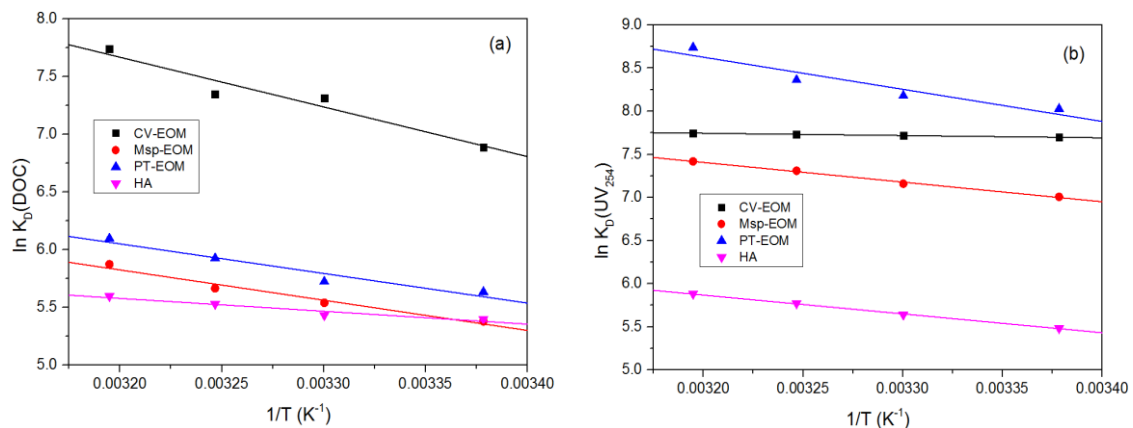
Figure 5.8 Plots of ln KD vs 1/T for the estimation of thermodynamic parameter for adsorption of DOM onto GAC in terms of DOC (a) andUV$_{254}$ (b).

The negative value of ΔG^0 (Table 5.3) indicates that the process is thermodynamically feasible and the adsorption is spontaneous. The decrease of ΔG^0 value with increase of temperature implied an increase in feasibility of adsorption at higher temperature. It was noted that ΔG^0 for UV$_{254}$ removal by adsorption was less than that of DOC removal, which indicated that aromatic substance represented by UV$_{254}$ in DOM was favorably removed than DOC. It has been reported that ΔG^0 for a physisorption process, where van der Waals force is the major interaction force, was usually less than 20 kJ/mol [11]. Values presented in Table 5.3 indicate both physi- and chemi-sorption are important for AOM adsorption on GAC. The values of ΔH^0 for all DOM were positive, verifying the adsorption of DOM under experimental condition were endothermic. Moreover, the positive values of ΔS^0 indicate a nonreversible process with increasing freedom of the adsorbate during adsorption. Although the adsorption of DOM from bulk solution onto GAC is an entropy decreasing process, due to the simultaneous desorption of water molecules with DOM adsorption, the total entropy increased with a net positive ΔS^0 [11]. The adsorption of DOM with larger volume of molecules cause desorption of higher number of water molecules.

Table 5.3 Thermodynamic parameters for adsorption of DOM by GAC at different temperatures.

Temperature (K)	ΔG^0(kJ/mol) for DOC removal				ΔG^0(kJ/mol) for UV$_{254}$ removal			
	CV-EOM	Msp-EOM	PT-EOM	HA	CV-EOM	Msp-EOM	PT-EOM	HA
296	-16.95	-13.24	-13.87	-13.28	-18.94	-17.24	-19.76	-13.49
303	-18.43	-13.63	-14.09	-13.68	-19.39	-17.62	-20.13	-14.20
308	-18.82	-13.94	-14.58	-14.16	-19.83	-18.26	-20.58	-15.01
313	-20.14	-14.46	-15.00	-14.56	-20.15	-18.26	-21.51	-15.30
ΔH^0 (kJ/mol)	35.80	21.82	21.33	9.27	2.19	18.97	30.98	18.15
ΔS^0(J/mol·K)	178.30	118.25	118.57	76.03	71.40	122.28	170.86	106.86
R^2	0.94	0.97	0.94	0.93	0.99	0.99	0.91	0.99

5.4. Conclusion

In this study, the adsorption equilibrium, kinetics and thermodynamics of the removal of extracellular algal matter of three different algae were compared with that of a commercial humic acid. The adsorptive removal of DOC was significantly affected by pH, while a marginal effect can be seen for UV_{254}. The isotherm adsorption data fitted well with both Langmuir and Freundlich models, though the Freundlich model presented relatively higher R^2 than the Langmuir model. The monolayer maximum adsorption capacity for each DOM was 31.45 mg/g and 4.235 mg/g, 22.88 mg/g and 15.69 mg/g for DOC of CV-EOM, Msp-EOM, PT-EOM and HA, respectively. Due to the predominantly hydrophilic nature of algal matter, the removal by GAC adsorption is moderate with a range from 23.29 % to 57.85 % in terms of DOC. Thermodynamic analysis demonstrates that the DOM adsorption onto GAC is spontaneous and endothermic process in nature. The pseudo-second-order rate model well described the adsorption of DOM by granular activated carbon. The second order kinetics also indicates the existence chemisorption mechanism, which is possible due to ionization of the surface carbon and ionized DOM of algae; however, needs to be confirmed by surface analysis.

References

[1]   L. Li, H.C. Guo, C. Shao, S.L. Yu, D.Q. Yin, N.Y. Gao, N. Lu, Effect of algal organic matter (AOM) extracted from Microcystis aeruginosa on photo-degradation of Diuron, Chemical Engineering Journal 281 (2015) 265-271.

[2]   Y. Zhang, J.Y. Tian, J. Nan, S.S. Gao, H. Liang, M.L. Wang, G.B. Li, Effect of PAC addition on immersed ultrafiltration for the treatment of algal-rich water, Journal of Hazardous Materials 186 (2011) 1415-1424.

[3]   W. Cheng, S.A. Dastgheib, T. Karanfil, Adsorption of dissolved natural organic matter by modified activated carbons, Water Research 39 (2005) 2281-2290.

[4]   Z. Zhao, W. Sun, M.B. Ray, A.K. Ray, T. Huang, J. Chen, Optimization and modeling of coagulation-flocculation to remove algae and organic matter from surface water by response surface methodology, Frontiers of Environmental Science & Engineering 13 (2019) 75.

[5]   Z. Zhao, W. Sun, A.K. Ray, T. Mao, M.B. Ray, Coagulation and disinfection by-products formation potential of extracellular and intracellular matter of algae and cyanobacteria, Chemosphere 245 (2020) 125669.

[6]   J.C. Jeon, C.H. Jo, I. Choi, S.B. Kwon, E. Jang, T.M. Hwang, Analysis on the Natural Organic Matter and Disinfection By-Products in Full-scale Advanced Water Treatment Plant and Conventional Water Treatment Plant, Desalination and Water Treatment 51 (2013) 6288-6298.

[7]   K.P. Lobanga, J. Haarhoff, S.J. van Staden, Treatability of South African surface waters by activated carbon, Water SA 39 (2013) 379-384.

[8]   S. Jamil, P. Loganathan, A. Listowski, J. Kandasamy, C. Khourshed, S. Vigneswaran, Simultaneous removal of natural organic matter and micro-organic pollutants from reverse osmosis concentrate using granular activated carbon, Water Research 155 (2019) 106-114.

[9]   S.J. Jones, Pesticide residues in surface waters of North Carolina rural and urban watersheds: Studies to determine and reduce residues in drinking water, North Carolina State University, Ann Arbor, 2003, pp. 298.

[10]   W. Beita Sandi, Removal of N-nitrosodimethylamine and trihalomethane precursors with powdered activated carbon, Clemson University, Ann Arbor, 2013, pp. 82.

[11]   J. Deng, Y.S. Shao, N.Y. Gao, S.Q. Zhou, X.H. Hu, Adsorption Characteristics of ss-Ionone in Water on Granular Activated Carbon, Clean-Soil Air Water 40 (2012) 1341-1348.

[12]   C.A. Chiu, K. Hristovski, S. Huling, P. Westerhoff, In-situ regeneration of saturated granular activated carbon by an iron oxide nanocatalyst, Water Research 47 (2013) 1596-1603.

[13]   B. Schreiber, D. Wald, V. Schmalz, E. Worch, Removal of dissolved organic compounds by granular activated carbon, in: L. Simeonov, E. Chirila (Eds.) Chemicals as Intentional and Accidental Global Environmental Threats, Springer, Dordrecht, 2006, pp. 397-+.

[14]   K. Watson, M.J. Farre, F.D.L. Leusch, N. Knight, Using fluorescence-parallel factor analysis for assessing disinfection by-product formation and natural organic matter removal efficiency in secondary treated synthetic drinking waters, Science of the Total Environment 640 (2018) 31-40.

[15]   N. Moona, K.R. Murphy, M. Bondelind, O. Bergstedt, T.J.R. Pettersson, Partial renewal of granular activated carbon biofilters for improved drinking water treatment, Environmental Science-Water Research & Technology 4 (2018) 529-538.

[16]   A.H. Sulaymon, A.F.M. Ali, S.K. Al-Naseri, Natural organic matter removal from Tigris River water in Baghdad, Iraq, Desalination 245 (2009) 155-168.

[17]   S. Alvarez-Torrellas, J.L. Sotelo, A. Rodriguez, G. Ovejero, J. Garcia, Influence of the natural organic matter in the removal of caffeine from water by fixed-bed column adsorption, International Journal of Environmental Science and Technology 14 (2017) 833-840.

[18]   S.Y. Zhang, S. Gitungo, L. Axe, J.E. Dyksen, R.F. Raczko, A pilot plant study using conventional and advanced water treatment processes: Evaluating removal efficiency of indicator compounds representative of pharmaceuticals and personal care products, Water Research 105 (2016) 85-96.

[19]   M. Pivokonsky, J. Naceradska, I. Kopecka, M. Baresova, B. Jefferson, X. Li, R.K. Henderson, The impact of algogenic organic matter on water treatment plant operation and water quality: A review, Critical Reviews in Environmental Science and Technology 46 (2016) 291-335.

[20]   L. Cermakova, I. Kopecka, M. Pivokonsky, L. Pivokonska, V. Janda, Removal of cyanobacterial amino acids in water treatment by activated carbon adsorption, Separation and Purification Technology 173 (2017) 330-338.

[21]   K.J. Zhang, N.Y. Gao, Y. Deng, M.H. Shui, Y.L. Tang, Granular activated carbon (GAC) adsorption of two algal odorants, dimethyl trisulfide and beta-cyclocitral, Desalination 266 (2011) 231-237.

[22]   A.A.M. Gad, S. El-Tawel, Effect of pre-oxidation by chlorine/permanganate on surface water characteristics and algal toxins, Desalination and Water Treatment 57 (2016) 17922-17934.

[23]   P. Xie, Y. Chen, J. Ma, X. Zhang, J. Zou, Z. Wang, A mini review of preoxidation to improve coagulation, Chemosphere 155 (2016) 550-563.

[24]   D. Gumus, F. Akbal, A comparative study of ozonation, iron coated zeolite catalyzed ozonation and granular activated carbon catalyzed ozonation of humic acid, Chemosphere 174 (2017) 218-231.

[25]   K. Kuśmierek, A. Świątkowski, Influence of Ph on Adsorption Kinetics of Monochlorophenols From Aqueous Solutions on Granular Activated Carbon, Ecological Chemistry and Engineering S 22 (2015) 95-105.

[26]   H. Eustáquio, C.W. Lopes, R.S.d. Rocha, B.D. Cardoso, S.B. Pergher, Modification of activated carbon for the adsorption of humic acid, Adsorption Science & Technology 33 (2015) 117-126.

[27]   P. Hnatukova, I. Kopecka, M. Pivokonsky, Adsorption of cellular peptides of Microcystis aeruginosa and two herbicides onto activated carbon: Effect of surface charge and interactions, Water Research 45 (2011) 3359-3368.

[28]   W. Zhang, T. Yu, X.L. Han, W.C. Ying, Removal of 2-ClBP from soil-water system using activated carbon supported nanoscale zerovalent iron, Journal of Environmental Sciences 47 (2016) 143-152.

[29]   H.Q. Chu, H. Yu, X.B. Tan, Y.L. Zhang, X.F. Zhou, L.B. Yang, D.Y. Li, Extraction procedure optimization and the characteristics of dissolved extracellular organic matter (dEOM) and bound extracellular organic matter (bEOM) from Chlorella pyrenoidosa, Colloids and Surfaces B-Biointerfaces 125 (2015) 238-246.

[30]   P.K. Curtis-Jackson, G. Masse, M. Gledhill, M.F. Fitzsimons, Characterization of low molecular weight dissolved organic nitrogen by liquid chromatography-electrospray ionization-mass spectrometry, Limnology and Oceanography-Methods 7 (2009) 52-63.

[31]   M. Baresova, M. Pivokonsky, K. Novotna, J. Naceradska, T. Branyik, An application of cellular organic matter to coagulation of cyanobacterial cells (Merismopedia tenuissima), Water Research 122 (2017) 70-77.

[32] T. Karanfil, J.E. Kilduff, M.A. Schlautman, W.J. Weber, Adsorption of organic macromolecules by granular activated carbon .1. Influence of molecular properties under anoxic solution conditions, Environmental Science & Technology 30 (1996) 2187-2194.

[33] Z. Zhang, L. Yan, H. Yu, T. Yan, X. Li, Adsorption of phosphate from aqueous solution by vegetable biochar/layered double oxides: Fast removal and mechanistic studies, Bioresource Technology 284 (2019) 65-71.

[34] M. Pivokonsky, O. Kloucek, L. Pivokonska, Evaluation of the production, composition and aluminum and iron complexation of algogenic organic matter, Water Research 40 (2006) 3045-3052.

[35] C.M. Chung, T. Tobino, K. Cho, K. Yamamoto, Alleviation of membrane fouling in a submerged membrane bioreactor with electrochemical oxidation mediated by in-situ free chlorine generation, Water Research 96 (2016) 52-61.

[36] H.S. Niasar, H. Li, T.V.R. Kasanneni, M.B. Ray, C. Xu, Surface amination of activated carbon and petroleum coke for the removal of naphthenic acids and treatment of oil sands process-affected water (OSPW), Chemical Engineering Journal 293 (2016) 189-199.

[37] A. Omri, M. Benzina, W. Trabelsi, N. Ammar, Adsorptive removal of humic acid on activated carbon prepared from almond shell: approach for the treatment of industrial phosphoric acid solution, Desalination and Water Treatment 52 (2014) 2241-2252.

[38] B. Schreiber, V. Schmalz, T. Brinkmann, E. Worch, The effect of water temperature on the adsorption equilibrium of dissolved organic matter and atrazine on granular activated carbon, Environmental Science & Technology 41 (2007) 6448-6453.

[39] B. Schreiber, T. Brinkmann, V. Schmalz, E. Worch, Adsorption of dissolved organic matter onto activated carbon - the influence of temperature, absorption wavelength, and molecular size, Water Research 39 (2005) 3449-3456.

[40] S. Saber-Samandari, S. Saber-Samandari, H. Joneidi-Yekta, M. Mohseni, Adsorption of anionic and cationic dyes from aqueous solution using gelatin-based magnetic nanocomposite beads comprising carboxylic acid functionalized carbon nanotube, Chemical Engineering Journal 308 (2017) 1133-1144.

[41] S. Nethaji, A. Sivasamy, A. Mandal, Adsorption isotherms, kinetics and mechanism for the adsorption of cationic and anionic dyes onto carbonaceous particles prepared from Juglans regia shell biomass, International Journal of Environmental Science and Technology 10 (2013) 231-242.

[42] A. Sari, O.D. Uluozlu, M. Tuzen, Equilibrium, thermodynamic and kinetic investigations on biosorption of arsenic from aqueous solution by algae (Maugeotia genuflexa) biomass, Chemical Engineering Journal 167 (2011) 155-161.

[43] U. Iriarte-Velasco, J.I. Alvarez-Uriarte, N. Chimeno-Alanis, J.R. Gonzalez-Velasco, Natural Organic Matter Adsorption onto Granular Activated Carbons: Implications in the Molecular Weight and Disinfection Byproducts Formation, Industrial & Engineering Chemistry Research 47 (2008) 7868-7876.

[44] R. Aravindhan, J. Raghava Rao, B. Unni Nair, Preparation and characterization of activated carbon from marine macro-algal biomass, Journal of Hazardous Materials 162 (2009) 688-694.

[45] H. Qiu, L. Lv, B.-c. Pan, Q.-j. Zhang, W.-m. Zhang, Q.-x. Zhang, Critical review in adsorption kinetic models, Journal of Zhejiang University-Science A 10 (2009) 716-724.

[46] H. Qian, Y.-L. Lin, B. Xu, L.-P. Wang, Z.-C. Gao, N.-Y. Gao, Adsorption of haloforms onto GACs: Effects of adsorbent properties and adsorption mechanisms, Chemical Engineering Journal 349 (2018) 849-859.

[47] M.-H. To, P. Hadi, C.-W. Hui, C.S.K. Lin, G. McKay, Mechanistic study of atenolol, acebutolol and carbamazepine adsorption on waste biomass derived activated carbon, Journal of Molecular Liquids 241 (2017) 386-398.

[48] A.E.A. Nayl, R.A. Elkhashab, T. El Malah, S.M. Yakout, M.A. El-Khateeb, M.M. Ali, H.M. Ali, Adsorption studies on the removal of COD and BOD from treated sewage using activated carbon prepared from date palm waste, Environmental Science and Pollution Research 24 (2017) 22284-22293.

Chapter 6

6 Granular Activated Carbon Adsorption of Algal Organic Matter in Mitigating Microfiltration Membrane Fouling

6.1. Introduction

Climate change, population growth and increased urbanization have contributed to the increasing frequencies of eutrophication worldwide [1]. The occurrence of harmful algal blooms in surface water has increased markedly over the last decade [2]. The metabolites of algae and other planktonic species are the major constituents of natural organic matter (NOM) in many surface water bodies, which are the sources of potable water in many areas. These substances cannot be removed well by the traditional drinking water treatment processes such as coagulation-flocculation and sedimentation, creating problems for downstream units such as clogging of filters, increase biofouling, reduce the efficiency of adsorption beds for the removal of trace contaminants, and increased disinfection by-products formation [3].

The extensive application of membrane process, including microfiltration (MF) and ultrafiltration (UF), for drinking water treatment has significantly increased since the last two decades for their effective removal of pathogens such as *Cryptosporidium oocysts*. and *Giardia cysts* and reduction of water turbidity with a comparable cost to conventional sand-charcoal filtration systems [4, 5]. Microfiltration (MF, 0.1-10 μm) is widely applied in water treatment plants to remove particulate materials [6]. However, membrane fouling caused by DOM significantly affects the filtration efficiency in water treatment. Membrane fouling due to the surrogate NOM such as commercial humic acid (HA) and Suwannee River NOM (SRNOM) is well-researched [7-10]; however, fouling due to real cellular materials of algae or cyanobacteria (most common eutrophic species) needs further attention due to ubiquitous nature of the issue and absence of comprehensive research in this area.

A previous investigation of membrane fouling by algal organic matters (AOM) indicated that algal species and the derived AOM compositions significantly affected membrane fouling behavior [11]. An extended Derjaguin–Landau–Verwey–Overbeek (XDLVO) theory was applied to investigate the fouling behavior of AOM fractions from *Aphanizomenon flos-aquae* and *Anabaena flos-aquae*. The results indicated that the interface between membrane and neutral hydrophilic fraction presented highest attractive energy, and controlled the membrane fouling in AOM microfiltration process [12]. Granular activated carbon (GAC) adsorption, as one of the cost-effective and environmentally-friendly process for water treatment plants to remove organic matter, has been extensively applied as a pre-treatment process for membrane filtration to mitigate membrane fouling [13, 14]. It is generally acknowledged that the performance of MF is influenced by the membrane type, feedwater characteristics, and operational conditions [6]. A hybrid membrane-activated carbon process was applied for the treatment of oil field produced water and the results presented that GAC pre-treatment enhanced the removal efficiency of COD and conductivity, also reduced cake layer formation on membrane surface[15]. A previous study presented that biopolymers, such as proteins and polysaccharides, could be effectively removed by GAC pre-treatment prior UF filtration to mitigate the membrane fouling [16]. Another study [17] further found that coupling GAC to downstream MF process provided a significant reduction in membrane fouling with improved product water quality and lower carbon usage rate than powder activated carbon (PAC). Zhang et.al. [18] investigated the effect of PAC on fouling by algal solution during ultrafiltration using two modes, i.e., addition of PAC to the bulk feed and pre-depositing PAC onto the membrane surfaces. Both modes improved the removal of EOM from the algal solution; however, the influence of PAC addition on the EOM fouling was weak.

As mentioned above, most of the previous studies on GAC/PAC adsorption-microfiltration process focused on NOM, and artificial organic micropollutants removal from drinking water treatment, only a few of the investigations reported an integrated system for the treatment of algae-laden water. A comprehensive investigation on the combination of GAC and microfiltration membranes is not available. Further experimental data are necessary for process optimization and for designing of such units. The objective of the current study is

to investigate the effect of GAC dosage and solution pH on fouling potential and the flux of microfiltration due to several species of algae and cyanobacteria.

6.2. Materials and methods

6.2.1. Algae cultivation and AOM extraction

The three species, *Chlorella vulgaris* (CV)*, Microcystis aeruginosa* (MA), and *Phaeodactylum tricornutum* (PT)*,* were obtained from the Canadian Phycological Culture Centre (CPCC) at Waterloo University (Waterloo, ON, Canada). The algal cell were cultivated in 2 L flasks in High Salt, 3N-BBM and F/2, respectively, at $23 \pm 2^{\circ}C$ under a fluorescent lamp (3000 lx) with a 16/8 hours of light/dark cycle [19]. Algae and the cyanobacteria were harvested at the stationary growth phase monitored by cell counting following the previous study [20].

AOM solution was extracted by following steps: 1) centrifugation of the harvested algal cultures at 3700 rpm and $23^{\circ}C$ for 30 min (Thermo Scientific Sorvall, Legend T Plus); and 2) subsequent filtration of the supernatant by a 1.2 µm filter (hydrophilic acrylic copolymer, Pall Corporation) to obtain EOM. 3) The deposited algae on the filter were washed three times using Milli-Q water, then subjected to three freeze/thaw cycles (-18 °C for 12 h/40 °C for 2.0 h) to destroy the cells [21], then followed by centrifugation and filtration process as described above to obtain IOM. The obtained AOM stock solutions were stored at $4^{\circ}C$ in a fridge for no more than 48 hours before characterization or preparing the feed solution with DOC of 8 ± 0.5 mg/L for GAC adsorption and microfiltration after pH adjustment by 1 mol/L NaOH and 1.0 mol/L HCl solution. For comparison with the fouling behavior of AOM, humic acid (98% grade, Thermo Fisher Scientific Chemicals, Inc. USA) solution was used to prepare working solution as the surrogate of natural organic matter for GAC-MF experiment.

6.2.2. GAC adsorption

The commercial GAC (Norit ROW 0.8 SUPRA, CAS Number: 7440-44-0) used in this study was purchased from Sigma-Aldrich Canada Co. The properties of GAC were

investigated in a previous study in our group [22] showed as following: surface area ≈1400 m^2/g, pore size ≈2 nm, total pore volume ≈0.7 cm^3/g, mesoporous area ≈ 634 m^2/g, and microporous area ≈ 766 m^2/g The GAC was screened by mesh sieves in order to collect the GAC with size range of 0.42-0.60 mm, followed by washing to remove the fines, then dried in an oven at 105 °C, and stored in a desiccator before adsorption experiments.

The adsorption experiments were carried out in 500 mL Erlenmeyer flasks containing 400 mL of AOM solution using a Bench-top Orbital Shaker (Max Q 400, Thermo Scientific, ON, Canada) operated at temperatures of 23 ±1.5°C under 200 rpm of shaking speed. Since surface and groundwater contains DOC in the range of 2-10 mg/L [23], 1.0 g/L GAC was added into the DOM solution with an initial DOC of 8.0 ± 0.5 mg/L. The pH of solution was adjusted using 1.0 mole/L HCl or 1.0 mol/L NaOH to reach the pH values of 5-8 before adsorption. After GAC adsorption with the retention time of 1.0 hour, the solution was filtered using a 1.2 µm filter (hydrophilic acrylic copolymer, Pall Corporation) to remove GAC particles.

6.2.2. Membrane and filtration unit

6.2.2.1. Fouling experiment assessment

The MF membrane used was a 0.45 μm nominal pore size hydrophilic PVDF membrane (Millipore Corporation, US) with the effective filtration area of 1.59×10^{-3} m^2 in a dead-end stainless steel filter holder at a constant transmembrane pressure (TMP) of 50 ± 0.5 kPa by compressed air and operation temperature of 25 ±0.5 °C. Prior to filtration, all fresh membranes were soaked in Milli-Q water for at least 24 h to remove possible organic contaminants. The filtrate weight was measured constantly by a digital balance (Denver SI-4002, Denver Instrument Co. USA) and data were automatically logged to a connected computer equipped with a data acquisition system shown in Figure 6.1.
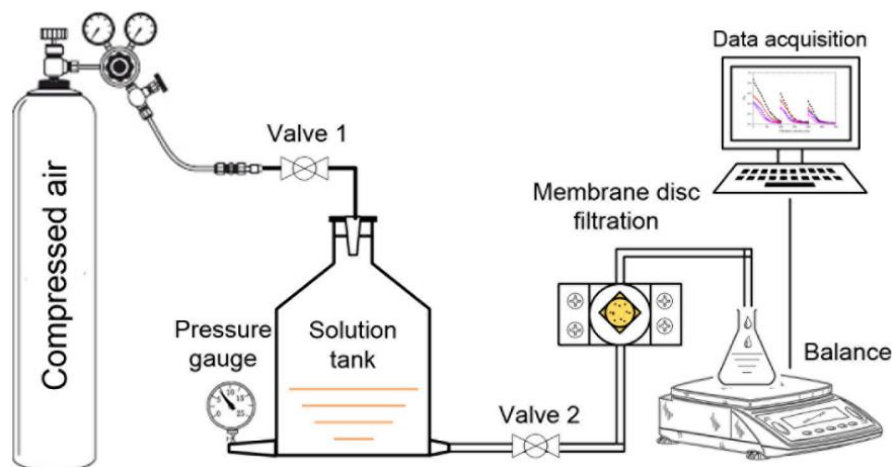
Figure 6.1 Schematic diagram of the apparatus for the MF system. (**Redraw from [11])**

All DOM solutions were diluted using Milli-Q water to DOC of 8.0 ± 0.5 mg/L from stock solution. Every filtration experiment was conducted for three continuous filtration cycles. Each cycle is comprised of 3 steps: (1) filtration with 100 mL Milli-Q water; (2) filtration of 100 mL feed solution (3) backwashing of membrane by placing the reverse side of membrane upwards and filtration of 100 mL Milli-Q water. The flux of feed solution is named $J_{s,n}$, with the number n (1-3) representing the cycle number. J_n represented the average flux in the filtration of Milli-Q water. The total fouling (TF), the reversible fouling (RF), and the accumulative irreversible fouling (IF) of each filtration cycle can be calculated as following Equation 6.1-6.3 [24].

$$TF_n = \frac{J_0 - J_{s,n}}{J_0} \qquad \text{(Eq. 6.1)}$$

$$IF_n = \frac{J_0 - J_n}{J_0} \qquad \text{(Eq. 6.2)}$$

$$RF_n = TF_n - IF_n \qquad \text{(Eq. 6.3)}$$

2.2.2. Membrane fouling resistance and mechanism

To elucidate fouling mechanisms, the classic filtration models, including complete blocking, standard blocking, intermediate blocking and cake filtration, were applied to understand the flux decline during the MF of the DOM solution under a constant pressure.

The instantaneous flux was calculated by numerically differentiating the cumulative volume filtered (V) per unit membrane area and analyzing it using blocking laws listed in Table 6.1.

Table 6.1 Equations of four classic filtration models [25, 26]**.**

Models	Equations	Description
Complete blocking	$J = J_0 - k_b V$	Particles block pores when reaching the membrane surfaces.
Standard blocking	$J = J_0\left(1 - \dfrac{k_s}{2}V\right)^2$	Particles deposit on the internal pore walls, decreasing the pore diameter.
Intermediate blocking	$J = J_0\exp\left(-k_i V\right)$	Particles settle on each other and may seal some membrane pores.
Cake filtration	$\dfrac{1}{J} = \dfrac{1}{J_0} + k_c V$	Particles deposit on the membrane surface and cake layer forms.

where J_0 is the initial permeate flux (m·s^{-1}), V is the accumulative volume (m^3) and k_b, k_s (m^{-1}), k_i (m^{-1}) and k_c (s·m^{-2}) are parameters describing complete blocking, standard blocking, intermediate block and cake filtration, respectively.

6.2.3. Analytical methods

DOC of AOM solution was measured using a TOC–V$_{CPN}$ analyzer (TOC–V$_{CPN}$, Shimadzu, Japan) with a detection limit of 0.1 mg/L calibrated by a standard glucose solution. Temperature and pH were measured using a pH meter (Orion Model STAR A111, USA). The UV absorbance at 254 nm (UV$_{254}$) was measured by a UV/Vis spectrophotometer (UV-3600, Shimadzu, Japan) and the specific UV absorbance (SUVA, L·mg^{-1}·cm) was calculated from UV$_{254}$ value divided by DOC concentration.

6.3. Results and discussion

6.3.1. Effect of GAC dosage on organic removal efficiency

The effect of GAC dosage on the removal of DOM was determined using dosage of 0- 1.5 g/L for different feed solution, and the results are shown in Figure 6.2. The percentage of

DOM removal (in terms of DOC (Figure 6.2 a) and UV_{254} (Figure 6.2 b) increased with the increase of GAC dosage, which may be attributed to an increasing number of available adsorption sites with the increasing adsorbent dosage. The removal of UV_{254} from each feed solution was higher than the removal of DOC. In terms of DOC for algal organic matter, the IOM for each algae presented higher removal efficiency than that of EOM. With a dosage of 1.5 g/L GAC, IOM of PT showed 40.03% of DOC removal, higher than that from EOM, followed by 37.68% from CV and 22.34% from MA. With respect to UV_{254}, there was 38.99% of UV_{254} removal from IOM, more than removed from EOM of CV, followed by 30.72%, 13.14% from MA and PT, respectively, which could be due to the higher aromatic or unsaturated components in IOM than EOM of the investigated algae [27-30]. Up to 23.21% of DOC and 24.06% of UV_{254} from PT-IOM was removed by the GAC-MF system with GAC addition of 1.5 g/L, more than DOC and UV_{254} was removed by the MF membrane without GAC addition.

It was found that GAC adsorption was effective for DOM removal, and similar results were found for DOC of lower molecular weight substances, when adsorbed onto GAC, and DOC of higher molecular weight can be removed by the cake formed on the surface of the MF membrane [31]. Comparison with DOM from algal organic matter, humic acid presented relatively lower removal efficiency. It was also noted that addition of GAC (1.5 g/L) showed (Figure 6.2) approximately 16.49 % and 16.67% greater DOC and UV_{254} removal than without GAC adsorption.
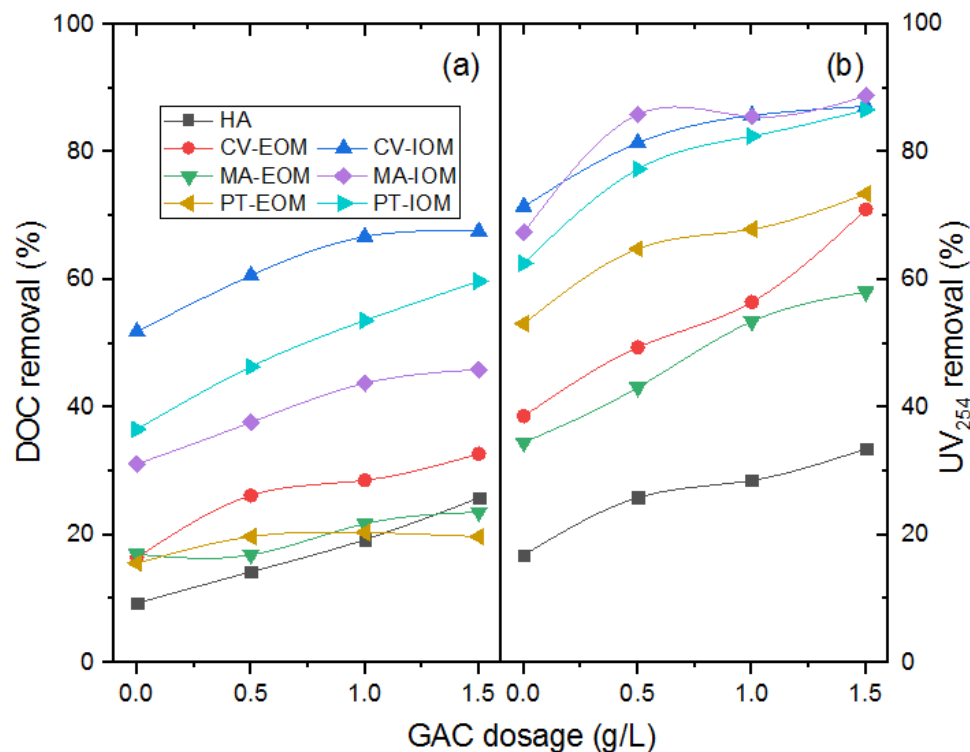
Figure 6.2 Effect of GAC dosage on DOM removal of DOC (a) and UV$_{254}$ (b) after microfiltration with GAC adsorption pretreatment at pH 7.0 and contact time of 1.0 hour.

6.3.2. Effect of GAC dosage on the flux and reversibility by DOM fouling

The normalized flux of each DOM for the MF with and without GAC addition is shown in Figure 6.3. The flux profiles demonstrated an initial sharp decrease (< 40 mL) followed by gradual decrease and a plateau during the later filtration phase. This phenomenon can be explained by the co-existence of irreversible pore blocking by low- MW fractions of the AOM and reversible cake layer formation resulting from the deposition of high-MW organics during the filtration period [32].
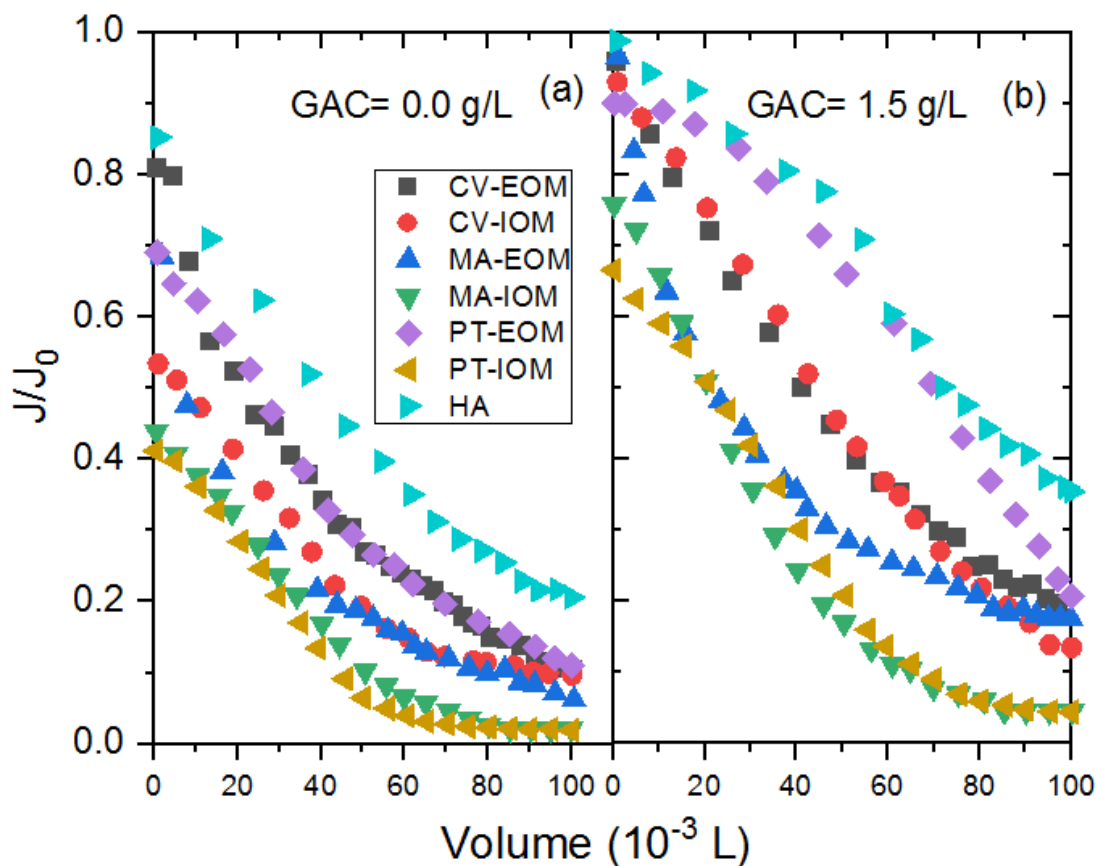
Figure 6.3 Flux profile for first filtration cycle of the DOM solution with and without GAC adsorption pretreatment.

Specifically, the feed solution from AOM presented a significant flux decline compared to humic acid, with more than 80% of flux decline occurred at the end of the single cycle filtration (Figure 6.3 a). A similar trend was also observed for the filtration of humic acid and AOM by Zhang et.al [33]. With 1.5 g/L GAC adsorption, the filtration flux for each DOM was improved, with a maximum 15 % improvement in flux occurred for HA, followed by PT-EOM, CV-IOM, CV-EOM, MA-EOM, and PT-IOM. It was noted that, even though filtration flux was increased for all AOM after GAC adsorption, about 80% decline in flux occurred for AOM. In comparison, flux for humic acid solution declined by 60%.
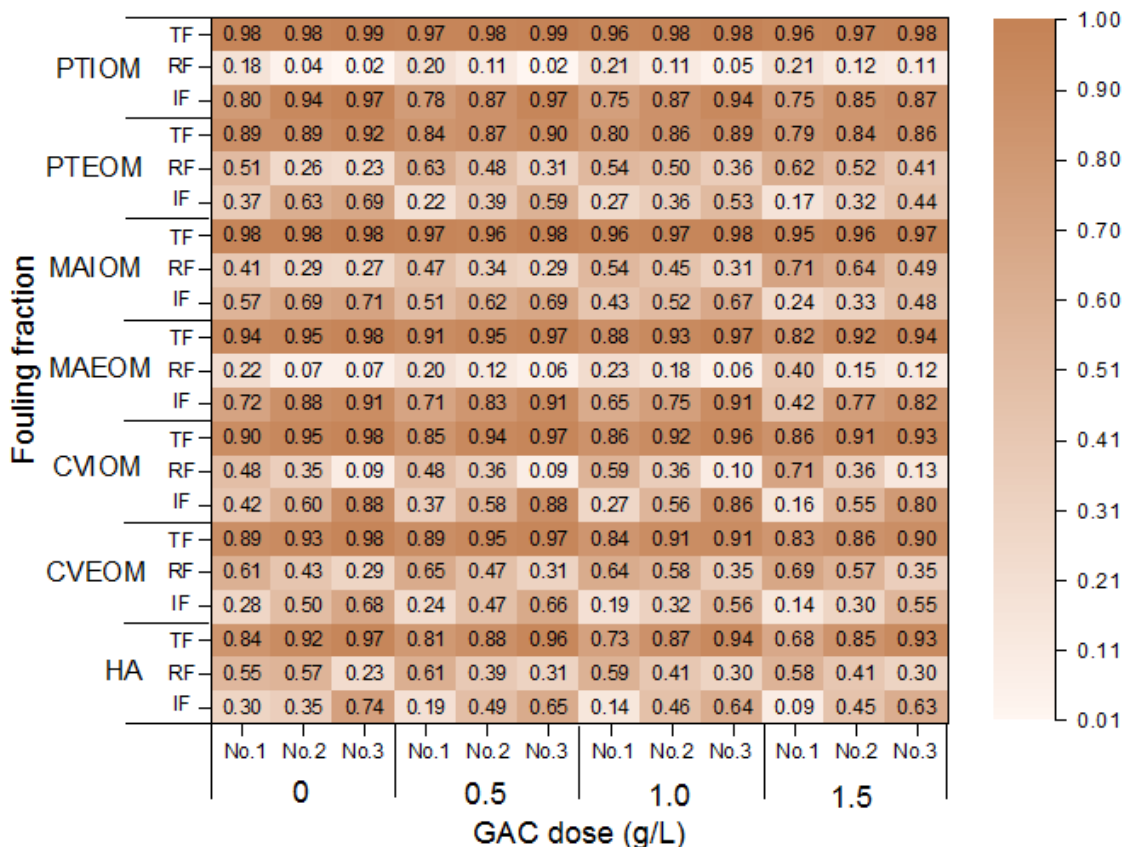
Figure 6.4 Effect of GAC dosage on the reversibility of DOM fouling (TF, RF and IF represented the total fouling, reversible fouling and irreversible fouling, respectively, No.1 to No.3 denoted the filtration cycle of each DOM).

Figure 6.4 shows the reversibility of fouling in terms of specific fouling contribution after each filtration cycle with different GAC addition. The results show that the irreversible fouling gradually increased at the cost of the reversible fouling decrease during the filtration cycles for each DOM. The decrease of irreversible fouling with the increase of GAC dosage indicated that GAC adsorption pretreatment improved the membrane reversibility considerably. Some protein-like compounds, hydrophobic in nature, and aromatic substances can be preferentially adsorbed by GAC, which was also validated by the UV_{254} removal in this study. An earlier study used biologically active carbon for the removal of hydrophilic compound for membrane filtration [34]. In this work, humic acid was observed to contribute lower irreversible fouling than the AOM investigated, probably due to higher hydrophilicity of the algal matter as shown earlier in Chapter 4. The EOM and IOM from

three algal species presented a comparable total fouling at identical experimental conditions; however, the irreversible fouling from IOM was higher than that of EOM due to higher percentage of hydrophilic protein-like substances with lower molecular weight (58.4%) than that in EOM (18.5%) [35]; probably by blocking of micropores of membrane or settling on already deposited substance resulting in the irreversible fouling.

6.3.3. Effect of pH on organic removal efficiency

The pH of the DOM solution not only alters the surface charge of the adsorbent, the dissociation of functional groups on the active sites of the adsorbent, but also affects ionization degree of the DOM in the solution [36, 37]. In this study, the pH dependence of DOM removal by microfiltration with GAC adsorption was performed in the pH range of 5.0-8.0.

As shown in Figure 6.5, the removal of DOM by GAC-MF combined system decreased with pH increasing from 5.0-8.0. Similar trend and relatively higher removal percentage of UV_{254} at lower pH for each DOM occurred, which indicated that aromatic and unsaturated compounds are favorably removed. The removal efficiency of each DOM decreased at neutral and alkaline pH. At alkaline condition, the anionic species from DOM, such as the carboxyl, hydroxyl, and amide groups of DOM, are deprotonated, resulting in the increase of negative charge of DOM, causing the decrease of DOM removal by GAC. The EOM solution showed higher removal efficiency than humic acid and IOM from each algal species.
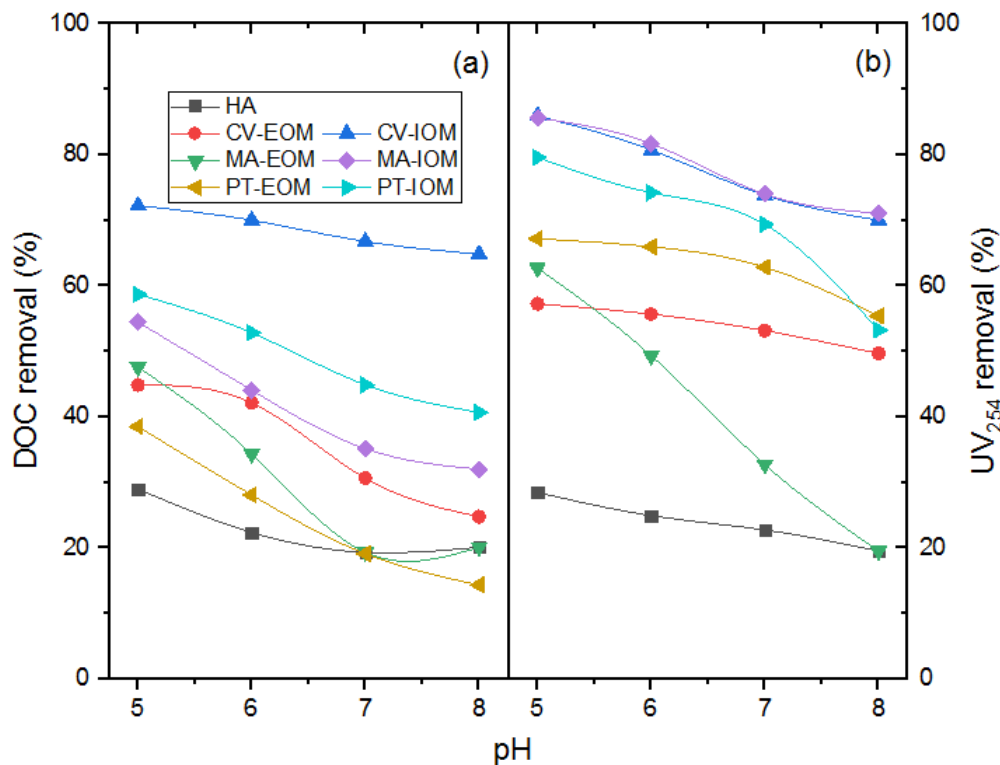
Figure 6.5 Effect of pH on DOM removal as DOC (a) and UV$_{254}$ (b) after microfiltration with GAC adsorption pretreatment (GAC dosage of 1.0 g/L and contact time of 1.0 hour).

6.3.4. Effect of pH on the flux decline and reversibility of DOM fouling

To probe the effect of feed solution pH on membrane permeate and degree of fouling after GAC adsorption for each DOM, experiments were performed at pH 5.0 and 8.0 for GAC adsorption with conditions mentioned above followed by three cycles of MF filtration without any additional pH control. As pH can alter the degree of ionization of the DOM presented in the solution, the electrostatic interaction between DOM and membrane would play a significant role. At higher pH, the repulsive force between negatively charged membrane and anionic species of DOM caused lower flux decline. On the contrary, at lower pH, the negatively charged membrane would attract protonated and positively charged DOM species, thus leading to the increased fouling and decrease of permeate flux [38]. In the present study, as seen from Figure 6.6, the flux decline increased at higher initial pH 8, which indicated that higher fouling occurred at higher pH. More than 30% of DOM of CV

was removed by GAC adsorption (with about 50% total removal by combining GAC-MF treatment). These results implied that the effectiveness of GAC adsorption at lower pH can reduce the permeate flux decline and mitigate membrane fouling. This was also seen in a previous study where decrease in the irreversible fouling of ultrafiltration occurred at lower pH for filtration of NOM [39]. This finding implied that the electrostatic attraction between DOM and membrane was not the dominant fouling mechanism in present experiments.
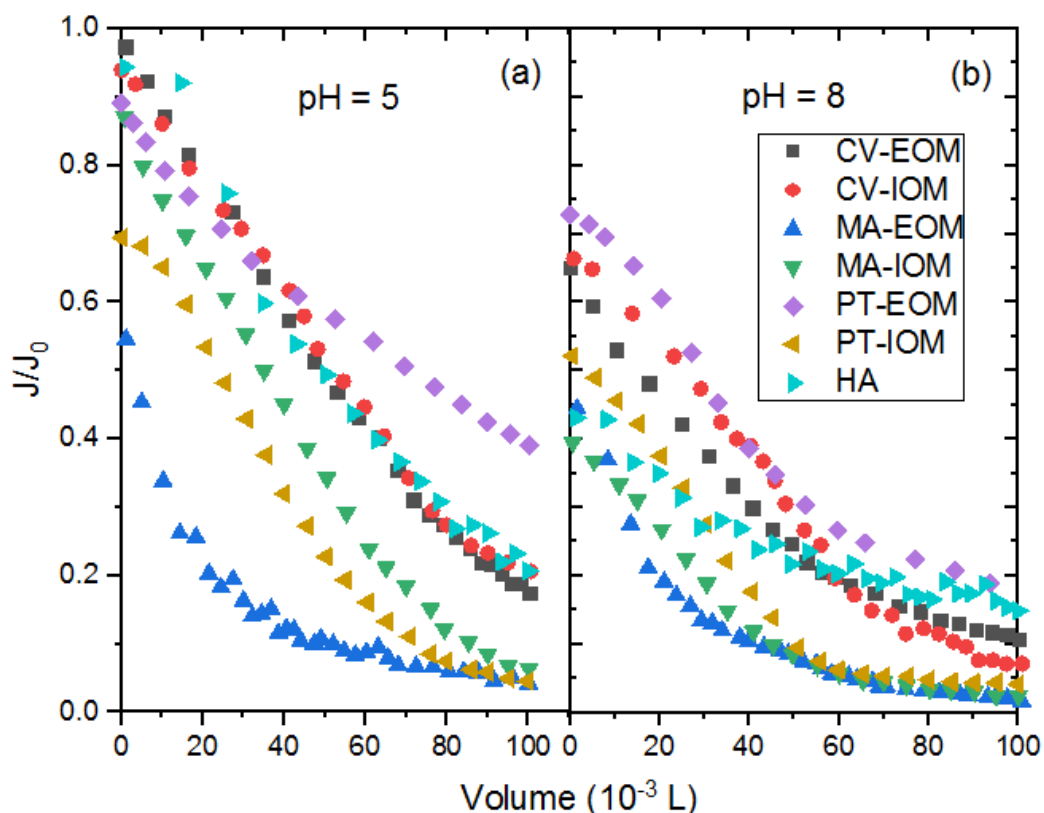
Figure 6.6 Flux profile for first filtration cycle of the DOM solution with GAC adsorption pretreatment at different solution pH.

The reversibility of membrane fouling with pH variation is shown in Figure 6.7. The results indicated that the irreversible fouling increased while the reversible fouling slightly decreased during the filtration cycles for each DOM. The decrease of irreversible fouling with the decrease of solution pH indicated that GAC adsorption pretreatment at lower pH can improve the membrane reversibility, due to higher removal of DOM by GAC at pH 5.
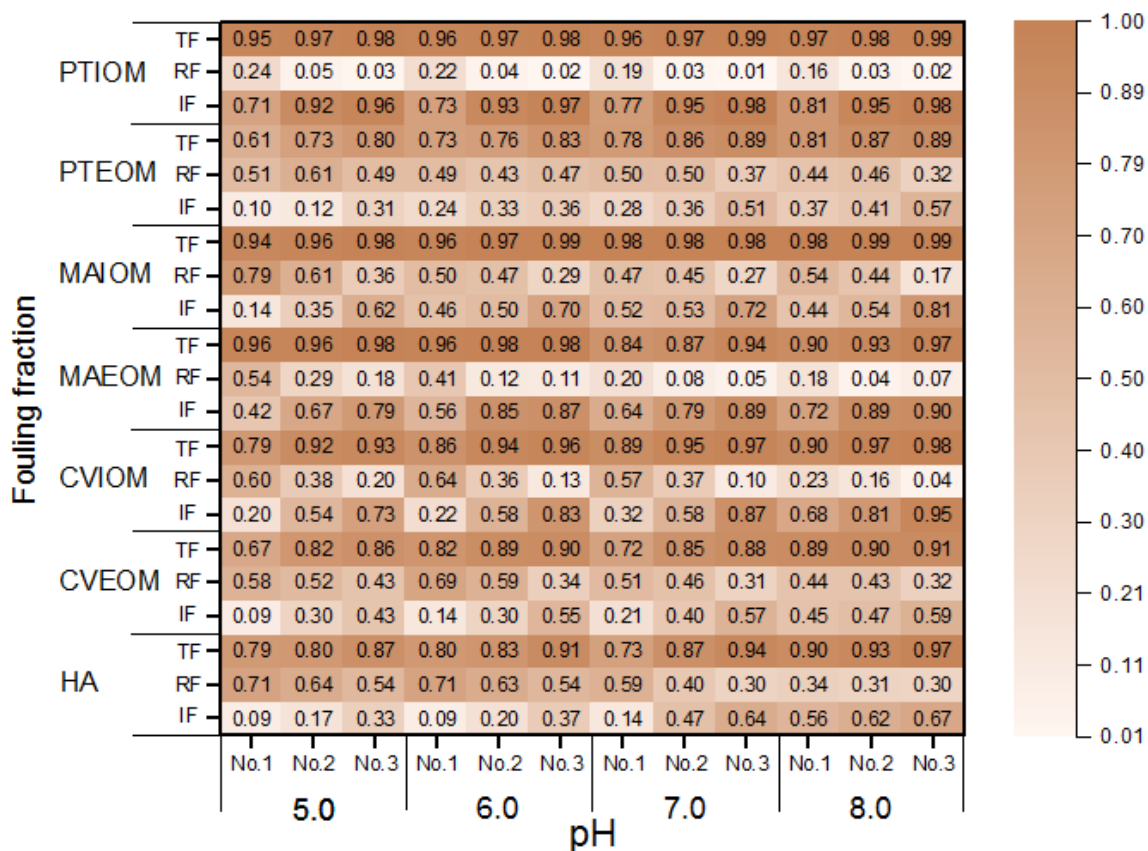
Figure 6.7 Effect of pH on the reversibility of DOM fouling (TF, RF and IF represented the total fouling, reversible fouling and irreversible fouling, respectively, No.1 to No.3 denoted the filtration cycle of each DOM).

To obtain a better understanding of the fouling of each DOM, the fouling reversibility with pH variation was analyzed and the results are shown in Figure 6.7. The decrease of irreversible fouling with the decrease of solution pH indicated that GAC adsorption pretreatment at lower pH in the experimental range can cause membrane reversibility, due to the considerable removal of DOM by GAC adsorption at lower pH. In addition, the effective radius of DOM may decrease due to reduced inter-chain electrostatic repulsion at low pH, which can make the molecules smaller and easier to be adsorbed onto the membrane and flow through the micropores of membrane matrix [40]. Comparing with humic acid, AOM presented higher irreversible fouling. In a comparative study on membrane fouling potentials showed that higher irreversible fouling was caused by AOM derived from MA than that from humic acid [41].

6.3.5. Fouling mechanisms of the AOM

To investigate the fouling mechanisms, instantaneous flux of the first cycle of MF after GAC adsorption was fitted with the classic filtration models (shown in Table 6.1). The regression results are presented in Figure 6.8 and Table 6.2. As shown in Table 6.2, among the four fouling models for each DOM solution, for CV-EOM and MA-IOM, membrane fouling was controlled by standard blocking with R^2 values of 0.997 for CV-EOM and 0.982 for MA-IOM. For the other DOM solutions, including humic acid, CV-IOM, MA-EOM, PT-EOM and PT-IOM with the maximum R^2 values 0.977, 0.973, 0.958, 0.995, and 0.977, respectively, the fouling mechanisms are predominated by intermediate blocking.

It can be seen that the comparable R^2 values of the fouling models implied that the fouling process was controlled by multiple mechanisms. This is attributed to the broad MW distribution of AOM [8, 29]. The low-MW substance may be trapped inside of membrane pores resulting standard blocking, and the high-MW components may be deposited on membrane surface and to form a cake layer. A previous study on the UF membrane fouling potential of EOM also demonstrated that multiple mechanisms, including cake filtration and standard blocking, dominated the fouling formation [41, 42].

In a comparative study on membrane fouling potentials of algal extracellular and intracellular organic matter, the cake filtration has been identified as an important mechanism for flux decline

Table 6.2 R^2 values of fouling models for each DOM during the first cycle of MF after GAC adsorption (GAC dosage of 1.0 g/L, pH 7.0 and 1.0 hour contact time)

Feed solution	Complete Blocking	Standard Blocking	Intermediate blocking	Cake filtration
HA	0.856	0.931	**0.977**	0.940
CV-EOM	0.990	**0.997**	0.993	0.953
CV-IOM	0.901	0.942	**0.973**	0.969
MA-EOM	0.622	0.937	**0.958**	0.938
MA-IOM	0.957	**0.982**	0.972	0.840
PT-EOM	0.983	0.992	**0.995**	0.980
PT-IOM	0.911	0.962	**0.977**	0.849

Note: The associated p value of each model is less than 0.0001.
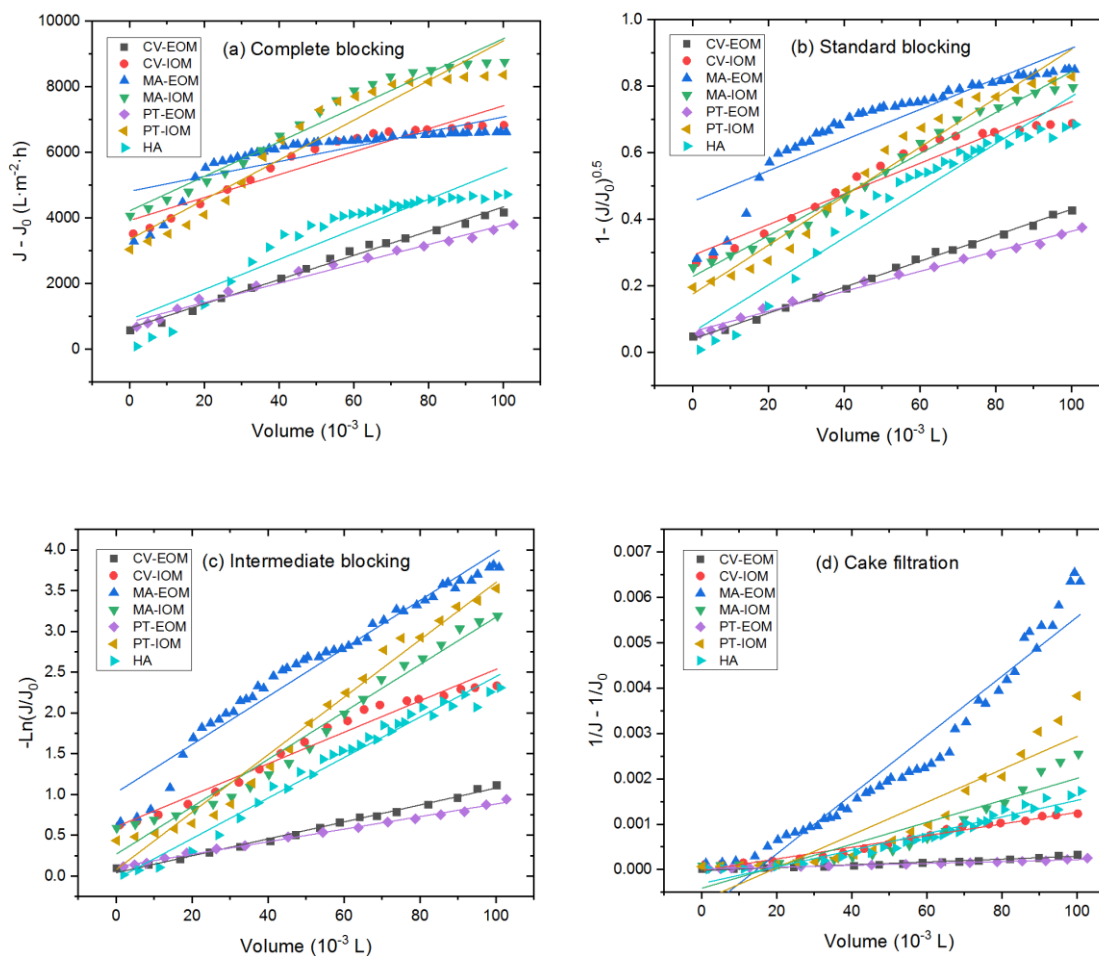
Figure 6.8 Regression analysis of membrane fouling behavior using classical fouling models for the first filtration cycle of individual DOM at pH 7 with 1.0 g/L GAC adsorption pretreatment.

It should be noted that multiple mechanisms might also take effect during filtration considering the relatively higher R^2 value, for instance, intermediate blocking and cake filtration dominated the fouling formation for humic acid, and standard blocking and intermediate blocking controlled the membrane fouling for most AOM, except for CV-IOM and humic acid for which intermediate blocking and cake filtration mechanisms governed the fouling formation. An earlier study demonstrated that cake filtration

dominated the fouling during ultrafiltration of AOM from MA; however, the difference is mainly due to the type of filtration [32].

6.4. Conclusions

The influence of GAC dosage and initial pH on microfiltration to remove DOM derived from three different algae, as well as humic acid, was investigated using a dead-end down-flow MF unit in batch scale. The combination of GAC adsorption and MF can significantly enhance DOM removal up to 72.23% and 85.95% for DOC and UV_{254} for CV-IOM. The addition of GAC can not only promote the DOM removal, but also mitigate the flux decline and reduce irreversible fouling. A Lower initial pH value within the experimental range (5-8) showed positive effects for DOM removal and the membrane reversibility. The total removal efficiency of AOM was higher than humic acid; however, a greater flux decline and higher irreversible fouling were observed from AOM than that humic acid. The AOM derived from CV showed better removal efficiency with less flux decline and irreversible fouling, followed by the cyanobacteria, MA and the diatom, PT. The analyses of fouling models indicate that intermediate blocking and standard blocking were the dominant membrane fouling mechanisms for most DOM except for the CV-IOM and humic acid where intermediate blocking and cake filtration controlled the fouling process. Although, IOM from each algal species showed relatively higher removal performance than EOM, considering the greater flux decline and irreversible fouling compared to EOM, to maintain the algal cell integrity and avoiding lysis to release IOM are important considerations for membrane treatment of algae-laden water.

References

[1]   J. Hoslett, T.M. Massara, S. Malamis, D. Ahmad, I. van den Boogaert, E. Katsou, B. Ahmad, H. Ghazal, S. Simons, L. Wrobel, H. Jouhara, Surface water filtration using granular media and membranes: A review, Science of the Total Environment 639 (2018) 1268-1282.

[2]   R. Kudela, E. Berdalet, S. Bernard, M. Burford, L. Fernand, S. Lu, S. Roy, G. Usup, P. Tester, R. Magnien, Harmful algal blooms. A scientific summary for policy makers, IOC/UNESCO, Paris, 2015.

[3]   W.S. Lopes, J.S. Buriti, B.S.O. Cebalos, J.T. Sousa, V.D. Leite, F.F. Vieira, Removal of Microcystin-LR from Drinking Water Using a System Involving Oxidation and Adsorption, Water Air and Soil Pollution 228 (2017) 14.

[4]   J.M. Wong, California leads way in drinking water membrane filtration, in: A. Maya (Ed.), WaterWorld Magazine, 2012.

[5]   U.S. Environmental Protection Agency, Method 1623: Cryptosporidium and Giardia in Water by Filtration/IMS/FA, Office of Ground Water and Drinking Water Technical Support Center, U.S. Environmental Protection Agency, Washington, DC., 2005.

[6]   S.G. Lehman, L. Liu, Application of ceramic membranes with pre-ozonation for treatment of secondary wastewater effluent, Water Research 43 (2009) 2020-2028.

[7]   C.A. Chiu, K. Hristovski, S. Huling, P. Westerhoff, In-situ regeneration of saturated granular activated carbon by an iron oxide nanocatalyst, Water Research 47 (2013) 1596-1603.

[8]   J.Y. Fang, X. Yang, J. Ma, C. Shang, Q.A. Zhao, Characterization of algal organic matter and formation of DBPs from chlor(am)ination, Water Research 44 (2010) 5897-5906.

[9]   M. Zhang, X. Wang, T.T. Du, H.H. Wang, H.Z. Hao, Y.Y. Wang, Y. Li, T.W. Hao, Effects of carbon materials on the formation of disinfection byproducts during chlorination: Pore structure and functional groups, Water Research 162 (2019) 1-10.

[10]   H.C. Kim, B.A. Dempsey, Membrane fouling due to alginate, SMP, EfOM, humic acid, and NOM, Journal of Membrane Science 428 (2013) 190-197.

[11]   W.W. Huang, H.Q. Chu, B.Z. Dong, J.X. Liu, Evaluation of different algogenic organic matters on the fouling of microfiltration membranes, Desalination 344 (2014) 329-338.

[12]   W.W. Huang, H.Q. Chu, B.Z. Dong, Understanding the fouling of algogenic organic matter in microfiltration using membrane-foulant interaction energy analysis: Effects of organic hydrophobicity, Colloids and Surfaces B-Biointerfaces 122 (2014) 447-456.

[13]   B.K. Mayer, C. Johnson, Y. Yang, N. Wellenstein, E. Maher, P.J. McNamara, From micro to macro-contaminants: The impact of low-energy titanium dioxide photocatalysis followed by filtration on the mitigation of drinking water organics, Chemosphere 217 (2019) 111-121.

[14]   Y. Rasouli, M. Abbasi, S.A. Hashemifard, Investigation of in-line coagulation-MF hybrid process for oily wastewater treatment by using novel ceramic membranes, Journal of Cleaner Production 161 (2017) 545-559.

[15]   B. Kose‑Mutlu, M.E. Ersahin, H. Ozgun, R. Kaya, C. Kinaci, I. Koyuncu, Influence of powdered and granular activated carbon system as a pre‑treatment alternative for membrane filtration of produced water, Journal of Chemical Technology & Biotechnology 92 (2017) 283-291.

[16]   P.M. Huck, S. Peldszus, J. Haberkamp, M. Jekel, Assessing the performance of biological filtration as pretreatment to low pressure membranes for drinking water, Environmental Science & Technology 43 (2009) 3878-3884.

[17]   J.W. Hatt, E. Germain, S.J. Judd, Granular activated carbon for removal of organic matter and turbidity from secondary wastewater, Water Science and Technology 67 (2013) 846-853.

[18]   Y. Zhang, X.Y. Wang, H.J. Jia, B.G. Fu, R.W. Xu, Q. Fu, Algal fouling and extracellular organic matter removal in powdered activated carbon-submerged hollow fiber ultrafiltration membrane systems, Science of the Total Environment 671 (2019) 351-361.

[19]   L.O. Villacorte, Y. Ekowati, T.R. Neu, J.M. Kleijn, H. Winters, G. Amy, J.C. Schippers, M.D. Kennedy, Characterisation of algal organic matter produced by bloom-forming marine and freshwater algae, Water Research 73 (2015) 216-230.

[20]   Z. Zhao, W. Sun, A.K. Ray, T. Mao, M.B. Ray, Coagulation and disinfection by-products formation potential of extracellular and intracellular matter of algae and cyanobacteria, Chemosphere 245 (2020) 125669.

[21]   L. Li, N.Y. Gao, Y. Deng, J.J. Yao, K.J. Zhang, Characterization of intracellular & extracellular algae organic matters (AOM) of Microcystic aeruginosa and formation of AOM-associated disinfection byproducts and odor & taste compounds, Water Research 46 (2012) 1233-1240.

[22]   J. Wan, T. Chakraborty, C. Xu, M.B. Ray, Treatment train for tailings pond water using Opuntia ficus-indica as coagulant, Separation and Purification Technology 211 (2019) 448-455.

[23] D. Gumus, F. Akbal, A comparative study of ozonation, iron coated zeolite catalyzed ozonation and granular activated carbon catalyzed ozonation of humic acid, Chemosphere 174 (2017) 218-231.

[24] H. Elcik, M. Cakmakci, B. Ozkaya, The fouling effects of microalgal cells on crossflow membrane filtration, Journal of Membrane Science 499 (2016) 116-125.

[25] R. Golbandi, M.A. Abdi, A.A. Babaluo, A.B. Khoshfetrat, T. Mohammadlou, Fouling study of TiO2-boehmite MF membrane in defatting of whey solution: Feed concentration and pH effects, Journal of Membrane Science 448 (2013) 135-142.

[26] E. Iritani, N. Katagiri, Developments of blocking filtration model in membrane filtration, KONA Powder and Particle Journal 33 (2016) 179-202.

[27] L.O. Villacorte, Y. Ekowati, H. Winters, G. Amy, J.C. Schippers, M.D. Kennedy, MF/UF rejection and fouling potential of algal organic matter from bloom-forming marine and freshwater algae, Desalination 367 (2015) 1-10.

[28] X. Zhang, L. Fan, F.A. Roddick, Understanding the fouling of a ceramic microfiltration membrane caused by algal organic matter released from Microcystis aeruginosa, Journal of Membrane Science 447 (2013) 362-368.

[29] G. Li, Y. Ren, L. Gu, Q. He, R. Deng, L.Z. Tang, Migration and transformation of nitrogen in algae organic matter (AOM) during the growth of Microcystis aeruginous, Desalination and Water Treatment 111 (2018) 79-87.

[30] H. Wang, D.M. Liu, P. Wang, F.Y. Cui, Structural characteristics of intracellular and extracellular organic matter from Microcystis aeruginosa, in: L. Zhang (Ed.) Environmental Technology and Resource Utilization Ii, Trans Tech Publications Ltd, Stafa-Zurich, 2014, pp. 163-166.

[31] K.Y. Kim, H.S. Kim, J. Kim, J.W. Nam, J.M. Kim, S. Son, A hybrid microfiltration-granular activated carbon system for water purification and wastewater reclamation/reuse, Desalination 243 (2009) 132-144.

[32] B. Liu, F.S. Qu, H. Liang, B. Van der Bruggen, X.X. Cheng, H.R. Yu, G.R. Xu, G.B. Li, Microcystis aeruginosa-laden surface water treatment using ultrafiltration: Membrane fouling, cell integrity and extracellular organic matter rejection, Water Research 112 (2017) 83-92.

[33] X.L. Zhang, L.H. Fan, F.A. Roddick, Impact of the Interaction between Aquatic Humic Substances and Algal Organic Matter on the Fouling of a Ceramic Microfiltration Membrane, Membranes 8 (2018) 10.

[34] B.K. Pramanik, F.A. Roddick, L.H. Fan, Impact of biological activated carbon pre-treatment on the hydrophilic fraction of effluent organic matter for mitigating fouling in microfiltration, Environmental Technology 39 (2018) 2243-2250.

[35] S.Q. Zhou, Y.S. Shao, N.Y. Gao, Y. Deng, L. Li, J. Deng, C.Q. Tan, Characterization of algal organic matters of Microcystis aeruginosa: Biodegradability, DBP formation and membrane fouling potential, Water Research 52 (2014) 199-207.

[36] K. Kuśmierek, A. Świątkowski, Influence of Ph on Adsorption Kinetics of Monochlorophenols From Aqueous Solutions on Granular Activated Carbon, Ecological Chemistry and Engineering S 22 (2015) 95-105.

[37] Z. Zhang, L. Yan, H. Yu, T. Yan, X. Li, Adsorption of phosphate from aqueous solution by vegetable biochar/layered double oxides: Fast removal and mechanistic studies, Bioresource Technology 284 (2019) 65-71.

[38] E.J. de la Casa, A. Guadix, R. Ibanez, E.M. Guadix, Influence of pH and salt concentration on the cross-flow microfiltration of BSA through a ceramic membrane, Biochemical Engineering Journal 33 (2007) 110-115.

[39] B.Z. Dong, Y. Chen, N.Y. Gao, J.C. Fan, Effect of pH on UF membrane fouling, Desalination 195 (2006) 201-208.

[40] A.S. Al-Amoudi, Factors affecting natural organic matter (NOM) and scaling fouling in NF membranes: A review, Desalination 259 (2010) 1-10.

[41] L. Li, Z.M. Wang, L.C. Rietveld, N.Y. Gao, J.Y. Hu, D.Q. Yin, S.L. Yu, Comparison of the Effects of Extracellular and Intracellular Organic Matter Extracted From Microcystis aeruginosa on Ultrafiltration Membrane Fouling: Dynamics and Mechanisms, Environmental Science & Technology 48 (2014) 14549-14557.

[42] Z.S. Yan, B. Liu, F.S. Qu, A. Ding, H. Liang, Y. Zhao, G.B. Li, Control of ultrafiltration membrane fouling caused by algal extracellular organic matter (EOM) using enhanced Al coagulation with permanganate, Separation and Purification Technology 172 (2017) 51-58.

Chapter 7

7 Impact of UV Irradiation on Disinfection By-Product Formation by Post Chlorination

7.1. Introduction

Ultraviolet (UV) irradiation has been increasingly applied in water treatment plants to inactivate a wide range of waterborne pathogens, such as *Cryptosporidum* [1] and *Giardia lamblia* [2], which are resistant to chlorination [3]. It has also been an alternative treatment for the removal of small concentrations of organics including the taste and odor compounds [4]. However, the main disadvantage of UV disinfection is that there is no residual inactivation capacity of UV radiation left once the treated water is in the distribution system [5]. Many treatment plants use post-chlorination or chloramination to address this for maintaining water quality. However, depending on the dissolved organic carbon (DOC) content in the UV-treated water, formation of disinfection by-products (DBP) is a concern post-chlorination. Algal organic matter is an important source of dissolved organic matter (DOM) in surface water, which can be the precursor of many harmful disinfection by-products [6], and is not removed effectively during coagulation.

UV radiation at 254 nm is known to degrade organics by the process of photolysis. Being a complex mixture of carbohydrate, sugar, lipid, and protein, AOM is susceptible to be degraded during UV disinfection. The complex mixture of intermediates subsequent to photolysis may cause the formation of harmful products after chlorination. However, the literature on UV photolysis of AOM followed by chlorination under control conditions is rather limited. It was reported that UV pretreatment enhanced the formation of nitrogenous DBP (N-DBP) during the subsequent chlor(am)ination of AOM, especially dichloroacetonitrile [7]. A few studies were conducted on UV irradiation followed by chlorination of humic acid solutions [3, 7-9]. It was found that UV irradiation did not alter the specific disinfection by-product formation potential (DBPFP) significantly based on the DOM characteristics, which indicated that most of the DBP precursors could not be removed by photodegradation [7, 9]. With the increasing events of harmful algal blooms

all over the world, a control study on the photolysis of AOM followed by chlorination is required to determine the effect of algal matter on drinking water treatment processes, which is the objective of this study.

In the previous study, disinfection by-products formation of both extracellular and intracellular materials of four algae and two cyanobacteria were determined [10]. However, intracellular materials are only released under stress conditions and certain treatment conditions such as pre-chlorination and pre-oxidation, hence was not covered in this study. In addition, only carbonaceous DBP was determined as the concentration of nitrogenous DBP is much lower than that small amount of intracellular materials may be released during the growth stage, hence, instead of denoting the algal organic matter as EOM, AOM will be used all through this chapter.

7.2 Materials and Methods

7.2.1. Algal cultivation

The three freshwater species, *Scenedesmus quadricauda* (SQ*)*, *Merismopedia* sp. (Msp) and *Phaedactylum tricornutum* (PT) were purchased from the Canadian Phycological Culture Centre (CPCC) at Waterloo University (Waterloo, ON, Canada). Algal strains were cultivated in 2 L conical flasks with a culture medium (High Salt medium for SQ, BG-11 for Msp and F/2 for PT) at $23 \pm 2^{\circ}$C with a light/dark cycle of 16/8 hours intermittent illumination (3000 lx). All solutions were prepared from reagent-grade chemicals and Milli-Q water, except the medium F/2, which was diluted by synthetic seawater prepared by Instant Ocean sea-salt (Instant Ocean Company, USA). The growth of algae were monitored by cell counting using a hemocytometer (LW Scientific, USA) under a microscope (ZEISS, Germany). Algae and cyanobacterial cultures were harvested during the stationary growth phase based on the previous study [11].

7.2.2. AOM extraction and characterization

AOM of the species was extracted by centrifuging algal cell suspension at 3700 rpm for 15 min. The supernatant was filtered with 0.45 μm hydrophilic acrylic copolymer filter (Pall Corp.) to obtain AOM. DOC of AOMs were determined by a Shimadzu TOC–V$_{CPN}$

analyzer (Shimadzu, Japan) with an ASI-L auto-sampler, and the detection limit was 0.1 mg-C/L on filtered samples. Glucose was used as the standard of dissolved organic carbon at a concentration of 2-20 mg/L to obtain the DOC standard calibration curve. Three replicates were measured and an average was reported with the coefficient of variance less than 2%.

Ultraviolet absorbance at 254 nm (UV_{254}) was obtained using a UV/Vis spectrophotometer (Model 3600, Shimadzu, Japan) in the range of 200 to 300 nm with a 1 cm quartz cuvette. The specific UV absorbance (SUVA) is widely used for characterizing aromaticity of NOM and predicting its DBPFP in water treatment. SUVA is defined as the UV absorbance at 254 nm (m^{-1}) normalized by the overall organic loading in terms of DOC (mg/L), which represents the average absorptivity at 254 nm from all the dissolved organics compounds [12]. The initial DOC of the AOM was kept below 5 mg/L, as this is the typical DOC that many treatment plants experience [13-17].
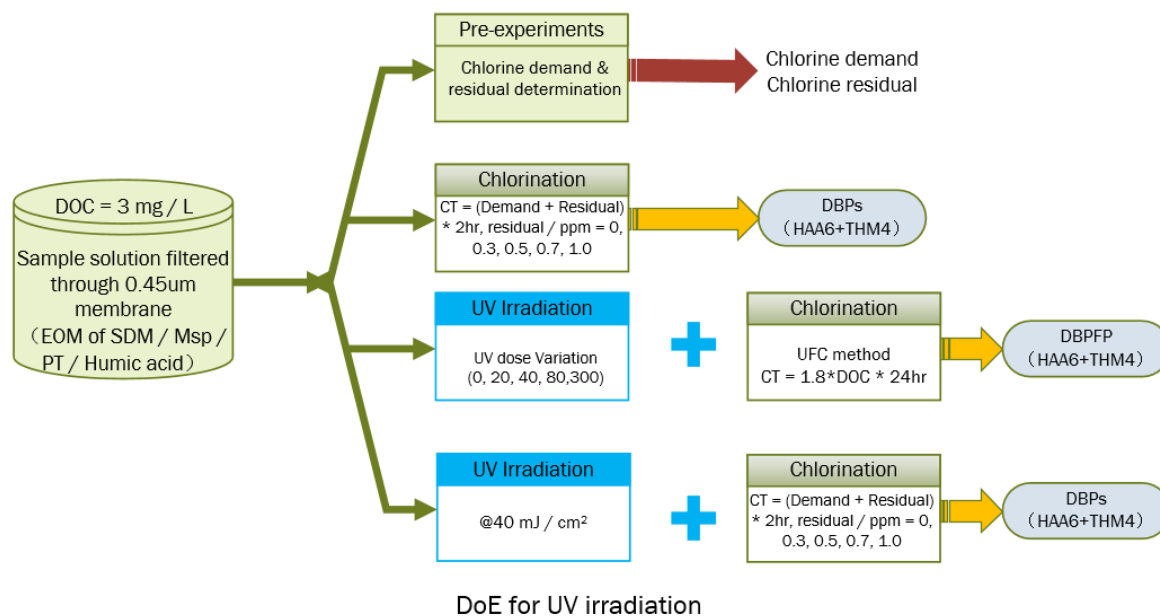
7.2.3. UV irradiation

The UV irradiation was performed in a bench-scale collimated beam enclosing a low pressure (LP) UV lamp and a collimated tube with a non-reflective inner surface (Trojan Technologies)[18]. UV intensity was monitored and calibrated by ILT1400 radiometer (International Technologies) and SED 240SEL detector at 254 nm. The UV intensity of 0.156 mW/cm^2 and UV dosages of 0-300 mJ/cm^2 were applied to 50 mL water samples containing algal matter in a Petri dish and placed under the UV lamp using constant stirring at room temperature. UV doses were calculated by multiplying the measured intensity and exposure time [4]. The initial pH of 8 was adjusted with 0.01 M H_2SO_4 or 0.1 M NaOH and borate buffer.

7.2.4. Post chlorination and DBPs quantification

Chlorination of water samples after UV irradiation treatment was conducted immediately in headspace-free amber glass bottles containing a calculated amount of hypochlorite-buffer solution and incubated under dark at ambient temperature ($23 \pm 1^{\circ}C$) for specific time. After (2 hours for DBP formation, 24 hours for DBPFP followed by UFC method

[19]) incubation, ammonium chloride was added to quench the residual chlorine [20] in water to obtain the trihalomethane formation potential (THMFP) and haloacetic acid formation potential (HAAFP) following the method of USEPA551.1 [21] and EPA552.3 [22] The free and total chlorine residual were measured following DPD method 8167 using a HACH DR5000 and a UV-Vis spectrophotometer (HACH Company, USA). The formation of four major THM$_4$, including trichloromethane (TCM), tribromomethane (TBM), bromodichloromethane (BDCM), and dibromochloromethane (DBCM) were extracted) via liquid-liquid extraction following the method of USEPA 551.1 [21]. The six HAA$_6$, bromochloroacetic acid (BCAA), dichloroacetic acid (DCAA), monochloroacetic acid (MCAA), trichloroacetic acid (TCAA), monobromoacetic acid (MBAA), and dibromoacetic acid (DBAA) were extracted with MTBE, methylated with acid methanol following the modified USEPA method 552.3 [22]. The chlorinated DBP were determined by gas chromatography coupled with an electron capture detector GC/ECD (Shimadzu GC-2014) with a BPX5 capillary column (30 m× 0.25 mm ID, 0.25 μm film thickness) following the previous study from same lab [10]. DBPFP (μg·mg C^{-1}) were obtained by dividing the concentration of DBP (in μg·L^{-1}) by the DOC (in mg L^{-1}). For better clarification, sequence of entire experimental scheme is shown in Figure 7.1.

Figure 7.1 Experimental sequence showing UV irradiation and chlorination of AOM.

7.3. Results and discussion

7.3.1. Chlorine residual with variation of chlorine dosage

From preliminary chlorine demand, water sample spiked with each DOM stock solution was dosed with different free chlorine concentrations to establish the chlorine demand curve for each specific water matrix. The total chlorine residual with variation of dosage under identical incubation and measurement conditions were shown in Figure 7.2. It can be seen that the AOM and humic acid solution demonstrated different total chlorine residual profile with chlorine dose. A linear equation with the highest correlation coefficient of 0.9985 can well fit the total chlorine of SQ in the experimental range. However, unlike the SQ, a longer lag phase occurred for Msp before total chlorine residual increased gradually following an exponential pattern. The PT and humic acid showed a similar increase pattern, thus a quadratic polynomial equation can fit the data with the correlation coefficient of 0.993 and 0.984 for PT and humic acid, respectively.
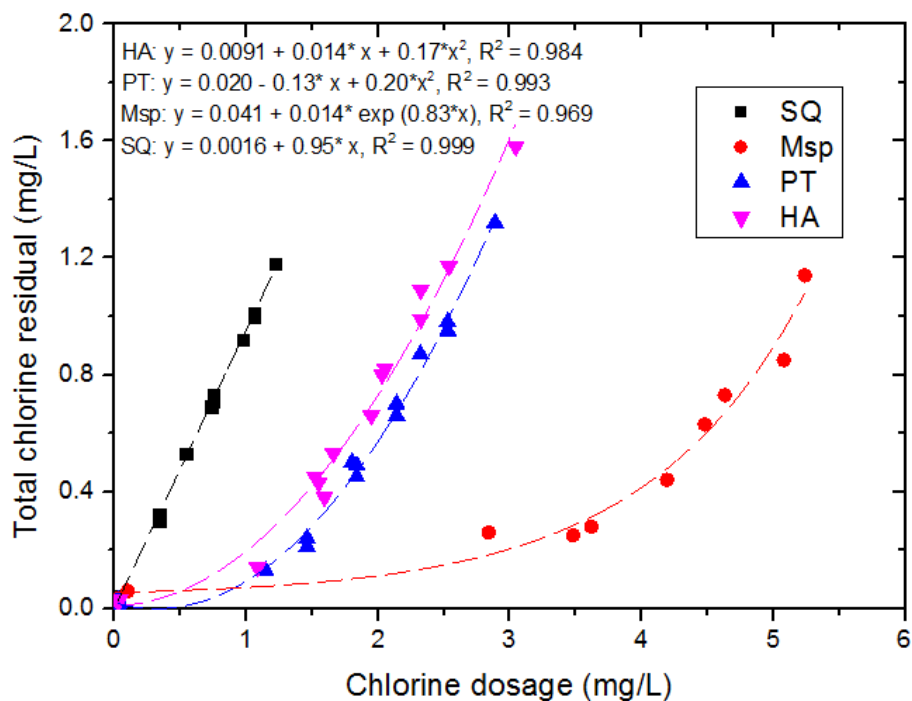
Figure 7.2 Total chlorine residual with variation of chlorine dosage after 2 hours incubation in dark at room temperature for AOM solution with initial DOC of 3.0 ± 0.2 mg/L.

It is interesting to see that although all DOM solution were dosed at similar initial DOC of 3 mg/L, different DOM showed different chlorine demand, with *Merismopedia* sp. showing the highest chlorine demand followed by PT and humic acid. Unfortunately, without detail characterization of all the different organics present in various species, reasons for the results shown in Figure 7.2 will be purely speculative. Since many water treatment plants keep a total chlorine residual of around 1-1.5 mg/L [23], different chlorine dosage will be required for different algal matter.

7.3.2. Effect of total chlorine residual on DBP formation

From the results of the chorine demand test presented above, the calculated amount of free chlorine was added into water samples of each DOM for the following DBP formation tests. DBP formation was evaluated for the water samples before and after UV irradiation to evaluate the influence of UV disinfection on the DBP formation under different total

chlorine residual after incubation in dark for 2 hours at room temperature as the post-chlorination process.

Under the chlorination conditions adopted, total DBP formation increased with the increasing total chlorine residual as shown in Figure 7.3. HAA formation was higher than THMs formation, and the diatom PT produced the highest amount of both types of DBP followed by the others in the order: PT>HA>MSP>SQ.
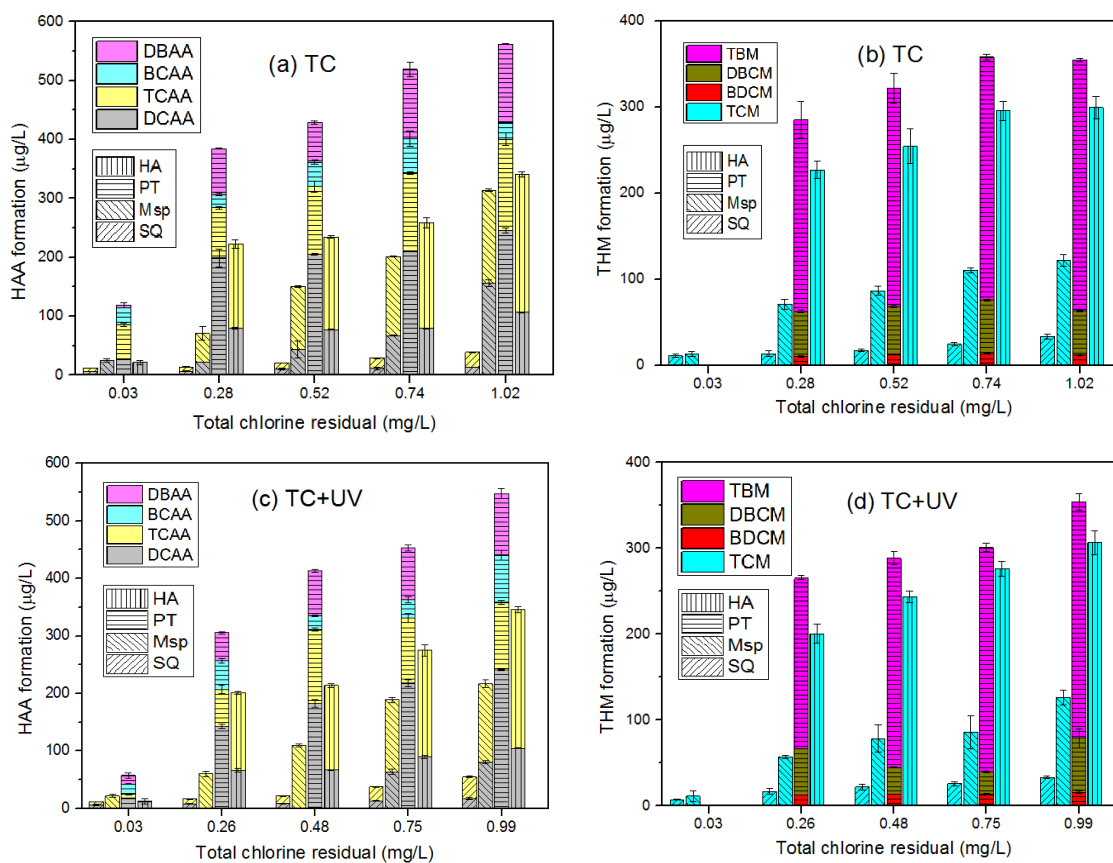
Figure 7.3 DBP formation with variation of chlorine residual (a) and (b), 40 mJ/cm^2 UV irradiation followed by chlorine dose (c) and (d) after 2 hour incubation in dark for DOM spiked water sample with initial DOC of 3.09 ± 0.19 mg/L.

Since PT can also be a marine algae, its medium was diluted by synthetic seawater prepared by commercial Instant Ocean sea salt, which contains 94.12 µg/L bromide in the final DOM solution. Thus, significant amounts of brominated DBP was formed after chlorination. This

is in agreement with an earlier work [10], where both IOM and EOM of PT showed the highest DBP formation. Since bromide is frequently observed in natural and marine water, it was found to be more active with DOM during chlorination [4]. It can alter the DBP speciation composition and promote brominated DBP formation which might be attributed to the reaction between bromide ion and hydroxyl radical. A previous study also demonstrated the increased brominated total organic halogen after UV irradiation/chlorination process [24].

For the other DOM, DCAA and TCAA were the dominant HAA species for SQ, Msp and HA with total HAA formation of 38.23 ± 1.25 μg/L, 313.56 ± 6.05 μg/L and 340.82 ± 9.29 μg/L, respectively, when the total chorine residual was around 1.0 mg/L. It should be noted that trichloromethane (TCM) was the only THM species formed from SQ, Msp and HA. Tribromomethane (TBM) (Figure 7.3b) was the most abundant species of THM for bromide-containing in PT. It was interesting to find that even Msp showed the highest chlorine demand (Figure 7.2), the DBP formation was much lower than PT and humic acid. Overall, except SQ, the DBP formation by other three DOM (i.e., Msp, PT and HA) always exceeded the DBP limit of 80 μg/L for HAA and 100 μg/L for THM as regulated by the guidelines for Canadian drinking water quality[25].

The effect of UV radiation at 40 mJ/cm^2, a typical dosage used for disinfection caused a slight decrease in DBP formation after chlorination, although the effect was insignificant (Figure 7.3). The comparison of the DBP formation between with and without UV irradiation is shown in Figure 7.4 and the regression coefficients are presented in Table 7.1. As can be seen from Figure 7.4, there was no increase in DBP formation after UV radiation for SQ and HA. This is reasonable as much higher dosage is required for effective photolysis of trace concentration of organics (micropollutants) [26]. However, there is still a small amount of DBP formation changes for PT and Msp, which both HAA and THM formation decreased for PT, but with a small increase in the same for Msp.
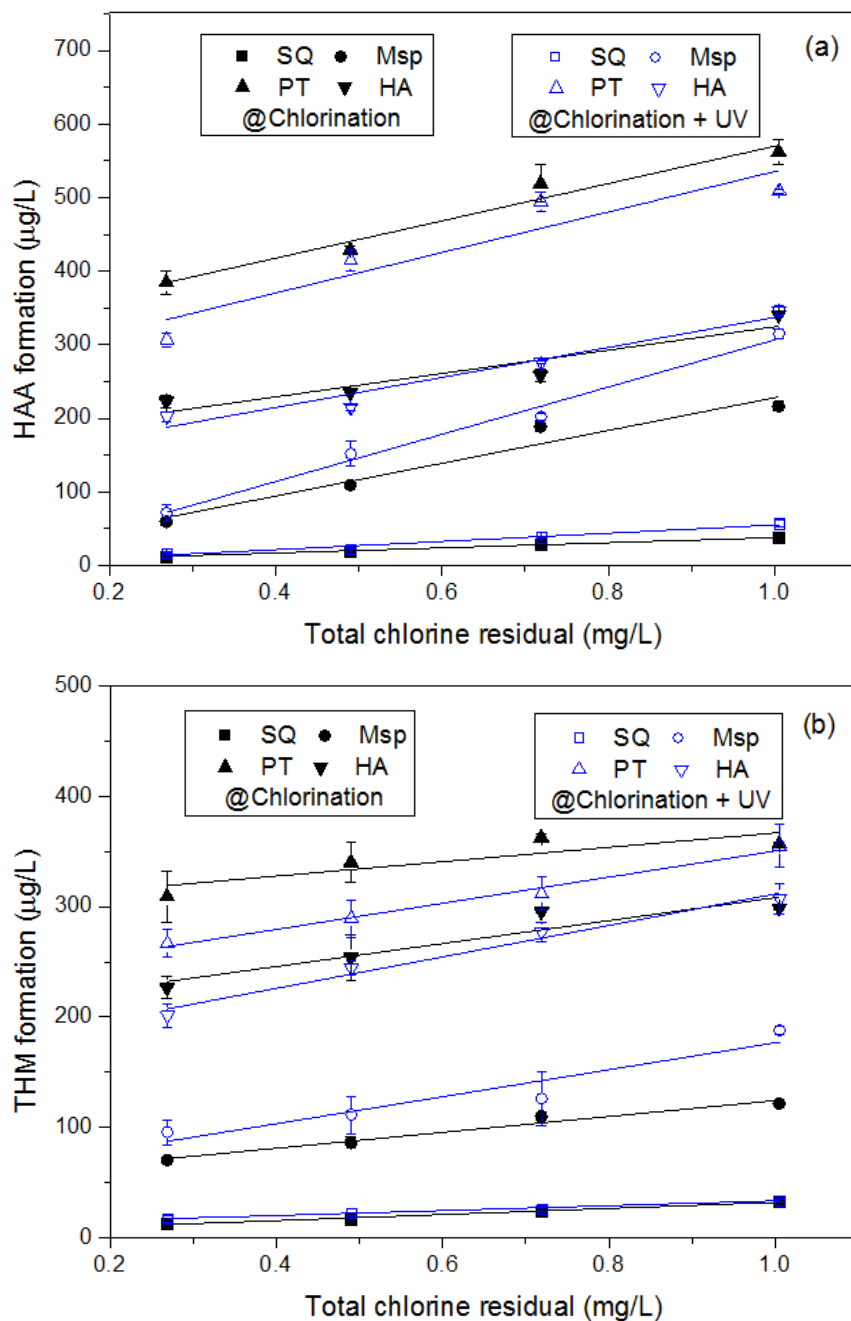
Figure 7.4 The comparison of DBP formation and the correlation with total chlorine residual of DOM spiked water sample between chlorination and UV irradiation of 40 mJ/cm² followed by chlorination after 2 hour incubation in dark.

Table 7.1shows the Pearson correlation coefficients between each of the HAAs/THMs and total residual chlorine. The strong correlations (0.936-0.999) found between HAAs/THMs

and total residual chlorine indicated that experimental conditions were well controlled and total chlorine residual as a variable showed robust correlations with DBP formation from each DOM. Similar results were found in a previous study [27].

Table 7.1 Regression parameters of total chlorine residual and DBP formation.

		SQ		Msp		PT		HA	
		TC	TC+UV	TC	TC+UV	TC	TC+UV	TC	TC+UV
HAA	Intercept	3.06	-2.06	-15.41	5.20	316.17	259.16	165.65	131.94
	Slope	34.82	56.00	321.18	222.82	253.56	275.32	158.68	204.30
	R^2	0.999	0.984	0.995	0.975	0.984	0.936	0.940	0.976
THM	Intercept	4.46	10.69	52.24	53.80	301.49	230.91	204.08	168.28
	Slope	27.53	22.18	71.98	122.21	65.21	115.12	103.92	42.58
	R^2	0.993	0.996	0.984	0.953	0.958	0.971	0.943	0.990

7.3.3. Effect of UV irradiation on DBP formation

To further investigate the DBP formation potential of each DOM with variation of UV dosage, a comparison was made under identical experimental conditions (UFC method) and results were shown in Figure 7.5. The AOM from PT presents the highest specific DBPFP up to 232 μg/mg C for HAAFP and 138.79 μg/mg C for THMFP. TBM species dominated more than an average of 56.28% of THM at each UV dosage, compared with around 24% brominated acetic acid formed, which indicated that TBM is subject be formed in the presence of bromide ions. It is clear to see that with the increase of UV dosage, both HAAFP and THMFP decreased, with the maximum reduction of 42.25 % and 13.75 % for HAAFP and THMFP at UV irradiation dosage of 300 mJ/cm^2, respectively. In a different study, about 16.4 % of THM reduction was found at a UV dosage of 100 mJ/cm^2 [4]. This is probably due to the photolysis of DOM to alter the SUVA by UV irradiation [18], thus, decreasing the final formation of DBP. A similar trend was also observed from THMFP of SQ, even though the effect was not significant. Except PT, the brominated species did not feature among HAAs and THMs assayed for SQ, Msp and HA during chlorination. It was noted that DBPFP of Msp increased slightly with the UV dosage increase, with the

maximum formation of 160.95 ± 3.30 µg/mg C, 80.44 ± 4.14 µg/mg C for HAAFP and THMFP, respectively, at UV irradiation dosage of 300 mJ/cm^2.
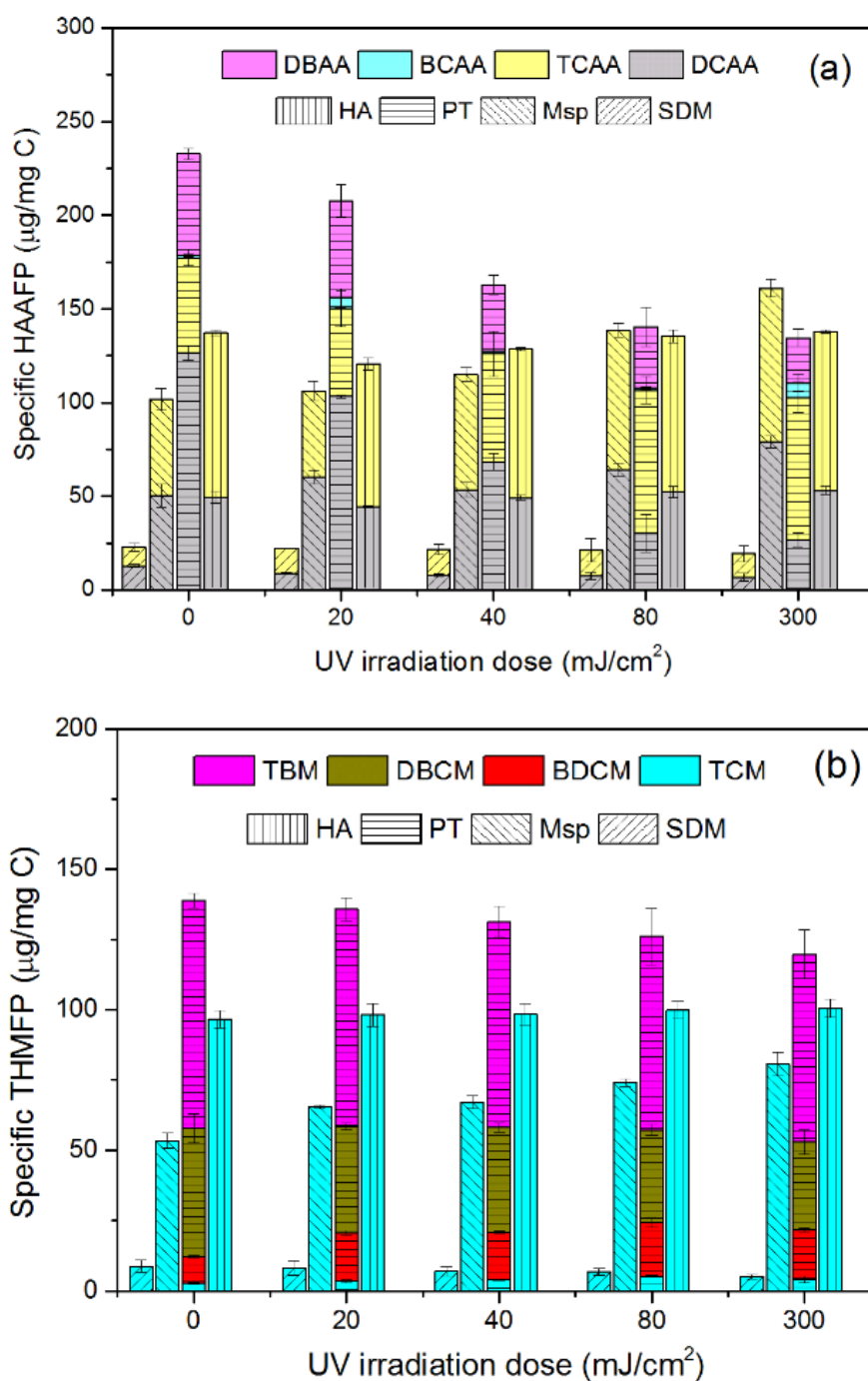
Figure 7.5 Specific DBP formation potential, (a) HAAFP, (b) THMFP of DOM spiked water sample.

Even though UV irradiation can eliminate aromatic, methyl, guaiacyl lignin group in HA and prevent the formation of TCM during subsequent chlorination, UV irradiation can also activate the phenolic hydroxyl group and promote DCAA and TCAA formation [28], and thus the final DBPFP of HA may not be changed significantly under moderate UV irradiation dosage.

7.4. Conclusions

The investigation of DBPFP of selected DOM with variation of total chlorine residual and UV irradiation was performed in this study. The positive correlation with high coefficients between total chlorine residual and DBP formation were established. Results showed that DBPs formation increased with total chlorine residual; AOM from PT presented the highest formation potential followed by HA, Msp, and SQ. The comparison of DBP formation between with and without UV irradiation for of each type of DOM indicates that 40 mJ/cm^2 UV irradiation may be insignificant to change the DBP formation from HA and SQ. However, it can decrease the DBP formation from bromide-containing AOM of PT, and can promote the DBP formation from AOM of Msp at various total chlorine residual. The maximum DBP formation potential (DBPFP) reduction of 42.25 % and 13.75 % for HAAFP and THMFP was obtained at UV irradiation dosage of 300 mJ/cm^2 for AOM of PT. However, for the AOM derived from Msp, a maximum increase of 58.1% and 51.1% of HAAFP and THMFP was observed. The results implied that further attention should be given to determine the effectiveness of UV irradiation on the degradation of algal matter.

References

[1]   P.A. Rochelle, D. Fallar, M.M. Marshall, B.A. Montelone, S.J. Upton, K. Woods, Irreversible UV inactivation of Cryptosporidium spp. despite the presence of UV repair genes, Journal of Eukaryotic Microbiology 51 (2004) 553-562.

[2]   G. Shin, K.G. Linden, G. Faubert, Reactivation of Giardia lamblia cysts after exposure to polychromatic UV light, Letters in applied microbiology 51 (2010) 395-399.

[3]   Z. Ye, W.J. Liu, W.J. Sun, X.B. Nie, X.W. Ao, Role of ammonia on haloacetonitriles and halonitromethanes formation during Ultraviolet irradiation followed by chlorination/chloramination, Chemical Engineering Journal 337 (2018) 275-281.

[4]   S. Chen, J. Deng, L. Li, N.Y. Gao, Evaluation of disinfection by-product formation during chlor(am)ination from algal organic matter after UV irradiation, Environmental Science and Pollution Research 25 (2018) 5994-6002.

[5]   H.B. Wang, C. Hu, X.X. Hu, Effects of combined UV and chlorine disinfection on corrosion and water quality within reclaimed water distribution systems, Engineering Failure Analysis 39 (2014) 12-20.

[6]   L.C. Hua, J.L. Lin, P.C. Chen, C.P. Huang, Chemical structures of extra- and intra-cellular algogenic organic matters as precursors to the formation of carbonaceous disinfection byproducts, Chemical Engineering Journal 328 (2017) 1022-1030.

[7]   T.Y. Zhang, Y.L. Lin, B. Xu, T. Cheng, S.J. Xia, W.H. Chu, N.Y. Gao, Formation of organic chloramines during chlor(am)ination and UV/chlor(am)ination of algae organic matter in drinking water, Water Research 103 (2016) 189-196.

[8]   T.Y. Zhang, Y.L. Lin, B. Xu, S.J. Xia, F.X. Tian, N.Y. Gao, Effect of UV irradiation on the proportion of organic chloramines in total chlorine in subsequent chlorination, Chemosphere 144 (2016) 940-947.

[9]   M.H. Lee, J. Hur, Photodegradation-Induced Changes in the Characteristics of Dissolved Organic Matter with Different Sources and Their Effects on Disinfection By-Product Formation Potential, Clean-Soil Air Water 42 (2014) 552-560.

[10]   Z. Zhao, W. Sun, A.K. Ray, T. Mao, M.B. Ray, Coagulation and disinfection by-products formation potential of extracellular and intracellular matter of algae and cyanobacteria, Chemosphere 245 (2020) 125669.

[11]   H. Wang, D. Liu, L. Lu, Z. Zhao, Y. Xu, F. Cui, Degradation of algal organic matter using microbial fuel cells and its association with trihalomethane precursor removal, Bioresource Technology 116 (2012) 80-85.

[12]   G. Hua, D.A. Reckhow, I. Abusallout, Correlation between SUVA and DBP formation during chlorination and chloramination of NOM fractions from different sources, Chemosphere 130 (2015) 82-89.

[13]   Z.B. Guo, Y.L. Lin, B. Xu, C.Y. Hu, H. Huang, T.Y. Zhang, W.H. Chu, N.Y. Gao, Factors affecting THM, HAN and HNM formation during UV-chlor(am)ination of drinking water, Chemical Engineering Journal 306 (2016) 1180-1188.

[14]   J. Fu, W.N. Lee, C. Coleman, M. Meyer, J. Carter, K. Nowack, C.H. Huang, Pilot investigation of two-stage biofiltration for removal of natural organic matter in drinking water treatment, Chemosphere 166 (2017) 311-322.

[15]   L.Y. Yang, D. Kim, H. Uzun, T. Karanfil, J. Hur, Assessing trihalomethanes (THMs) and N-nitrosodimethylamine (NDMA) formation potentials in drinking water treatment plants using fluorescence spectroscopy and parallel factor analysis, Chemosphere 121 (2015) 84-91.

[16]   C.A. Mash, B.A. Winston, D.A. Meints, A.D. Pifer, J.T. Scott, W. Zhang, J.L. Fairey, Assessing trichloromethane formation and control in algal-stimulated waters amended with nitrogen and phosphorus, Environmental Science-Processes & Impacts 16 (2014) 1290-1299.

[17]   H.Z. Xu, H.Y. Pei, Y. Jin, H.D. Xiao, C.X. Ma, J.M. Sun, H.M. Li, Characteristics of water obtained by dewatering cyanobacteria-containing sludge formed during drinking water treatment, including C-, N-disinfection byproduct formation, Water Research 111 (2017) 382-392.

[18]   X. Hu, Formation Potential of Disinfection By-products after Coagulation of Algal Matters, University of Western Ontario (2016).

[19]   R.S. Summers, S.M. Hooper, H.M. Shukairy, G. Solarik, D. Owen, Assessing DBP yield: uniform formation conditions, American Water Works Association. Journal 88 (1996) 80.

[20]   I. Kristiana, A. Lethorn, C. Joll, A. Heitz, To add or not to add: the use of quenching agents for the analysis of disinfection by-products in water samples, Water Res 59 (2014) 90-98.

[21]   D.J. Munch, D.P. Hautman, Method 551.1: Determination of chlorination disinfection byproducts, chlorinated solvents, and halogenated pesticides/herbicides in drinking water by liquid-liquid extraction and gas chromatography with electron-capture detection, Methods for the Determination of organic compounds in drinking water (1995).

[22]   M. Domino, B. Pepich, D. Munch, P. Fair, Y. Xie, Method 552.3 Determination of haloacetic acids and dalapon in drinking water by liquid-liquid microextraction, derivatization, and gas chromatography with electron capture detection, Methods for the Determination of organic compounds in drinking water (2003).

[23]   D.K. Roth, D.A. Cornwell, DBP Impacts From Increased Chlorine Residual Requirements, Journal American Water Works Association 110 (2018) 13-28.

[24]   Q. Zhao, C. Shang, X.R. Zhang, G.Y. Ding, X. Yang, Formation of halogenated organic byproducts during medium-pressure UV and chlorine coexposure of model compounds, NOM and bromide, Water Research 45 (2011) 6545-6554.

[25]   X. Wang, Y. Mao, S. Tang, H. Yang, Y.F. Xie, Disinfection byproducts in drinking water and regulatory compliance: A critical review, Frontiers of Environmental Science & Engineering 9 (2015) 3-15.

[26]   P. Chowdhury, S.R. Sarathy, S. Das, J. Li, A.K. Ray, M.B. Ray, Direct UV photolysis of pharmaceutical compounds: Determination of pH-dependent quantum yield and full-scale performance, Chemical Engineering Journal 380 (2020) 122460.

[27]   R. Dyck, G. Cool, M. Rodriguez, R. Sadiq, Treatment, residual chlorine and season as factors affecting variability of trihalomethanes in small drinking water systems, Frontiers of Environmental Science & Engineering 9 (2015) 171-179.

[28]   H.B. Wang, Y. Zhu, C. Hu, X.X. Hu, Treatment of NOM fractions of reservoir sediments: Effect of UV and chlorination on formation of DBPs, Separation and Purification Technology 154 (2015) 228-235.

Chapter 8

8 Conclusions and Recommendations

8.1 Major conclusions

Presence of algal organic matter in source water is a critical issue for the sustainability of drinking water supply all across the world. Among the myriads of problems due to the presence of AOM in water, mentioned in this thesis earlier, the most detrimental factor for human consumption of water is the possibility of higher disinfection byproducts formation potential due to chlorination. Conventional drinking water treatment process includes multiple steps; each treatment step faces challenge during algal bloom conditions. Using both raw water and synthesized water, this research was performed to characterize the impact of algae and algal organic matter on drinking water treatment processes including coagulation-flocculation, GAC adsorption, microfiltration and chlorination / UV irradiation. Although bench scale study was performed, the parameters were selected based on actual operating conditions.

Earlier research in this area had shown that coagulation was not effective for the removal of dissolved AOM and the performance was specific to algae. Similarly, unit processes such as granular activated carbon adsorption, membrane filtration and UV disinfection were conducted with some selected AOM. Often contradictory results were found, which indicated the need of comprehensive control study with several species of algae with diverse characteristics and following their behavior through the entire treatment train adopted in most drinking water treatment plants. The comprehensive research conducted in this thesis has produced the following results that are useful for formulating an optimal treatment scheme for the water treatment plants for minimizing disinfection by-products formation from algal matter. Following conclusions can be drawn.

- Combination of coagulation-flocculation is the primary and most cost-effective treatment process in a multiple barrier system of a conventional drinking water treatment plant. At optimum coagulation condition of pH 6 and alum dosage of 40

mg/L, an average of 47.4 and 40.4% AOM removal in terms of DOC and UV_{254} can be achieved.

- The hydrophobicity of AOM can be determined using a resin fractionation method. The coagulation efficiency correlated well with the hydrophobicity/(hydrophilicity and transphilicty) ratio and specific UV absorbance (SUVA). It was concluded that SUVA and hydrophobicity of AOM can be used as surrogate parameters to predict the coagulation performance and subsequent DBPFP.

- Although, hydrophobic fraction of the AOM was removed better by coagulation-flocculation, higher DBPFP also occurred for this fraction for most algal species due to the presence of aromatic compounds.

- GAC adsorption can remove low MW fraction of AOM, however, with only moderate equilibrium capacity. However, GAC adsorption as a pre-treatment can mitigate the fouling of microfiltration membrane to some extent. The irreversible fouling caused by DOM can be reduced by a dosage of 1.5 g/L of activated carbon.

- The total removal efficiencies of AOM by microfiltration were higher than humic acid, however, a greater flux decline and higher irreversible fouling were observed from AOM than humic acid.

- DBP formation increased linearly with total chlorine residual from 0.28 to 1.02 mg/L, and at a DOC concentration of 3.0 mg/L, both , both haloacetic acids (HAA) and trihalomethane (THM) concentration were much higher than the maximum acceptable concentrations of THM and HAA.

- UV irradiation of each AOM indicted that 40 mJ/cm^2 did not significantly alter the DBP formation; however, more attention should be given to determine the effectiveness of enhanced dosage of UV irradiation on the degradation of algal matter as some algae (*Phaeodactylum tricornutum* and *Merismopedia* sp.) showed contrasting results in UV + chlorination.

8.2 Recommendations for future study

As the algal or cyanobacterial bloom are an on-going global challenge for water treatment plants, and the research indicated that at a concentration of 3.0 mg/L, DBP formation can

exceed the maximum acceptable concentrations, future research should explore further removal of AOM followed by coagulation. Enhanced coagulation can be achieved using polymers.

- More advanced characterization of AOM, such as FTIR, 3D-EEM, NMR, XPS might be required to probe detail information for DBP formation mechanism.

- N-DBP derived from AOM as the emerging group of DBP is of great concern due to the higher carcinogenicity and toxicity than regulated C-DBP needs further investigation.

- The future research can be directed towards surface modification of GAC and operating conditions for better removal of hydrophilic and transphilic AOM. Other low cost adsorbent and membranes can be explored for better removal of AOM.

- High intensity and energy-efficient UV irradiation with capability to mineralize or degrade dissolve organic matter prior to chlorination can be employed to reduce chlorine dosage and DBP formation.

Although, above are the end of pipe solutions for algal bloom, greater effort should be directed towards reducing nutrient overload in the wastewater effluent. More holistic approach is needed so that the surface water sources are managed better.

Appendices

Appendix A: Supplementary material of chapter 3
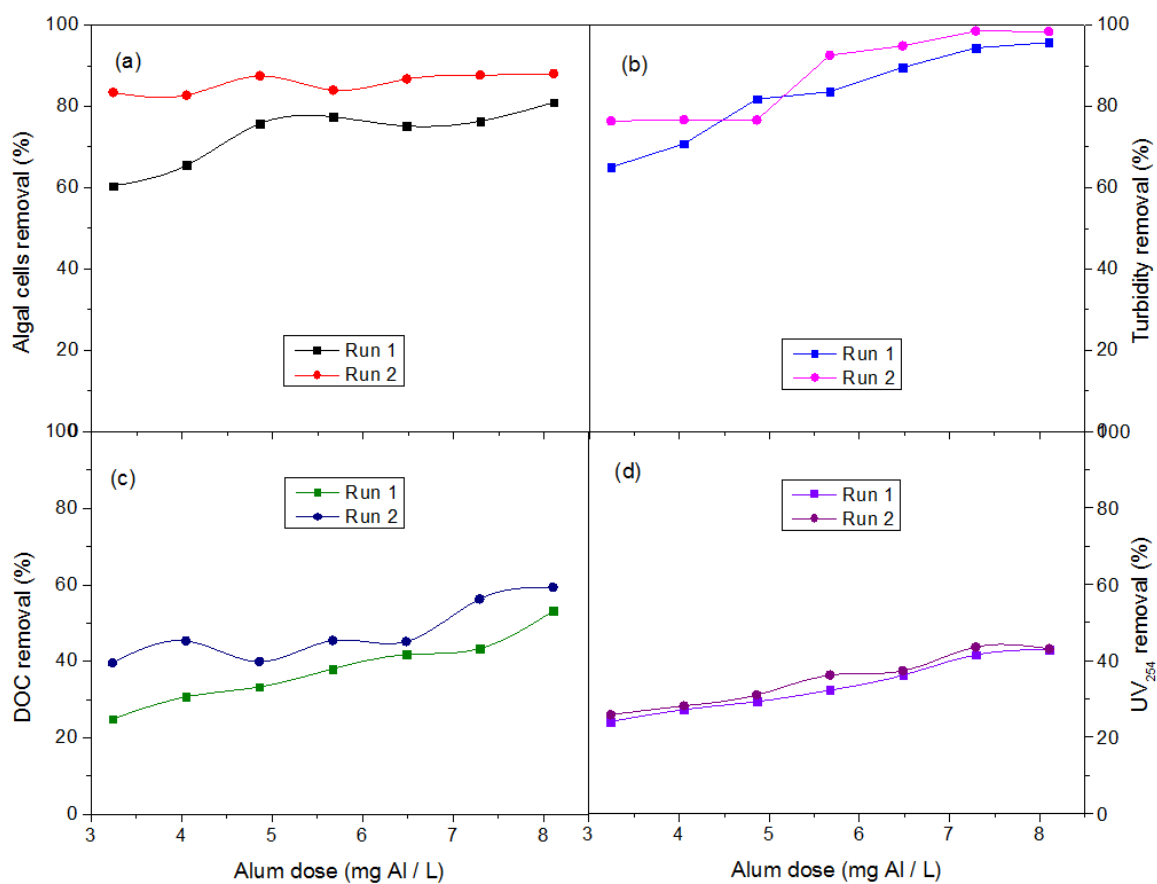
Figure S1 Removal efficiency with variation of alum dose by coagulation for the water samples with cell density of 4.55×10^6 cell/ml without pH adjustment, (a) - (d) represent the removal efficiency of algal cell, turbidity, DOC and UV_{254}, respectively.
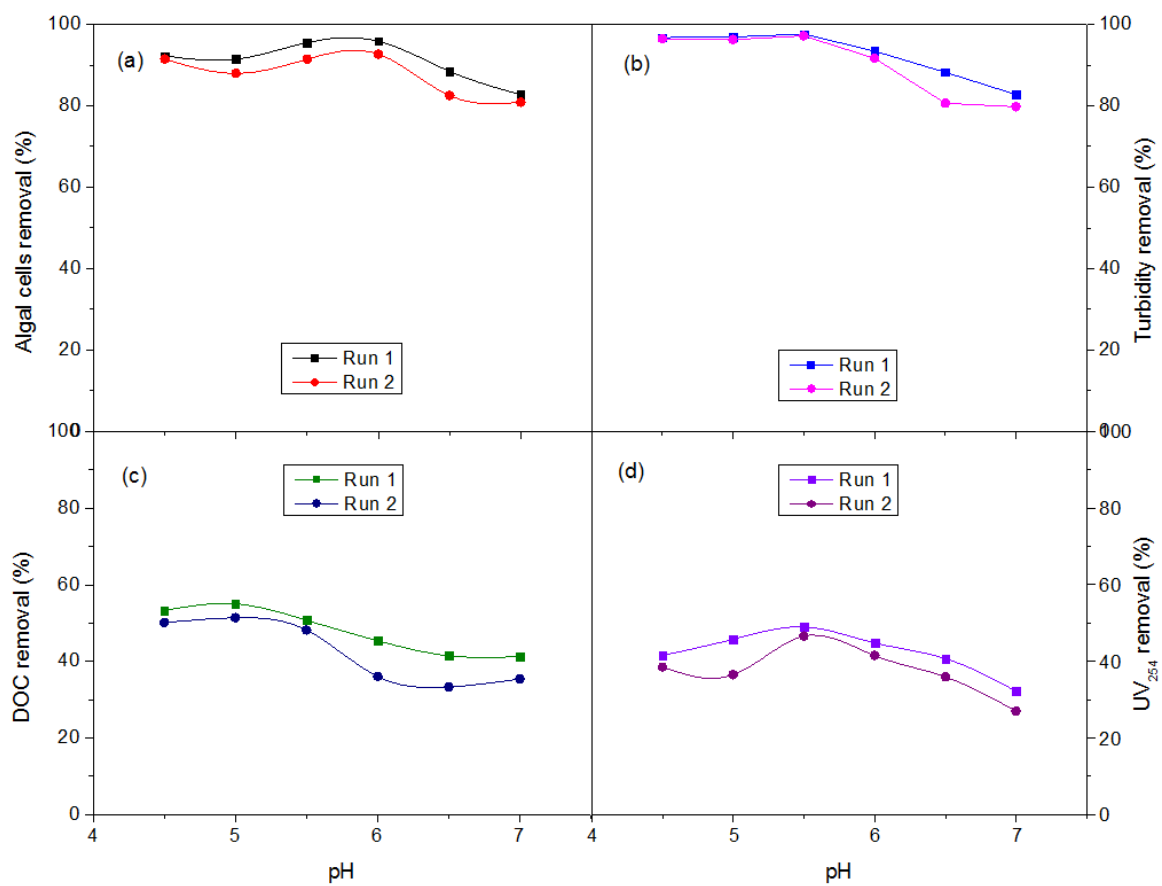
Figure S2 Effect of pH on coagulation performance for the water samples with cell density of 4.5×10^6 cell/ml under the alum dosage 7.30 mg Al/L, (a) - (d) represent the removal efficiency of algal cell, turbidity, DOC and UV_{254}, respectively.
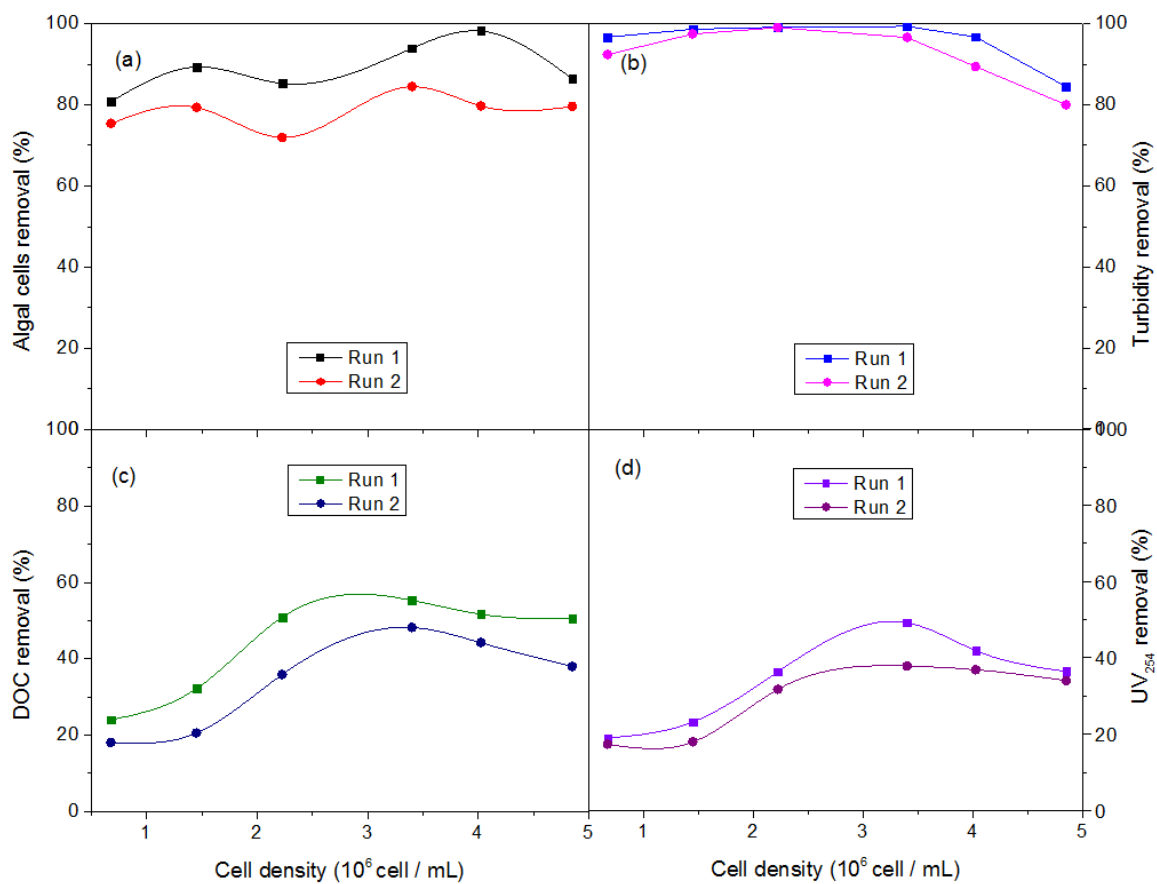
Figure S3 Effect of initial cell density on coagulation performance under the alum dosage 7.30 mg Al/L and pH of 5.5, (a) - (d) represent the removal efficiency of algal cell, turbidity, DOC and UV$_{254}$, respectively.

Appendix B: Permission to reuse copyrighted material of published chapter 3 and chapter 4

Copyright Clearance Center — RightsLink

Home | Account Info | Help

SPRINGER NATURE

Title: Optimization and modeling of coagulation-flocculation to remove algae and organic matter from surface water by response surface methodology

Author: Ziming Zhao, Wenjun Sun, Madhumita B. Ray et al

Publication: Frontiers of Environmental Science & Engineering

Publisher: Springer Nature

Date: Jan 1, 2019

Copyright © 2019, Higher Education Press and Springer-Verlag GmbH Germany, part of Springer Nature

Logged in as:
Ziming Zhao
Western University
Account #: 3001461673

LOGOUT

Order Completed

Thank you for your order.

This Agreement between Western University -- Ziming Zhao ("You") and Springer Nature ("Springer Nature") consists of your license details and the terms and conditions provided by Springer Nature and Copyright Clearance Center.

Copyright Clearance Center — RightsLink

Home | Help | Email Support | Ziming Zhao ⌄

Coagulation and disinfection by-products formation potential of extracellular and intracellular matter of algae and cyanobacteria

Author: Ziming Zhao,Wenjun Sun,Ajay K. Ray,Ted Mao,Madhumita B. Ray

Publication: Chemosphere

Publisher: Elsevier

Date: April 2020

© 2019 Elsevier Ltd. All rights reserved.

Please note that, as the author of this Elsevier article, you retain the right to include it in a thesis or dissertation, provided it is not published commercially. Permission is not required, but please ensure that you reference the journal as the original source. For more information on this and on your other retained rights, please visit: https://www.elsevier.com/about/our-business/policies/copyright#Author-rights

BACK | CLOSE WINDOW

Curriculum Vitae

Name	Ziming Zhao
Post-secondary Education and Degree	The University of Western Ontario, London, Ontario, Canada, 2015-2019 Ph. D.
	The University of Western Ontario, London, Ontario, Canada, 2013-2014 M.Eng.
	Shaanxi University of Science and Technology, Xi'an, Shaanxi, China, 2002-2005, M. E.Sc.
	Shaanxi University of Science and Technology, Xi'an, Shaanxi, China, 1998-2002, B. Eng.

Honors and Awards:

The University of Western Ontario Graduate Research Scholarship, 2015-2019

3rd Prize for Liaoning Province Science &Technology Progress Award, July 2012

3rd Prize for Liaoning Province Science &Technology Progress Award, Dec. 2009

Related Work Experience

Teaching Assistant, The University of Western Ontario, 2015-2019

Research Assistant, The University of Western Ontario, 2014-2019

Research Associate, Dalian Institute of Chemical Physics, Chinese Academy of Sciences, Dalian, China, 2005-2013

Publications:

Ziming Zhao, Wenjun Sun, Madhumita B. Ray, Ajay K. Ray, Tianyin Huang, and Jiabin Chen. (2019). Optimization and modeling of coagulation-flocculation to remove algae and organic matter from surface water by response surface methodology. *Frontiers of Environmental Science & Engineering* 13(5), 75.

Ziming Zhao, Wenjun Sun, Ajay K Ray, Ted Mao, and Madhumita B. Ray. (2020). Coagulation and disinfection by-products formation

potential of extracellular and intracellular matter of algae and cyanobacteria. *Chemosphere*. 245, 125669.

Ziming Zhao and Madhumita B. Ray. (2020). Adsorption isotherms, kinetics and mechanism for the adsorption of dissolved organic matter onto granular activated carbon. (To be submitted)

Ziming Zhao and Madhumita B. Ray. (2020). Granular activated carbon adsorption of algal organic matter in mitigating microfiltration membrane fouling. (To be submitted)

Ziming Zhao, Wenjun Sun, Ted Mao, and Madhumita B. Ray. (2020). Impact of UV irradiation on disinfection by-product formation by post chlorination. (To be submitted)

Ziming Zhao, George Nakhla, and Madhumita B. Ray. (2020). Overview of the application of microalgae for nutrients utilization and contaminants removal in wastewater treatment process. (To be submitted)

Conferences   **Ziming Zhao**, Hassan Gomaa and Madhumita B. Ray. Coagulation performance for the removal of six algae and algal organic matter for drinking water treatment. *CSChE 2017 Conference and Exhibitio*n. October 22nd - 25th, 2017, Edmonton, AB. CA. (Oral presentation)

Ziming Zhao, Hassan Gomaa and Madhumita B. Ray. Removal of algal matter by coagulation both in presence and absence of pre-oxidation. *17AIChE annual meeting*, Oct. 29 to Nov. 3, 2017, Minneapolis, MN, USA. (Oral presentation)